

UNIVERSITÉ DE LILLE

MCMASTER UNIVERSITY

CO-TUTORIAL DOCTORAL THESIS

Computational Actinide Chemistry: Structure, Bonding and Thermodynamics

---

Author:

Sophie KERVAZO

A thesis submitted in fulfillment of the requirements
for the degree of Doctor of Philosophy
in:

PHYSICS - DILUTED MEDIUM AND FUNDAMENTAL OPTICS

in the doctoral school

Sciences de la Matière, du rayonnement et de l'environnement

in:

Laboratoire Physique des Lasers, Atomes et Molécules

Department of Chemistry and Chemical Biology

Defense October 26th 2018

Protractors	
Pr. Nathalie GUIHERY	Université P. Sabatier Toulouse III
Dr. Emmanuel FROMAGER	Université de Strasbourg
Examiners	
Pr. Laurent MARON	Université P. Sabatier Toulouse III
Dr. Dominique GUILLAUMONT	CEA Marcoule
Supervisors	
Dr. Valérie VALLET	Université de Lille
Pr. Paul AYERS	McMaster University
Co-supervisors	
Dr. Florent REAL	Université de Lille
Dr. André SEVERO PEREIRA GOMES	Université de Lille

This page intentionally left blank

UNIVERSITÉ DE LILLE

MCMASTER UNIVERSITY

THÈSE EN COTUTELLE

Computational Actinide Chemistry: Structure, Bonding and Thermodynamics

---

Auteur:
Sophie KERVAZO

En vue de l'obtention du

DOCTORAT DE L'UNIVERSITÉ DE LILLE

en

PHYSIQUE: MILIEUX DILUÉS ET OPTIQUE FONDAMENTAL

de l'école doctorale

Sciences de la Matière, du rayonnement et de l'environnement

au sein des laboratoires:

Laboratoire Physique des Lasers, Atomes et Molécules

Department of Chemistry and Chemical Biology

Défence: 26/10/2018

Rapporteurs	
Pr. Nathalie GUIHERY	Université P. Sabatier Toulouse III
Dr. Emmanuel FROMAGER	Université de Strasbourg
Examinateurs	
Pr. Laurent MARON	Université P. Sabatier Toulouse III
Dr. Dominique GUILLAUMONT	CEA Marcoule
Superviseurs	
Dr. Valérie VALLET	Université de Lille
Pr. Paul AYERS	McMaster University
Co-encadrants	
Dr. Florent REAL	Université de Lille
Dr. André SEVERO PEREIRA GOMES	Université de Lille

This page intentionally left blank

Abstract

The main question of this thesis is: do we have today the tools to efficiently describe the structure, the bonding and the thermodynamics of actinide systems? This broad question is answered thanks to three studies. The first two are directly applied to the plastic industry and the nuclear plant safety. The last one, more fundamental, concerns the benchmarking of newly developed theoretical approach on f-element systems.

First, actinides and transition metal arene-coordinated alkyl cations have been recently proven to be efficient catalysts for ethylene polymerizations. Interestingly, thorium, uranium and zirconium alkyl cations catalytic activity depends on the solvent. To understand these behaviours and to confirm the tendency of these complexes to engage in unusual-arene coordination, relativistic DFT calculations combined with a characterization of the interaction thanks to the ETS-NOCV method are used.

Second, in accident scenario along the reprocessing of spent nuclear fuel, plutonium can be released in various volatile forms (PuO_2, PuO_3 or $PuO_2(OH)_2$, ...). The exploration of these scenarios by the use of simulations requires, among the various parameters, the knowledge of the thermodynamic properties of the possibly formed elements. Our in-silico study focusses on the determination of the enthalpies of formation of the former two species for which experimental uncertainties remain, using multi-configurational relativistic wavefunction method.

The last part of the thesis focusses on the benchmark of the B2-PLYP functional for f-element systems, which turns out quite accurate with respect to the experimental data and the gold-standard CCSD(T) method.

ABSTRACT

La question générale traitée dans cette thèse est de déterminer si, aujourd'hui, nous disposons d'outils théoriques efficaces pour d'écrire la structure, la liaison et les propriétés thermodynamiques de système comprenant un actinide. Cette large question va être abordée à l'aide de trois études différentes. Les deux premières sont directement liées à l'industrie plastique et à la sureté nucléaire. La dernière, plus fondamentale concerne une analyse comparative d'une approche théorique nouvellement développée sur des systèmes comprenant des éléments f.

Tout d'abord, les cations alkyles contenant un actinide (Th, U) ou un métal de transition (Zr) coordonné à un arène se sont révélés efficaces pour la catalyse de la synthèse du polyéthylène. Étonnamment, les activités catalytiques des cations alkyles dépendent du solvant. Pour comprendre cela et confirmer la tendance quónt ces complexes à se lier à l'arène, une étude en DFT dans un contexte relativiste combinée à une caractérisation de liaison avec la méthode ETS-NOCV fut faite.

La deuxième étude vise à étoffer les bases de données thermodynamiques qui servent à explorer numériquement les scénarios d'accidents. Notre étude in silico porte sur la détermination des enthalpies de formation des deux espèces pour lesquelles des incertitudes expérimentales subsistent (PuO_3 ou $PuO_2(OH)_2$, ...), en utilisant une méthode quantique multiconfigurationnelle et relativiste.

La dernière partie de la théorie se concentre sur l'estimation de la précision de la fonctionnelle B2-PLYP pour les éléments f, qui sávère assez précise en comparaison aux données expérimentales et à la méthode de référence CCSD(T).

Acknowledgements

First, I want to thank the protractors Emmanuel Fromager and Nathalie Guihery the jury Dominique Guillaumont and Laurent Maron who take the time to read, listen and give me a feedback on my work. I would like to acknowledge David Emslie et Randy Dumont for getting up so early to attend my PhD defence. My directors also need to be thanked, the four of them is the perfect mixture and is the whole spectrum in their scientific knowledges, listening, advices and managing skills. In science, collaboration is a key to success and I was lucky enough to work with amazing searchers: Franǫis Virot, David Emslie, Stefan Knecht, Leon Freitag and Benjamin Helmich-Paris.

A french comedian Pierre Desproges in one of his chronicles of ordinary hatred said the humanity is divided in four categories: relations, friends, close friends and people you do not know. The the people I do not know, thank you for reading this lines. I hope it can help for your project or to fight insomnia.

Friends/ colleagues: during a PhD, the time spend with friends being inversely proportional to that spend with the colleagues so I thank you all for enlightening scientific conversions, nice beers or a nice scientific conversions with enlightening beers. Family (not describe by Desproges): I have the luck to have a great family, always there when needed or just to share a slice of pizza. Thank you for being here, it is also a pleasure to go home thanks to you all. Close friend: Desproges said that you can count them on the Baron Empain's hand or Django Reihart's for the most misanthrope of us. Nonetheless, you are still being here, thank you !

Desproges was then adding the woman he loved. I will just change the gender to thank to man who is here for me day after day. Finally I think Desproges forget another type of people: the mothers. I thank mine for always supporting me and being there.

Remerciements

Premièrement, je voudrais remercier les rapporteurs Emmanuel Fromager et Nathalie Guihery et le jury Dominique Guillaumont et Laurent Maron qui ont pris le temps de lire et d'écouter mon travail et pris celui de me donner un retour sur celui-ci. Je souhaite aussi remercier David Emslie et Randy Dumont qui ont dû se lever de bonne heure pour suivre ma soutenance de thèse. Je me dois aussi de remercier mes directeurs, à eux quatre, ils furent un parfait mélange, représentant un spectre total dans leurs connaissances scientifiques, leurs écoutes, leurs conseils et leurs façns d'encadrer un thésard. Les collaborations sont importantes en sciences et j'ai eu la chance de travailler avec de formidables chercheurs merci à Françis Virot, David Emslie, Stefan Knecht, Leon Freitag et Benjamin Helmich-Paris.

Pierre Desproges dans une de ses chroniques de la haine ordinaire disait que lhumanité se divise en quatre grandes catégories les relations, les copains, les amis et les gens qu'on ne connait pas. Les gens qu´ on ne connaît pas, merci de me lire en espérant que cela vous aide dans vos recherches ou dans la lutte contre l'insomnie.

Les copains/collègues, en thèse, le temps passé avec les uns étant directement inversement proportionnel à celui passé avec les autres, je vous remercie que ce soit pour une conversion scientifique éclairante, une sympathique petite bière ou pour une sympathique conversation scientifique autour d'une bière éclairante. La famille (qui n'était pas une catégorie de Desproges) : avoir la chance d'avoir une famille en arrière-plan toujours là, que ce soit pour les déménagements, faire des punchs ou manger une pizza en parlant de tout et de rien mais toujours dans la bonne humeur, c'est un réel luxe dont j'ai eu la chance d'héritée. Merci à chacun d'entre vous pour être qui vous êtes, car rentrer en Normandie est toujours un plaisir et me donne un nouveau souffle grâce à vous. Les amis, disait Desproges se comptent sur les doigts de la main du baron Empain voir de Django Reihart pour les plus misanthropes. Néanmoins, vous êtes encore présent aujourd'hui, alors merci !

Desproges, aux quatre catégories y ajouté la femme qu'on aime. Je passerai donc à la version masculine pour remercier celui qui me supporte au quotidien.Enfin, je pense que Desproges a oublié une catégorie très importante : les mamans. Je remercie la mienne pour m' avoir toujours soutenu, que ce soit par un coup de pied au cul (plus ou moins littéral) quand j'en en avait besoin que par le petit Tupperware du dimanche soir qui en réduit la mélancolie.

Contents

List of Figures

List of Tables

List of Abbreviations

AMFI	**A**verage **M**ean **F**ield **I**ntegrals
ANO	**A**tomic **N**atural **O**rbitals
ASTEC	**A**ccident **S**ource **T**erm **E**valuation **C**ode
BSSE	**B**asis **S**ets **S**uperpositon **E**rror
CASSCF	**C**omplete **Actif** **S**pace **S**elf **C**onsistent **F**ield
CASPT2	**C**omplete **Actif** **S**pace **P**erturbation **T**heory at the $\mathbf{2}^{nd}$ order
CBS	**C**omplete **B**asis **S**et
CC	**C**oupled **C**luster
CCSD(T)	**C**oupled **C**luster with **S**ingles and **D**ouble and **T**riple
CI	**C**onfiguration **I**nteraction
CPP	**C**ore **P**olarisation **P**otential
CSF	**C**onfiguration **S**tate **F**unction
DFT	**D**ensity **F**unctional **T**heory
DKH	**D**ouglas **K**roll **H**ess
DMRG	**D**ensity **M**atrix **R**enormalisation **G**roup
EA	**E**lectronic **A**finity
ECP	**E**ffective **C**ore **P**otential
EOM	**E**quation **O**f **M**otion
ETS	**E**xtended **T**ransition **S**tate
FCI	**F**ull **C**onfiguration **I**nteraction
FORA	**F**irst **O**rder **R**egular **A**pproximation
GGA	**G**eneralized **G**radient **A**pproximation
HF	**H**artree **F**ock
IP	**I**onisation **Potential**
IRSN	**I**nstitut **R**adioprotection et de **S**ureté **N**ucléaire
KS	**K**ohn **S**ham
GTO	**G**aussian **T**ype **O**rbitals
LCAO	**L**inear **C**ombimaison of **A**tomic **O**rbitals
LDA	**L**ocal **D**ensity **A**pproximation
MAD	**M**ean **A**verage **D**eviation
MO	**M**olecular **O**rbital

MP	**M**øller-**P**lesset
MP2	**M**øller-**P**lesset at the **2**nd order
NEVPT2	**N** -**E**lectron **V**alence state **P**erturbation **T**heory at the **2**nd order
NOCV	**N**atural **O**rital for **C**hemical **V**alence
PE	**P**oly**E**tylene
PT	**P**erturbation **T**heory
PUREX	**P**lutonium **U**ranium **R**edox **EX**traction
RASSI	**R**estricted **Actif S**pace **S**tate **I**nteraction
RECP	**R**elativistic **E**ffective **C**ore **P**otential
RHF	**R**estricted **H**artree **F**ock
SA	**S**tate **A**verage
SCF	**S**elf **C**onsistent **F**ield
SF	**S**pin **F**ree
SO	**S**pin **O**rbit
SOC	**S**pin **O**rbit **C**oupling
SR	**S**calar **R**elativistic
SS	**S**tate **S**pecific
STO	**S**later **T**ype **O**rbitals
TDDFT	**T**ime **D**ependent **D**ensity **F**unctional **T**heory
TPH	**T**tetra-**P**ropylene
UCCSD(T)	**U**nrestricted **C**oupled **C**luster with **S**ingle **D**ouble and (**T**riple)
UHF	**U**nrestricted **H**artree **F**ock
ZORA	**Z**eroth **O**rder **R**egular **A**pproximation
ZPE	**Z**ero **P**otential **E**nergy

Chapter 1

General Introduction

Actinides are located in the last row of the periodic table, with an atomic number of 89 to 103 and even if they are large atoms with limited natural availability, for some of them, their use are present in our daily life. The plastic piece holding this pages together and the electric power used to write them do not contain actinides but could be the result of the daily exploitation of actinides complexes.

As quantum chemist, the modelling actinides can be a challenge for two main reasons. The first is the inclusion of relativistic effects, the second is how to properly take into account the electronic correlation within the partially occupied 7s, 5f and 6d valence orbitals of actinides. The main question of this thesis is: do we have today the tools to efficiently describe the structure, the bonding and the thermodynamics of actinide systems ?

This broad question is answered thanks to three studies. The two first are directly applied to the plastic industry and the nuclear plant safety. The last one, more fundamental, concerns the benchmarking of double hybrid functional on f-element systems.

The first applied use of actinides we are interested in is the use of actinides complexes as catalyst for the ethylene polymerisation. As with many great discoveries in chemistry, and sciences in general, polyethylene (PE) was first synthesised in Germany by accident in 1898 by Hans von Pechmann. It has now an important position in our daily life since it is used in many plastic items such as plastic bags, bottles, etc...

The most widely used ethylene polymerisation catalysis process is the Ziegler-Natta that allows an ethylene coordination and 1,2 insertion [1] in arene solvent in industry [2] or alkane one in academic laboratory [3]. Many patents are filled as the industrial application of new and better catalysts for ethylene polymerisation could really

be lucrative. The most interesting patent here was filled by Dow Chemical Company in 1987 in order to base, for the first time, the polymerisation of ethylene on actinides and more precisely on a mixture of bis(metallocene) precursor [$Cp^*_2AnX_2$] and [Cp^*AnX_3] (An = Th, U and X = Cl, Me, CH_2SiMe_3) with different activating agents.
With the goal of improving the polymerisation of polyethylene, Pr David Emslie and his former PhD student Nicholas R. Andreychuk at McMaster University worked on new compounds based on actinides as catalysts. They could obtain the arene-coordinated alkyl cations $[(XA_2)An(CH2SiMe_3)(arene)]^+$ with (An = Th, U; XA_2 = 4,5-bis(2,6-diisopropylanilido)-2,7-di-*tert*-butyl-9,9-dimethylxanthene); arene = benzene, toluene, bromobenzene or fluorobenzene) (Figure 1.1) and $[B(C_6F_5)_4]^-$ as counter ion and the close equivalent $[(XN_2)Zr(CH_2SiMe_3)(arene)]^+$ with the same arenes and (XN_2) being the 4,5-bis(2,4,6-triisopropylanilido)-2,7-di-*tert*-butyl-9,9-dimethylxanthene.

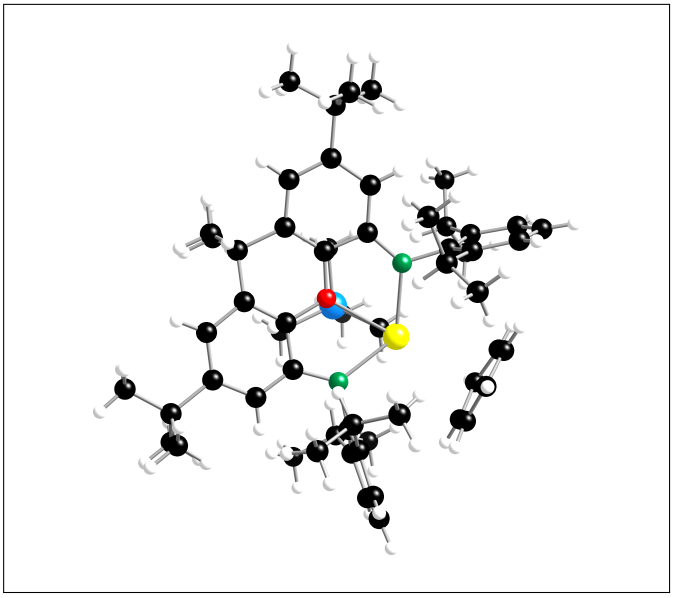

FIGURE 1.1: $(XA_2)U(CH2SiMe_3)(benzene)^+$

The activity of the catalyst does not only dependent on the arene but also of the metallic center. Our theoretical contribution, presented in Chapter 3 aims at understanding the mechanism of the catalysis by an in-depth study of the bond between the arene and the transition metal Zr or an actinide (Th or U) center

As second study, we worked with the French Radioprotection and Nuclear Safety agency (IRSN). While in the past decades the climate change and the future nuclear plants are at the heart of political debate, it is important to recall that no matter the prospective political decisions, nuclear safety must be addressed now. One of the challenge of nuclear power plants is the recycling of the nuclear fuel. Wordwide

the chosen recycling process is the PUREX (Plutonium Uranium Redox EXtraction) one. It uses a liquid-liquid extraction in order to separate the fission products from Plutonium and Uranium in order to reinject the former in the nuclear cycle. The problem with PUREX process is that the solvent tetra-propylene (TPH) could ignite itself and lead to a release, among numerous species, of gaseous plutonium in the atmosphere. This actually happened three times, twice at Savannah River (USA) in 1953 and 1975 and at Tomsk (Russia) in 1993. Even if the plutonium species only represents 0.9% of the fission products it is still responsible for 50% of the radiotoxicity after 100 years (see Figure 1.2).

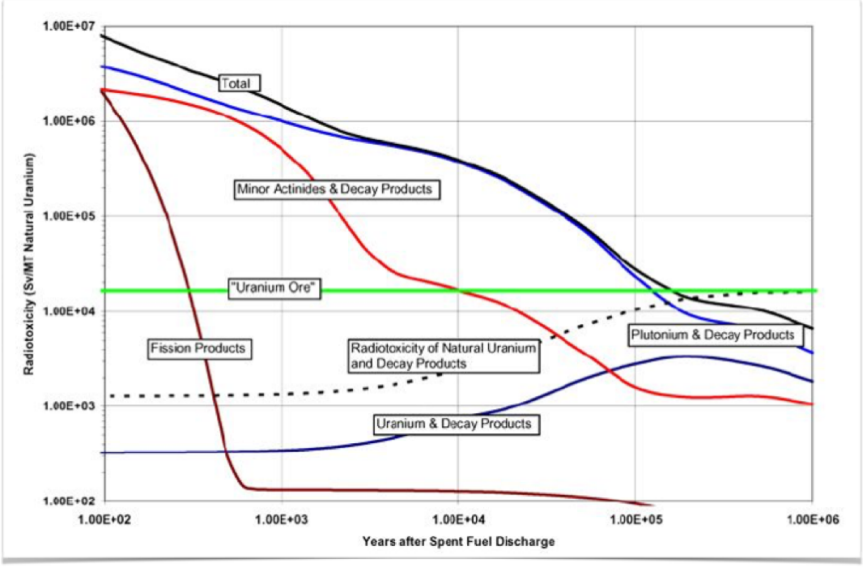

FIGURE 1.2: Radiotoxicity of spend nuclear fuel [4]

To perform nuclear safety analysis, the chemical behaviour of the Pu species need to be known. Experimental studies are complicated to pursue for safety reason. Since Pu can have multiple degrees of oxidation including (VI) it cannot be replaced by the less radioactive Th or Ce for the experiments. The volatile species expected to be formed in the contact with oxygen are the dioxide PuO_2, trioxide PuO_3 and oxy-hydroxide ($PuO_2(OH)_2$) of plutonium. Horeover, the experiments conducted in the past 30 years disagree on the formation of PuO_3 *i.e.* some analysis of experimental data proposed that PuO3 could be formed along the chemical processes, while others do not. Thus theoretical simulations of an accident is the best solution to answer this question. The ASTEC (Accident Source Term Evaluation Code) simulator code, developed by the IRSN, can simulate the accident condition of pression and temperature but precise thermodynamic data such as heat capacities, entropies and enthalpies of formation of the different species involved are needed as input parameters. This study will limit itself to the plutonium oxides PuO_2 and PuO_3 and the

oxyhydroxide $PuO_2(OH)_2$. Those thermodynamic values can be obtained computationally thanks to a detailed knowledge of their electronic structure which implies to take into account thoroughly relativistic effects and electronic correlation. The challenging aspect of this work as detailed in Chapter 4, is the multiconfigurational character of the ground-state wave function.

The treatment of electronic correlation is still source of new developments in quantum chemistry. For the past 10 years, the DFT community tried to better account for electronic correlation in the functionals by proposing new approaches. One of them is the so-called double-hybrid method, which is based on the use of a hybrid functional combined with the MP2 correlated method. This family of functionals has proven its efficiency for a lot of system but so far it was never applied to f-elements. During this thesis, one double hybrid (B2-PLYP) was tested for f-elements systems and representative chemical reaction in Chapter 5

In this thesis the general methods of quantum chemistry are first presented in Chapter 2. These will be followed in Chapter 3 by the exploration of the bonding between alkyl cations and arenes to rationalise the catalytic process of polyethylen. A third part (Chapter 4) will be devoted to the determination of thermodynamic properties of plutonium oxides and oxyhydroxide. The last chapter (Chapter 5) will evaluate the performances of double hybrid functional B2-PLYP for the determination of thermodynamic properties of f-elements containing systems. We will close this manuscript with general conclusions and perspectives.

Chapter 2

Methods

2.1 Introduction to Quantum Chemistry

As discussed in the introduction, the experimental expertise is complementary to theoretical studies. In this chapter, I will define all the necessary tools to understand what is solved from a computational point of view and all the important concepts that were used during my PhD work. As we already mentioned, the context of this study implies accounting for relativistic effects due to the presence of actinides. However, for the sake of clarity, we will start with the presentation of quantum chemical mechanics notions in a non-relativistic framework before introducing the relativistic Dirac equation and the other flavors of relativistic approximate Hamiltonians. Last but not least the concept of basis sets will be presented.

2.1.1 Schrödinger equation

The time-dependent Schrödinger equation describes the physics of a molecular system with respect to time [5]:

$$\hat{H}\psi = i\hbar\frac{\partial\psi}{\partial t} \tag{2.1}$$

Where ψ(t) is the wave function of the state under consideration, in general the ground state (or an excited state), $\hat{H}$ the Hamiltonian operator, i the imaginary number and $\hbar$ the Planck contants divided by 2π. The first approximation is to consister the system as stationary at a moment t [6] and thus the equation becomes an eigenvalue equation, independent of time:

$$\hat{H}(\boldsymbol{r},\boldsymbol{R})\psi(\boldsymbol{r},\boldsymbol{R}) = E\psi(\boldsymbol{r},\boldsymbol{R}) \tag{2.2}$$

with $\psi(\boldsymbol{r}, \boldsymbol{R})$ the wave function of the system made on our case of electrons at positions $\{\boldsymbol{r} = r_1, ..., r_n\}$ and nuclei at the positions $\{\boldsymbol{R} = R_1, ..., R_N\}$ and E being the total energy. $\hat{H}$ is written for a molecule, in atomic units as:

$$\hat{H} = -\sum_i \frac{1}{2} \bigtriangledown_i^2 - \sum_A \frac{1}{2M_A} \bigtriangledown_A^2 - \sum_{i,A} \frac{Z_A}{r_{iA}} + \frac{1}{2} \sum_{i \neq j} \frac{1}{r_{ij}} + \frac{1}{2} \sum_{A \neq B} \frac{Z_A Z_B}{R_{AB}} \tag{2.3}$$

i and j are indices running over the electrons while A and B indices are related to the nuclei. r_{ij} is the distance between the electron i and j , r_{iA} the one between an electron i and a nucleus A and R_{AB} is the distance between two nuclei. Finally, Z_A is the atomic number of nucleus A. The two-first terms of equation 2.3 represent the kinetic energies terms of the electrons and the nuclei, respectively. The last three terms are the standard Coulomb interaction potential terms for electron-nucleus, electron-electron and nucleus-nucleus interactions.

2.1.2 Born-Oppenheimer approximation

As a proton is heavier than an electron (mass ratio of 1 836) the velocity of the nucleus considered to be negligible. Thus, it is possible to decouple the Hamiltonian as a sum of the electronic Hamiltonian $\hat{H}^{el}$ and the nuclear one $\hat{H}^{nuc}$

$$\hat{H} = \hat{H}^{el} + \hat{H}^{nuc} \tag{2.4}$$

In the adiabatic approximation [7] or Born-Oppenheimer approximation, the wave function $\psi(\boldsymbol{r}, \boldsymbol{R})$ can be written as a product of the electronic contribution, ψ^{el}, and the nuclear one ψ^{nuc}:

$$\psi(\boldsymbol{r}, \boldsymbol{R}) = \psi^{el}_{\boldsymbol{R}}(\boldsymbol{r}) \psi^{nuc}(\boldsymbol{R}) \tag{2.5}$$

The electronic Hamiltonian operator is define as:

$$\hat{H}^{el} = -\sum_i \frac{1}{2} \bigtriangledown_i^2 - \sum_{i,A} \frac{Z_A}{r_{iA}} + \frac{1}{2} \sum_{i \neq j} \frac{1}{r_{ij}} + \frac{1}{2} \sum_{A \neq B} \frac{Z_A Z_B}{R_{AB}} \tag{2.6}$$

It can be shown that the contribution of the nucleus-nucleus interaction term is just a constant in the total energy calculation. The eigenvectors are the electronic wave functions $\psi^{el}_{\boldsymbol{R}}(\boldsymbol{r})$ that depend parametrically on $\boldsymbol{R}$. Therefore, the electrons move on a potential energy surface (PES), $E^{el}_{\boldsymbol{R}}$, that can be obtained by solving the following:

$$\hat{H}^{el}\psi^{el}_{\boldsymbol{R}} = E^{el}_{\boldsymbol{R}}\psi^{el}_{\boldsymbol{R}} \tag{2.7}$$

The methods presented in the following pages have for purpose to solve this eigenvalue problem.

2.1.3 Constraints on the wave-function

The first hypothesis is to consider the electrons as independent particules. Thus the n-particule wave function can be written as the product of N one-particule orbitals ϕ (see Section 2.5.1).

$$\psi(r_1, r_2, ..., r_N) = \phi_1(r_1)...\phi_N(r_N) \tag{2.8}$$

A prerequisite for the form of the electronic wave function (now written as ψ), because it characterises fermion particules, is its anti-symmetric character with respect to the particle exchange:

$$\psi(i, j) = -\psi(j, i) \tag{2.9}$$

A a manifestation of the Pauli exclusion principle [8], which states that two fermions cannot occupied the same quantum state, *i.e.* they cannot have the same four quantum numbers (n, l, m and s).

A trial wave function that satisfies both criteria is the Slater determinant [9] composed of orthonormal spin orbitals.

$$\psi(r_1, r_2, ..., r_N) = \frac{1}{\sqrt{N!}} \begin{vmatrix} \phi_1(r_1) & \phi_2(r_1) & ... & \phi_N(r_1) \\ \phi_1(r_2) & \phi_2(r_2) & ... & \phi_N(r_2) \\ \vdots & \vdots & \ddots & \vdots \\ \phi_1(r_N) & \phi_2(r_N) & ... & \phi_N(r_N) \end{vmatrix} \tag{2.10}$$

with the spin orbitals in column and the electron coordinates in row. From now on, ψ will denote Slater determinants.
One can notice:

- The anti-symmetry of the wave-function is present since the exchange of two rows changes the sign of the determinant.

- The Pauli principle and the indiscernibility of the electrons remains. Indeed, having two electrons in the same state will give a determinant equals to zero since two columns will be equal.
- The normalisation constant is $\frac{1}{\sqrt{N!}}$.

2.2 Single-Reference Methods

In this section, the methods common to the three thesis projects using the single-reference approximation will be presented. The specific methods proper to each of them are introduced in the chapter in question.

2.2.1 Hartree-Fock method

In the context of Wave Function Theory, equation 2.10 can be solved thanks to different approximations. The Hartree-Fock approach [10] is the foundation of many other methods and more specifically the so-called *post* Hartree-Fock methods, presented later. It rests on the mean-field approximation which assumes that a given electron is sujected to the average potential (which as discussed below, consists of a classical (electrostatic) and a non-classical (exchange) interaction) of the other electrons, rather than the individual electron-electron interactions. The Hartree-Fock wave function is determined by the variation principle by minimising the energy of the system:

$$E_{HF} = \frac{\langle \Phi | H^{el} | \Phi \rangle}{\langle \Phi | \Phi \rangle} \geq E \tag{2.11}$$

E_{HF} being the HF energy and E the exact total energy of the system. Since the N-electrons problem can be decomposed in N one-electron problems, the solution Φ can be described by a Slater determinant built from the orbitals ϕ_i. The variational conditions on the orbitals lead to a new effective one-electron operator, the Fock operator [6] $\hat{F}_i$.

$$\hat{\boldsymbol{F}}_{\boldsymbol{i}} \phi_i = \epsilon_i \phi_i \tag{2.12}$$

Its eigenvector, ϕ_i is the molecular spin-orbital of the electron i and its eigenvalue ϵ_i the corresponding orbital energy. The Fock operator can be written as:

$$\hat{\boldsymbol{F}}_{\boldsymbol{i}}(\boldsymbol{r}) = \hat{\boldsymbol{h}}_{\boldsymbol{i}}(\boldsymbol{r}) + \sum_{j=1}^{N} |\hat{\boldsymbol{J}}_j(\boldsymbol{r}) - \hat{\boldsymbol{K}}_j(\boldsymbol{r})| \tag{2.13}$$

The one-electron core Hamiltonian $\hat{h}_i(\mathbf{r})$ is composed of the kinetic energy of the electron i and the nucleus-electron potential energy:

$$\hat{\boldsymbol{h}}_{\boldsymbol{i}}(\boldsymbol{r}) = -\frac{1}{2} \bigtriangledown_i^2 - \sum_{K=1}^{N} \frac{Z_K}{r_{iK}} \tag{2.14}$$

The second part of the equation 2.13 is composed by the two one-electron operators. The Coulomb operator J_j, corresponds to the classic representation of the repulsion between two electrons (i and j). The second operator is the non-classical exchange operator and arises from the indiscernability of the electrons and the anti-symmetry of the wave-function. It forbids electrons with identical spins to occupy the same spatial position. Applying the exchange and Coulomb operators on ϕ_j gives:

$$\hat{\boldsymbol{J}}_j \phi_i(\boldsymbol{r_i}) = \left[\int \frac{\phi_j^*(\boldsymbol{r_j}) \phi_j(\boldsymbol{r_j})}{\boldsymbol{r_{ij}}} d\boldsymbol{r_j} \right] \phi_i(\boldsymbol{r_i}) \tag{2.15}$$

$$\hat{\boldsymbol{K}}_j \phi_i(\boldsymbol{r_i}) = \left[\int \frac{\phi_j^*(\boldsymbol{r_j}) \phi_i(\boldsymbol{r_j})}{\boldsymbol{r_{ij}}} d\boldsymbol{r_j} \right] \phi_j(\boldsymbol{r_i}) \tag{2.16}$$

Thus the eigenvalue ϵ_i of the eigenfunction ϕ_i in the equation 2.12 is:

$$\epsilon_i = \langle \phi_i | \, \hat{\boldsymbol{F}}_{\boldsymbol{i}} \, | \phi_i \rangle = \langle \phi_i | \, \hat{\boldsymbol{h}}_{\boldsymbol{i}} \, | \phi_i \rangle + \langle \phi_i | \sum_{j=1}^{N} (\hat{\boldsymbol{J}}_j - \hat{\boldsymbol{K}}_j) \, | \phi_i \rangle \tag{2.17}$$

Finally, the whole energy Hartree-Fock is:

$$\boldsymbol{E}_{HF} = \sum_{i=1}^{N} h_{ii} + \frac{1}{2} \sum_{i=1}^{N} \sum_{j=1}^{N} (\boldsymbol{J}_{ij} - \boldsymbol{K}_{ij}) = \sum_{i=1}^{N} [\epsilon_i - \frac{1}{2} \sum_{j=1}^{N} (\boldsymbol{J}_{ij} - \boldsymbol{K}_{ij})] \tag{2.18}$$

Where N remains the number of electrons and ϵ_i, $\boldsymbol{J}_{ij}$ and $\boldsymbol{K}_{ij}$ follow the description of the equations 2.17 and:

$$\boldsymbol{J}_{ij} = \int \phi_i^* \hat{J}_i \phi_i; \boldsymbol{K}_{ij} = \int \phi_i^* \hat{K}_i \phi_i \tag{2.19}$$

One can note that the total energy Hartree-Fock is not the sum or the energy of the spin-orbitals of the equation 2.17 otherwise the electronic repulsion would be counted twice for each electron.

2.2.2 The problem of Electron Correlation

Definition

As mentioned above, in the HF approximation, the instantaneous electron-electron interaction was replaced by an average potential while this approximation can yield to a fairly good representation of the physical systems. It is, nevertheless, still far from the exact solution as far as physico-chemical process are concerned. The missing interactions are what is referred as electronic correlation E_{corr} [11] which is defined as the difference between the total exact non relativistic energy of the system E_{tot} and the Hartree-Fock one E_{HF} (for a given basis set limit, see Section 2.5):

$$E_{corr} = E_{tot} - E_{HF} \tag{2.20}$$

Though electron correlation represents only 5 to 10% of the total energy of the system it can change the whole picture of the wave function and impact molecular properties and thus cannot be neglected [12]. From a physical point of view, electronic correlation is due to two types of instantaneous repulsions. The first one is the repulsion between the two negative charges, leading to the Coulomb hole. The second type of repulsion prevents two particules with the same spin to be at the same position corresponding to the Fermi hole.

One can distinguish between the dynamical and non-dynamical (or static) electronic correlation. The static correlation, occurring in case of near orbitals degeneracy, implies that the wave function has to be described by more than one Slater determinant. The dynamical correlation, is connected to the instantaneous correlation of the electron motions and is accounted for by post-Hartree-Fock methods discussed after.

Møller-Plesset Perturbation Theory

In order to include dynamical correlation into a single reference wavefunction, Perturbation Theory (PT) [13] can be used. One can rewrite the Schrödinger equation as:

$$\hat{H}\psi = E\psi \tag{2.21}$$

with :

$$\hat{H} = \hat{H}_0 + \hat{H}' \tag{2.22}$$

where $\hat{H}_0$ is the HF Hamiltonian and $\hat{H}'$ the perturbation one defined in the equation 2.26.

The energy and the wave function can be written as Taylor expansion of λ (being the strength of the perturbation) since E_{PT} and ψ are continuous functions between zero and infinity:

$$E_{PT} = \lambda^{(0)}E_0 + \lambda^{(1)}E_1 + \lambda^{(2)}E_2 + ... \tag{2.23}$$

$$\psi = \lambda^{(0)}\psi_0 + \lambda^{(1)}\psi_1 + \lambda^{(2)}\psi_2 + ... \tag{2.24}$$

If λ = 1, the n-th order energy and wavefunction are of all the terms with indices $\leq$ n.

In the Møller-Plesser (MP) Perturbation Theory, $\hat{H}_0 = \hat{H}_{HF}$ thus it consists in the introduction of a perturbation to a reference (HF) wave function. In other words, excited Slater determinants are included.

We will focus on Møller-Plesset to the 2^{nd} order (MP2), for which double excitations are included. Since it is easily proven that MP1 (Møller-Plesser to the 1^{st} order) is actually equivalent to HF [10] with the Brillouin theorem. The Brillouin theorem stating that the singly excited configurations do not contribute to the 1^{st} order correction to the wave function. By single excitation, one has to understand the promotion of one electron to an unoccupied orbital is allowed (see Figure 2.1), for double excitations, it is two electrons. The number of excited determinants is directly linked to the size of the basis set implying that, the computational cost will be also dependent on it (see Table 2.1 and Section 2.5.1 for the definition of a basis set). Let us have a look at E_{MP2} starting from λ = 1 and equation 2.23 .

$$E_{MP2} = E_0 + E_1 + E_2 = \sum_i \epsilon_i - \frac{1}{2}\sum_{ij} \langle ij| \, |ij\rangle \tag{2.25}$$

As mentioned before, MP2 includes single and double excitations (if non-canonical/open-shell orbitals are used). The matrix elements with singly excited determinants Φ_i^a are:

$$\begin{aligned} \langle \Phi_0| \, \hat{H}' \, |\Phi_i^a\rangle &= \langle \Phi_0| \, \hat{H}_0 - \sum_j^{N_{elec}} \hat{\boldsymbol{F}}_j \, |\Phi_i^a\rangle \\ &= \langle \Phi_0| \, \hat{H}_0 \, |\Phi_i^a\rangle - \langle \Phi_0| \sum_j^{N_{elec}} \hat{\boldsymbol{F}}_j \, |\Phi_i^a\rangle \\ &= \langle \Phi_0| \, \hat{H}_0 \, |\Phi_i^a\rangle - \left(\sum_j^{N_{elec}} \epsilon_j \right) \langle \Phi_0 | \Phi_i^a \rangle \end{aligned} \tag{2.26}$$

Where the subscript of Φ, *i,j, ...* are the occupied orbitals the electron is promoted from and *a, b, ...* the virtual orbitals. Φ_0 and Φ_i^a are two orthogonal states so the

second term is equals to zero. For the first term, the Brillouin theorem [14] states that (for closed shell systems) if two orthogonal states satisfying HF equation are different by only one orbital then: $\langle \Phi_0 | \hat{H}_0 | \Phi_i^a \rangle = 0$, so that $\langle \Phi_0 | \hat{H}' | \Phi_i^a \rangle = 0$. Thus, E_2 only involves doubly excited determinants:

$$E_2 = \sum_{i<j}^{occ} \sum_{a<b}^{vir} \frac{\langle \Phi_0 | \hat{H}' | \Phi_{ij}^{ab} \rangle \langle \Phi_{ij}^{ab} | \hat{H}' | \Phi_0 \rangle}{E_0 - \epsilon_{ij}^{ab}} \tag{2.27}$$

Because of the Koopmans' Theorem [15] the difference in total energy between two Slater determinants is the difference in Molecular Orbitals (MO) energies thus the second-order energy for a closed-shell system can be written with a sum over the spatial orbitals a, b, r and s as:

$$E(MP2) = 2 \sum_{abrs}^{N/2} \frac{\langle ab | |rs\rangle - \langle rs | |ab\rangle}{\epsilon_a + \epsilon_b - \epsilon_r - \epsilon_s} - \sum_{abrs}^{N/2} \frac{\langle ab | |rs\rangle - \langle rs | |ba\rangle}{\epsilon_a + \epsilon_b - \epsilon_r - \epsilon_s} \tag{2.28}$$

The two main advantages of MP2 are the low computational cost compared to variational methods (such as CI see Section 4.2.1) and its size extensivity [1].

Higher orders of perturbation such as MP3 (with the third order energy) or MP4 (with the fourth order energy) allow to include more dynamical correlation but at a greater cost. However, it has been shown that MP perturbation theory may not always converge [17], converge slowly or even oscillate. The issue of convergence, as well as the fact that other approaches such as coupled cluster have a similar cost than MP3, MP4 etc... but are more reliable, means that these approaches are mow seldom used.

TABLE 2.1: Computational Cost and Amount of Correlation Included In the different Møller-Plesser Perturbation Theories. (see section 2.5.1 for the definition of M_{basis})

Method	Computational Cost	Amount of Correlation Included
MP2	M_{basis}^5	80 - 90 %
MP3	M_{basis}^6	90 - 95 %
MP4	M_{basis}^7	95 - 97 %

[1] Size-extensivity is a mathematical concept introduced by Bartlett [16] to characterised a method with a linear scaling between the energy and the number of electrons. The size consistency is also a property of a method, refering to the fact that if A and B are two subsystems sharing no electrons the following equality is true: E(A + B) = E(A) + E(B).This property is particularly important when a dissociation curve is explored.

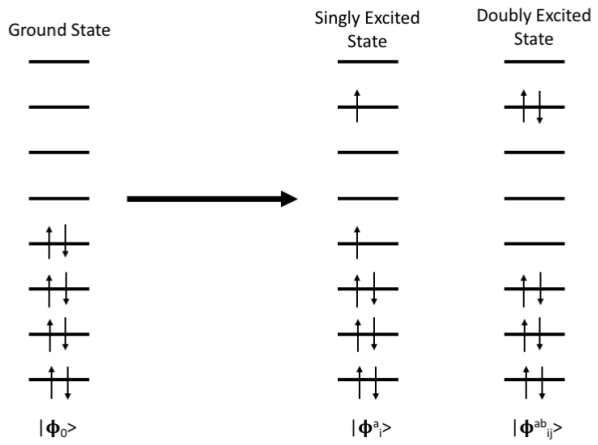

FIGURE 2.1: Single Excitation from a Ground State [17]

Coupled Cluster Method

The coupled cluster (CC) method [18–21] is an approach based on the Many-Body Perturbation Theory where high-order excitations are included efficiently. Thus, the Schrödinger equation can be written as:

$$\hat{H}\Psi_{CC} = E\Psi_{CC} \tag{2.29}$$

Ψ_{CC} is defined with an excitation operator $\hat{T}$ acting on a reference wave function:

$$\Psi_{CC} = e^{\hat{T}}\Psi_0 \tag{2.30}$$

The exponential term can be expanded as:

$$e^{\hat{T}} = 1 + \hat{T} + \frac{1}{2!}\hat{T}^2 + \frac{1}{3!}\hat{T}^3 + ... = \sum_{k=0}^{\infty}\frac{1}{k!}\hat{T}_k \tag{2.31}$$

the excitation operator $\hat{T}$ is the sum:

$$\hat{T} = \sum_{i=1}^{N}\hat{T}_i \tag{2.32}$$

the subscript being the excitation order and N the number of electrons in the system. The excitation order corresponds to the number of electrons excited from an

occupied to an unoccupied orbital, for example:

$$\hat{T}_1\Psi_0 = \sum_{i}^{occ}\sum_{a}^{virtual} t_i^a \Phi_i^a \tag{2.33}$$

and

$$\hat{T}_2\Psi_0 = \sum_{i<j}^{occ}\sum_{a<b}^{virtual} t_{ij}^{ab} \Phi_{ij}^{ab} \tag{2.34}$$

represent single and double excitations, where t_i^a and t_{ij}^{ab} are the amplitudes of the excitations and so on. Here, the variational principle generally used to find the energy cannot be applied. Indeed, non-vanishing terms all the way up to the order of N arise because of the expansion in equation 2.31. Therefore, the energy is determined by projecting equation 2.29 onto the reference wave function Φ_0. The coupled-cluster E_{CC} energy is then expressed as:

$$E_{CC} = \langle\Phi_0| e^{-\hat{T}}\hat{H}e^{\hat{T}} |\Phi_0\rangle \tag{2.35}$$

This method, similar to MP2 in the idea, retrieves the dynamical correlation of the system but still describes it with a single reference determinant. However, in contrast to MP2, the single excited T_1 operators are known to introduce orbital relaxation [22] and make CC method more reliable than MP2 in cases the HF orbitals are not optimal

If no constraints on the excitation order are put in place, one would arrive at the FCI calculation and the method 4.2.1 would only be applicable for very small systems, so a truncated form was developed including only the single and double electrons excitations [23]. This truncated CC, called CCSD, remains size extensive and affordable for medium systems. Higher-order truncations are available such as CCSDT[24] including explicitly the triple excitations or CCSDTQ adding the quadruple ones, but they are too expensive for the gain in electronic correlation retrieved. The triple excitations, that might be important for the description of some wave functions, are then included perturbatively, leading to CCSD(T) being the most wisely used triple variant [25][2].

Unfortunately, the restricted CCSD(T) depicted above is inadequate to describe open-shell molecules such as the ones under study. Thus, one must turn to the unrestricted version of this method UCCSD(T). The first formulations of it [16, 27, 28] use an

[2]CCSD(T) is different from CCSD[T] were the contribution of the single excitations are not taken into account and from CCSD-T where triples corrections are computed as defined by M. J. O. Deegan *et al.*[26]

Unrestricted-HF (UHF) reference wave function. However this idea has the disadvantages of being expensive and leading to spin contamination (artificial mixing of multiple electronic spin states). This is why different studies decided to start with a restricted HF reference [29, 30] but the spin contamination of the wave-function was still present. In 1993, Knowles *et al.* [20, 21] proposed a RHF-UCCSD formulation.

Today, UCCSD(T) is considered as the "gold standard" for single reference cases, but may fail for multi-reference ones. The T_1 [31] and D_1 diagnostics [32, 33] can be used to qualitatively spot a multi-reference character. Defining T_1 with the one-electron excitation amplitudes t_1:

$$T_1 = \frac{||t_1||}{\sqrt{N}} \tag{2.36}$$

And the D_1 for open-shell [34]:

$$D_1 = max(||f_i^a||_2, ||f_x^a||_2, ||f_i^x||_2) \tag{2.37}$$

where the 2-norm of a matrix, $||R||_2$, is the maximum Euclidean norm of the vectors formed by the multiplication of R with a unit vector [35], and the f amplitudes being linked to the t amplitudes by:

$$f_i^a = \frac{t_{i\alpha}^{a\alpha} + t_{i\beta}^{a\beta}}{2} \tag{2.38}$$

$$f_x^a = \frac{t_{x\alpha}^{a\alpha}}{\sqrt{2}} \tag{2.39}$$

$$f_i^x = \frac{t_{i\beta}^{x\beta}}{\sqrt{2}} \tag{2.40}$$

If for lighter elements a T_1 diagnostic higher than 0.02 is usually a sign of multi-reference character the value is raised at 0.05 [36, 37] for systems with transition metals and other heavy elements.

2.3 Density Functional Theory

At the birth of quantum chemistry in the 1960's, the limited computational power raised difficulties to perform accurate calculations using large basis sets (see Section 2.5.1) or including many atoms with HF method. In this context, the great adventure of Density Functional Theory (DFT) started in 1964 with Hohenberg and Kohn [38]

when they demonstrated that the exact energy of the ground state of any electron gas in an external potential is a functional of the density F [ρ].

$$E[\rho] \equiv \int \nu(\boldsymbol{r})\rho(\boldsymbol{r})d\boldsymbol{r} + F[\rho] \tag{2.41}$$

where ν would be the Coulomb attraction between the nuclei and the electrons. ρ, the total electron density of N electrons is defined as:

$$\rho(\boldsymbol{r}) = N \int ... \int |\Psi(\boldsymbol{x}_1, \boldsymbol{x}_2, ...\boldsymbol{x}_n)|^2 d\sigma d\boldsymbol{x}_2 ... d\boldsymbol{x}_N \tag{2.42}$$

σ being the arbitrary spin of the electron one, $\boldsymbol{x}_i$ being the map of the spin-spatial coordinated of the other N-1 electrons.

F[ρ] is a universal functional of the total electron density ρ that corresponds to the sum of the two electron energy functional W[ρ] and the kinetic energy terms T[ρ]. Considering F[ρ], it can be rewritten as:

$$F[\rho] = T[\rho] + W[\rho] \tag{2.43}$$

Thus the "only" down side is the determination of the universal functional F[ρ], since the energy is simply obtained by the variational principle. Hohenberg and Kohn stated themselves the problem of obtaining this universal functional in the conclusion of their paper: *"We have developed a theory of electronic ground state which is exact in two cases : The case of a nearly constant density [...] and the case of a slowly varying density. Actual electronic systems do not belong to either of them."*

The answer to this problem arrived one year later in 1965, with Kohn and Sham [39] by proposing that the exchange-correlation term, at the heart of the problem of Hohenberg and Kohn (and more generally in quantum chemistry), can be approximate by using the true chemical potential $\mu(\rho)$ of the homogeneous interacting electron gas.

$$\frac{\delta E}{\delta \rho} = \mu \tag{2.44}$$

First, the density is rewritten as a slater determinant of spin orbitals ϕ_i for a non interacting reference system.

$$\rho(\boldsymbol{r}) = \sum_i^N \phi_i^*(\boldsymbol{r})\phi_i(\boldsymbol{r}) \tag{2.45}$$

Then, the variational principle is applied to equation 2.41 in order to obtain N coupled one-particle equations for the non-interacting electrons, the so-called the Kohn-Sham equations:

$$\left\{ -\frac{1}{2m} \bigtriangledown^2 + \phi(\boldsymbol{r_i}) + v_{xc}(\rho(\boldsymbol{r_i})) \right\} |\phi_i\rangle = \epsilon_i |\phi_i\rangle \tag{2.46}$$

with:

$$\phi(\boldsymbol{r}) = v_{ext}(\boldsymbol{r}) + \int \frac{\rho(\boldsymbol{r'})}{|\boldsymbol{r} - \boldsymbol{r'}|} d\boldsymbol{r'} \tag{2.47}$$

and

$$v_{xc}(\rho(\boldsymbol{r})) = \frac{\delta E_{xc}[\rho]}{\delta \rho(\boldsymbol{r})} \tag{2.48}$$

Here, the issue is the formulation of E_{xc}. In practice, the exact functional is replaced by an approximated one with a certain number of exact conditions being enforced [10] as listed below:

- For a hydrogen-like system the functional should give the exact exchange energy and a correlation energy equals to zero.
- For solid-state physics, it is important to recover the electron gas solution when the density becomes constant. However, it is less true for molecular densities since as the electron gas model does not properly describe a molecular system.
- Multiplying by a constant factor the molecular coordinates ($\rho\lambda$(x,y,z) = $\lambda^3\rho(\lambda$x, λy, λz)) should result in a linear scaling of the exchange energy. $E_x[\rho_\lambda] = \lambda E_x[\rho]$.
- On the contrary, there is no full scaling concerning the correlation energy.
- The exact functional should fulfill the Lieb-Oxford inequality saying that $E_x[\rho] \geq E_{xc}[\rho] \geq 2.273\ E_x^{LDA}[\rho]$ (see Section 2.3.1).
- As $\boldsymbol{r}$ tends to infinity the exchange potential should have an asymptotic behaviour in $-\boldsymbol{r}^{-1}$ while the correlation potential shows a $-\frac{1}{2}\alpha\boldsymbol{r}^{-4}$ behaviour (α being the polarisability of the N_{elec} - 1 system).

A good starting point to find the universal or approximate functional is to separate the exchange term from the correlation one in equation **??**, such as $E_{xc}[\rho] = E_x[\rho] + E_c[\rho]$, with :

$$E_x[\rho] = \int \rho(\boldsymbol{r}) \epsilon_x([\rho], \boldsymbol{r}) d\boldsymbol{r} \tag{2.49}$$

$$E_c[\rho] = \int \rho(\boldsymbol{r}) \epsilon_c([\rho], \boldsymbol{r}) d\boldsymbol{r} \tag{2.50}$$

The exchange energy, by definition, involves only electrons with identical spins while the correlation due to electrons with the same spin is different, and thus separable, from the correlation from electrons with opposite spins:

$$E_x[\rho] = E_x^{\alpha}[\rho_\alpha] + E_x^{\beta}[\rho_\beta] \tag{2.51}$$

$$E_c[\rho] = E_c^{\alpha\alpha}[\rho_\alpha] + E_c^{\beta\beta}[\rho_\beta] + E_c^{\alpha\beta}[\rho_\alpha, \rho_\beta] \tag{2.52}$$

With $\rho = \rho_\alpha + \rho_\beta$ and $\rho_\alpha = \rho_\beta$ for a closed-shell singlet state.

Now that the basis of DFT are exposed, the next part will focus of the expressions of $E_x[\rho]$ and $E_c[\rho]$ and the approximations leading to their formulations.

2.3.1 Local Density Approximation

In the Local Density Approximation (LDA)[39–41], the exchange energy is given by the Dirac formula:

$$E_x^{LDA}[\rho] = -C_x \int \rho(\boldsymbol{r})^{\frac{4}{3}} d^3\boldsymbol{r} \tag{2.53}$$

In the case of an open-shell system where α and β densities are different, LSDA (Local Spin Density Approximation) is used, the exchange energy reads :

$$E_x^{LSDA}[\rho] = -C_x \int (\rho_\alpha(\boldsymbol{r})^{\frac{4}{3}} + \rho_\beta(\boldsymbol{r})^{\frac{4}{3}}) d^3\boldsymbol{r} \tag{2.54}$$

Concerning the correlation part, it is fitted on high precision calculations performed with Quantum Monte Carlo method to a uniform electron gas. The analytic interpolation formula used for this fit defines the functional, for example Vosko, Wilk and Nusair' one [41] (VWN) or the popular PW92 constructed by Perdew and Wang in 1992 [40].

2.3.2 Generalised Gradient Approximation

The goal of the Generalised Gradient Approximation's (GGA) [42] is to improve the exchange and correlation energies by including the electron density and its derivative, at given point (removing the *local* or homogeneous character of LDA) in the functional. For example, in this thesis, we have used the Perdew-Burke-Ernzerhof (PBE) [43] GGA functional defined by its exchange functional:

$$\epsilon_x^{PBE} = \epsilon_x^{LDA} F(x) \tag{2.55}$$

where x is a gradient of the density:

$$x = \frac{|\nabla\rho|}{\rho^{\frac{4}{3}}} \tag{2.56}$$

and

$$F(x) = 1 + a - \frac{a}{1 + bx^2} \tag{2.57}$$

a and b being parameters. The correlation part is expressed as:

$$\epsilon_c^{PBE} = \epsilon_c^{LDA} H(x) \tag{2.58}$$

$$H(x) = cf_3^3 \ln\left[1 + dt^2\left(\frac{1 + At^2}{1 + At^2 + A^2t^4}\right)\right] \tag{2.59}$$

$$A = d\left[exp\left(-\frac{\epsilon_c^{PBE}}{cf_3^3}\right) - 1\right]^{-1} \tag{2.60}$$

$$f_3(\zeta) = \frac{1}{2}\left[(1+\zeta)^{\frac{2}{3}} + (1-\zeta)^{\frac{2}{3}}\right] \tag{2.61}$$

$$t = \left[2(3\pi^3)^{\frac{1}{3}} f_3\right]^{-1} x \tag{2.62}$$

The parameters a, b and c are determined in a non-empirical way. ζ is the relative spin polarisation (= ($n_\uparrow$ - $n_\downarrow$) /n with n = 3/4 π r_s^3, r_s being the Wigner-Seitz radius that is the radius of a sphere whose volume is equal to the mean volume per atom in a solid).

2.3.3 Hybrid-Generalised Gradient Approximation

Hybrid-GGA functionals combine a LDA part, a GGA part and an exact HF exchange weighted in order to fit experimental data. For example in this work, the well-used B3LYP [44] and PBE0 [45, 46] functionals have been used. The B3LYP functional is:

$$E_{xc}^{B3LYP} = (1-a)E_x^{LSDA} + aE_x^{exact} + b\delta E_x^{B88} + (1-c)E_c^{LSDA} + cE_c^{LYP} \tag{2.63}$$

The LYP and B88 part of the correlation and exchange energies are obtained with the GGA approximtion. E_x^{exact} is obtained when the KS orbitals used are identical to HF one. E_x^{LSDA} is described in the equation 2.54. The default values for a, b and c are 0.2, 0.7 and 0.8 respectively, however most of the quantum chemistry codes allow the user to modify these values. The defaults values are kept in the present work.

PBE0 consists in the addition of 25% of E_x^{exact} to the PBE functional presented in the previous paragraph.

2.3.4 Strengths and Weaknesses of DFT

As one understood, DFT is a great tool for quantum chemists. It is fast and black box once the functional is (smartly) chosen. Its computational cost scales as N^3 (N being the number of orbitals). On the other side, the impossibility to systematically improve results and the problem of describing spin states are severe drawbacks [47, 48]. In a vision restricted to the treatment of actinides, the main deficiency of DFT is its single determinant description, while the large number of unpaired f, s and d actinides electrons may results in a strongly multi-determinantal wave-function.

We can also point out that the exchange-correlation functional does not account for long-range ($\frac{C_6}{R_6}$) correlation corresponding to the London part of the dispersion energy notably present when Van der Waals interaction are important.

Dispersion can be patched to KS energies as proposed by Grimme *et al.* [49–51] with the D3 empirical correction:

$$E_{disp} = E^{(2)} + E^{(3)} \tag{2.64}$$

With the two-body $E^{(2)}$ term defined as:

$$E^{(2)} = \sum_{AB} \sum_{n=6,8,10} s_n \frac{C_n^{AB}}{r_{AB}^n} f_{d,n}(r_{AB}) \tag{2.65}$$

with

$$f_{d,n}(r_{AB}) = \frac{1}{1 + 6(\frac{r_{AB}}{s_{r,n} R_0^{AB}})^{-\alpha_n}} \tag{2.66}$$

C_n^{AB} are tabulated for atom pairs, s_n and $s_{r,n}$ are a scaling factor adjusted for each functional and R_0^{AB} is the cutoff radii

The three-body $E^{(3)}$ term is:

$$E^{(3)} = \sum_{ABC} f_{d,(3)}(\bar{r}_{ABC}) E^{ABC} \tag{2.67}$$

$\bar{r}_{ABC}$ being the geometrically averaged radii of atoms A, B and C and E^{ABC} the triple dispersion term:

$$E^{ABC} = \frac{C_9^{ABC}(3cos\theta_a cos\theta_b cos\theta_c + 1)}{(r_{AB}r_{BC}r_{CA})^3} \tag{2.68}$$

where C_9^{ABC} is a constant and θ_a, θ_b and θ_c are the internal angles of the triangle formed by r_{AB}, r_{BC} and r_{CA}

This dispersion correction can be efficient but still relies on empirical corrections. A second solution is a new type of functionals, the Double Hybrids described in Chapter 5.

2.4 Treatment of relativistic effects

All the methods presented so far were based on the non-relativistic Schrödinger equation. For relatively light atoms (Z < 36), this approximation is fully legitimate but increasing the atomic number of the atom implies for the electrons closer to the nucleus to have a velocity approaching the speed of light [52], making relativistic effects no longer negligible and affecting their electronic structure.

Relativistic effects can be separated in two types: those independent of the electron spin (or scalar) and those dependent of the electron spin (or spin-orbit). The first steams from the fact that, because of the stronger nuclear attraction (as Z increases), the inner electrons are accelerated and get closer to the nucleus. The consequence is, the contraction and the stabilisation of the *s* and *p* orbitals. Furthermore, as the inner *s* and *p* electrons are drawn towards the core, they increasingly more effective in screening outer shells and as consequence, the *d* and *f* electrons are destabilised. The second category, the spin-orbit one, can be seen, in a classic representation, as the interaction of the electron magnetic moment and the magnetic induction created by the kinetic orbital motion and results in the splitting of orbitals with angular momenta greater than 0.

2.4.1 Dirac equation

According to relativistic theory, since the speed of light and the Physics laws are the same in all inertial frames, the researched equation must be invariant under Lorentz transformation [53][3]. We see, for instance, the time-dependent Schrödinger equation:

$$\frac{-\hbar}{2m}\left[\frac{\partial^2\psi(\boldsymbol{r},t)}{\partial x^2} + \frac{\partial^2\psi(\boldsymbol{r},t)}{\partial y^2} + \frac{\partial^2\psi(\boldsymbol{r},t)}{\partial z^2}\right] = -i\hbar\frac{\partial\psi(\boldsymbol{r},t)}{\partial t} \tag{2.69}$$

[3]Invariant under Lorentz transformation means that the value of a quantity is the same in all Galileen referentials

does not fulfil this requirement, since the spatial coordinates x, y and z appear as quadratic derivatives while the time appears as its first derivative.

Paul. A. M. Dirac [54] suggested instead an Hamiltonian with linear derivatives of both time and space, introducing the algebraic quantities $\boldsymbol{\alpha}$ and $\boldsymbol{\beta}$. The Dirac equation, in an external electromagnetic potential describes the relativistic motion of an electron as:

$$\left(\beta m_0 c^2 + e\phi + \boldsymbol{\alpha}.\boldsymbol{\pi} - ih\frac{\partial}{\partial t}\right)\psi = 0 \tag{2.70}$$

with

$$\boldsymbol{\pi} = \boldsymbol{p} + e\boldsymbol{A} \tag{2.71}$$

recalling :

$$\boldsymbol{p} \rightarrow p - q\boldsymbol{A}; E \rightarrow -q\phi \tag{2.72}$$

ϕ being the scalar potential and $\boldsymbol{A}$ the vector potential describing the magnetic field and q = -e for an electron and q = +e for a positon. $\boldsymbol{\alpha}$ retains the information about the spin of the particle. Both $\boldsymbol{\alpha}$ and $\boldsymbol{\beta}$ are 4 x 4 matrices defined as:

$$\alpha_x = \begin{pmatrix} 0 & 0 & 0 & 1 \\ 0 & 0 & 1 & 0 \\ 0 & 1 & 0 & 0 \\ 1 & 0 & 0 & 0 \end{pmatrix}, \alpha_y = \begin{pmatrix} 0 & 0 & 0 & -i \\ 0 & 0 & i & 0 \\ 0 & -i & 0 & 0 \\ i & 0 & 0 & 0 \end{pmatrix}, \alpha_z = \begin{pmatrix} 0 & 0 & 1 & 0 \\ 0 & 0 & 0 & -1 \\ 1 & 0 & 0 & 0 \\ 0 & 1 & 0 & 0 \end{pmatrix} \tag{2.73}$$

$$\beta = \begin{pmatrix} 1 & 0 & 0 & 0 \\ 0 & 1 & 0 & 0 \\ 0 & 0 & -1 & 0 \\ 0 & 0 & 0 & -1 \end{pmatrix} \tag{2.74}$$

This can be rewritten with the Pauli matrices, the zero 2 x 2 matrix 0_2 and the 2 x 2 Identity matrix 1_2:

$$\alpha_x = \begin{pmatrix} 0_2 & \sigma_x \\ \sigma_x & 0_2 \end{pmatrix}, \alpha_y = \begin{pmatrix} 0_2 & \sigma_y \\ \sigma_y & 0_2 \end{pmatrix}, \alpha_z = \begin{pmatrix} 0_2 & \sigma_z \\ \sigma_z & 0_2 \end{pmatrix} \tag{2.75}$$

$$\beta = \begin{pmatrix} 1_2 & 0_2 \\ 0_2 & -1_2 \end{pmatrix} \tag{2.76}$$

The Pauli matrices being:

$$\sigma_x = \begin{pmatrix} 0 & 1 \\ 1 & 0 \end{pmatrix}, \sigma_y = \begin{pmatrix} 0 & -i \\ i & 0 \end{pmatrix}, \sigma_z = \begin{pmatrix} 1 & 0 \\ 0 & -1 \end{pmatrix} \tag{2.77}$$

Since $\boldsymbol{\alpha}$ and $\boldsymbol{\beta}$ appears in the equation 2.70 as 4 x 4 matrices the wave function must be a four-component vector:

$$\psi(\boldsymbol{r}, t) = \begin{pmatrix} \psi_1(\boldsymbol{r}, t) \\ \psi_2(\boldsymbol{r}, t) \\ \psi_3(\boldsymbol{r}, t) \\ \psi_4(\boldsymbol{r}, t) \end{pmatrix} \tag{2.78}$$

Among the four components, two (one for the spin α and one for the β) are the large (L) ones and the other two are the small (S) components (also one for the spin α and one for the β) we can rewrite $\psi(\boldsymbol{r}$, t) as:

$$\psi(\boldsymbol{r}, t) = \begin{pmatrix} \psi^L(\boldsymbol{r}, t) \\ \psi^S(\boldsymbol{r}, t) \end{pmatrix} = \begin{pmatrix} \psi^L_\alpha(\boldsymbol{r}, t) \\ \psi^L_\beta(\boldsymbol{r}, t) \\ \psi^S_\alpha(\boldsymbol{r}, t) \\ \psi^S_\beta(\boldsymbol{r}, t) \end{pmatrix} \tag{2.79}$$

The solution of the time-independent Dirac equation for a free electron can then be found by solving the matrix equation:

$$\begin{pmatrix} mc^2 - E & c(\boldsymbol{\sigma}.\boldsymbol{p}) \\ c(\boldsymbol{\sigma}.\boldsymbol{p}) & -mc^2 - E \end{pmatrix} \begin{pmatrix} \psi^L \\ \psi^S \end{pmatrix} = 0 \tag{2.80}$$

leading to the four two-fold degenerate solutions, corresponding to the large and small components:

$$E^+ = +\sqrt{c^2p^2 + m^2c^4} \tag{2.81}$$

and

$$E^- = -\sqrt{c^2p^2 + m^2c^4} \tag{2.82}$$

indicating that an electron could occupy a positive or negative state. Since the physical meaning of the former states would be a problem, Dirac supposed all the negative states to be occupied [55], That so the electrons would not be able to occupy them

due to the Pauli principle. In the presence of a potential such as the nucleus (V = $e\phi = \frac{-Z}{r}$ see equation 2.71), two continuum of states appear, with one corresponding to electronic (positive) states and one for the negative solutions, and bound states in between the continuum.

In this formalism only the one electron equation can be exactly resolved, therefore, some approximations must be made to describe many-electrons systems.

2.4.2 Dirac-Coulomb-Breit Hamiltonian

While multiple electrons are present their motions are dependent from each other. Thus we introduce the many-electron Dirac-Coulomb-Breit Hamiltonian $\hat{H}^{DCB}$ as the sum of the Dirac one-electronic Hamiltonian and the two-electronic Breit correction term g^B_{ij}:

$$\hat{H}^{DCB} = \sum_{i=1}^{N} \hat{h}_i + \sum_{i<j} \hat{g}^B_{ij} \tag{2.83}$$

where

$$\hat{g}^B_{ij} = -\frac{1}{2r_{ij}} \left(\boldsymbol{\alpha}_i . \boldsymbol{\alpha}_j + \frac{(\boldsymbol{\alpha}_i . \boldsymbol{r}_{ij})(\boldsymbol{\alpha}_i . \boldsymbol{r}_{ij})}{r^2_{ij}} \right) \tag{2.84}$$

the first term in parenthesis being the Gaunt interaction [56] and the second the retarded effect important for long distance interactions [57, 58].

2.4.3 Dirac Equation approximations

Since working with the four-component framework can be expensive even for relatively small systems, simplifying the Dirac equation by keeping only two components, the large ones, could save a lot of computational effort. To do so, the large and small components must be separated. It can be done with the elimination of the small components or by decoupling the small and large components with a unitary transformation.

Small Components elimination

In a similar way than in equation 2.80, the time independent Dirac equation for one free electron can be written to take into account an external potential V (shifting by

-mc^2 to set the electronic solutions to zero):

$$\begin{pmatrix} V-E & c(\boldsymbol{\sigma}.\boldsymbol{p}) \\ c(\boldsymbol{\sigma}.\boldsymbol{p}) & V-2mc^2-E \end{pmatrix} \begin{pmatrix} \psi^L \\ \psi^S \end{pmatrix} = 0 \tag{2.85}$$

which is equivalent to resolve the two equations system:

$$\begin{aligned} c(\boldsymbol{\sigma}.\boldsymbol{p})\psi^S + V\psi^L &= E\psi^L \\ c(\boldsymbol{\sigma}.\boldsymbol{p})\psi^L + (V-2mc^2)\psi^S &= E\psi^S \end{aligned} \tag{2.86}$$

Thus it is possible to express ψ^S as a function of ψ^L:

$$\psi^S = K(E)\frac{\boldsymbol{\sigma}.\boldsymbol{p}}{2mc}\psi^L \tag{2.87}$$

with K(E) a local multiplicative operator that depends on the electron energy:

$$K(E) = \left(1 - \frac{V-E}{2mc^2}\right)^{-1} \tag{2.88}$$

By inserting equation 2.87 in the first equation 2.86 we obtained the 2-component equation:

$$\left(\frac{1}{2m}(\boldsymbol{\sigma}.\boldsymbol{p})K(E)(\boldsymbol{\sigma}.\boldsymbol{p}) + V\right)\psi^L = E\psi^L \tag{2.89}$$

This equation allows to retrieve the Schrödinger equation in the non-relativistic limit (c $\rightarrow \infty$ and K $\rightarrow$ 1).

Pauli Hamiltonian

The K(E) term can be expanded as a geometric series as:

$$K(E) = \sum_{k=0}^{\infty}\left(\frac{V-E}{2mc^2}\right)^k \tag{2.90}$$

The Pauli approximation is obtained by retaining the two first terms of the series:

$$K(E) \approx K^{Pauli}(E) = 1 + \frac{V-E}{2mc^2} \tag{2.91}$$

This expansion is only valid if

$$|V - E| << 2mc^2$$

but is not the case in the region close to the nucleus. As r $\rightarrow$ 0 and V = $\frac{-Z}{r} \rightarrow \infty$, making the condition | V - E | < < 2mc^2 not true. Away from the nucleus, K(E) can be expanded to the first order leading to the Pauli Hamiltonian $\hat{H}^{Pauli}$ [59, 60]:

$$\hat{H}^{Pauli} = \hat{T} + V - \frac{1}{8m^2c^2}\boldsymbol{p}^4 + \frac{\hbar^2}{8m^3c^2}(\nabla^2 V) + \frac{\hbar}{4m^2c^2}\boldsymbol{\sigma}.(\nabla V) \times \boldsymbol{p} \tag{2.92}$$

$\hat{T}$ being the kinetic energy operator, V remains the potential created by the nucleus ($-\frac{Ze^2}{r}$) the third term being the mass-speed correction term coming from the relativistic variation of the mass with the speed. The fourth term is a correction due to the fast oscillation of the electron around its mean position. It is also called the Darwin term. Finally the last term is the spin-orbit coupling.

Zeroth Order Relativistic Approximation Hamiltonian

To obtain an approximate Hamiltonian valid in all regions of space one can expanded K(E) differently as:

$$K(E) = \left[1 + \frac{E}{2mc^2 - V}\right]^{-1} = 1 - \frac{E}{2mc^2 - V} + \left[\frac{E}{2mc^2 - V}\right]^2 + ... \tag{2.93}$$

Thus, by keeping the zeroth order of expansion 2.93, we obtain the Zeroth Order Relativistic Approximation (ZORA) Hamiltonian:

$$\hat{H}^{ZORA} = V + (\boldsymbol{\sigma}.\boldsymbol{p})\frac{c^2}{2mc^2 - V}(\boldsymbol{\sigma}.\boldsymbol{p}) \tag{2.94}$$

Of course, this formulation retains the spin-orbit coupling in $\boldsymbol{\sigma}.\boldsymbol{p}$, it is easy to disregard this part to obtain the Scalar Relativistic (SR) ZORA Hamiltonian. In 1998, Christoph van Wüllen [61] showed that the scalar relativistic effects could be fully included in a kinetic operator $\hat{T}_{SR}^{ZORA}$:

$$\hat{T}_{SR}^{ZORA} = \boldsymbol{p}\frac{c^2}{2mc^2 - V}\boldsymbol{p} \tag{2.95}$$

This new operator is really useful when the SOC is small enough to be disregarded and allows to decrease the computational cost.

Decoupling small and large components with unitary transform: the Douglas-Kroll-Hess Hamiltonian

The Douglas-Kroll-Hess (DKH) [62, 63] Hamiltonian does not rely on the elimination of the small components as before but is derived from a unitary transformation U, acting on the Dirac-Coulomb Breit Hamiltonian $\hat{H}^{DCB}$, in order to obtain a diagonal Hamiltonian:

$$U^{\dagger}\hat{H}^{DCB}U = \begin{pmatrix} h_{+} & 0 \\ 0 & h_{-} \end{pmatrix} \tag{2.96}$$

with $U^{\dagger}U = 1$.

The first transformation in the DKH approximation is actually the Foldy Wouthuysen transformation [64] in a free particule case.

$$\hat{U}^{(0)} = \hat{A}_i(a + \beta\boldsymbol{\alpha}\boldsymbol{P}_i) \tag{2.97}$$

with

$$\hat{A}_i = \sqrt{\frac{\hat{E}_i + m_e c^2}{2\hat{E}_i}}; \boldsymbol{P}_i = \frac{c\boldsymbol{p}_i}{\hat{E}_i + m_e c^2} \tag{2.98}$$

with $\hat{E}_i$ the kinetic energy operator for the positive energy states, defined as:

$$\hat{E}_i = \sqrt{m_e^2 c^4 + p_i^2 c^2} \tag{2.99}$$

After this first transformation the resulting Hamiltonian matrix, $\hat{H}^{DKH1}$ is not diagonal but the coupling is already reduced. The potential $\hat{V}$ needs to be now added and the decomposition to be pushed one step further.

$$\hat{U}^{(1)} = \sqrt{1 + \hat{W}_1^2} + \hat{W}_1 \tag{2.100}$$

with

$$\hat{W}_1(i) = \hat{W}_1\phi(\boldsymbol{p}_i) = \int d^3p_j \hat{W}(\boldsymbol{p}_i, \boldsymbol{p}_j)\phi(\boldsymbol{p}_j) \tag{2.101}$$

where:

$$\hat{W}(\boldsymbol{p}_i, \boldsymbol{p}_j) = \int d^3p_j \hat{A}_i(\boldsymbol{\sigma}\boldsymbol{P}_i - \boldsymbol{\sigma}\boldsymbol{P}_j)\hat{A}_j \frac{\hat{V}(\boldsymbol{p}_i, \boldsymbol{p}_j)}{\hat{E}_i + \hat{E}_j}\phi(\boldsymbol{p}_j) \tag{2.102}$$

$\hat{V}(\boldsymbol{p}_i, \boldsymbol{p}_j)$ being the the Fourier transform of the potential energy and $\phi(p_i)$ the (bi-spinor) wave function associated to an electron having the momentum $\boldsymbol{p}_i$. The decoupled Hamiltonian for two particles is thus:

$$\hat{H}^{Decoupled} = \beta\hat{E}_i + \hat{A}_i(\hat{V} + \boldsymbol{\sigma P}_i\hat{V}\boldsymbol{\sigma P}_i)\hat{A}_i - \beta(\hat{W}_1\hat{E}_i\hat{W}_1 + \frac{1}{2}[\hat{W}_1^2, \hat{E}_i]_+) \tag{2.103}$$

Using the Dirac relation $((\boldsymbol{\sigma}.\boldsymbol{u})(\boldsymbol{\sigma}.\boldsymbol{v}) = \boldsymbol{u}.\boldsymbol{v} + \mathrm{i}\ \boldsymbol{\alpha}(\boldsymbol{u} \times \boldsymbol{v}))$, it is possible to separate the terms spin-independent to the spin-dependent leading to the $\hat{H}^{SF}$ and $\hat{H}^{SO}$, respectively.

$$\hat{H}^{SF} = \sum_i \hat{E}_i + \sum_i \hat{V}_{eff}^{SF}(i) + \sum_{i<j} \frac{1}{r_{ij}} \tag{2.104}$$

with

$$\begin{aligned} \hat{V}_{eff}^{SF}(i) &= -\hat{A}_i[V(i) + \boldsymbol{P}_i V(i)\boldsymbol{P}_i]\hat{A}_i - \hat{W}_1(i)\hat{E}_i\hat{W}_1(i) - \frac{1}{2}[\hat{W}_1^2(i), \hat{E}_i] \\ V(i) &= \sum_\alpha \frac{Z_\alpha}{r_{i\alpha}} \end{aligned} \tag{2.105}$$

and $\hat{H}^{SO}$:

$$\begin{aligned} \hat{H}^{SO} =& \alpha\hbar c\Bigg\{ \sum_i \sum_a Z_a \frac{\hat{A}_i}{\hat{E}_i + m_e c^2}\boldsymbol{\sigma}_i(\frac{\boldsymbol{r}_{ia}}{r_{ia}^3} \times \boldsymbol{p}_i)\frac{\hat{A}_i}{\hat{E}_i + m_e c^2} \\ &- \sum_{i\neq j} \frac{\hat{A}_i\hat{A}_j}{\hat{E}_i + m_e c^2}.(\boldsymbol{\sigma}_i\frac{\boldsymbol{r}_{ij}}{r_{ij}^3} \times \boldsymbol{p}_i)\frac{\hat{A}_i\hat{A}_j}{\hat{E}_i + m_e c^2} - 2\boldsymbol{\sigma}_i(\frac{\boldsymbol{r}_{ij}}{r_{ij}^3} \times \boldsymbol{p}_i)\frac{\hat{A}_i\hat{A}_j}{\hat{E}_i + m_e c^2}\Bigg\} \end{aligned} \tag{2.106}$$

This SO Hamiltonian is the sum of one-electron and two-electrons terms. The matrix elements of the SO operator are still expensive to calculate. A solution is to approximate this Hamiltonian. The Atomic Mean Field Approximation (AMFI) is used to reduce the number of integrals to calculate using a "simple" idea since the SO interaction is short range as it behaves (as $\frac{1}{r^3}$), it is relevant to disregard all multi-center two-electron SO integrals [65]. For a balanced treatment of SO effects, it is also appropriate to only include one-center one-electron SO integrals.

To simplify the SO Hamiltonian in a context of CI-SO coupling, Hess *et al.*[65] showed that the doubly excited determinants SO contributions can be negligible if the matrix elements of the SO operator between two Slater determinant that differ from only one single-excitation (from the spin orbital i to the spin orbital j) are modified

in a way that defines the effective mean field one-electronic operator as:

$$\hat{H}_{ij}^{SO} = \langle\phi_i(1)|\,\hat{h}^{SO}(1)\,|\phi_j(2)\rangle + \frac{1}{2}\sum_k n_k \Big\{ \langle\phi_i(1)|\,\widetilde{H}_{kk}^{SO}(1)\,|\phi_j(1)\rangle - \langle\phi_i(1)|\,\widetilde{H}_{kj}^{SO}(1)\,|\phi_k(1)\rangle - \langle\phi_k(1)|\,\widetilde{H}_{ik}^{SO}(1)\,|\phi_j(1)\rangle \Big\} \tag{2.107}$$

with

$$\langle\phi_i(1)|\,\widetilde{H}_{kk}^{SO}(1)\,|\phi_j(1)\rangle = \langle\phi_i(1)[\phi_k(2)|\,\widetilde{H}_{1,2}^{SO}\,|\phi_k(2)]\phi_j(1)\rangle \tag{2.108}$$

$$\langle\phi_i(1)|\,\widetilde{H}_{kj}^{SO}(1)\,|\phi_k(1)\rangle = \langle\phi_i(1)[\phi_k(2)|\,\widetilde{H}_{1,2}^{SO}\,|\phi_j(2)]\phi_k(1)\rangle \tag{2.109}$$

$$\langle\phi_k(1)|\,\widetilde{H}_{ik}^{SO}(1)\,|\phi_j(1)\rangle = \langle\phi_k(1)[\phi_i(2)|\,\widetilde{H}_{1,2}^{SO}\,|\phi_k(2)]\phi_j(1)\rangle \tag{2.110}$$

and :

$$\hat{h}^{SO}(1) = \alpha\hbar c\Big\{ \sum_a Z_\alpha \frac{\hat{A}_1}{\hat{E}_1 + m_e c^2}\boldsymbol{\sigma}_1\Big(\frac{\boldsymbol{r}_{1a}}{r_{1a}^3}\times\boldsymbol{p}_1\Big)\frac{\hat{A}_1}{\hat{E}_1 + m_e c^2}\Big\} \tag{2.111}$$

$$\widetilde{H}_{1,2}^{SO} = \alpha\hbar c\Big\{ \frac{\hat{A}_1\hat{A}_2}{\hat{E}_1 + m_e c^2}.\Big(\boldsymbol{\sigma}_1\frac{\boldsymbol{r}_{12}}{r_{12}^3}\times\boldsymbol{p}_1\Big)\frac{\hat{A}_1\hat{A}_2}{\hat{E}_1 + m_e c^2} - 2\boldsymbol{\sigma}_1\Big(\frac{\boldsymbol{r}_{12}}{r_{12}^3}\times\boldsymbol{p}_1\Big)\frac{\hat{A}_1\hat{A}_2}{\hat{E}_1 + m_e c^2}\Big\} \tag{2.112}$$

n_k is the occupation of spin-orbital k, ϕ_i an occupied and ϕ_j a virtual orbital. Since equation 2.107 describes the valence electrons in a field created by the electrons in the orbitals k $\neq$ i, n_k and ϕ_k must have a physical meaning. For this reason, the AMFI module must be used with atomic natural orbitals such as the relativistic contracted ANO-RCC basis sets (see Section 2.5.1).

2.4.4 Relativistic Effective Core Potential

In chemistry, many molecule's properties involve the valence electrons and eventually the sub-valence shells. It is then possible to speed up the calculation by replacing the core electrons by an effective core potential (ECP) [66]. Since the number of electrons is smaller and the number of functional basis can be reduced, the calculation becomes less expensive. The second advantage of ECP is its convenience because it can be used with DFT and wave function methods. The Hamiltonian is reduced to the sum of the interaction between the valence electrons and the interaction of the former with the nucleus/core electrons and called the valence Hamiltonian $\hat{H}^v$:

$$\hat{H}^v = \sum_i^{n_{valence}} -\frac{1}{2}\hat{\nabla}_i^2 + \sum_{i<j}^{n_{valence}} \frac{1}{r_{ij}} + \sum_i^{n_{valence}}\sum_I^N V_{cv}^I(i) + \sum_{I<J}^N \frac{Q_I Q_J}{R_{IJ}} + V_{CPP} \tag{2.113}$$

The first term is the kinetic energy of the valence electrons. The second is the interaction between the valence electrons, the third one is the interaction between the electron/nuclei and valence electrons. The fourth term is the repulsion between effective cores. The last term is the core polarisation potential (CPP). V_{cv} in equation 2.113 is parametrised to include not only to the scalar relativistic effects but also the spin-orbit relativistic effects so it is adjusted to reproduce data with great accuracy.

$$V_{cv}^{I}(i) = \sum_{i}^{n_{valence}} \frac{Q_I}{r_{iI}} + \sum_{i}^{n_{valence}} V_{PP}^{I}(i) \tag{2.114}$$

The name of the ECP is given under the form ECPnXY where usually XY represents the level of the fully relativistic method used to generate the target all-electron data to which the ECP parameters are adjusted: MWB for multi-configurational Wood-Boring or MDF for multi-configuration Dirac-Fock [67].

2.5 Basis Sets, Basis Sets Superposition Error and Complete Basis Set Extrapolation

2.5.1 Basis Sets

Back to equation 2.10, the wave-function is described by a Slater determinant composed of orthonormal spin-orbitals. In a molecule, each spin-orbital represents a molecular orbital (MO) ϕ_i which can be represented by a Linear Combination of Atomic Orbitals (LCAO) [68], χ_k.

$$\phi_i = \sum_{j}^{N_{AO}} c_{ij}\psi_i = \sum_{j}^{N_{AO}} c_{ij} \sum_{k}^{Nb} d_{jk}\chi_k \tag{2.115}$$

d_{jk} being the expansion coefficients, χ_k the atomic basis functions, and Nb the number of the basis function used. A minimum basis set contains roughly[4] as much basis function as there are atomic orbitals.

The only restriction for mathematical functions to be used as basis functions is to decay to zero as the distance between the nuclei and the electron increases. In practice, two families of orbitals are used: the Slater Type Orbitals (STO) [69] and the Gaussian Type Orbitals (GTO) [70] both products of a radial part $\mathcal{R}_l(r)$ and a spherical harmonic function $Y_{lm_l}(\theta\phi)$.

[4] sometimes extra orbitals are added for polarization

- Slater Type Orbitals

Slater-type orbitals, the radial part only depends on n as

$$\mathcal{R}_n = N_{Slater} r^{n-1} e^{-\zeta r} \tag{2.116}$$

n being the principal quantum number, N_{Slater} the normalisation constant, r is the distance between the electron and the nucleus and ζ a constant related to the effective charge of the nucleus Z^* such that the energy level of this orbital equals to

$$E_n = \frac{1}{2}\left(\frac{Z^*}{n}\right)^2 \tag{2.117}$$

STO basis are successful for atoms as they describe the cusp at the nucleus. However, their limitation is that two-electrons integrals involving 3 or 4 centres cannot be computed analytically.

- Gaussian Type Orbitals

To overcome the integration issue, GTO (Gaussian Type Orbitals) were introduced defined as:

$$\mathcal{R}_n = N_6(\alpha) r^{n-1} e^{-\alpha r^2} \tag{2.118}$$

for their radial part. If the GTOs allow the calculations to be performed faster, the r^2 dependency alter the description of the electron behaviour near the nucleus [10]. Therefore a larger basis will be needed to reach the same accuracy as with an STO.

Linear combinations (contractions) of primitive GTOs functions are able to approximate the nodal structures of atomic orbitals (AO). The quality of a basis set is linked to the number of Gaussian primitives and to the optimisation of the contraction coefficients.

In the current work, we aim at computing reaction energies with an accuracy of a few kJ.mol^{-1}. Thus the choice of the atomic basis set is crucial. In all the PhD projects, basis sets of at least triple-ζ quality were used to determine the optimal geometries, using correlation consistent Dunning's basis sets [71, 72], aug-cc-pVTZ/aug-cc-pVQZ, and the proper small-core RECP basis sets for the heavy elements. For the largest molecular complexes (See Chapter 3), efficient computational speed up was achieved with the resolution of the identity algorithm, using Ahlrichs def2-TZVP basis sets and their auxiliary counterparts [73, 74]. Note that for heavy elements, the def2-basis sets are bound to small-core RECPs.

To reach chemical accuracy (or higher) for thermodynamics properties of plutonium gas-phase molecules, the electronic energies were extrapolated to the complete basis set limit, from calculations with the extended all-electron atomic natural orbital relativistic correlation consistent (ANO-RCC) Roos's basis sets [75–77], which offer from triple to quadruple-ζ quality expansions in the Douglas-Kroll-Hess relativistic framework [78].

We will comment on the choice of the basis sets in the appropriate introductory sections of each research project.

2.5.2 Basis Sets Superposition Error

The Basis Sets Superposition Error (BSSE) introduced by Boys and Bernardi [79] occurs when 2 atoms (A and B) are close to each other. The basis set of the atom A will be superposed with the basis set of the atom B describing twice the same stabilising energy. Thus, the total energy is lower than what it should be and must be corrected.

$$E_{corrected} = E_{uncorrected} + E_{BSSE} \tag{2.119}$$

In order to compute the corrected total energy, the energy of atom A has to be calculated in the presence of the basis of the atom B and the energy of atom B in the presence of the basis of the atom A.

$$E_{BSSE} = E_A^A - E_A^{AB} + E_B^B - E_B^{AB} \tag{2.120}$$

where the superscripts refers to the basis set used and the subscripts the atom.

2.5.3 Complete Basis Set Extrapolation

A way to avoid BSSE, among others, is to extrapolate the energy to the Complete Basis Set (CBS) limit *i.e.* to approach the results with infinite basis sets (see Figure 2.2).

In this work we compared two ways of extrapolating energies, one by extrapolating the total energy, the second by extrapolating separately the SCF energy and the correlated energy before summing the two.

FIGURE 2.2: Theoretical convergence to the complete basis set limite with increasing the number of basis functions

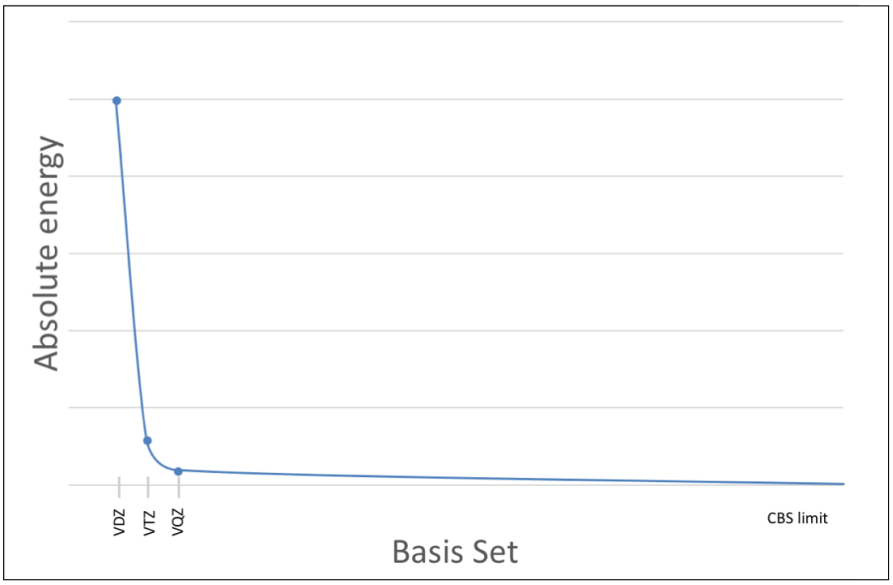

The total energy CBS value can be derived from a two-points extrapolation formula [80]:

$$E_{XY}^{CBS} = \frac{X^3 E_X - Y^3 E_Y}{X^3 - Y^3} \tag{2.121}$$

where X and Y are the size of the basis sets (typically n=3 and n=4 for triple and quadruple-ζ basis sets).

Peterson *et. al.* [81] proposed specific formulas for the uncorrelated energy E_{CBS}^{SCF} and the correlated energy E_{CBS}^{Corr} extrapolations:

$$E_n^{SCF} = E_{CBS}^{SCF} + A(n+1)e^{-6.57\sqrt{n}} \tag{2.122}$$

$$E_n^{corr} = E_{CBS}^{corr} + \frac{B}{(n+\frac{1}{2})^4} \tag{2.123}$$

In these formulas n is the size of the basis set (typically n=3 and n=4 for triple and quadruple-ζ basis sets), E^{SCF} is either the SCF or CASSCF energy and E^{corr} the correlation part of the total energy.

2.6 Conclusion

As mentioned before, only a few and basic methods of Quantum Chemistry were depicted here. Nonetheless, it already triggers some general questions at the heart of the modelling of Actinides.
How to properly describe the relativistic effects ?
How the retrieve electronic correlation ?
If the first question is almost answered in the present section, the former question will be addressed more particularly in the Chapter 4. Indeed, a good way to describe the static correlation is to use methods including multiple Slater determinants in the wave function. These methods are called "multi-reference" quantum chemical methods.

Chapter 3

Coordination of Alkyl cations $[(XA_2)X(CH_2SiMe_3)]$ (X = Th, U) or$[(XN_2)Zr(CH_3)]$ with an arene for Ethylene polymerisation: Exploration of the bonding

3.1 Introduction

The amount of polyethylene produced every year implies a constant need for improving the industrial production process. Since the pioneering process by Karl Ziegler and Giulio Natta in the early 1950's on the polymerisation of simple olefins, there had been intense interest in the application of early transition metal catalysts for the selective polymerisation of inexpensive olefins. Following to Ziegler-Natta catalysts [82] , metallocene catalysts were discovered in the late 1980's and resulted in numerous industrial processes for improving the properties of polyolefinic materials along with performance parameters. In particular, beside the requirement of higher activity, research have focused on the control of particle size, particle size distribution, and the morphology of the resultant polyolefin (number of carbon in the chain). In the metallocene family, group 4 transition metal metallocene complexes have the largest activity, such as $[Cp_2ZrMe][B(C_6F_4TBS)_4]$ synthesised by Marks and co-workers [83–91] 1.1 x 10^7g of polyethylene.(mol of M=Zr)$^{-1}$.h^{-1}.atm^{-1}[92]). The brother complex with Th was also synthesised but is an order of magnitude less active than the Zr-complex (9.2 x 10^5g of polyethylene.(mol of Th)$^{-1}$.h^{-1}.atm^{-1}), suggesting that the nature of the metallic centre may play a key role in the catalytic

activity. In the 1990s, new catalysts with well-defined metal complexes and other ligand motifs were summarised as the "post metallocenes" family [93].

During my first-year PhD stay at Mc Master University in Hamilton (Ontario, Canada), discussions were initiated with David Emslie's research group, currently working on the synthesis of cationic metal alkyl complexes, that are open post-metallocene catalysts of electropositive metals. These are typically generated by reaction of a neutral dialkyl complex with strong electrophiles such as $[CPh_3][B(C_6F_5)_4]$, $[HNMe_2Ph][B(C_6F_5)_4]$, $B(C_6F_5)_3$ or $(Al(CH_3)xOy)n$ (Methylaluminoxane-MAO). The subsequent polymerisation is achieved by repeated ethylene coordination and 1,2-insertion steps [1]. These activation and polymerization reactions are commonly conducted in arene or alkane solvents; the former is standard in academic laboratories [2], while the latter is favoured in industry [3, 94]. However, in sterically open post-metallocene catalysts of electropositive metals, arene solvents have significant potential to coordinate, negatively impacting ethylene polymerisation activity. At the same time arene coordination is known to increase the thermal stability of metal alkyl cations prior to exposure to ethylene, which is of key importance for industrial polymerisation processes often conducted at elevated temperatures (140 °C). Therefore, Emslie's group has explored, in a systematic fashion, the suitability of tetravalent actinides, namely Thorium and Uranium, to create thermally robust and highly reactive cationic monoalkyl derivatives, as an alternative to the Zirconium based ones.

The chapter begins with a review of all the Zr, Th, and U complexes that were synthesised and crystallised when possible for structural characterisation. We will also present the evaluated ethylene polymerisation activities at room and elevated (70-80 °C) temperatures. The experimental work scanned several arene solvents, from benzene, toluene, to halogenated derivatives of benzene (bromo-benzene, fluorobenzene and di fluorobenzene), with different electron donor capabilities, noting for example that Hayes *et al.* showed a good activity for a scandium complex in Bromobenzene [95, 96]. In an attempt to link the catalytic properties with the complexes structures and coordination, the second part will present the quantum chemical calculations that allow an in-depth discussion of the influence of the cation and the impact of arene solvent coordination. We finally investigate the strength of the interaction between cationic metal alkyl complex with ethylene to shed some light on the competition between ethylene and arene coordination in the initial steps of the catalytic reaction.

3.2 Systems presentation and theoretical studies

3.2.1 Catalysts synthesis strategy, structures and catalytic power

Using a neutral dialkyl **1-X** (X = Th, U or Zr) the arene-coordinated alkyl cations could be derived, where the arene (benzene, toluene, bromo-benzene, fluorobenzene or the (o)-difluoro-benzene) is introduced by the solvent. The catalytic power and the robustness of the compounds were tested by exposing them to ethylene during 30 min at temperatures between 20 and 70 °C (80 °C for **n-Zr**). It is important to note that early transition metal and f-element olefin polymerisation catalysts are frequently generated *in situ* without isolation and characterisation, this lack of information is the main source of uncertainties in the mechanism.

TABLE 3.1: Name of the different ligands, counter ion and arene of the compounds discussed in this Chapter

	Formula	Name
Ligands	XA_2	4,5-bis(2,6-diisopropylanido)-2,7-di-tert-butyl-9,9-dimethylxanthene
Ligands	XN_2	4,5-bis(2,4,6-triisopropylanido)-2,7-di-tert-butyl-9,9-dimethylxanthene
	CH_2SiMe_3	(trimethylsilyl)methyl
Counter ion	$B(C_6F_5)_4^-$	diskal tetrakis(pentafluorophenyl)borate
Arene	C_6H_6	Benzene
	$C_6H_5CH_3$	Toluene
	C_6H_5Br	Bromobenzene
	C_6H_5F	Fluorobenzene
	$C_6H_5F_2$	Difluorobenzene
	C_2H_2	Ethylene

The different metallic centres are chosen first because the literature reports their efficiency (see Section 3.1) and because of their electronic structure in the tetravalent oxidation state. Zr(IV) is a $4d^0$-element with the smallest ionic radius, while Th(IV) is a $5f^0$-element and U(IV) a $5f^2$-element with larger ionic radii (see Table 3.3). In the actinides, while the 5f-orbitals are expected to participate into the bonding, the 6d-orbitals in U(IV) complexes may also play a role in the bonding, allowing back donation electron transfer [97].

The choice of the arene is made in order to tune the donating capacity. This donating power is directly connected to the strength of the cation arene bond. If too strong it could hinder or even shutter ethylene coordination and impact the catalytic activity (see Section 3.2.2).

We start the a survey on Emslie's work with the cation derivatives of the neutral dialkyl **1-Th**. **2-Th**, **3-Th** and **5-Th** cations [99–102]. All of them could be synthesised but only **2-Th** could be characterised with X-ray diffraction (see Figure 3.1). Unfortunately only **5-Th** exhibits a catalytic power but it is not thermally robust (see Table

TABLE 3.2: Numbers and Formula of the different compounds of the present Chapter

Number	Formula	X-ray structure
1-U	$[(XA_2)U(CH_2SiMe_3)_2]$	yes
2-U	$[(XA_2)U(CH_2SiMe_3)(C_6H_6)]^+[B(C_6F_5)_4]^-$	yes
3-U	$[(XA_2)U(CH_2SiMe_3)(C_6H_5CH_3)]^+[B(C_6F_5)_4]^-$	yes
4-U	$[(XA_2)U(CH_2SiMe_3)(C_6H_5Br)]^+[B(C_6F_5)_4]^-$	no
5-U	$[(XA_2)U(CH_2SiMe_3)(C_6H_5F)]^+[B(C_6F_5)_4]^-$	yes
6-U	$[(XA_2)U(CH_2SiMe_3)(C_6H_4F_2)]^+[B(C_6F_5)_4]^-$	no
E-U	$[(XA_2)U(CH_2SiMe_3)(C_2H_2)]^+[B(C_6F_5)_4]^-$	not synthesised
1-Th	$[(XA_2)Th(CH_2SiMe_3)_2]$	no
2-Th	$[(XA_2)Th(CH_2SiMe_3)(C_6H_6)]^+[B(C_6F_5)_4]^-$	yes
3-Th	$[(XA_2)Th(CH_2SiMe_3)(C_6H_5CH_3)]^+[B(C_6F_5)_4]^-$	no
4-Th	$[(XA_2)Th(CH_2SiMe_3)(C_6H_5Br)]^+[B(C_6F_5)_4]^-$	not synthesised
5-Th	$[(XA_2)Th(CH_2SiMe_3)(C_6H_5F)]^+[B(C_6F_5)_4]^-$	no
6-Th	$[(XA_2)Th(CH_2SiMe_3)(C_6H_4F_2)]^+[B(C_6F_5)_4]^-$	not synthesised
2'-Th	$[(XN_2)Th(CH_3)(C_6H_6)]^+[B(C_6F_5)_4]^-$	not synthesised
E-Th	$[(XA_2)Th(CH_2SiMe_3)(C_2H_2)]^+[B(C_6F_5)_4]^-$	not synthesised
2-Zr	$[(XA_2)Zr(CH_2SiMe_3)((C_6H_5CH_3))]^+[B(C_6F_5)_4]^-$	not synthesised
2'-Zr	$[(XN_2)Zr(CH_3)(C_6H_6)]^+[B(C_6F_5)_4]^-$	no
3'-Zr	$[(XN_2)Zr(CH_3)(C_6H_5CH_3)]^+[B(C_6F_5)_4]^-$	yes
4'-Zr	$[(XN_2)Zr(CH_3)\ (C_6H_5Br)]^+[B(C_6F_5)_4]^-$	no
5'-Zr	$[(XN_2)Zr(CH_3)\ (C_6H_5F)]^+[B(C_6F_5)_4]^-$	not synthesised
6'-Zr	$[(XN_2)Zr(CH_3)\ (C_6H_4F_2)]^+[B(C_6F_5)_4]^-$	not synthesised
E'-Zr	$[((XN_2)Zr(CH_3)(C_2H_2)]^+[B(C_6F_5)_4]^-$	not synthesised

TABLE 3.3: Ionic Radii of metallic center in Å from [98]

Element	Ionic Radius
Zr	0.72
Th	0.94
U	0.89

3.5). **4-Th** could not be synthesised and no attempt was made for the generation of **6-Th**.

The benzene **2-U** and toluene **3-U** derivatives of **1-U**, are more soluble than their thorium equivalents [103–107]. Thus it could be crystallised to obtain a deep brown solids (see Figures 3.2 and 3.3 for structure). The distances are, as expected from the ionic radii, shorter in the uranium complexes than in the thorium ones (see Table 3.4). **4-U** (bromobenzene) was readily obtained but not structurally characterised

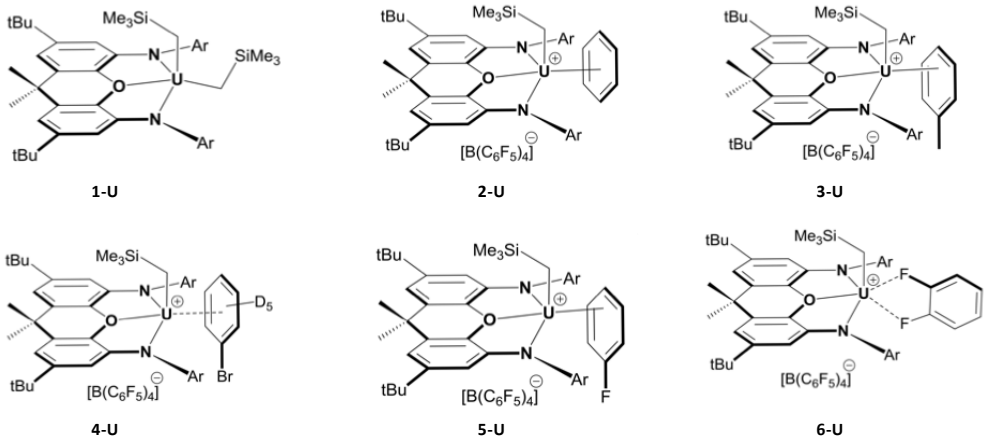

FIGURE 3.1: Structures of the catalysts containing uranium, thorium ones are strictly equivalent.

and catalytically silent.

TABLE 3.4: Important bond lengths in Å and angles in degree for the neutral **1-U** and the cationic **2-U**, **2-Th**, **3-U**, **3'-Zr** and **5-U** given by X-ray diffraction [108].

Compounds	**1-U**	**2-U**	**2-Th**
An-O	2.484(5), 2.504(4)	2.441(2)	2.496(5)
An-N	2.261(5), 2.262(5), 2.272(5), 2.280(5)	2.224(2), 2.236(6)	2.278(3), 2.288(3)
An-C_{arene}	–	3.099(3) - 3.248(3)	3.18 - 3.31
$N_1 \ldots N_2$	4.00, 4.02	3.94	4.04
Arene Bend Angle [1]	17.5, 18.8	18.9	8.7
O-An-C_{apical}	94.8(2),95.0(2)	87.26(8)	91.3(1)
An-C-Si	128.2(3), 130.4(3), 130.5(4), 130.8(3)	133.7(2)	131.0(2)

Compounds	**3-U**	**3'-Zr**	**5-U**
An-O	2.417(9)	2.220	2.431(3)
An-N	2.21(1), 2.22(1)	2.138; 2.122	2.215(3), 2.218(3)
An-C_{arene}	3.05(2) - 3.78(2)	2.697 - 2.840	3.129(5) - 3.598(6)
$N_1 \ldots N_2$	3.98	3.91	3.98
Arene Bend Angle[1]	5.9		7.2
O-An-C_{apical}	88.8(4)		89.6(1)
An-C-Si	136.8(7)	–	134.8(2)

[1] Angle between the carbons of the arene and the planar ligand.

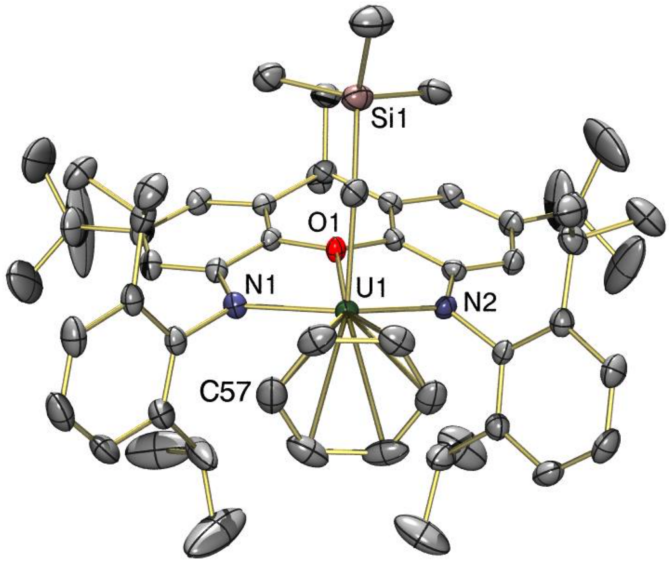

FIGURE 3.2: X-ray crystal structure of η^6**-2-U** [108]. Hydrogen atoms are not represented

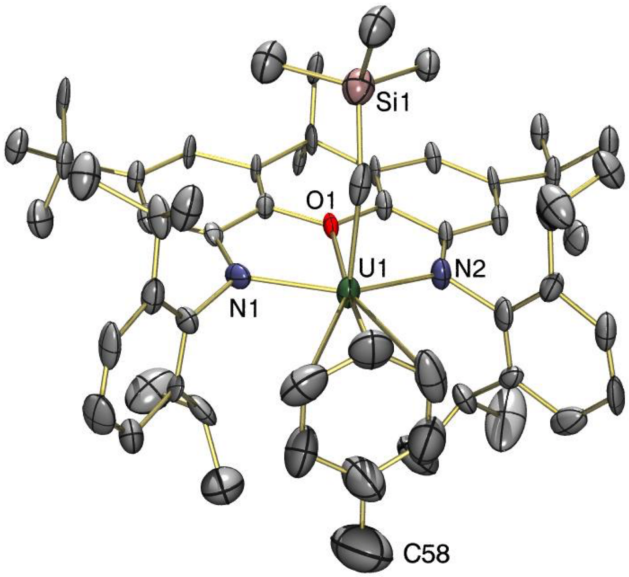

FIGURE 3.3: X-ray crystal structure of η^6**-3-U** [108]. Hydrogen atoms are not represented

Bromobenzene was then exchanged (conceptually) with fluorobenzene to have an expected less donating ligand character, leading to **5-U** which could be X-ray analysed (see Figure 3.4). This makes it the first 5*f*-element complex bearing a π-coordinated

fluoroarene ligand crystallographically characterised. Table 3.4 shows a ressemblance between **5-U** and **3-U** with the same distance N_1-$_2$ (3.98 Å) and the smallest arene bend angle (7.2 °and 5.9°, respectively).

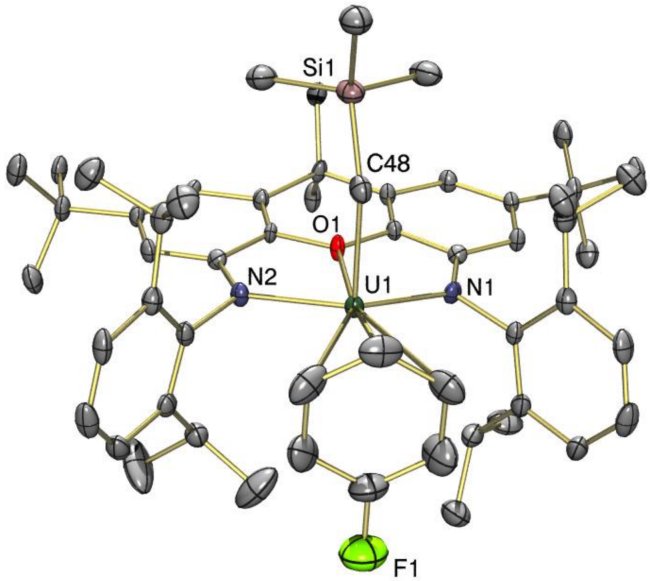

FIGURE 3.4: X-ray crystal structure of η^6**-5-U** [108]. Hydrogen atoms are not represented

In order to further decrease the coordination between arene and the uranium mettalic center, the cation with *o*-difluorobenzene was synthesised but could not be crystallised.

The activity of **5-U** is slightly larger than **6-U**, 1.12 x 10^4g of polyethylene.(mol of U)$^{-1}$.h^{-1}.atm^{-1} at 20 °C (see Table 3.5). However, at higher temperature (70 °C) no polymerisation is observed, indicating that **6-U** has a reduced thermal stability. An attempt was made to use the *m*-difluorobenzene, unfortunately no polyethylene was formed after 30 minutes at 20 °C.

At the same time, close equivalents were synthesised with a zirconium center [109].

2'-Zr polymerises so slowly that its activity is negligible. **3'-Zr** presents excellent performance with an activity of 2.73 x 10^5g.mol $^{-1}$.h^{-1}.atm^{-1} observed after 30 minutes at 20 °C and 1.11 x 10^5g.mol $^{-1}$.h^{-1}.atm^{-1} observed after 30 minutes at 80 °C. The decrease of the activity as the temperature increases can probably be explained by the decomposition of the catalyst. **4'-Zr** could be obtained (see Figure 3.6) and presents an activity close to that of **3'-Zr**. Its structure could not be resolved since

TABLE 3.5: Activities of complexes at and 1 atm in g of polyethylene.(mol of X=Th, U or Zr)$^{-1}$.h^{-1}.atm^{-1} and after 30 min of ethylene exposure.

Complex	Activity (20°C)	Activity (70°C)[1]
2-U	0	0
3-U	0	0
4-U	0	0
5-U	12 800	39 200
6-U	11 200	0
2-Th	0	0
3-Th	0	0
5-Th	16 800	57 600
2′-Zr	NA	NA
3′-Zr	273 000	113 000
4′-Zr	52 200	NA

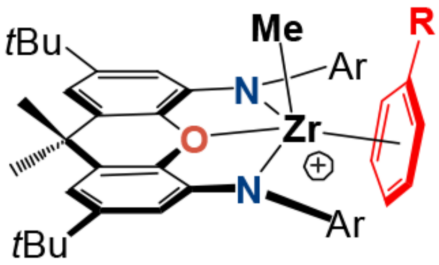

FIGURE 3.5: Structures of the compounds containing zirconium, with R = H, CH_3, F, Br .

the synthesis leads to a mixture of two isomers (see Figure 3.6). There is no report of synthesis concerning **5′-Zr** or **6′-Zr** yet.

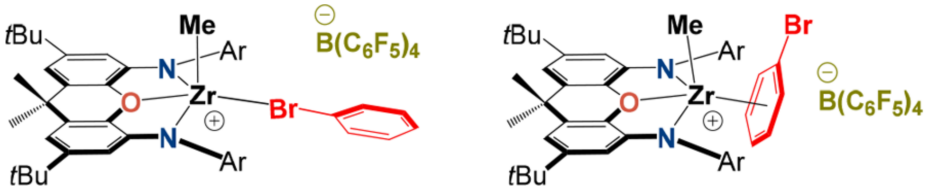

FIGURE 3.6: Possible structures of **4′-Zr** [109]

3.2.2 Finding the catalytic mechanism

The rationalisation of the catalytic mechanism is not easy since several hypotheses can be put forward:

- First, is it a concerted mechanism like in Figure 3.7 where both arene and ethylene are bonded at the same time to the metallic center or not ?
- If not, the relative bonding strengths of ethylene versus arene with the metal will be important. If the arene-metal bond is too strong, the ethylene will not be able to insert itself and the catalysis will not occur.

The success of the zirconium complexes over the actinides ones raises the question on the nature of the arene bonds to the metals. Having the smallest ionic radius Zr could be expected to form stronger bonds than the Th and U, contradicting the observed efficiency.

Gardner *et al.* [110] reported a larger catalytic power for Th complexes ([Th{N(CH_2CH_2 $NSiPri_3$)$_2$($CH_2CH_2NSiPri_2C$[H]$MeCH_2$)}]) than for the U ones (as for **5-U** and **5-Th**), and proposed as an explanation that electrostatic interactions are dominant in Th-complexes making the Th-ligand bond reacting more easily than the U-ligand one. Conversely, Domeshek *et al.* [111], in their complexes bis(N,N'-bis(trimethylsilyl)-2-pyridylami-dinate)An(μ-Cl)$_2$Li(TMEDA) (An = Th, U) found that U-complexes are more efficient than the Th ones. They proposed three explanations. The first is that the $5f^2$ electrons of uranium can participate to a back-donation leading to an improved coordination to the olefin facilitating the activation of the double bond. The second is that the thorium complexes form stronger bonds with the arene making the insertion of ethylene harder. Another explanation is that the 5f orbitals in the U complex could stabilise the 4-member transition state (Figure 3.7), thus facilitating the catalysis [112].

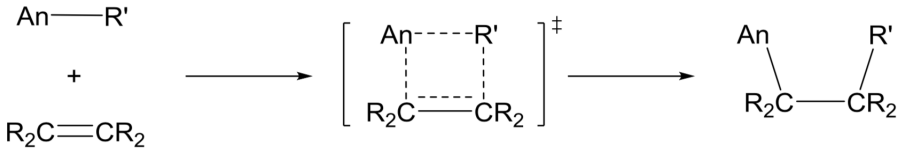

FIGURE 3.7: Four-center transition state in neutral organoactinide-mediated transformation where R' is the arene [108]

The last explanation appears as the simplest, as the larger size of Th(IV) might make it sterically more accessible than the U(IV) .

Of course, the true explanation can be a mixture of these hypothesis calling for a theoretical study of the systems to rationalise their catalytic activities and the mechanism of polymerisation by answering the following questions:

- Why do Zr complexes present such short bonds between the arene and the metal?
- What is the dominant nature of the bonding (electrostatic, covalent?...)?
- What is the participation of d and f orbitals into the bonding?
- What is the strength of the ethylene-metal versus the arene-metal bond?

3.2.3 Theoretical Studies of the Th, U and Zr cationic complexes

The theoretical studies of the complexes cited in the previous section are very limited. One theoretical study explored the catalysis reaction path [110]. It includes a full geometry optimisation followed by an anharmonic frequency calculation with the B3PW91 [113, 114] functional. Scalar relativistic effects were included by the Stuttgart-Dresden RECP [115, 116] and the corresponding basis sets. These articles emphasised the important role of the 5f-orbitals of thorium [110] and uranium [110, 117].

This study confirm that the explanations proposed by experimentalists such as electrostatic interaction, back-donation and strength of the bonds must be tested and assessed by an in-depth exploration of the bond between the various metallic centre and the arene solvents. In this context, we have used the ETS-NOCV bonding analysis [118, 119] that has been proven useful to elucidate the nature of the bonding interaction in multiple transition metal complexes [97, 120–129].

We start by optimising the structures of the complexes and compare the computed geometries to X-ray data, when available. Ultimately our results should address the previous and the following questions:

- How well do quantum chemistry structures agree with X-ray data?
- Is it possible to predict the geometries of the uncrystallised complexes?
- What are the driving forces of the cation interactions? How do they relate to the catalytic activity?

3.3 Optimisation of the Arene-Coordinated Uranium, Thorium or Zirconium Alkyl Cations

The complexes were optimised at the DFT level with the TURBOMOLE package [130]. Def-TZVP with RECP [131] was used for U, Th and Zr, and def2-TZVP basis

set [73] for all the other atoms. The resolution of identity for the Coulomb integrals was used to reduce the computational cost. We first considered the pure GGA PBE functional but it was not satisfying. Indeed in the η^6**-2-U** and η^6**-2-Th** benzene complexes, the benzene ended up being tilted in the optimised structured deviating from its expected orientation observed in the crystal. The hybrid PBE0 [45] functional previously reported good geometrical agreement with the experimental data for Actinides containing molecules [132] . In our case PBE0 brought the theoretical structure in excellent agreement with the experimental one. All the geometries provided by Emslie's team are available in Appendix A. The inclusion of the solvent effect with the COSMO continuum solvent model marginally affected the geometries while significantly increasing the computational time. This lead us to consider only gas-phase optimised geometries.

3.3.1 Optimisation of Benzene-Coordinated Alkyl Cations

For η^6**-2-Th** and η^6**-2-U**, X-ray structures were available and were used as starting points (see Table 3.2). For the **2'-Zr** no X-ray structure was available. Thus the X-ray structure of η^6**-3'-Zr** was used by substituting the methyl group of toluene by a hydrogen atom. As a complement of information concerning the influence of the (trimethylsilyl)methyl group, the structure η^6**-2-Zr**, being the strict equivalent of η^6**-2-Th** and the structure η^6**-2'-Th** being the strict equivalent of η^6**-2'-Zr**, were optimised. The starting points of those optimisations were the optimised η^6**-2-Th** and η^6**-2'-Zr** geometries where the Th atom was substituted by a Zr atom and vice versa respectively..

3.3.2 Optimisation of Toluene-Coordinated Alkyl Cations

For η^6**-3-U** and η^6**-3'-Zr**, X-ray structures were available and were used as starting points. Since the X-ray data of η^6**-3-U** and η^6**-3'-Zr** present the arene facing the metallic center (as in the benzene complexes), we only tested the orientation of the methyl group of the arene for the toluene structure η^6**-3-Th**. By convention, as in [96], we will name as "exo" structure the structure where the methyl group is on the same side as the CH_2SiMe_3 group and as "endo" structure, the structure where the methyl group sits on the opposite side of CH_2SiMe_3 as illustrated by Figure 3.8.

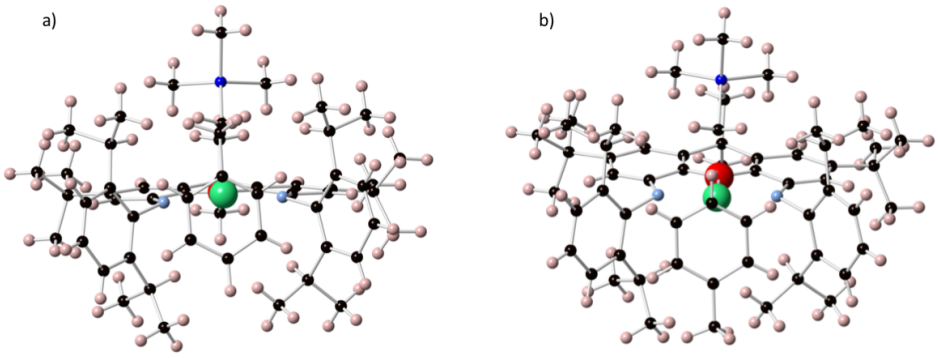

FIGURE 3.8: Starting geometries for the optimisation of the toluene complex η^6**-3-Th** with a) the "exo" starting point b) the "endo" starting point.

3.3.3 Optimisation of Halogeno-Coordinated Alkyl Cations

The X-ray structure of fluorobenzene, η^6**-5-U**, is also presenting a "endo" structure. Thus we also expect a "endo" structure for η^6**-5-Th**. We also explored the orientation of the arene in the fluorobenzene complexes η^1**-5-Th** and η^1**-5'-Zr** having the fluorobenzene of the arene ring facing the metallic centre, with the "horizontal" and the "vertical" orientations as shown in Figure 3.9.

The bromo-benzene **4-U** and fluorobenzene **5-U** were optimised with the η^6**-5-U** X-ray structure as starting point substituting fluorine by bromine.

The η^6**-3-Th**, η^6**-3-U** and η^6**-5-U** have a similar orientation of the methyl group of the toluene or the fluor of the fluorobenzene; all are in the "endo" orientation. Thus the bromo-benzene η^6**-4-Th** and η^6**-4-U** were optimised in the "endo" convention.

For the **4'-Zr**, Motolko *et al.* [109] reported the "exo" and the "horizontal" structures as possible structures and probably a mixing of the two. Thus we tested these two orientations presented in Figure 3.10.

3.3.4 Optimisation of Difluoro-Coordinated Alkyl Cations

For difluoro-benzene complexes, only the **6-Th** was optimised so far. There are no X-ray data for any of the metallic center thus, five orientations were tested. Three

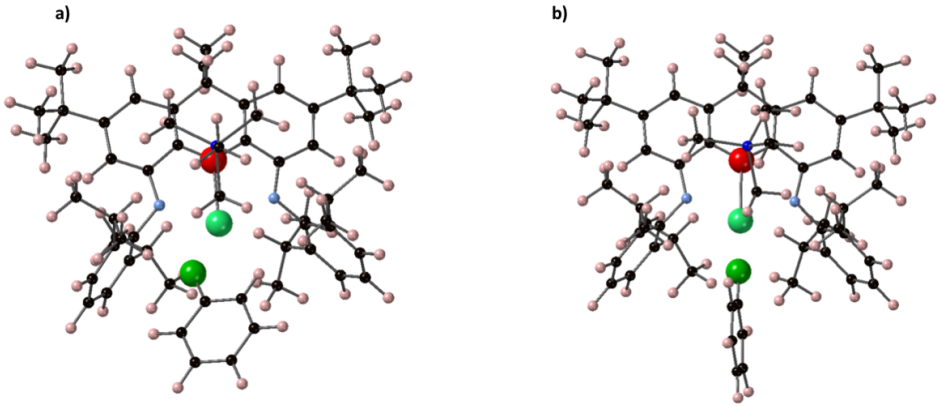

FIGURE 3.9: Starting geometries for the optimisation of η^1**-5-Th** with a) the "horizontal" starting point and b) the "vertical" starting point.

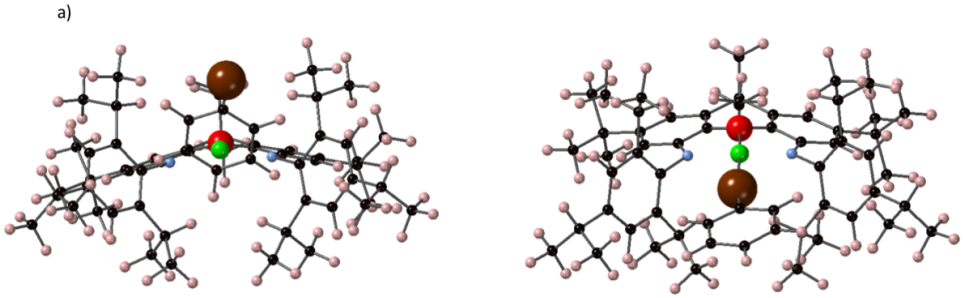

FIGURE 3.10: Starting geometries for the optimisation of the bromobenzene complex **4'-Zr** with a) the "exo" starting point and b) the "horizontal" starting point.

correspond to the arene facing Th with different initial positions of the two fluor atoms. Again, we kept the "exo" and "endo" notations, adding the label "side" to the third possibility as it can be seen in Figure 3.11. The last two starting points are the "horizontal" and the "vertical" presented earlier.

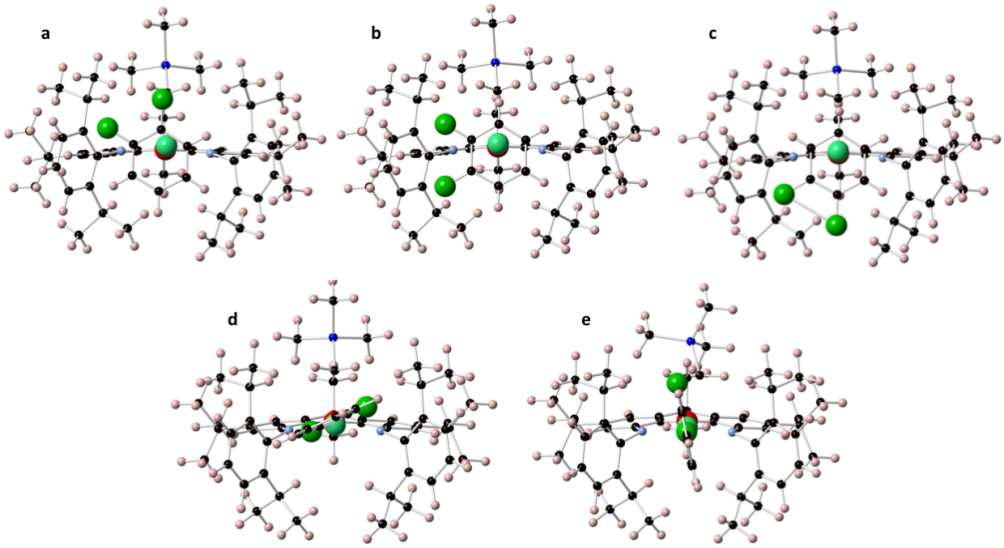

FIGURE 3.11: Starting geometries for the optimisation of **6-Th**: (a) η^6**-6-Th-exo**, (b) η^6**-6-Th-side**, (c) η^6**-6-Th-endo**, (d) η^1**-6-Th-horizontal** and (e) η^1**-6-Th-vertical**.

3.3.5 Optimisation of Ethylene-Coordinated Alkyl Cations

The **E′-Zr**, **E-Th** and **E-U** are optimised with two starting points, one with CH_2 pointing to the metal one with the two carbons of the ethylene facing the metal/actinide centre. The starting structures are the optimised structures of the benzene **2′-Zr**, **2-Th** and **2-U**.

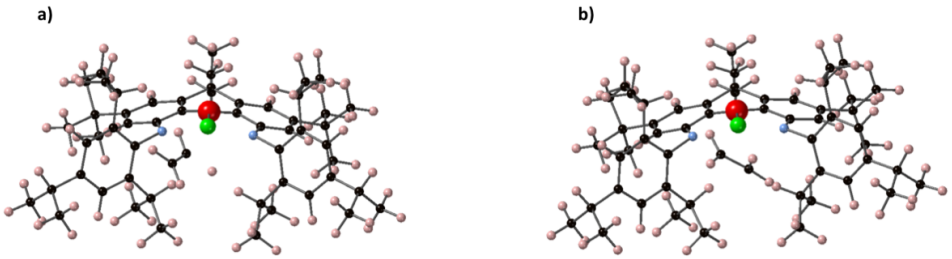

FIGURE 3.12: Starting geometries for the optimisation of **E′-Zr**: (a) η^1**-E′-Zr** and (b) η^2**-E′-Zr**.

3.4 Bonding studies

3.4.1 Dissociation curves - Benzene-Coordinated Alkyl Cations

For the benzene complexes, to quantify the strength and the nature of the benzene cation bonds, interaction curves were computed scanning the cation benzene distance from 2.7 Å to 4.0 Å for Th and U and from 2.2 Å to 3.4 Å in steps of 0.1 Å plus additional points at 4.5, 5, 6 and 10 Å.

Since the curves were smooth and presented only a single minimum (see Figure 3.17), the estimation of the binding energy was done at the structures accounting for the BSSE correction as described in the following paragraph.

3.4.2 Estimation of the binding energies at the equilibrium including BSSE and dispersion

For the BSSE calculation, the complex is divided into two fragments the first one (A) being composed of the catalyst and the second fragment (B) corresponding to the arene. If all the setup from the previous calculation was kept (DFT-TURBOMOLE-PBE0), tests on basis sets, using larger ones, such as def2-QZVP, def2-TZVPP and aug-cc-pVTZ for **2'-Zr** were performed. The interaction energies changed by a few kJ/mol with a largest basis sets proving that def2-TZVP is sufficiently accurate.

Because of the π-coordination of the arene to the metallic center, dispersion effects might be important. They can be captured by the MP2 method at considerable computational cost, or with a DFT-based approach with an empirical dispersion correction, namely the D3 correction [50].

3.4.3 Decomposition of the bond energy: the ETS-NOCV method

The ETS-NOCV method [118, 119], implemented in the ADF package, decomposes the interaction between two fragments within a system chosen by the user, to offer a quantitative picture of the chemical bond.

ETS - Extended Transition State decomposition analysis

The total energy between the interacting fragments is divided in 4 components [133]:

$$\Delta E_{tot} = \Delta E_{dist} + \Delta E_{elstat} + \Delta E_{Pauli} + \Delta E_{orb} \tag{3.1}$$

- ΔE_{dist}: the distorsion term corresponding to the energy between the free fragments and their geometry within the complex.
- ΔE_{elstat}: the electrostatic stabilising interaction between the 2 fragments when they are brought to their position in the final complex.
- ΔE_{Pauli}: the destabilising repulsive interaction between the occupied orbitals of the 2 fragments.
- ΔE_{orb}: the stabilising interaction between the occupied orbitals of one fragment and the unoccupied orbitals of the other one and the mixing of the unoccupied and occupied orbitals of a same fragment (intrafragment polarisation) once the two fragments have been united.

The change in the electronic density $\Delta\rho$ responsible for ΔE_{orb} can be written as:

$$\Delta\rho(1) = \sum_{\lambda}\sum_{\nu}\Delta P_{\lambda\nu}\lambda(1)\nu(1) \tag{3.2}$$

With "(1)" corresponding to the molecular orbital, λ are the occupied orbitals and ν the unoccupied orbitals of the 2 fragments and $\Delta P_{\lambda\nu}$ the deformation density function of λ and ν. Then ΔE_{orb} can be written as:

$$\Delta E_{orb} = \sum_{\lambda}\sum_{\nu}\Delta P_{\lambda\nu}F^{TS}_{\lambda\nu} \tag{3.3}$$

where $F^{TS}_{\lambda\nu}$ is the Kohn-Sham Fock matrix element that can be defined in terms of potential (transition state -TS) that is midway between the combined fragments and the final molecule (this is why it is called transition state).

NOCV - Natural orbitals for chemical valence

Derived from Nalewajski-Mrozek valence theory [134, 135], the deformation density is defined as :

$$\Delta\rho(r) = \rho^{system} - \sum_i \rho_i^{frag}(r) \tag{3.4}$$

The deformation density $\Delta\rho$ can be expanded as a sum of pairs of (Ψ_{-k}, Ψ_k) the natural orbitals for chemical valence (NOCV) that provide an orbital representation of the deformation density:

$$\Delta\rho(r) = \sum_{k=1}^{M/2} \nu_k[-\Psi_{-k}^2(r) + \Psi_k^2(r)] = \sum_{k=1}^{M/2} \Delta\rho_k(r) \tag{3.5}$$

In equation 3.5, Ψ_{-k} and Ψ_k NOCV are the eigenvectors of the ΔP matrix corresponding to eigenvalues $\pm\ \nu_k$, where ΔP = P_{AB} - (P_A + P_B), and P_{AB}, P_A and P_B are the molecular, and the fragment charge and bond order matrices [134, 135].

As a result the orbital interaction can be expressed in terms of the NOCV orbitals as:

$$\Delta E_{orb} = \sum_{k=1}^{M/2} \Delta E_{orb}(k) = \sum_{k=1}^{M/2} \nu_k[-F_{-k,-k}^{TS}(r) + F_{k,k}^{TS}(r)] \tag{3.6}$$

where $F_{-k,-k}^{TS}$ and $F_{k,k}^{TS}$ are the diagonal Kohn-Sham matrix elements defined over NOCVs with respect to the TS density. In this expression, only few complementary NOCV pairs (often 2 to 4) contribute significantly to ΔE_{orb}. Each pair represents one charge-transfer contribution $\Delta\rho_k$, with its energy contribution ΔE_{orb}(k). To discuss trends across complexes the same fragment types must be used *i.e.* the fragments A and B must describe the same parts of the molecule.

ETS-NOCV calculations were performed for all the benzene complexes with the PBE0 functional, QZ4P basis sets and included scalar relativistic effects with the ZORA Hamiltonian. As for the BSSE calculation, the first fragment includes the cationic complex and the second one the arene. One has to note that ETS-NOCV analysis cannot be performed with spin-orbit coupling. Nevertheless, for benzene complexes a simple-point calculation with Spin-Orbit ZORA Hamiltonian was ran showing that spin-orbit coupling has no effect on the interaction energy.

3.5 Results and discussions

3.5.1 Geometries of the arene-coordinated uranium, thorium or zirconium alkyl cation with the arene solvent

Geometries of benzene-coordinated alkyl cations

TABLE 3.6: Important bond lengths in Å and angles in degree for η^6**-2-U** (X-ray and optimised structures), η^6**-2-Th** (X-ray and optimised structures),η^6**-2′-Th** (optimised structure), η^6**-2′-Zr** (optimised structure) and η^6**-2-Zr** (optimised structure).

Compounds	η^6**-2-U** X-ray	η^6**-2-U** opt	η^6**-2′-U** opt
M-O	2.441(2)	2.428	2.473
M-N	2.224(2), 2.236(6)	2.222, 2.231	2.221, 2.220
M-C_{arene}	3.099(3) - 3.248(3)	3.028 - 3.795	3.127 - 3.248
M-Arene Centroid	2.932	3.136	3.177
$N_1 \ldots N_2$	3.94	3.99	3.896
Arene Bend			
Angle[1]	18.9	23.5	1.1
O-M-C_{apical}	87.26(8)	91.90	81.25
M-C-Si	133.7(2)	135.7	–
Compounds	η^6**-2-Th** X-ray	η^6**-2-Th** opt	η^6**-2′-Th**
M-O	2.496(5)	2.487	2.500
M-N	2.278(3), 2.288(3)	2.278, 2.282	2.273, 2.274
M-C_{arene}	3.18 - 3.31	3.19 - 3.41	3.171-3.302
M-Arene Centroid	2.950	2.999	2.925
$N_1 \ldots N_2$	4.04	4.02	3.963
Arene Bend			
Angle[1]	8.7	10.8	0.8
O-M-C_{apical}	91.3(1)	91.4	82.8
M-C-Si	131.0(2)	132.4	–
Compounds	η^6**-2′-Zr** opt	η^6**-2-Zr** opt	
M-O	2.248	2.263	
M-N	2.144, 2.149	2.103, 2.099	
M-C_{arene}	2.781 - 2.881	4.43 - 2.699	
M-Arene Centroid	2.470	3.403	
$N_1 \ldots N_2$	3.87	3.829	
Arene Bend			
Angle[1]	2.4	30.1	
O-M-C_{apical}	82.2	96.2	
M-C-Si	–	132.3	

[1] Angle between the carbons of the arene and the planar ligand.

Table 3.6 gathers all the results for the benzene complexes. The distances between the metal centres and both the oxygen and nitrogen atoms of the XA_2 (4,5-bis(2,4,6-triisopropylanilido)-2,7-di-tert-butyl-9,9-dimethylxanthene) group almost perfectly vary with respect to the ionic radii variations; for instance the Th-O distance in η^6**-2-Th** comes out 0.22 Å longer the Zr-O one in η^6**-2-Zr**, and 0.06 Å longer than the U-O one in η^6**-2-U**. Contrariwise the metal-arene distances do not follow the ionic radii trends since the Th-C_{arene} distance are about 0.47 Å and 0.17 Å longer than the Zr-C_{arene} and U-C_{arene} ones respectively, suggesting that the various cations interact differently with the benzene ring. The computed structure of η^6**-2′-Zr** is also reported though it could not be crystallised by Emslie *et al.* The difference between η^6**-2′-Zr** and η^6**-2-Zr** is that a methyl group is attached to Zr in the former while the latter carries a bulkier CH_2SiMe_3 group. This is confirmed by the fact that η^6**-2′-Th** present similar O-M-C_{apical} angle and arene bend angle than η^6**-2′-Zr**. As consequences, η^6**-2′-Th** also present a short distance M-Arene Centroid than η^6**-2-Th**. Albeit Zr-O and Zr-N distances are nearly the same in both η^6**-2-Zr** and η^6**-2′-Zr** complexes, the Zr-C_{arene} distance is shorter in the former than in the latter.

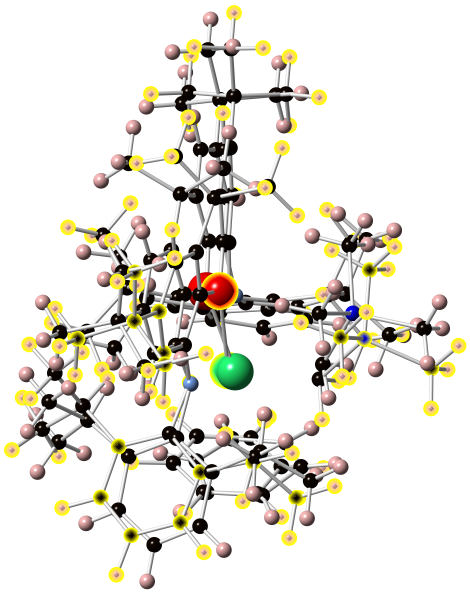

FIGURE 3.13: Superposition of the X-ray and the optimised (yellow atoms) structures of η^6**-2-Th**

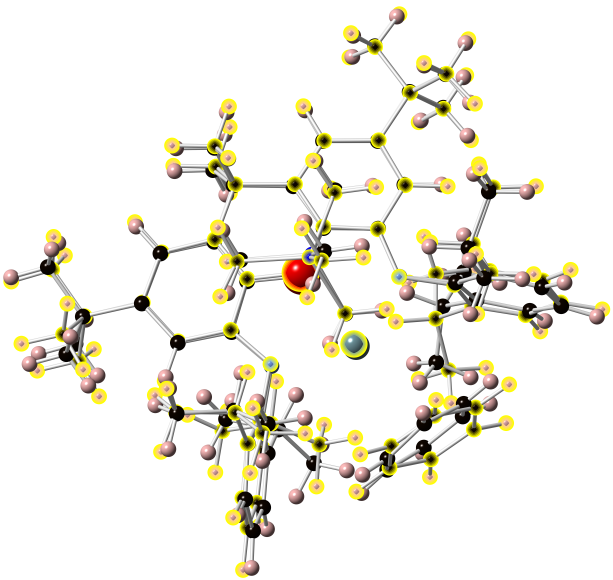

FIGURE 3.14: Superposition of the X-ray and the optimised (yellow atoms) structures of η^6**-2-U**

Geometries of toluene-coordinated alkyl cations

TABLE 3.7: Important bond lengths in Å and angles in degree for η^6**-3-U** (X-ray structures), η^6**-2-Th** (optimised structure) and η^6**-3′-Zr** (X-ray and optimised structures).

Compounds	η^6**-3-U-endo** X-ray	η^6**-3-Th-endo** opt	η^6**-3′-Zr-exo** opt	η^6**-3′-Zr-exo** X-ray
M-O	2.480	2.417(9)	2.247	2.220
M-N	2.21(1), 2.22(1)	2.277, 2.273	2.161, 2.148	2.138, 2.142
M-C_{arene}	3.05(2) - 3.78(2)	3.084 - 4.005	2.747 - 2.908	2.697 - 2.840
M-Arene Centroid	3.138	3.271	2.449	2.383
$N_1 \ldots N_2$	3.98	4.04	3.91	3.91
Arene Bend Angle[1]	11.8	13.4	12.7	
O-M-C_{apical}	5.9	92.20	87.7	81.0
M-C-Si	136.8(7)	133.8	–	–

[1] Angle between the carbons of the arene and the planar ligand.

The structures of η^6**-3-U-endo** and η^6**-3-Th-exo** are not be obtained yet. For those available the computed geometries agree well with the available crystallographic data (see Table 3.7). The main observation is that the M-C_{arene} distances in toluene complexes are slightly shorter than in the benzene ones.

Geometries of halogeno-coordinated alkyl cations

The structures of bromobenzene η^6**-4-U** and the fluorobenzene η^6**-5-U** and η^1**-5-Th-horizontal** are not reported yet.

The fluorobenzene η^6**-5′-Zr-exo** is slightly more stable than η^1**-5-Th-vertical** with a difference in energy of 0.35 kJ.mol^{-1}. This difference is so small that both structures will be kept for the rest of the study. The η^1**-5′-Zr-vertical** relaxed to an "horizontal" orientation but forming an important tilt angle with the molecular plane. The most stable is the optimised **5′-Zr-vertical**, with an energy 4.2 kJ.mol^{-1} lower than that obtained with the η^1**-5′-Zr-horizontal**. The last isomer, η^6**-5′-Zr-exo** is the least stable lying 15.7 kJ.mol^{-1} above η^1**-5′-Zr-vertical**. Nevertheless, as the structures are close in energy both the η^1**-5′-Zr-horizontal** (from the optimised $\eta^{'}$**-5′-Zr-vertical** starting point) and η^1**-5′-Zr-exo** are kept for the next steps of the study. The currently optimised structures cannot be compared to crystal data, though, they reveal very

similar bond distances to the toluene ones.

TABLE 3.8: Important bond lengths in Å and angles in degree for η^6**-5-U** (optimised and X-ray structures), η^6**-5-Th** (optimised structure), η^6**-5′-Zr** (optimised structure) and η^1**-5′-Zr -horizontal** (optimised structure) and the relative energy ΔE in kJ.mol^{-1} with respect to the most stable isomer.

Compounds	η^6**-5-U** X-ray	η^6**-5-Th-endo** opt	η^1**-5-Th-vertical**
M-O	2.431	2.477	2.476
M-N	2.215, 2.218	2.267, 2.275	2.267, 2.270
M-C$_{arene}$	3.128 - 3.598	3.140 - 3.822	–
M-Arene Centroid	3.077	3.204	–
$N_1 \ldots N_2$	3.98	4.033	4.040
Arene Bend			
Angle [1]	1.6	8.4	78.9
O-M-C$_{apical}$	89.6	92.3	94.9
M-C-Si	134.8	133.2	132.5
ΔE		0.0	0.3
Compounds	η^6**-5′-Zr-exo** opt	η^1**-5′-Zr -horizontal** opt	
M-O	2.277	2.257	
M-N	2.088, 2.082	2.068, 2.070	
M-C$_{arene}$	2.687 - 4.417	–	
M-Arene Centroid	3.401	–	
$N_1 \ldots N_2$	3.790	3.813	
Arene Bend			
Angle [1]	10.7	11.1	
O-M-C$_{apical}$	91.3	101.5	
M-C-Si	–	–	
ΔE	15.7	0.0	

[1] Angle between the carbons of the arene and the planar ligand.

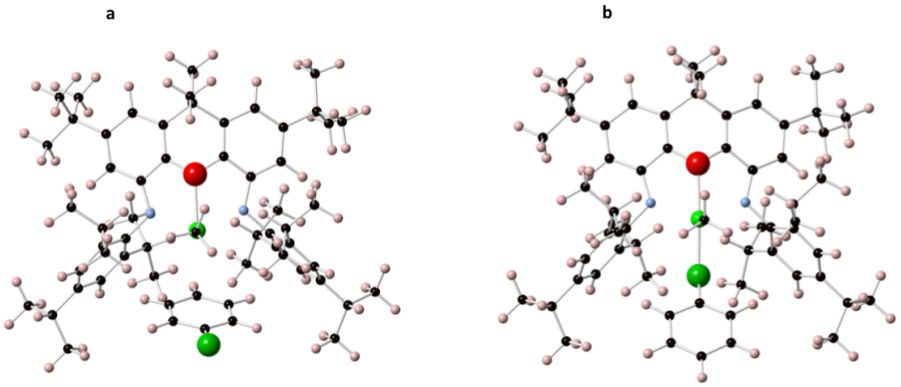

FIGURE 3.15: Optimised geometries for a) η^6**-5′-Zr-exo**, b) η^1**-5′-Zr-horizontal**

TABLE 3.9: Important bond lengths in Å and angles in degree for η^6**-4-Th** (optimised structure) and **4′-Zr** (optimised structures) and the relative energy ΔE in kJ.mol^{-1} with respect to the most stable isomers.

Compounds	η^6**-4-Th-endo** opt	η^6**-4′-Zr-exo** opt	η^1**-4′-Zr-horizontal** opt
M-O	2.472	2.276	2.260
M-N	2.263, 2.263	2.082, 2.088	2.069, 2.077
M-C_{arene}	3.058 - 4.335	2.697 - 4.406	–
M-Arene Centroid	3.481	3.390	–
$N_1 \ldots N_2$	4.03	3.789	3.789
Arene Bend Angle [1]	4.9	11.4	13.5
O-M-C_{apical}	92.9	91.1	90.8
M-C-Si	133.3	–	–
ΔE		0.0	9.7

[1] The angle between the carbons of the arene and the planar ligand.

In the case of bromobenzene isomers, η^6**-4′-Zr-exo** is more stable than η^1**-4′-Zr-horizontal** by 9.7 kJ.mol^{-1} but since David Emslie suspected the presence of these two isomers from NMR analysis [109], both will be kept for the next steps of the bonding study.

Geometries of difluorobenzene-coordinated alkyl cations

η^1**-6-Th-vertical** and η^1**-6-Th-horizontal** are converging to the same η^1**-6-Th-vertical** structure, thus only this one will be kept for the results. The most stable isomer is the η^1**-6-Th-vertical** and the other three are less than 15 kJ.mol^{-1} higher in energy, forcing us to consider all of them. Nonetheless the final structure of η^1**-6-Th-horizontal**

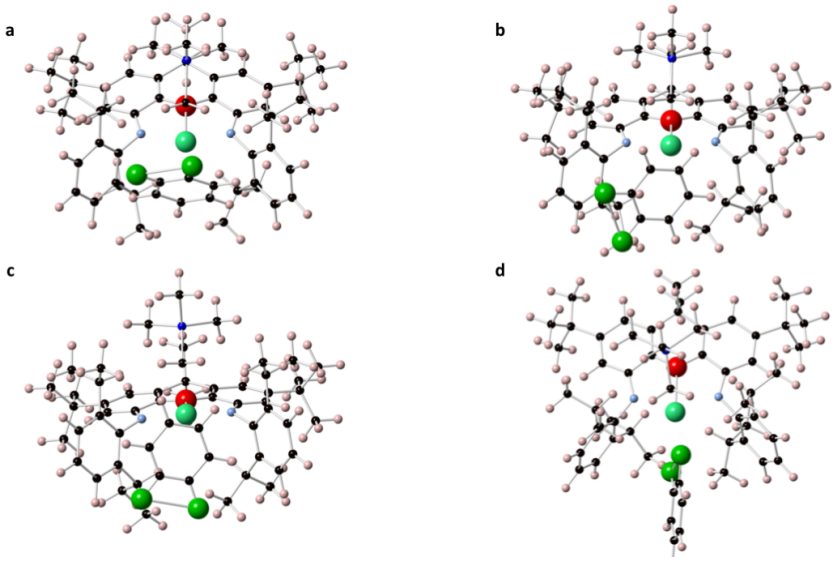

FIGURE 3.16: Optimised geometries for a) η^6**-6-Th-exo**, b) η^6**-6-Th-side**, c) η^6**-6-Th-endo** and, d) η^1**-6-Th-vertical**

TABLE 3.10: Important bond lengths in Å and angles in degree for η^6**-6-Th-exo**, η^6**-6-Th-side**, η^6**-6-Th-endo**, η^1**-6-Th-horizontal** and η^1**-6-Th-vertical** optimised structures and the relative energies ΔE in kJ.mol^{-1} with respect to the most stable isomer.

Compounds	η^1**-6-Th-vertical** opt	η^6**-6-Th-exo** opt	η^6**-6-Th-side** opt	η^6**-6-Th-endo** opt
M-O	2.46	2.492	2.477	2.475
M-N	2.252, 2.254	2.279, 2.280	2.259, 2.258	2.262, 2.258
M-C$_{arene}$	–	3.060 - 4.298	3.107 - 4.373	3.030 - 4.326
M-Arene Centroid	–	3.461	3.531	3.464
$N_1 \ldots N_2$	4.000	4.036	4.004	4.014
Arene Bend Angle [1]	–	28.6	24.9	13.0
O-M-C$_{apical}$	93.6	93.5	93.3	93.5
M-C-Si	132.3	133.8	132.4	132.3
ΔE	0.0	12.4	15.5	9.6

[1] The angle between the carbons of the arene and the planar ligand.

The arene bend angles in the η^6**-6-Th-exo** and η^6**-6-Th-side** isomers are larger than in the η^6**-6-Th-endo** one because of the steric repulsion of the two fluorine atoms.

Optimisation of Ethylene-Coordinated Alkyl Cations

The **E′-Zr** optimised structures with both starting points are giving the same result with the two carbons of the ethylene facing the zirconium atom. For this reason, for U and Th complexes, the optimisation where the CH_2 is pointing to the actinide is disregarded. The important information on the complexes can be found in Table 3.11

TABLE 3.11: Important bond lengths in Å and angles in degree for η^2**-E′-Zr** and η^2**-E-Th** optimised structures.

Compounds	**E′-Zr**	**E-Th**
M-O	2.268	2.467
M-N	2.070, 2.076	2.251, 2.254
M-$C_{ethylene}$	2.796, 2.842	3.113, 3.094
$N_1 \ldots N_2$	3.790	4.005
Ethylene Bend		
Angle [1]	37.4	12.9
O-M-C_{apical}	92.1	95.6
M-C-Si	–	131.4

[1] The angle between the carbons of the ethylene and the planar ligand.

All the distance M-$C_{ethylene}$ are shorter than in the other complexes thus a stronger bond could be expected. Unfortunately, as I write this lines, no result about η^2**-E-U** is available.

3.5.2 Bonding studies

Dissociation curves - Benzene-Coordinated Alkyl Cations

Figure 3.17 presents the results for the dissociation of benzene from the alkyl Zr, Th and U cations. The curves display only one minimum corresponding to the distance benzene - metallic center found in the geometry optimisations. The bonding energies derived from the curves are -145.5 kJ.mol^{-1}, -90.4 kJ.mol^{-1} and -80.3 kJ.mol^{-1} for η^6**-2′-Zr**, η^6**-2-Th** and η^6**-2-U**, respectively.

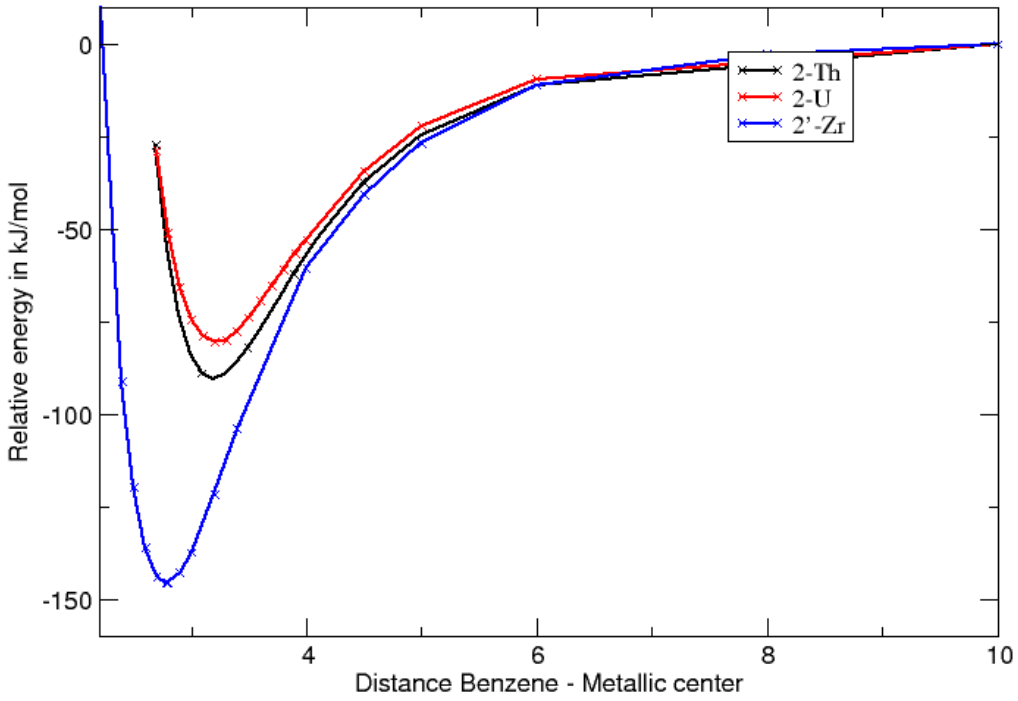

FIGURE 3.17: Dissociation curves for η^6**-2-Th** (black), η^6**-2-U** (red) and η^6**-2′-Zr** (blue) for a benzene - metallic center distance between 2.2 Å and 10 Å

TABLE 3.12: BSSE corrections (in kJ.mol^{-1}) to the benzene interaction energies in η^6**-2′-Zr** computed at different levels of calculation with different basis sets.

	ΔE	ΔE(BSSE)	$\Delta E_{corrected}$
PBE0-def2-TZVP	-147.4	-4.6	-142.8
(PBE0 + D3)-def2-TZVP	-204.4	-4.6	-199.9
MP2-def2-TZVP	-281.9	-42.2	-239.7
MP2-def2-TZVPP	-289.4	-36.9	-252.6
MP2-aug-cc-pVTZ	-305.2	-45.0	-260.2

BSSE corrections and decompositions of the bond energies: an ETS-NOCV study

To evaluate the accuracy of the QM methods on the bonding energies, we have performed PBE0, PBE0 + D3 and MP2 calculations for the η^6**-2′-Zr** complex (see Table 3.12). MP2 energies are somewhat sensitive to the size of the basis set; increasing

the basis quality from def2-TZVP to def2-TZVPP and aug-cc-PVTZ increases the binding energy by 13 and 20 kJ.mol^{-1} (< 10% of the total interaction energy), respectively, while expanding significantly the computational time. Thus, the def2-TZVP basis sets are kept for all other complexes.

TABLE 3.13: Bonding energies in kJ.mol^{-1} for the benzene molecules η^6**-2′-Zr**, η^6**-2-Zr**, η^6**-2-Th** and η^6**-2-U** at PBE0, PBE0 + D3 and MP2 levels.

	ΔE			ΔE(BSSE)			$\Delta E_{corrected}$		
	PBE0	PBE0 + D3	MP2	PBE0	PBE0 + D3	MP2	PBE0	PBE0 + D3	MP2
η^6**-2′-Zr**	-147.4	-204.4	-305.2	-4.6	-4.6	-45.0	-142.8	-199.9	-260.2
η^6**-2-Zr**	-92.8	-147.1	-190.5	-3.2	-3.2	-29.1	-89.6	-143.8	-161.5
η^6**-2-Th**	-92.5	-141.7	-189.7	-3.5	-3.5	-25.7	-89.0	-138.1	-164.1
η^6**-2-U**	-77.8	-128.0		-3.5	0.2		-74.2	-128.2	

From Table 3.13, we note that for both Zr and Th complexes, the MP2 energies are larger than the PBE0 ones. Assuming that PBE0 with D3 correction captures most of the dispersion effects, it is interesting to note that the PBE0 trends across the metal centres match the MP2 ones. However, the MP2 values come out lower than the PBE0 + D3 ones, which is in line with the fact that MP2 is known to overestimate

dispersion contributions [136, 137].

TABLE 3.14: Bonding energy decomposition in kJ.mol^{-1} for the zirconium cations with the ETS-NOCV method .

	η^2-**E′-Zr**	η^6-**2′-Zr**	η^6-**2-Zr**	η^6-**3′-Zr-exo**
ΔE_{Dist}	29.7	95.4	38.1	112.0
ΔE_{Pauli}	130.8	296.4	137.6	311.7
ΔE_{elstat} [1]	-119.3 (54%)	-200.5 (45%)	-105.6 (45%)	-217.6 (45%)
ΔE_{orb} [1]	-99.6 (46%)	-242.2 (55%)	-126.3 (55%)	-263.2 (55%)
ΔE^{σ}_{orb} [2]	-62.8 (63%)	-45.2 (19%)	–	-46.0 (19%)
$\Delta E^{\pi}1_{orb}$ [2]	-12.5 (13%)	-60.2 (25 %)	-71.1 (56%)	-66.1 (25%)
$\Delta E^{\pi}2_{orb}$ [2]	–	-63.2 (26%)	-13.0 (10%)	-66.9 (25%)
ΔE^{other}_{orb} [2]	-24.7 (24%)	-77.0 (30%)	-41.0 (32%)	-84.1 (31%)
ΔE^{PBE0}_{int}	-88.1	-146.3	-94.3	-169.2
ΔE_{Disp} [3]	-33.1	-52.5	-51.0	-61.9
$\Delta E^{PBE0+D3}_{int}$	**-91.5**	**-103.4**	**-107.2**not finish	**-119.1**
	η^6-**4′-Zr-exo** *	η^1-**4′-Zr-horizontal**	η^6-**5′-Zr-exo**	η^1-**5′-Zr-horizontal**
ΔE_{Dist}	36.3	29.1	30.7	22.3
ΔE_{Pauli}	133.3	115.3	136.7	100.3
ΔE_{elstat} [1]	-95.1 (43%)	-97.5 (48%)	-103.0 (45%)	-108.7 (54%)
ΔE_{orb} [1]	-125.6 (57%)	-105.9 (52%)	-125.3 (55%)	-91.7 (44%)
ΔE^{σ}_{orb} [2]	-73.6 (59%)	-65.5 (62%)	-74.5 (59%)	-44.5 (49%)
$\Delta E^{\pi}1_{orb}$ [2]	-10.5 (8%)	-10.8 (10%)	-9.6 (8%)	-14.2 (15%)
$\Delta E^{\pi}2_{orb}$ [2]	-8.4 (7%)	–	-8.4 (7%)	-9.6 (10%)
ΔE^{other}_{orb} [2]	-33.4 (26%)	-30.2 (28%)	-33.1 (24%)	-23.8 (26%)
ΔE^{PBE0}_{int}	-87.3	-88.1	-91.5	-100.0
ΔE_{Disp} [3]	-55.5	-47.3	-52.5	-36.8
$\Delta E^{PBE0+D3}_{int}$	**-106.5**	**-106.3**	**-113.0**	**-114.5**

* Most stable isomers.

[1] Values in parenthesis give the percentage contribution to the total attractive interaction (ΔE_{elstat} +ΔE_{orb}).

[2] Values in parenthesis give the percentage contribution to the total orbital energy for the σ- and π-donor NOCV-pair contributions.

[3] ΔE_{Disp} is the difference between ΔE^{PBE0}_{int} and $\Delta E^{PBE0+D3}_{int}$ with the BSSE correction.

Tables 3.14 and 3.15 summarise the energy decomposition analysis performed at the PBE0 level and the dispersion contributions that range from 40 to 70 kJ.mol^{-1}, representing at least 27% of the bonding energy. Thus, dispersion does not change the trends observed but is not negligible. Comparing the benzene η^6-**2′-Zr** and the

toluene η^6**-3′-Zr-exo** in Table 3.14, we see that the η^6**-3′-Zr-exo**, which is catalytically more active than η^6**-2′-Zr**, exhibits a stronger bond between Zr and the toluene solvent, which is counter intuitive with the hypothetical mechanism. η^6**-2-Zr** does not present an important σ interaction while η^6**-2′-Zr** does. It can come from the fact that η^6**-2-Zr** presents a large arene bond angle (30.1°) which prevents σ overlaps.

Fluorobenzene **5′-Zr** forms the weakest arene bond to zirconium. In case of the η^6**-5′-Zr-exo** isomer, it can be explained by the fact that the center of the fluorobenzene ring is shifted upwards as a result of hydrogen bonding between fluorine and a hydrogen atom of the CH_2SiMe_3 group.

The weakest bond is observed between the ethylene and the zirconium. Such a weak bond discredits the hypothesis of a competition between the arene from solvent and the ethylene. Nonetheless, the ethylene complexe is presenting a bond different from the one between the arene and the zirconium. Indeed, in present a σ donation from the ethylene carbons to the 4d and 5s orbitals of the zirconium and a π-retrodonation from the 2p orbitals of the carbons around Zr to the 2p orbitals of the ethylene carbons (see Figure **??**). Further explorations of possible transition states involving both

ethylene and the arene are foreseen.

TABLE 3.15: Bonding energy decomposition in kJ.mol^{-1} for the thorium cations with the ETS-NOCV method.

	η^2-**E-Th**	η^6-**2-Th**	η^6-**2′-Th**	η^6-**3-Th-endo**
ΔE_{Dist}	1.4	15.5	29.8	17.3
ΔE_{Pauli}	90.4	143.9	153.5	119.7
ΔE_{elstat} [1]	-87.6 (56%)	-115.6 (49%)	-120.8 (48%)	-102.0 (49%)
ΔE_{orb} [1]	-69.3 ((44%))	-120.9 (51%)	-130.3 (52%)	-104.9 (51%)
ΔE^{σ}_{orb} [2]	-43.1(62%)	-22.6 (19%)	-24.5 (19%)	-10.5 (10%)
$\Delta E^{\pi}1_{orb}$ [2]	-8.7 (12%)	-33.0 (27%)	-35.6 (27%)	-39.7 (38%)
$\Delta E^{\pi}2_{orb}$ [2]	–	-26.4 (22%)	-28.5 (22%)	-20.9 (20%)
ΔE^{other}_{orb} [2]	-17.8 (26%)	-39.7 (33%)	-42.6 (32%)	-34.2 (32%)
ΔE^{PBE0}_{int}	-66.5	-92.6	-97.6	-87.1
ΔE_{Disp} [3]	-25.2	-45.6	-50.5	-52.1
$\Delta E^{PBE0+D3}_{int}$	**-90.2**	**-122.7**	**-118.3**	**-121.9**
	η^6-**4-Th-endo**	η^6-**5-Th-endo**	η^1-**5-Th-verical**	
ΔE_{Dist}	8.1	-0.6	-6.1	
ΔE_{Pauli}	94.4	113.1	63.4	
ΔE_{elstat} [1]	-72.7 (45%)	-91.4 (48%)	-72.4 (55%)	
ΔE_{orb} [1]	-87.8 (55%)	-97.8 (52%)	-59.3 (45%)	
ΔE^{σ}_{orb} [2]	–	-11.7 (12%)	–	
$\Delta E^{\pi}1_{orb}$ [2]	–	-33.5 (34%)	–	
$\Delta E^{\pi}2_{orb}$ [2]	–	-21.3 (22%)	–	
ΔE^{other}_{orb} [2]	-87.8 (100%)	-32.1 (32%)	-59.3 (100%)	
ΔE^{PBE0}_{int}	-66.1	-76.1	-68.3	
ΔE_{Disp} [3]	-50.8	-48.7	-21.3	
$\Delta E^{PBE0+D3}_{int}$	**-108.8**	**-125.4**	**-95.7**	
	η^1-**6-Th-vertical***	η^6-**6-Th-exo**	η^6-**6-Th-side**	η^6-**6-Th-endo**
ΔE_{Dist}	6.5	6.8	6.8	31.8
ΔE_{Pauli}	70.2	97.3	89.6	93.2
ΔE_{elstat} [1]	-80.2 (56%)	-71.4 (45%)	-68.6 (45%)	-69.8 (44%)
ΔE_{orb} [1]	-62.0 (44%)	-87.0 (55%)	-82.2 (55%)	-89.0 (56%)
ΔE^{σ}_{orb} [2]		– -15.5 (18%)	-38.0 (46%)	-41.4 (47%)
$\Delta E^{\pi}1_{orb}$ [2]	–	-39.7 (46%)	-16.2 (20%)	-13.8 (16%)
$\Delta E^{\pi}2_{orb}$ [2]	–	–	–	–
ΔE^{other}_{orb} [2]	-62.0 (100%)	-32.3 (37%)	-28.6 (34%)	-34.4 (37%)
ΔE^{PBE0}_{int}	-72.0	-61.1	-61.2	-65.6
ΔE_{Disp} [3]	-22.7	-45.9	-44.2	-44.4
$\Delta E^{PBE0+D3}_{int}$	**-88.2**	**-100.2**	**-98.6**	**-78.2**

* Most stable isomers.

[1] Values in parenthesis give the percentage contribution to the total attractive interaction (ΔE_{elstat} +ΔE_{orb}).

[2] Values in parenthesis give the percentage contribution to the total ornital energy

We can see that the bonding interaction decreases along the arene series of the Th-complexes (see Table 3.15); as the bonding strength decreases, so does the 7s and 5f characters of the acceptor orbital while the 6d character increase in the main deformation densities contributions (See figure 3.18, **??** and the Appendix C).

Regarding the **6-Th** isomers, η^6**-6-Th-vertical** is the most stable one and presents the strongest arene-metal interaction. In η^1**-6-Th-vertical** and η^6**-6-Th-endo** the orbital interaction is composed of multiple small interactions. In η^1**-6-Th-vertical**, the arene ring orientation does not favour any bonding symmetry, while η^6**-6-Th-endo**, the arene ring is shifted perpendicularly to the molecular plane. Just as in Zr complexes, η^2**-E-Th** presents the weakest bond and the π retrodonation from the 2p orbitals of the carbons close to the Th center and the 4d orbitals of the thorium to the 2p orbitals of the ethylene carbons. The same exploration of transition state must then be done to shed light on the mechanism.

Finally the useful complexes to compare the metals are the η^6**-2-Th**, η^6**-2-Zr**, η^6**-2′-Th** and η^6**-2′-Zr** ones (see Tables 3.14 and 3.15 and Figures 3.18, **??**, 3.19 and **??**). The interaction strength is roughly the same comparing metals but the Zr benzene bond is somewhat more covalent than the Th-benzene one (larger ΔE_{orb} percentage). Again the absence of σ interaction in **2-Zr** is explained by the large arene bend angle. Being smaller in the thorium equivalent, the σ donation contributions into the 6d and 5f orbitals of Th amounts to 20% while π-type interactions sums up to 49% of the covalent contribution.

3.6 Conclusion and Perspectives

Although a lot of information have been already collected, the catalytic mechanism could not be revealed. So far we have shown that our QM calculations are able to reproduce X-ray data and certainly predict the geometries of uncrystallised complexes. We have seen that the Zr-cations have a bonding interaction slightly more covalent than the Th-ones, in which the arene interaction is electrostatically driven. The stronger bonds in thorium systems mainly involve 7s and 5f orbitals while the weakest involve mainly 6d orbitals. The study of hypothetic transition states will be done to explore the possible reaction paths.

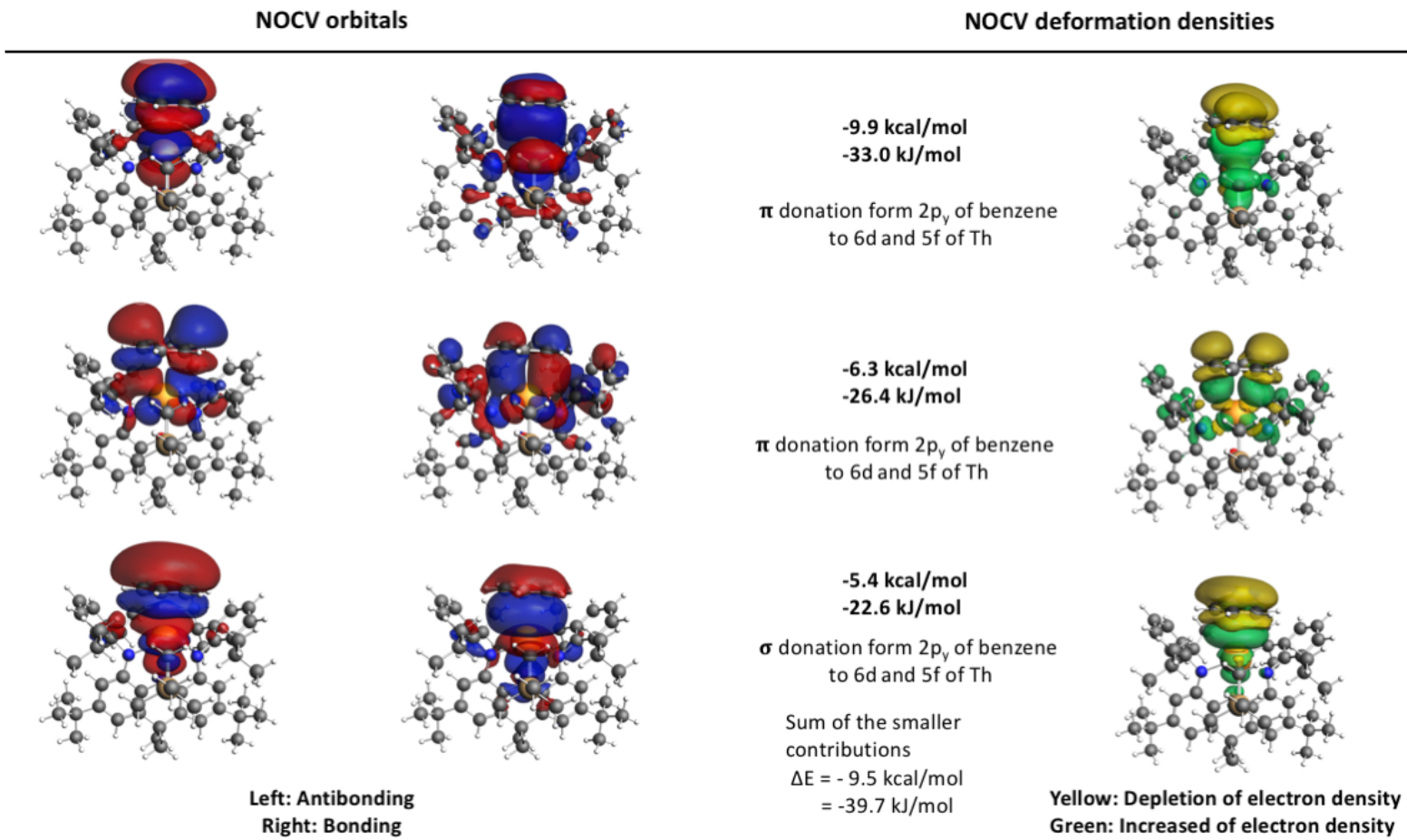

FIGURE 3.18: On the left hand side: the NOCV Orbitals (with isosurfaces set to 0.01) and on the right hand side ETS-NOCV deformation density contributions, Increased (green) and decreased (yellow) electron density is presented relative to that in the isolated fragments (isosurfaces are set to 0.0001) for the molecule η^6**-2-Th**.

FIGURE 3.19: On the left hand side: the NOCV Orbitals (with isosurfaces set to 0.01) and on the right hand side ETS-NOCV deformation density contributions, Increased (green) and decreased (yellow) electron density is presented relative to that in the isolated fragments (isosurfaces are set to 0.0001) for the molecule η^6**-2-Zr**.

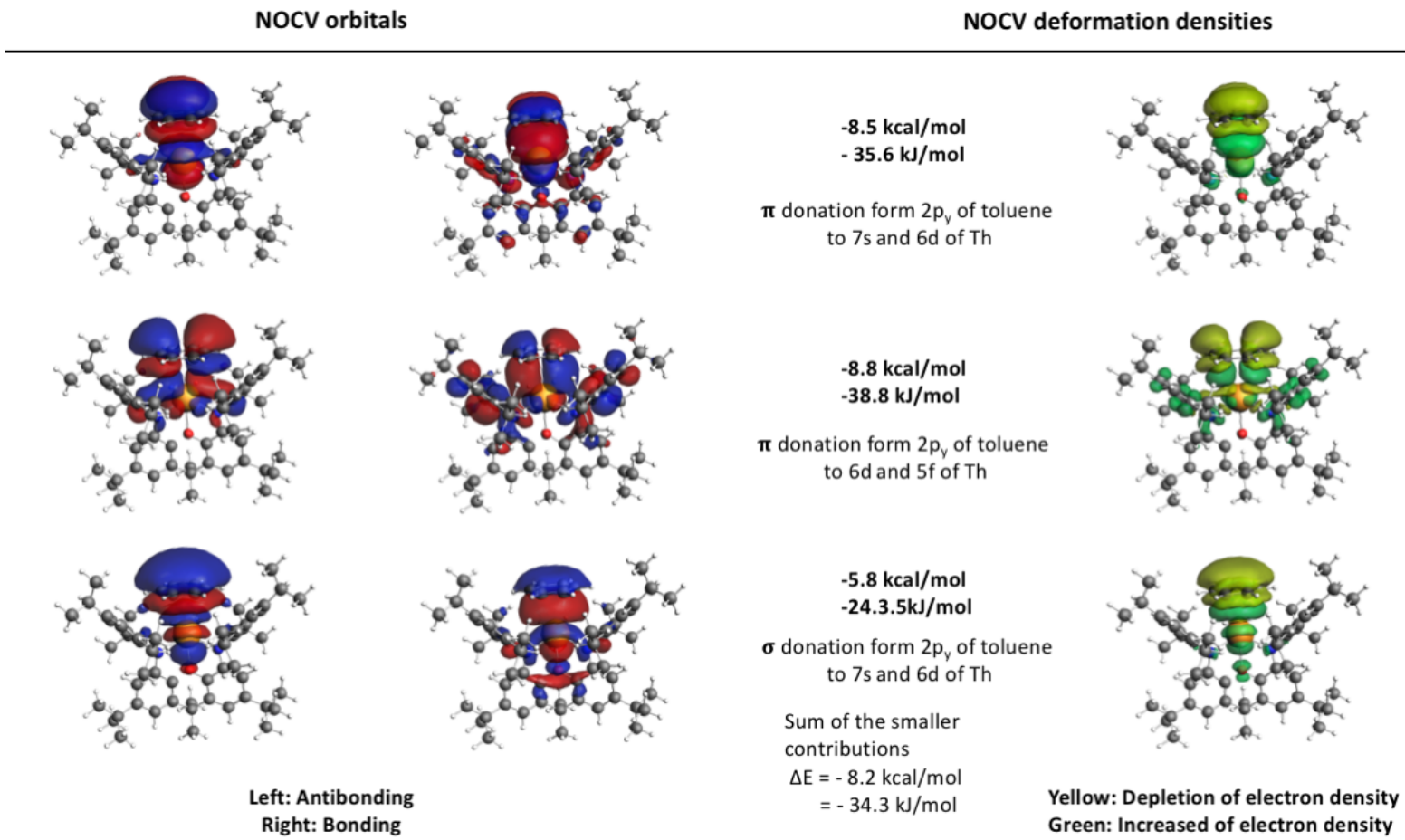

FIGURE 3.20: On the left hand side: the NOCV Orbitals (with isosurfaces set to 0.01) and on the right hand side ETS-NOCV deformation density contributions, Increased (green) and decreased (yellow) electron density is presented relative to that in the isolated fragments (isosurfaces are set to 0.0001) for the molecule η^6**2′-Th**.

FIGURE 3.21: On the left hand side: the NOCV Orbitals (with isosurfaces set to 0.01) and on the right hand side ETS-NOCV deformation density contributions, Increased (green) and decreased (yellow) electron density is presented relative to that in the isolated fragments (isosurfaces are set to 0.0001) for the molecule η^6**2'-Zr**.

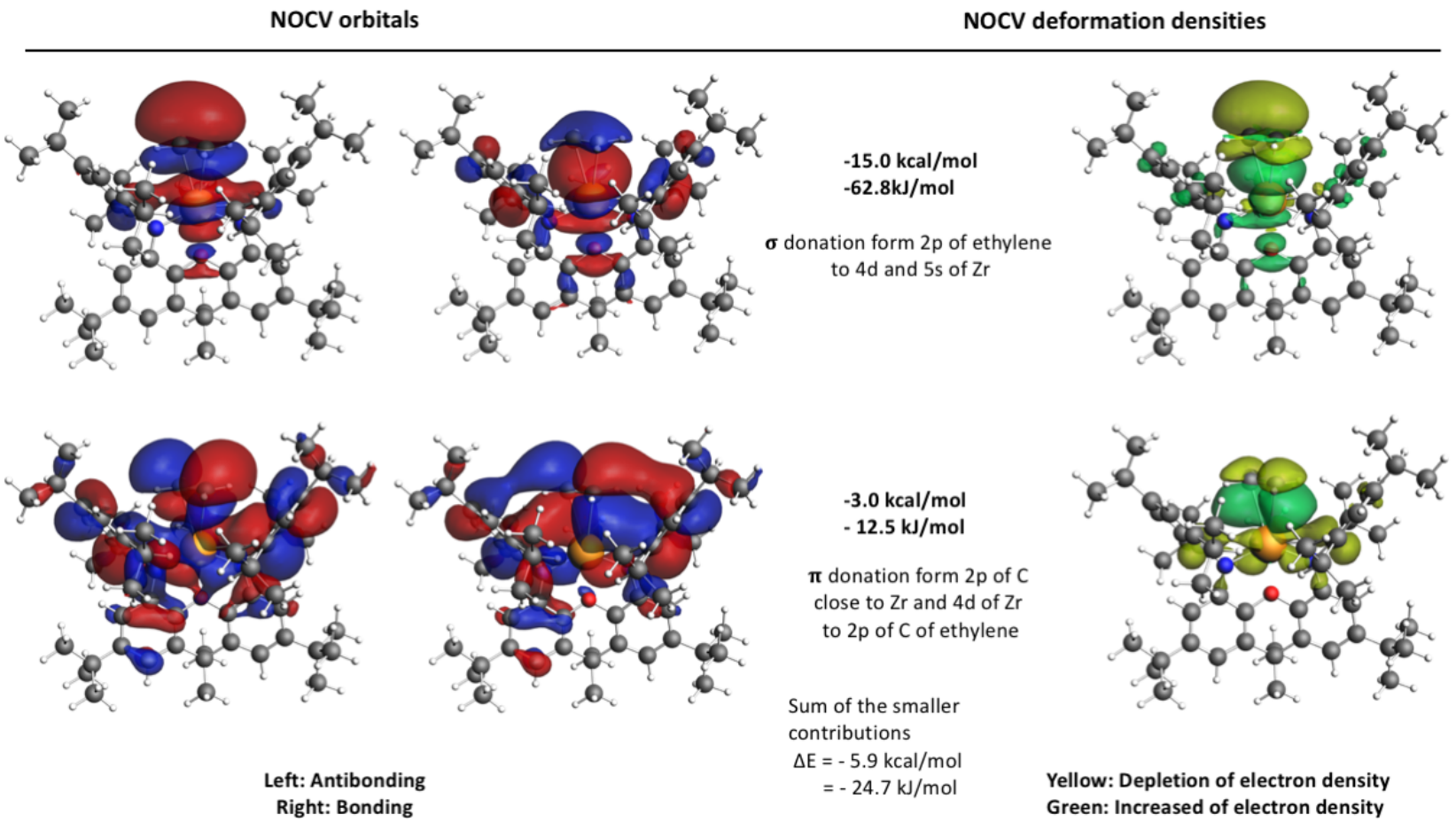

FIGURE 3.22: On the left hand side: the NOCV Orbitals (with isosurfaces set to 0.01) and on the right hand side ETS-NOCV deformation density contributions, Increased (green) and decreased (yellow) electron density is presented relative to that in the isolated fragments (isosurfaces are set to 0.0001) for the molecule η^2**-E′-Zr**.

FIGURE 3.23: On the left hand side: the NOCV Orbitals (with isosurfaces set to 0.01) and on the right hand side ETS-NOCV deformation density contributions, Increased (green) and decreased (yellow) electron density is presented relative to that in the isolated fragments (isosurfaces are set to 0.0001) for the molecule η^2-**E-Th**.

Chapter 4

Thermodynamic properties and electronic structures of Plutonium Oxides

Contents

As mentioned previously a nuclear accident would release numerous compounds. To confine this compounds would first imply to know the amount of the species released. This is what the IRSN (French Institute for Radioprotection and Nuclear Safety) aims to do. They decided to focused on Plutonium and its oxide because of its toxicity and volatility mentioned in the Introduction. In order to make a good prediction, the enthalpies of formation, the heat capacity and the entropy of each molecule involved must be known with the highest possible accuracy. In this Chapter, the enthalpies of formation of PuO_2, PuO_3 and $PuO_2(OH)_2$ will be discussed. Before a discussion of the computational protocol used and of the results obtained for these species, the existing experimental and theoretical results are reviewed below.

4.1 Review of available data for Plutonium Oxides

4.1.1 Experimental data

From a number of experimental investigations on PuO_2 [138–144], the most rescent which adresses the determination of $\Delta_f H^\circ$ is that of Gotcu-Freis *et al.* [138]. They carried out the measurements of the vapour pressure with a Knudsen cell coupled with a quadrupole mass spectrometer. This apparatus is designed for the study of radioactive materials at high temperature and built in a glove box shielded by 5 cm thick lead bricks. This simple description of the experimental setup is enough to emphasize the difficulty of manipulating plutonium. Gotcu-Freis *et al.* extracted the values $\Delta_f H^\circ$ = -(428.7 $\pm$ 7.0) kJ.mol^{-1} and $\Delta_f H^\circ$ = -(440$\pm$ 7.0) kJ.mol^{-1}, using the 2^{nd} and 3^{rd} law of thermodynamics, respectively. Previously the values reported in the thermodynamic databases were slightly higher $\Delta_f H^\circ$ = -(412 $\pm$ 20.0) kJ.mol^{-1} [139] and $\Delta_f H^\circ$ = -(410$\pm$ 20.0) kJ.mol^{-1} [140]. Konings in his 2014's review [141] selected $\Delta_f H^\circ$ = -(428.7 $\pm$ 20.0) kJ.mol^{-1} as the preferred value.

Unfortunately, the thermodynamic properties of PuO_3 and $PuO_2(OH)_2$ are not as much documented (see Table 4.1). The first molecule was observed in a small amount by Ronchi *et al.* [145] after sublimation of free surfaces of PuO_2 in presence of oxygen but no thermodynamic data was reported. Krikorian *et al.* [146] favoured the transpiration method starting from a PuO_2 solid sample and flows of O_2 or H_2O to generate PuO_3 and $PuO_2(OH)_2$ molecules respectively. They reported the values of standard enthalpy of formation of -(562.8 $\pm$ 5.0) kJ.mol^{-1} for PuO_3 and -(1 018.2 $\pm$ 3.3) kJ.mol^{-1} for $PuO_2(OH)_2$. This study is the unique source of experimental data

for $PuO_2(OH)_2$. Konings *et al.* [141] reported the value of $\Delta_f H^\circ$ = -(567.6 $\pm$ 15.0) kJ.mol^{-1} for PuO_3. One can note that the measurement of $\Delta_f H^\circ$ is never direct as they are derives from measured reaction quantities (such as the partial vapour pression) for a given chemical reaction. Thus the validity of the results on $PuO_2(OH)_2$ and PuO_3 needs to be confirmed.

Accounting for the fact that the manipulation plutonium is neither easy or safe, a reasonable alternative is to determine the enthalpies of formation with accurate relativistic correlated quantum chemical methods.

However, simulations of such systems remain challenging and to prove the capabilities of *ab initio* methods one has to answer to the following questions:

- Is it possible to reproduce the $\Delta_f H^\circ$ value for PuO_2 ?
- Can we confirm the values of $\Delta_f H^\circ$ for PuO_3 and $PuO_2(OH)_2$?

4.1.2 Computational protocol for prediction of thermochemistry data

On the quantum chemical side, these molecules have been studied from a structural point of view but, predictions of enthalpies of formation are lacking, justifying our study.

Since our goal is to calculate the enthalpies of formation $\Delta_f H^\circ$ of different species, we need to define the target quantities. The enthalpy H is defined as:

$$H = U + pV \tag{4.1}$$

U being the internal energy of the system, p its pressure and V its volume. The enthalpy of formation of a molecule is then the change in enthalpy to form one mole of the molecule. Hess law states that the enthalpy of a given reaction is the sum of standard enthalpies of formation of products minus the sum of the reactants.

$$\Delta_r H^\circ = \sum_i \nu_i \Delta_f H^\circ \tag{4.2}$$

with ν_i the stoechiometric number.

In practice $\Delta_r H^\circ$ is calculated as:

$$\Delta_r H^\circ = \sum_i (E_i + ZPE_i + H_{corr,i}) \tag{4.3}$$

summing up the electronic energy E_i, the Zero Point Energy (ZPE) and the thermal correction to enthalpy $H_{corr,i}$.

The enthalpy of formation of the molecule of interest can thus be extracted by the computation of the $\Delta_r H^\circ$ for a chosen reaction as in the equation 4.4 and the subtraction of the known $\Delta_f H^\circ$ of the other reactants and products (see Table 4.2). For example for the reaction : A + Pu $\rightarrow$ PuX + C we can obtain $\Delta_f H^\circ$ as:

$$\Delta_f H^\circ(PuX) = \Delta_r H^\circ - \Delta_f H^\circ(A) - \Delta_f H^\circ(Pu) + \Delta_f H^\circ(C) \tag{4.4}$$

where $\Delta_f H^\circ$(Pu), $\Delta_f H^\circ$(A) and $\Delta_f H^\circ$(C) are tabulated. Sing the enthalpy of formation is path independent, the results from the reactions R_1 to R_5 should be close to each other. The average of the results will be our final $\Delta_f H^\circ$ and the mean deviation the reported error.

Since it is established that DFT is able, even for open-shell systems, to yield good geometries and vibrational frequencies that contribute to the Zero Point Energy (ZPE) and the thermal correction to the enthalpy (H_{corr}), this will be the method of choice to estimate these thermodynamic contributions. However, the accurate estimation of the electronic energy of each molecules remains the most sensitive part, in particular for Pu and its derivatives since one can expect large contributions of the electron correlation as well as the relativistic effects. This will thus concentrate most of our attention in the following paragraphs.

Among the prior theoretical investigations on Pu oxides [147–152], the only one that focussed on the trioxide and oxyhydroxide molecules is that of Boguslawski *et al.* [147] employing the spin-free DMRG method which underlines the complexity of the electronic structure of $PuO_2(OH)_2$, PuO_2 and PuO_3. This method, allowing to include all the valence orbitals in the active space for the DMRG wave-function, can indicate which orbitals are important for the description of the correlation *via* an entanglement figure (see section 4.2.3). The entanglement diagrams show that the 5f-orbitals plutonium orbitals and the p-orbitals of bonded oxygens are important for the description of the non-dynamical correlation and that the wave-function has a strong multi-reference character.

This study, however, only provides a partial picture of the problem as it lacks the treatment of SOC in order to establish the true nature of the ground state.

While there are no subsequent theoretical investigations for $PuO_2(OH)_2$ reported in the literature, for PuO_3, a study, based on CASSCF/CASPT2 + RASSI simulations by Kovacs *et al.* [148] represents a priori a good starting point for a deeper understanding of its electronic structure. Despite a different active space from what

Boguslawski *et al.* predicted, they reached an agreement on the nature ground state (spin-free $^3B_2$ in the symmetry C_{2v}).

Concerning PuO_2, its electronic structure was studied by Liao *et al.* [149], Moskaleva *et al.* [152] and Archibong *et al.* [150] using single reference approaches, U-DFT for the two first and U-CCSD(T) for the last one, and only including the scalar relativistic effects. The only theoretical study of PuO_2 including the SOC was carried out by La Macchia *et al.* [151]. While all spin-free studies (i.e all aforementioned papers including the one using DMRG) proposed that the lowest $^5\Sigma_g$ state as the molecule's ground state, La Macchia *et al.* found that the SOC effect is so important that the ground state is no longer mainly composed of the $^5\Sigma_g$, as there is a strong contribution of the $^5\Phi_u$, and that the geometry of the molecule is strongly modified compared to the spin-free on, with SOC being responsible for a decrease of the Pu-O bond length of 0.048 Å.

TABLE 4.1: $\Delta_f H^\circ$ (kJ/mol) of the different compounds given in the literature.

Molecule	References	$\Delta_f H^\circ$
PuO_2	Gotcu-Freis *et al.* [138]	-(428.7 ± 7)
	Gotcu-Freis *et al.* [138]	-(440± 7)
	Glushko *et al.* [139]	-(412 ± 20)
	Cordfunke *et al.* [140]	-(4120 ± 20)
	Konings *et al.* [141]	-(428.7 ± 20)
PuO_3	Krikorian *et al.* [146]	-(562.8 ± 5)
	Konings *et al.* [141]	-(567.6 ± 15)
$PuO_2(OH)_2$	Krikorian *et al.* [146]	-(1 018.2 ± 3.3)

The results discussed above raise a few questions that will condition our capability of computing the desired thermodynamics:

- What is the geometry and nature of ground state of PuO_2 ?
- What is the ground state electronic structure of PuO_3 and $PuO_2(OH)_2$?
- Have static and dynamical correlation effects been treated properly before?

An appealing choice would be to use four-component-based multireference methods, such as 4c-FSCC [153–155] or EOM-CC [156] to answer these questions. Unfortunately, the relativistic FSCC implementation at our disposal at this time, cannot be used to investigate PuO_3 and $PuO_2(OH)_2$; it requires that the reference wave function to be a single determinant. For these systems, such a reference is a very poor choice. For PuO_2, on the other hand, once SOC is included self-consistently in the calculation as it is done in four-component approach, the ground state can be represented by a single determinant and the CCSD(T) method (and EOM-CC) applied.

Another option would be to extend the work of Boguslawski *et al.* and include a better description of the electronic correlation, in particular the dynamic contribution, and also include the effect of the spin-orbit coupling. Recent developments make it now possible to use DMRG-SCF and DMRG-NEVPT2 to include, respectively static and dynamic correlation, with an active space up to 50 electrons in 50 orbitals. Though, SOC is still only included via State Interaction (see Section 4.2.2). Preliminary calculations, however, were not successful and require further investigation that will pursued beyond this thesis.

For these reasons, the only generally applicable method to treat such highly correlated systems in a relativistic framework is the CASPT2 method, combined with a posteriori treatment of SOC.

In this chapter, we provide a detailed description of the CASSCF approach that relies on the selection of important orbitals (active space) for the treatment of the static correlation. The choice of the active space is at the heart of this work and will be discussed in details for the three molecules.

4.2 Multireference Approaches

All the quantum chemical methods listed so far in Chapter 2 refer to single determinant wave function, thus not applicable for the foreseen multi-reference gas-phase plutonium molecules. Indeed, partial population of the valence 7s, 5f and 6d orbitals can induce significant multi-reference contributions to the wave functions and connected to the presence of quasi-degenerated electronic states, reflected by strong static correlation. We will now describe the various multi-reference methods that can account for static and dynamical correlation.

4.2.1 The ideal multi reference method: Full Configuration Interaction

The most complete way to capture electronic correlation, for the ground state or excited states, is to use the Full Configuration Interaction (FCI) method, for which the wave function is written as a linear combination of all the possible determinants created by single up to N-excitations from the HF determinant, N being the number of electrons:

$$|\psi_{FCI}\rangle = c_0 |\Phi_{HF}\rangle + \sum_{a,r} c_a^r |\Phi_a^r\rangle + \sum_{\substack{a<b \\ r<s}} c_{ab}^{rs} |\Phi_{ab}^{rs}\rangle + \sum_{\substack{a<b<c \\ r<s<t}} c_{abc}^{rst} |\Phi_{abc}^{rst}\rangle + ... \tag{4.5}$$

One recognises Φ_{HF} the HF solution the excited determinants from the HF one. Φ_a^r is a singly excited (S-type) determinant generated by the promotion of one electron from the spin orbital a to the spin orbital r; the ψ_{ab}^{rs} is a doubly excited (D-type) determinant created by the promotion of two electrons from the spin orbitals a and b to the spin orbitals r and s etc...

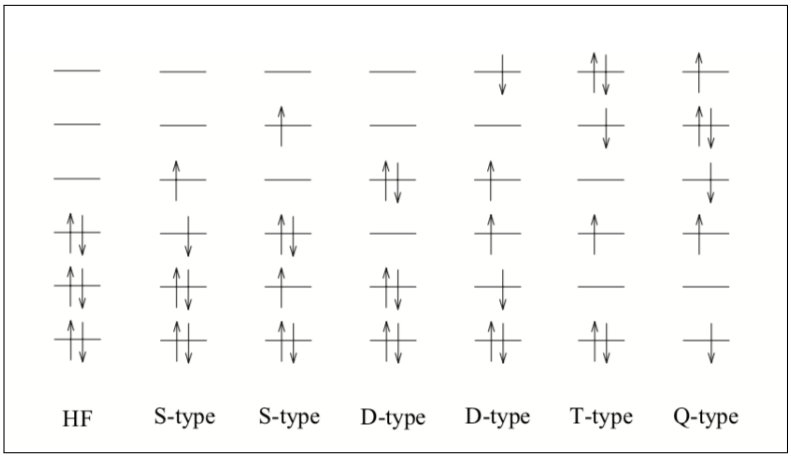

FIGURE 4.1: Various Excited Slater determinants generated from a HF reference [10]

The expansion coefficients are determined from a variational procedure in order to minimise the energy. In order to find the expansion coefficients all the possible excited determinants must be generated but also all the combinaisons of them : the Configurational State Functions (CSFs). It is the number of CSFs that will limit the use of this method. Indeed it was shown [10] that just for singlet the number of generated CSFs is:

$$\frac{M!(M+1)!}{(\frac{N}{2})!(\frac{N}{2}+1)!(M-\frac{N}{2})!(M-\frac{N}{2}+1)!} \tag{4.6}$$

M being the number of basis functions and N the number of electrons. If one takes the plutonium atom as example, the number of electron is 94 and the chosen basis set is the contracted ANO-RCC-TZP corresponding to 87 basis functions, the number of CSFs is $4.461\,424\,5 \times 10^{48}$ only for singlet configurations (!!). For this reason, one is forced to cut the number of excitations to obtain a *truncated*-CI expansion or reduce the number of determinants by selecting the orbitals that can participate into the excited determinants.

4.2.2 Multiple-steps correlated methods

Inclusion of static correlation: Complete Active Space Self Consistent Field

The main idea of the Complete Active Space Self Consistent Field (CASSCF) method is to proceed to a FCI calculation but only with a set of selected orbitals forming the so-called active space. The molecular orbitals are thus divided in three groups: the inactive orbitals, lowest in energy and doubly occupied, the active space containing at most 18 electrons in 18 active orbitals. The occupations of the active orbitals can vary between zero and two electrons. The third and last type of orbitals are the unoccupied orbitals also called virtual orbitals (see Figure 4.2) which will remain unoccupied.

CASSCF is far from "black box" being a method since the selection of the active space is in general not trivial especially due to the constraint of the number of electrons and the active obitals. The choice of active space, and making sure it accurately represents the physics of the system, represent the main challenges if this type of calculation. That said, one can follow the rules proposed by Roos *et al.* [157] to built an active space suitable for the ground state or excited states of a given system:

- the orbitals participating to the target state.
- the valence orbitals (*i.e.* first row for light atoms; 7s, 5f and 6d for an actinide atom).
- orbitals with an occupation between 0.05 and 1.95 electron from the MP2 first-order density matrix.
- if bonding orbitals are taken, the corresponding anti-bonding should be included as well.

Certainly, the number of electrons and orbitals corresponding to the point above can quickly be greater than 18. So, the choice of the orbitals to exclude is left to the appreciation of the user, nonetheless, this choice must be argued.

One solution to extend the size of the active space is to use the Restricted Active Space Self Consistent Field (RASSCF) method, Figure 4.2. The RAS1 is composed of doubly occupied orbitals, the RAS2 is the full CI active space and RAS3 includes unoccupied orbitals. A FCI will be done in the RAS2 space and excitations from RAS1 orbitals to RAS3 ones are added with a user-defined constrain on the maximum numbers of holes and particles in RAS1 and RAS3, respectively.

In order to compute the Spin-Orbit Coupling (SOC) in the system not only the ground state is needed but also some of the excited states (this need will be explain in the

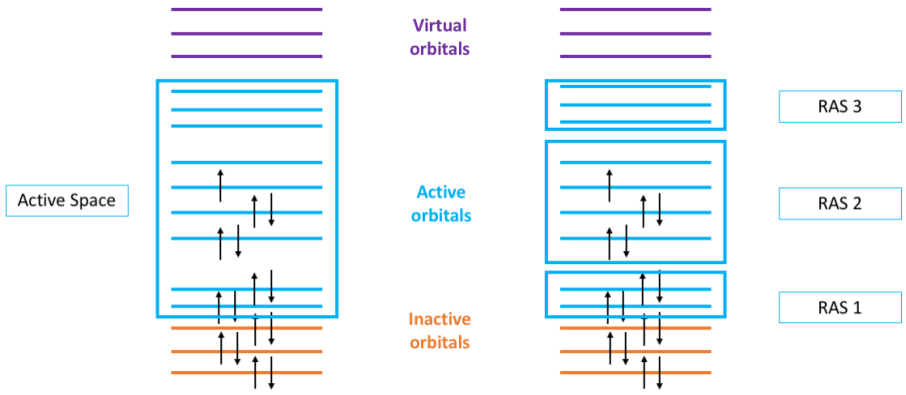

FIGURE 4.2: Representation of the CASSCF and RASSCF approaches. On the left hand side, the CASSCF method within the active space (9;9) on the right hand side, the RASSCF method with the active spaces: RAS1(4;2), RAS2(5;4);, RAS3(0,3).

section 4.2.2) that can be coupled by the SO operator. If only one state is computed at a time, we refer to a State Specific (SS) calculation, for a ground or excited state. The SS approach has the main disadvantages to be computationally expensive since a specific set of orbitals is optimised for each state. Instead, it is faster to use the SA procedure for which a set of common orbitals to several state sharing the same multiplicity and symmetry is optimised.

Note that SA-CASSCF energies will be higher than the SS ones but as we often only consider energy differences, the errors on the individual energies will compensate.

This multi-reference method CASSCF or RASSCF thoroughly includes the static electronic correlation but only a limited part of the dynamical correlation, since only double excitations are included within the active space. A rather economical way of including dynamical correlation, due to the excitations from active space to the virtual orbitals, is to use second-order perturbation theory.

Multi-Reference Perturbation Theory at the 2^{nd} order

The Complete Active Space Perturbation Theory at the 2^{nd} order or CASPT2 is, as indicated by his name a perturbative method. It allows to account for the dynamical correlation to the wave function, starting from a CASSCF calculation by adapting the MP2 approach introduced in Section 2.2.2. The contributing single and double excitations are represented in Figure 4.3. They are classified according to the number of holes and particules. It is useful to by-pass the diagonalisation problem of the

operator $\hat{H}'$. Instead of the diagonalisation of the full $\hat{H}'$ will be done by block *i.e.* for each excitation type at a time.

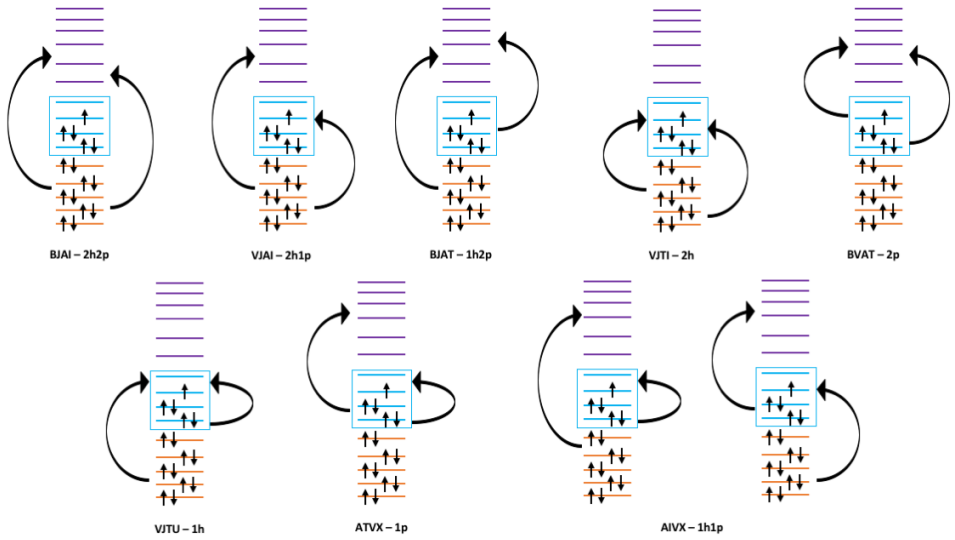

FIGURE 4.3: Representation of the possible di-excitation in CASPT2 method. NAME of the excitation in CASPT2 method - number of ***h***oles (electron(s) outside the active space promoted to the active or virtual orbitals) number of ***p***article (electron occupying a virtual orbital - outside the active space - after the perturbation).

Originally, the Hamiltonian used was the Zeroth-Order Hamiltonian with the standard Fock matrix formulation [158]:

$$\hat{H}_0 = \hat{P}_0\hat{F}\hat{P}_0 + \hat{P}_k\hat{F}\hat{P}_k + \hat{P}_{SD}\hat{F}\hat{P}_{SD} + \hat{P}_{TQ\ldots}\hat{F}\hat{P}_{TQ\ldots} \tag{4.7}$$

where $\hat{P}_0$ in the projector on the one-dimensional space V_0, spanned by the CAS reference wave function ϕ_0 under consideration, $\hat{P}_k$ is the projector on the space V_k, spanned by the orthogonal complement to ϕ_0 in the restricted FCI subspace used to generate the CAS wave function. $\hat{P}_{SD}$ is the projector on the space V_{SD}, spanned by all the single and double replacement states generated from V_0, finally $\hat{P}_{TQ\ldots}$ in the projector on the space V_{TQ}, spanned by all higher excitation not included in V_k and V_{SD}.

This formulation raises the intruder state problem [159]. When excited determinants are close in energy to the reference ones, their contribution will diverge due to a denominator approaching zero. Those intruder states can be spotted by a low (< 0.60)

value of the weight of the CAS/RAS wave function in the final wave function. To eliminate this problem a level shift of the active orbitals was introduced. Based on the Ionisation Potential (IP) and Electronic affinity (EA) [160], the IPEA shift was determined thanks to a benchmark on atomic data. During our study IPEA value was kept at its default value: 0.25 a.u.. Since it is known that the higher states are much more sensitive to the value of the level shift [159] it was decided to use the available "imaginary shift". It actually uses real quantities to treat the potential energy function differently from the IPEA level shift in order to reduce the sensitivity of the energies to the size of the imaginary shift. It was fixed at 0.05 a.u., the smallest value reported by Forsberg *et al.* [159] to reach accurate results.

Finally, another possibility to fix the problem of intruder states is to use the Hamiltonian by Angeli *et al.* [161] which is based on the generalised zeroth order Hamiltonian by Dyall [162]. It behaves as a true many-body Hamiltonian inside the CAS subspace, including all two-electrons interactions, while the CASPT2 method uses the monoelectronic Fock Hamiltonian. N-Electron Valence state Perturbation Theory at the 2^{nd} order (NEVPT2) method is intrinsically intruder state free; however, current implementations limit its use to active spaces of 14 electrons in 14 orbitals, thus inapplicable to our systems.

A posteriori treatment of spin orbit coupling : the RASSI method

The Restricted Active Space State Interaction (RASSI) methods is able to compute the coupling elements for any one-electron operator between CASSCF/RASSCF wavefunction that can be non-orthogonal. In our case, the one-electron operator is SOC, computed with the atomic mean field spin-orbit operator described by equation 2.106 in Section 2.4.3, that couples states of different spins and spatial symmetries. In order to also include the dynamical correlation, the method was adapted by Malmqvist *et al.* [163] to use the CASPT2 wave-functions as basis. So the diagonal RASSI matrix [65] is dressed with the CASPT2 energies while the spin orbit matrix elements (V_{SO}) appear as off-diagonal elements. The so-constructed matrix is diagonalised to obtain the SO-eigenstates.

The lowest eigenvalue is the energy of ground state at spin-orbit CASPT2 (SO-CASPT2) level. Every SO-state is expressed as a linear combinaison of the Spin-Free (SF) states that constituted the basis. The SOC contribution to the molecule total energy is thus energy difference between the lowest SO state and the lowest SF state.

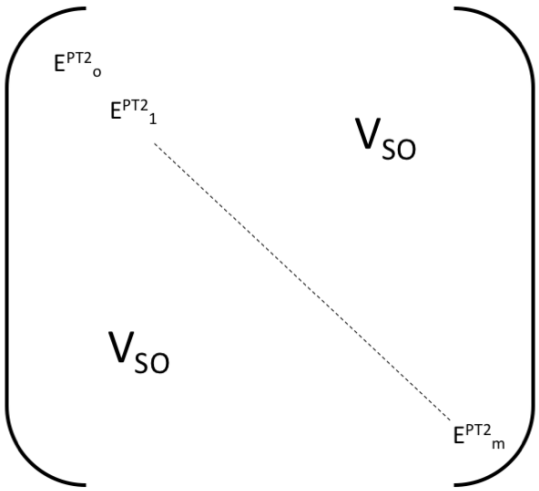

FIGURE 4.4: Matrix representation with, in diagonal, the CASPT2 energies and outside the diagonal, the spin orbit element.

4.2.3 Opening the active spaces to include electronic correlation: the Density Matrix Renormalisation Group

TABLE 4.2: $\Delta_f H^\ominus$ of the different compounds given in kJ/mol

Species	$\Delta_f H^\ominus$	$\Delta\Delta_f H^\ominus$
O (^{3}P)	249.23 [164]	0.00
H (^{1}S)	218.00 [165]	0.01
Pu (^{5}F)	349.00 [166]	3.0
H_2 (1S)	0.00[165]	0
H_2O	-241.81[164]	0.03
H_2O_2	-135.88 [167]	
O_2	0.00[165]	0.00
OH	37.36 [164]	0.13

4.3 Technical Considerations and Computational details

4.3.1 Geometries, enthalpic corrections and basis sets

The first information a computational chemist needs is the geometry of the system under study. In our case, all the geometries (except PuO_2 see section 4.3.1) were optimised with DFT (see section 2.3) and the B3LYP functional [168, 169] using the GAUSSIAN09 [170] package. The plutonium atom was described by a relativistic effective core potential (RECP) ECP60MWB [171] with the corresponding basis set of

TABLE 4.3: Reactions used to calculate $\Delta_r H^\circ$

	PuO_2	PuO_3	$PuO_2(OH)_2$
R_1	$Pu + O_2 \longrightarrow PuO_2$	$Pu + \frac{3}{2} O_2 \longrightarrow PuO_3$	$Pu + O_2 + 2H_2 \longrightarrow PuO_2(OH)_2$
R_2	$Pu + 2O \longrightarrow PuO_2$	$Pu + 3O \longrightarrow PuO_3$	$Pu + 4O + 2H \longrightarrow PuO_2(OH)_2$
R_3	$Pu + H_2O_2 \longrightarrow PuO_2 + H_2$	$Pu + \frac{3}{2} H_2O_2 \longrightarrow PuO_3 + \frac{3}{2} H_2O$	$Pu + 3H_2O_2 \longrightarrow PuO_2(OH)_2 + 2H_2O$
R_4	$Pu + OH \longrightarrow PuO_2 + 2H$	$Pu + 3OH \longrightarrow PuO_3 + 3H$	$Pu + 4OH \longrightarrow PuO_2(OH)_2 + 2H$
R_5	$Pu + 2H_2O \longrightarrow PuO_2 + 2H_2$	$Pu + 3H_2O \longrightarrow PuO_3 + 3H_2$	$Pu + 4H_2O \longrightarrow PuO_2(OH)_2 + 2H_2$

quadruple ζ [71] quality, while for the lighter atoms by augmented triple ζ (aug-cc-pVTZ) basis sets were used. This basis set quality is known to reproduce properly the geometries and the enthalpic corrections. All the geometries are available in Annex A. The calculation of harmonic frequencies is necessary to compute the zero point energy (ZPE) and the thermal corrections to the enthalpy of equation 4.3 and the entropy. Anharmonic frequencies were also computed but no significant difference in the value of the entropies S were seen in comparison to the harmonic ones, thus only contributions obtained at the harmonic level were kept.

Once the geometries of the different molecules were obtained and to reach accurate electronic energies for the determination of $\Delta_f H^\circ$, two methods were used. The first is the UCCSD(T) method which represents the gold standard for single-reference wave function. The second is the multi-reference wave-function method that involves CASSCF plus CASPT2 calculations to check whether the wave function has a multi-reference character or not. In both cases, the scalar relativistic effects are included via the DKH2 Hamiltonian and the SOC was calculating with the RASSI procedure and added to the UCCSD(T) and CASPT2 spin free energies. All atoms are described with the ANO-RCC basis sets [172, 173] with qualities sequentially increased from triple-ζ (n=3) to quadruple-ζ (n=4) to extrapolate the energies to the CBS limit with the total energy extrapolation (CBS-TE) and the extrapolation separating the uncorrelated and correlated energies (CBS-CE). The two extrapolation methods yield to small differences of a few kJ.mol^{-1} for the reaction energies.

Geometry of PuO_2

Because of disagreement in literature [147, 149, 152, 174] concerning the distance Pu-O and the nature of the ground state, a more accurate exploration of the potential energy surface was needed. It was first done with the State Specific-Spin-Free-CASPT2 method for the lowest quintet A_g and A_u states in D_{2u} symmetry. Scanning distances from 1.724Å to 1.884Å in steps of 0.02 Å.

In addition to the CASPT2 calculations, Andre Gomes performed calculations based on the molecular mean-field [175] approximation to the Dirac–Coulomb ($^2DC^M$)

Hamiltonian, at MP2, CCSD and CCSD(T) [176, 177] levels of theory with the DIRAC electronic structure code [178] using $D_{\infty h}$ symmetry. The Dyall basis sets [179, 180] of triple- and quadruple-zeta qualities were employed for the plutonium atom, and Dunning's aug-cc-pVXZ (X=T, Q) sets[181] for the oxygen atoms. In all calculations, the $(SS|SS)$-type two-electron integrals were approximated by a point-charge model [182]. Electrons in molecular spinors with energies comprised between -3 and 100 au were included in the correlated treatment, which amounted to correlating 28 electrons for PuO_2.

The SCF calculations were closed-shell ones, with 52 and 58 electrons in g and u irreducible representations, respectively. The equilibrium structure and spectroscopic constants for each electronic structure method were determined via a polynomial fit of the potential energy surface constructed from single-point calculations for Pu-O internuclear distances between 1.750 Å and 1.880 , in steps of 0.005 . Energies and potential energy curves at the complete basis set limit were obtained with the two-point extrapolation (see equation 2.121).

4.3.2 Results of the single-reference gold standard method: UCCSD(T)

The UCCSD(T) [183] calculations were performed with the Molpro Quantum Chemistry software [156]. The frozen orbitals were the 1s orbital of O and 1s to 5d (included) orbitals of Pu. No core-valence correlation was considered here due to the excessive computational cost and that we expect them not to exeed few kJ mol^{-1} for actinide molecules [184].

In order to look at the influence of the inclusion of the spin-orbit *a priori*, ^{2}DC^M-CCSD(T) calculation were performed (by Andre Gomes). It could be done on Pu, PuO_2, H_2, OH, H_2O and H_2O_2 allowing us to obtain the energies for reactions R_3, R_4 and R_5 for PuO_2. The setup from the PES exploration of PuO_2 was kept (see Section 4.3.1).

In addition, thanks to the recent implementation made by Andre Gomes used recent implementation in DIRAC code [185] of variant of EOM-CCSD, we were able to compute the ionization potential for atomic Pu and PuO_2 (EOM-IP-CCSD) and the excitation energies (EOM-EE-CCSD) for PuO_2.

In the case of EOM-IP-CCSD for Pu, we requested the number of states as follows: five $\Omega = 1/2_g$, two $\Omega = 3/2_g$, one $\Omega = 5/2_g$, three $\Omega = 1/2_u$, two $\Omega = 3/2_u$ and one $\Omega = 5/2_u$, whereas for PuO_2 we requested two $\Omega = 1/2_g$, one $\Omega = 3/2_g$, three $\Omega = 1/2_u$, two $\Omega = 3/2_u$ and one $\Omega = 5/2_u$ states. In the case of EOM-EE-CCSD

we requested the number of states as follows: six $\Omega = 0_g$, four $\Omega = 1_g$, three $\Omega = 2_g$, two $\Omega = 3_g$, one $\Omega = 4_g$, one $\Omega = 5_g$, ten $\Omega = 0_u$, nine $\Omega = 1_u$, seven $\Omega = 2_u$, five $\Omega = 3_u$, three $\Omega = 4_u$, and one $\Omega = 5_u$.

4.3.3 Multi-reference calculations: Actives Spaces, Number of States and Shifts

Actives spaces

All the multi-reference wave-function calculations were performed with the MOLCAS software [186]. As previously mentioned the choice of active space is crucial since a poor choice of active space can lead not only to poor accuracy but to false results. The easiest choice of active space is the one for the atomic plutonium. One would be tempted to wisely but simply consider the 5f-orbitals. The Paris-Sud database [167] reports the nonet ^{9}H, involving the 6d and 7s orbitals, as the closest in energy to the septuplet ground state. Thus the former orbitals were also included to lead to an active space of 8 electrons in 13 orbitals (8,13). First calculations yield for the appearance of a spurious orbital in the CAS, making us reconsider our previous active space. Finally, we proposed the following organisation: the 7s orbital in the RAS1 with 1 hole allowed, the 5f orbitals in the RAS2 and the 6d orbitals in the RAS3 with one particule permitted. Concerning the molecules with no plutonium atom, the active space is simply composed of the oxygen valence orbitals. For those molecules, spin-orbit coupling was not imputed as it is expected to be negligible.

Concerning the plutonium oxides and oxyhydroxides, the choice of the active space was guided by the DMRG study of Boguslawski *et al.* [147], to which our research team contributed. This study followed the rules laid out in the Section 4.2.2 to define the 'full valence" space. The analysis of the entanglement diagrams lead to the definition of "optimal active spaces" listed in Table 4.4.

TABLE 4.4: Full active space and optimal active space presented in the article of Boguslawski *et al.* [147]

Molecules	Full Valence	Optimal Active Space
PuO_2	(28,25)	(18,17)
PuO_3	(34,26)	(14,14)
$PuO_2(OH)_2$	(42,35)	(20,22)

Note that neither orbital optimisation nor SOC were included in [147]. The suggested optimal active space for $PuO_2(OH)_2$ is too large for the CASSCF method.

Instead, we restricted ourselves to a minimal active space of 2 electrons in 4 orbitals (see Figure 4.5). Concerning PuO_3 and PuO_2 attempts to use the optimal active spaces was made but turned out unsuccessful as these are suited for the ground state only but do not apply for the excited states. Thus the active spaces had to be modified.

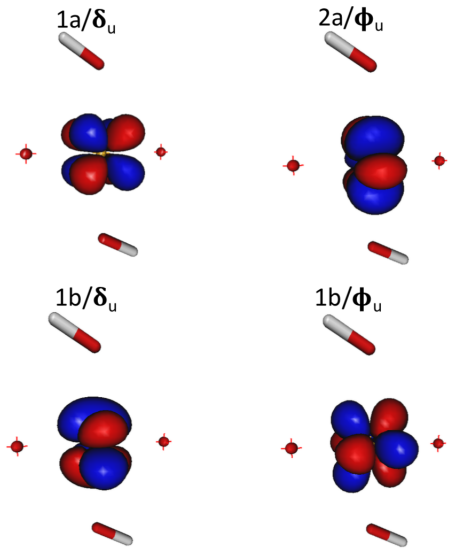

FIGURE 4.5: Molecular orbitals of $PuO_2(OH)_2$ at the CASSCF level. Isosurface = 0.05 a.u.

- **PuO_2 active space**

For PuO_2, the optimal active space matches the MO diagram of the uranyl moleculeproposed by Denning *et al.* [187]. This paper emphasised the mixing of the 5f, 6d and the 2p-orbitals of the oxygens, thus a chemically relevant model should include (14, 18) which is already approaching the limit of the CASSCF code. Moreover we would like to add the 7s orbitals that have been proven important for the description of plutonium and for PuO_2 [147], bringing the active space to 16 electrons in 19 orbitals, which is undoable.

After a close look at the DFT-B3LYP results for PuO_2, it appears that the lowest orbitals of the (16;19) active space are the degenerate π_g orbitals formed by the combination of Pu's 6d and oxygen 2p-orbitals. These orbitals did not appear as strongly entangled to the other valence orbitals in the entanglement diagram on the Figure 3 in [147] and can thus be eliminated from the active space cutting it down to a CAS(12, 17) (see Table 4.5 for details). This is slightly larger than the one used in the study of La Macchia *et al.* but the results can still be comparable.

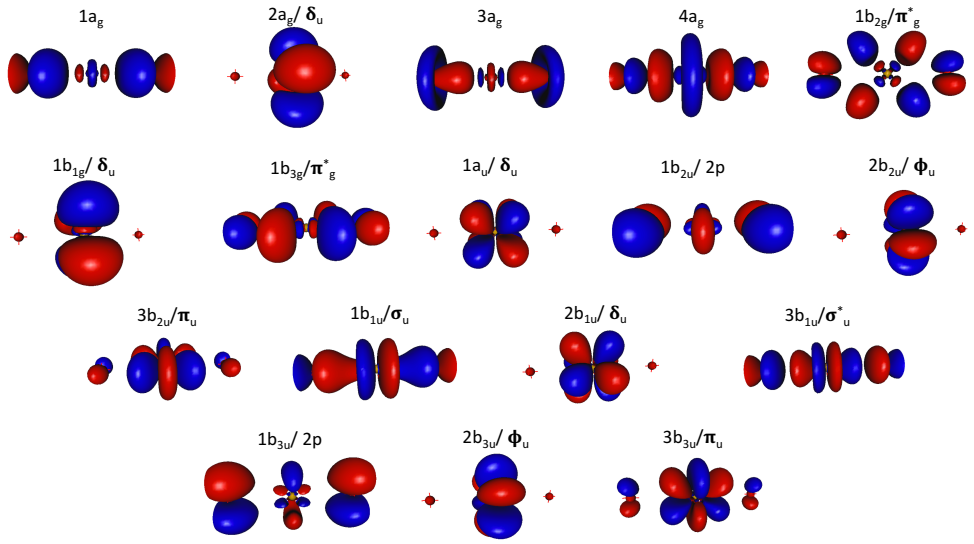

FIGURE 4.6: Molecular orbitals of PuO_2 at the CASSCF level; Isosurface = 0.05 a.u.

TABLE 4.5: Active spaces for the various plutonium oxides and oxyhydroxides.

Molecule	Active Space (electron, orbitals)	Orbitals
PuO_2	(12,17)	$\pi_u(2)$, $\pi_g(2)$, σ_g, σ_u, $\pi^*_u(2)$, $\pi^*_g(2)$, σ^*_g, σ^*_u, $f_\delta(2)$, $f_\phi(2)$
PuO_3	(14,13)	$1a_1$, $2a_1/\pi_u$,$2a_1$, $4a_1/p^o_x$,$5a_1/\phi_u$, $6a_1/\pi_u$, $1b_1/\phi_u$, $2b_1/\pi_u$, $1b_2/p^o_z$,$2b_2/\sigma_u$, $3b_2/\delta_u$, $4b_2/\sigma^*_u$, $1a_2/\delta_u$
$PuO_2(OH)_2$	(4,4)	$1a/\delta$, $2a/\phi$, $1b/\delta$, $2b/\phi$
Pu	(8,13)	7s, 5f, 6d
O	(6,4)	2s, $2p_x$, $2p_y$, $2p_z$
O_2	(12, 8)	σ_{2s}, σ^*_{2s}, $\sigma_{2p}(3)$, $\sigma^*_{2p}(3)$
OH	(7,5)	σ, σ_{nb}, $2p^O_x$, $2p^O_y$, σ^*,
H_2O_2	(14, 10)	1 σ^{O-O}, 1 σ^{*O-O}, σ^{O-H} (2), 2 σ^{O-O}, π^{O-O}, $2p^O$, $1\sigma^{*O-O}$, $\sigma^{O-H}(2)$
H_2O	(8,6)	$2a_1$,$1b_2$, $3a_1$, $1b_1$, $4a_1$, $1b_2$
H_2	(2, 2)	σ,σ^*
H	(1,1)	1s

- **PuO_3 active space**

Concerning PuO_3, from a chemical view point, assuming Pu to be in oxidation state (VI), we can depict it as a plutonyl PuO_2^{2+} in interaction with a O^{2-} anion. Thus from the PuO_2 active space we selected all the orbitals that could mix with the 2p-orbitals of the apical oxygen, leading to an active space of 12 electrons in 10 orbitals ($2p_x$ and $2p_z$ of the oxygen plus the $2b_{2u}/\phi_u$, $2b_{3u}/\phi_u$, $1b_{1u}/\sigma_u$, $2b_{1u}/\delta_u$, $3b_{1u}/\sigma^*_u$, $1a_u/\delta_u$,

TABLE 4.6: Totale energy of the ground state of Pu, PuO_3 and $PuO_2(OH)_2$ for different value of the imaginary shift.

Molecule	0.01	0.05	0.01	No Imaginary shift
Pu	-29539.80490586	-29539.80507744	-29539.80592767	-29539.80604535
PuO_3	-29765.45793749	-29765.45814830	-29765.45837134	-29765.45737950
$PuO_2(OH)_2$	-29841.93260283	-29841.93266384	-29841.93267515	-29841.93267545

$3b_{3u}/\pi_u$ and $3b_{3u}/\pi_u$ of PuO_2). It is enough for the description of the ground state but not for the excited states. Thus, 2 electrons and 3 orbitals (corresponding to the $1a_g$, $1b_{2u}$/2p and the visible of Figure 4.6 and the $1a_g$ of Figure 4.7) were added to obtain the active space mentionned in the Table 4.5 or in Figure 4.7.

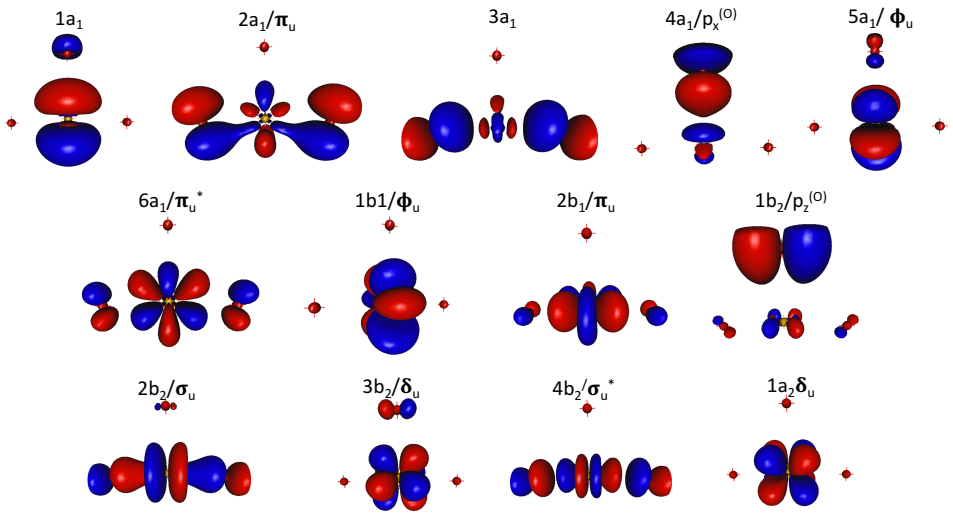

FIGURE 4.7: Active CASSCF orbitals of PuO_3 at the CASSCF level; Isosurface = 0.05 a.u.

- **CASPT2 - Numbers of state computed**

The number of states that are computed at CASSCF levels was dependent on the number of states that could be described properly (with a significant (> 0.6) reference weight) at the CASPT2 level. To keep high reference weights, beside the default IPEA value (0.25 a.u.), an imaginary shift had to be added. Indeed the Molcas manual recommends its use to improve the description of CASPT2 excited states results when transition metals or actinides are involved to avoid intruder state problems. Since the computation of PuO_2 is quite expensive, tests on the value of the imaginary shift was done on Pu, PuO_3 and $PuO_2(OH)_2$ only with smaller active spaces, (6,7), (12,10) and (2,4) for Pu, PuO_3 and $PuO_2(OH)_2$, respectively.

As shown in [159] the total energy is barely modified and the minimal value of the shift with noticeable effect on the description of the excited states is 0.05 a.u.. This

is the value kept in all the CASPT2 calculations since the 0.01 does not increase the number of states properly described and the value 0.1 impact the total energies and the excitation energies.

TABLE 4.7: Number of electronic states at CASSCF level of calculations

Multiplicity	Pu (C_i)	PuO_2 (D_{2h})								PuO_3 (C_{2v})				$PuO_2(OH)_2$ (C_2)	
symmetry	A_g	A_g	B_{2g}	B_{1g}	B_{3g}	A_u	B_{2u}	B_{1u}	B_{3u}	A_1	B_1	B_2	A_2	A	B
Singulet	0	5	5	5	5	5	5	5	5	20	20	20	20	7	4
Triplet	50	5	10	10	10	7	10	7	10	20	20	20	20	2	4
Quintuplet	120	5	5	5	5	5	5	5	5	20	20	20	20	0	0
Septuplet	110	0	0	0	0	0	0	0	0	0	0	0	0	0	0
Nonet	35	0	0	0	0	0	0	0	0	0	0	0	0	0	0

TABLE 4.8: Number of electronic states at CASPT2 level of calculations

Multiplicity	Pu (C_i)	PuO_2 (D_{2h})								PuO_3 (C_{2v})				$PuO_2(OH)_2$ (C_2)	
symmetry	A_g	A_g	B_{2g}	B_{1g}	B_{3g}	A_u	B_{2u}	B_{1u}	B_{3u}	A_1	B_1	B_2	A_2	A	B
Singulet	0	2	0	2	0	3	3	3	3	10	9	7	7	7	4
Triplet	27	2	3	3	3	6	7	6	7	16	15	13	14	2	4
Quintuplet	113	4	3	2	3	4	4	4	4	8	7	6	7	0	0
Septuplet	103	0	0	0	0	0	0	0	0	0	0	0	0	0	0
Nonet	35	0	0	0	0	0	0	0	0	0	0	0	0	0	0

Concerning the number of states included in the CASPT2, all of the 16 states were incorporated for $PuO_2(OH)_2$. Nonetheless, it was not possible for the atom of Pu or for the di and tri oxides (see Table 4.9). Thus we set a limit at 3 eV from the ground state for PuO_3 and only 2 eV for Pu and PuO_2. Even if these limits can seem arbitrary, they ensure a good description of all states introduced in the SO-RASSI calculations and which couple to the spin-free ground states.

TABLE 4.9: Number of states available for computation and states taken for computation for the plutonium atom and the various plutonium oxides and oxyhydroxides.

	Pu	PuO_2	$PuO_2(OH)_2$	PuO_3
Number of available states	20 825	136 634 576	16	2 740 106
Number of states included in RASSI	278	81	16	119

TABLE 4.10: Fine structure transition energies (cm^{-1}) of atomic Pu computed at the SO-CASPT2 with the ANO-RCC-TZVP basis set, and analysis of the various J-states in terms of the dominating LS terms.

Exp.[188–190]	This work	J-value	Weight of LS states
0	0	0	54% ^7F , 38% ^5D , 7% ^3P
2204	1806	1	64% ^7F , 32% ^5D
4300	4208	2	82% ^7F , 17% ^5D
6145	6353	3	88% ^7F , 10% ^5D
7775	8091	4	93% ^7F
9179	9552	5	90% ^7F
10 238	11 010	6	85% ^7F , 10% ^5G
9773	12 499	0	44% ^7F , 21% ^5D , 8% ^3P
13 528	13 612	1	66% ^9H , 9% ^7F , 7% ^7G

4.4 Results and Discussions

4.4.1 Electronic Structures Analysis

Atomic Pu

To compute the enthalpies of formation of the plutonium molecules, an accurate description of the plutonium atom, i.e. its electronic structure, is mandatory. Thus, in Table 4.10 (the higher excited states can be found in the Appendix B), the SO-CASPT2 calculations are reported and compared to available data from the literature [188–190]. The *ab initio* energy levels are able to accurately reproduce the experimental assignments with errors between 91 and 397 cm^{-1} for the first five excited states under 9500 cm^{-1}. Deviations between our results and the available data appear after the sixth state. The experimental assignment predicts the sixth state at 9773 cm^{-1} with a $J = 0$ while such state is found at 12 488 cm^{-1} in the current study though uncertainties remain for the attribution of this electronic state. The computed seventh state with $J = 6$ is about 800 cm^{-1} higher energy than the experimental value. Looking closely at the nature of the Pu low-lying states, one can first notice the remarkable mixing between the ^7F, ^5D and ^3P spin-orbit free states and that the contribution of the ^5D state decreases as the energy increases. Finally, the most important result is the overall good reproduction of the SO splitting of ^7F spin-free state, making us confident for the exploration of the other plutonium molecules.

PuO_3 and $PuO_2(OH)_2$

For PuO_3, at the spin-orbit level, we report the description of the ground state and the six lowest excited states in Table **??**, (the higher excited states can be found in the Appendix B). It is noteworthy that the $1a_g$, $2a_g/\delta_u$ and $3a_g$ orbitals are doubly occupied in all the calculated spin-free states. The PuO_3 orbitals are composed of a mixture of orbitals belonging to the plutonyl subunit and the distant oxygen. Thus, for the sake of clarity, we labelled these orbitals with the labels associated to those of the PuO_2^{2+} ion (with linear energy D_{2h} notations), and those of the distant oxygen atom are denoted by $p^{(O)}_{x,y,z}$. The SO ground state is composed of 47% $^3B_2$, 24% $^3A_2$ and 14% $^3B_1$ spin-free states. The composition is similar to the one previously reported by Kovács [191] (52% $^3B_2$ and 24% $^3A_2$). More striking is the difference between our computed vertical excitation energies with that of Kovács's SO-CASPT2 spectrum [191]. While we predict the first excited state to be at 1235 cm^{-1}, he places it at 471 cm^{-1}. The overall determined spectrum from our calculations is much denser and lower by about 4000 cm^{-1} than his. Such discrepancy may find its origin in the description of the spin-free states. We agree with Kovács that the spin-free ground state has $^3B_2$ symmetry, though with a different orbital character. Indeed, the $^3B_2$ exhibits a strong multi-determinantal character with 57% corresponding to the configuration in which the $4a_1/p^{(O)}_z$ and $2b_2/\sigma_u$ orbitals are doubly occupied (See Table **??** and Figure 4.7) and the singly occupied orbitals $5b_1/\Phi_u$, $1b_2/p^{(O)}_z$, $3b_2/\delta_u$ and $1a_2/\delta_u$ and 22% from the electronic configuration in which of the $4a_1/p^{(O)}_z$, $1b_2/p^{(O)}_z$ and $2b_2/\sigma_u$ orbitals are doubly occupied and the $5b_1/\Phi$ and $1a_2/\delta_u$ singly occupied. Kovács, however, finds the ground state to be mainly composed of plutonyl orbitals (79%). Such a difference can be explained by the fact that the considered active spaces are different (a CAS(10,16) in his case and CAS(14,13) in our work). Looking closely at the entanglement diagram of PuO_3 derived from DMRG calculations [147] (Figure 6a, Full-Valence CAS) there is a strong correlation within the non-bonding plutonyl-like orbitals ($5f_\delta$, $5f_\phi$) and also between the $b_2/p^{(O)}$ and the $5f_{\delta_u}$ orbitals, in agreement with our analysis of the $^3B_2$ ground-state wave function.

Concerning $PuO_2(OH)_2$, the low energy part of the vertical spectrum including SO coupling reported in the Table **??** shows two close-lying states separated by about 323 cm^{-1}, followed by a state at 2222 cm^{-1}. The analysis of the two lowest states shows that they correspond to a fifty-fifty combination of $^3A(1)$ and $^3B(1)$ spin-free states, with a small contribution (6% in each case) of the $^3B(2)$. The next three states also have strong SO-mixings between triplet states but also singlet excited states of $^1A(1)$ and $^1B(1)$ symmetries, placed at the spin-free level at about 5764 and 7444 cm^{-1}, respectively.

TABLE 4.11: Lowest electronic levels in cm^{-1} of PuO_3, computed at the SF-CASPT2 and SO-CASPT2 levels with the ANO-RCC-TZVP basis set, and analysis of the various states.

	No.	Term Symbol	ΔE	Character : % [orbital(number of electron)]
SF	1	$^3B_2(1)$	0	36% [$4a_1/p^{(O)}(2)$, $1b_1/\Phi_u(1)$, $1b_2/p^{(O)}(\bar{1})$, $2b_2/\sigma_u(2)$, $3b_2/\delta_u(1)$, $1a_2/\delta_u(1)$]
				21% [$4a_1/p^{(O)}(2)$, $1b_1/\Phi_u(1)$, $1b_2/p^{(O)}(1)$, $2b_2/\sigma_u(2)$, $3b_2/\delta_u(\bar{1})$, $1a_2/\delta_u(1)$]
				22% [$4a_1/p^{(O)}(2)$,$1b_1/\Phi_u(1)$,$1b_2/p^{(O)}(2)$,$2b_2/\sigma_u(2)$,$1a_2/\delta_u(1)$]
	2	$^3A_2(1)$	3161	43% [$4a_1/p^{(O)}(2)$, $5a_1/\Phi_u(1)$,$1b_2/p^{(O)}(\bar{1})$,$2b_2/\sigma_u(2)$,$3b_2/\delta_u(1)$,$1a_2/\delta_u(1)$]
				23% [$4a_1/p^{(O)}(2)$, $5a_1/\Phi_u(1)$,$1b_2/p^{(O)}(1)$,$2b_2/\sigma_u(2)$,$3b_2/\delta_u(\bar{1})$,$1a_2/\delta_u(1)$]
				17% [$4a_1/p^{(O)}(2)$, $5a_1/\Phi_u(1)$,$1b_2/p^{(O)}(2)$,$2b_2/\sigma_u(2)$,$1a_2/\delta_u(1)$]
	3	$^3B_1(1)$	4663	38% [$4a_1/p^{(O)}(2)$,$5a_1/\Phi_u(1)$,$1b_1/\Phi_u(1)$,$1b_2/p^{(O)}(\bar{1})$,$2b_2/\sigma_u(2)$,$3b_2/\delta_u(1)$]
				12% [$4a_1/p^{(O)}(2)$, $5a_1/\Phi_u(1)$, $2b_1/\pi_u(1)$,$1b_2/p^{(O)}(\bar{1})$,$2b_2/\sigma_u(2)$,$3b_2/\delta_u(1)$]
				12% [$4a_1/p^{(O)}(2)$, $5a_1/\Phi_u(1)$,$1b_1/\Phi_u(1)$,$2b_1/\pi_u(2)$,$1b_2/p^{(O)}(2)$]
	4	$^1A_1(1)$	7239	32% [$4a_1/p^{(O)}(2)$,$1b_2/p^{(O)}(1)$,$2b_2/\sigma_u(2)$,$3b_2/\delta_u(\bar{1})$,$1a_2/\delta_u(2)$]
				28% [$4a_1/p^{(O)}(2)$,$1b_2/p^{(O)}(2)$,$2b_2/\sigma_u(2)$,$1a_2/\delta_u(2)$]
				11% [$4a_1/p^{(O)}(1)$, $5a_1/\Phi_u(\bar{1})$,$1b_2/p^{(O)}(2)$,$2b_2/\sigma_u(2)$,$1a_2/\delta_u(2)$]
	5	$^3A_2(2)$	7287	20% [$4a_1/p^{(O)}(2)$,$1b_1/\Phi_u(1)$,$1b_2/p^{(O)}(1)$,$2b_2/\sigma_u(2)$,$3b_2/\delta_u(2)$]
				18% [$4a_1/p^{(O)}(1)$,$5a_1/\Phi_u(\bar{1})$,$1b_1/\Phi_u(1)$,$1b_2/p^{(O)}(2)$,$2b_2/\sigma_u(2)$,$3b_2/\delta_u(1)$]
				17% [$4a_1/p^{(O)}(2)$,$1b_1/\Phi_u(1)$,$1b_2/p^{(O)}(2)$,$2b_2/\sigma_u(2)$,$3b_2/\delta_u(1)$]
	6	$^3B_1(2)$	8038	31% [$4a_1/p^{(O)}(1)$,$5a_1/\Phi_u(\bar{1})$,$1b_2/p^{(O)}(2)$,$2b_2/\sigma_u(2)$,$3b_2/\delta_u(1)$,$1a_2/\delta_u(1)$]
				11% [$4a_1/p^{(O)}(2)$,$5a_1/\Phi_u(1)$,$2b_1/\pi_u(1)$,$1b_2/p^{(O)}(\bar{1})$,$2b_2/\sigma_u(2)$,$3b_2/\delta_u(1)$]
				10% [$4a_1/p^{(O)}(2)$,$1b_2/p^{(O)}(2)$,$2b_2/\sigma_u(2)$,$3b_2/\delta_u(1)$,$1a_2/\delta_u(1)$]
				10% [$4a_1/p^{(O)}(2)$,$1b_1/\Phi_u(1)$,$2b_1/\pi_u(1)$,$1b_2/p^{(O)}(\bar{1})$,$2b_2/\sigma_u(2)$,$1a_2/\delta_u(1)$]
SO		X	0	47% $^3B_2(1)$ + 24% $^3A_2(1)$ + 14% $^3B_1(1)$
		a	1235	59% $^3B_2(1)$ + 25% $^3A_2(1)$
		b	1783	73% $^3B_2(1)$
		c	3777	51% $^3A_2(1)$
		d	5660	24% $^3B_1(1)$ + 18% $^1A_1(1)$ + 17% $^3A_2(2)$ + 10% $^3B_1(2)$

TABLE 4.12: Lowest electronic levels in cm^{-1} of $PuO_2(OH)_2$, computed at the SF-CASPT2 and SO-CASPT2 levels with the ANO-RCC-TZVP basis set, and analysis of the various states.

	State	ΔE	Character : % [orbital(number of electron)]
SF	$^3B(1)$	0	49% [2a/Φ_u(1) ,1b/δ_u(1)]
			48% [1a/δ_u(1) , 2b/Φ_u(1)]
	$^3A(1)$	889	41% [1a/δ_u(1) , 2a/Φ_u(1)]
			59% [1b/δ_u(1) , 2b/Φ_u(1)]
	$^3B(2)$	2136	75% [1a/δ_u(1) , 1b/δ_u(1)]
			20% [2a/Φ_u(1) , 2b/Φ_u(1)]
	$^3A(2)$	4698	59% [1a/δ_u(1) , 2a/Φ_u(1)]
			41% [1b/δ_u(1) , 2b/Φ_u(1)]
	$^3B(3)$	5351	52% 2a/Φ_u(1), 1b/δ_u(1)
			46% [1a/δ_u(1), 2b/Φ_u(1)]
	$^1A(1)$	5764	[58% 1b/δ_u(1) , 2b/$\Phi_u(\bar{1})$]
			30% [1a/δ_u(1) , 2a/$\Phi_u(\bar{1})$]
			5%[2a/Φ_u(2)]
	$^1B(1)$	7444	50% [1a/δ_u(1), 1b/$\delta_u(\bar{1})$]
			28% [2a/Φ_u(1), 2b/$\Phi_u(\bar{1})$]
			16%[1a/δ_u(1), 2b/$\Phi_u(\bar{1})$]
	$^1A(2)$	9626	39% [1a/δ_u(1) , 2a/$\Phi_u(\bar{1})$]
			29 % [2a/Φ_u(2)]
			13% [1b/δ_u(1) , 2b/$\Phi_u(\bar{1})$]
			10% [1a/δ_u(2)]
			7 %[2a/Φ_u(2)]
SO	X	0	46% $^3A(1)$, 41% $^3B(1)$, 6% $^3B(2)$
	a	323	45.% $^3B(1)$, 45% $^3A(1)$, 6% $^3B(2)$
	b	2222	35% $^3B(2)$, 25% $^3B(1)$, 14% $^1A(1)$, 13% $^3A(2)$, 10% $^3B(3)$
	c	3757	40% $^3A(2)$, 25% $^3B(2)$, 19% $^1B(1)$, 7% $^3B(1)$, 6% $^3A(1)$
	d	4158	36% $^3B(3)$, 34% $^3B(2)$, 14% $^1A(2)$, 11% $^3B(1)$,

PuO_2 molecule

- PuO_2 Geometry

As explained in the section 4.1 La Macchia *et al.* showed that the spin-orbit coupling was of great importance not only to describe the electronic structure but also the geometry of PuO_2. In their study, the spin-free results gave a $^5\Sigma_g^+$ as ground state with a Pu-O distance of 1.792 Å. At the spin-orbit level, the ground state was found to be a 1_u composed by 96% of the $^5\Phi_u$ with a bond length of 1.744 Å. At the latter, our SO-CASPT2 calculation predicted a 0_g ground state.

The $^5\Sigma_g^+$ is the lowest at SF level as found in La Macchia's study by the similarities stop here. The equilibrium distance is here longer with 1.804 Å(versus 1.792 Åof La Macchia *et al.*). At this distance, the energy gap to the $^5\phi_u$ state is estimated to 7992 cm^{-1}, while it was equal to 1800 cm^{-1} in La Macchia's study. In spite of this disagreement, the "reduction" of the bond distance while the spin orbit is included might be true and must be tested.

TABLE 4.13: Comparison of CBS extrapolated $^2DC^M$-EOM-CCSD and SO-CASPT2 PuO_2 vertical transition energies in cm^{-1} computed at the 1.744 and 1.808 Å Pu−O distances.

	d(Pu-O)=1.744 Å			d(Pu-O)=1.808 Å	
Ω	$^2DC^M$-EOM-CCSD	SO-CASPT2		$^2DC^M$-EOM-CCSD	SO-CASPT2
	This work	This work	Ref. [192]	This work	
0_g	0	0	1794	0	0
1_g	2435	1438	2315	2325	2462
2_g	6012	4235	4131	5378	5904
1_u	5721	1778	0	8548	5851
2_u	5926	1805	535	8782	6265
3_u	6622			9882	
4_u	12 751			15 471	

At the $^2DC^M$ level, the PuO_2 ground-state is found to be well-described a closed-shell ($\Omega = 0_g$) determinant, corresponding to occupied $f_{3/2}$ and $f_{5/2}$ spinors. This allowed us to employ accurate single-reference approaches such as CCSD(T) to determine the optimal Pu−O bond length, which is equals to 1.808 Å after extrapolation, with a corresponding harmonic vibrational frequency of 793 cm^{-1}. We note that the CBS-$^2DC^M$-CCSD(T) Pu−O bond length is longer than the one predicted by La Macchia et al. [192] at the SO-CASPT2 level.

TABLE 4.14: CBS extrapolated Ionization Potentials of PuO_2 in eV computed at the $^2DC^M$-EOM-CCSD level (d(Pu-O)= 1.808 Å) and comparison with experiments.

$^2DC^M$-EOM-CCSD		Exp			
State	IP	[[193]]	[[194]]	[[195]]	[[196]]
		9.4	10.1	7.03	6.6
$3/2_u$	7.65				
$5/2_u$	7.90				
$1/2_u$	9.81				
$3/2_u$	10.81				

Furthermore, our $^2DC^M$-EOM-EE-CCSD calculations (see Table 4.13) confirm that, at the CBS-$^2DC^M$-CCSD(T) equilibrium structure, the $\Omega = 0_g$ state is indeed the ground-state: it is sufficiently well-separated from the lowest-lying states of both g ($\Omega = 1_g$, by over 2000 wavenumbers) and u ($\Omega = 1_u$, by over 5000 wavenumbers), and considering a shorter bond length–namely 1.744 Å, as was proposed by La Macchia et al. [192] for the ground state from SO-CASPT2–does not alter this picture. Thus, our results differ qualitatively from La Macchia et al., since they suggest the PuO_2 ground-state is of $\Omega = 1_u$ symmetry, and corresponding mainly to the occupation of the two $5f_\delta$, one $5f_\phi$ and the 7s orbitals (See Figure 4.6).

From Table 4.13, we observe significant variations for the u states (of nearly 3000 wavenumbers) when the internuclear distance is varied from 1.808 Å to 1.744 Å, while the g states remain more or less at the same energies. With this, at the longer distance, the $\Omega = 2_g$ state becomes lower than the $\Omega = 1_u$ one.

- PuO_2 Electronic Structure

The SO-CASPT2 transition energies computed at the $^2DC^M$ optimal bond length are reported in Table 4.15 (the higher excited states can be found in the Appendix B). The spin-orbit 0_g ground state is composed by the spin-free ground state $^5\Sigma_g^+(1)$ up to 48% and by the $^3\Sigma_g(1)$ up to 22%, which lies 10.308 cm above it. La Macchia *et al.* also found large SO effects this with a SO-value of 8548 cm^{-1}. Note that the vertical transition energies computed at the SO-CASPT2 level are in very good agreement with the $^2DC^M$ ones for the g-states, but the u-states come out about 2300 cm^{-1} lower in energy at the SO-CASPT2 than at the $^2DC^M$-EOM-CCSD level. However, we note that the electronic state spacing within either the g or u symmetries agrees with the SO-CASPT2 calculations. This thus points out to the importance of the choice of the active space to accurately predict the relative energies of g states involving mostly non-bonding 5f Pu atomic-centered orbitals, versus the u states involving the more diffuse plutonium 7s orbital.

TABLE 4.15: Lowest electronic levels in cm^{-1} of PuO_2, computed at the SF-CASPT2 and SO-CASPT2 levels (d(Pu-O)= 1.808 Å) with the ANO-RCC-TZVP basis set, and analysis of the various states.

	State	ΔE	Character : % [orbital(number of electron)]
SF	$^5\Sigma_g^+$	0	84% [$1a_u/\delta_u(1)$, $2b_{2u}/\Phi_u(1)$, $2b_{1u}/\delta_u(1)$, $2b_{3u}/\Phi_u(1)$]
	$^5\Sigma_g$	4798	45% [$1a_u/\delta_u(1)$, $3b_{2u}/\pi_u(1)$, $2b_{1u}/\delta_u(1)$, $2b_{3u}/\Phi_u(1)$]
			45% [$1a_u/\delta_u(1)$, $2b_{2u}/\Phi_u(1)$, $2b_{1u}/\delta_u3(1)$, $3b_{3u}/\pi_u(1)$]
	$^5\Phi_{u(1)}$ ($^5B_{3u}(1)$)	5421	85% [$3a_g(1)$, $1a_u/\delta_u(1)$, $2b_{1u}/\delta_u(1)$, $2b_{3u}/\Phi_u(1)$]
	$^5\Phi_{u(2)}$ ($^5B_{2u}(1)$)	5421	85% [$3a_g(1)$, $1a_u/\delta_u(1)$, $2b_{1u}/\delta_u(1)$, $2b_{3u}/\Phi_u(1)$]
	$^5\Delta_{u(1)}$ ($^5A_u(1)$)	7452	79% [$3a_g(1)$, $2b_{2u}/\Phi_u(1)$, $2b_{1u}/\delta_u(1)$, $2b_{3u}/\Phi_u(1)$]
	$^5\Delta_{u(2)}$ ($^5B_{1u}(1)$)	7462	80% [$3a_g(1)$, $1a_u/\delta_u(1)$, $2b_{2u}/\Phi_u0(1)$, $2b_{3u}/\Phi_u(1)$]
	$^3\Sigma_g^-$	10 308	24% [$1a_u/\delta_u(1)$, $2b_{2u}/\Phi_u(2)$, $2b_{1u}/\delta_u(1)$]
			24% [$1a_u/\delta_u(1)$, $2b_{1u}/\delta_u(1)$, $2b_{3u}/\Phi_u(2)$]
			19% [$2b_{2u}/\Phi_u(1)$, $2b_{1u}/\delta_u(2)$, $2b_{3u}/\Phi_u(1)$]
			16% [$1a_u/\delta_u(1)$, $2b_{2u}/\Phi_u(1)$, $2b_{3u}/\Phi_u(1)$]
SO	0_g^-	0	48% $^5\Sigma_g^+$, 22% $^3\Sigma_g^-$
	1_g	2462	67% $^5\Sigma_g^+$, 15% $^3\Sigma_g^-$
	1_u	5851	27% $^5\Phi_{u(1)}$, 27% 21% $^5\Phi_{u(2)}$, 13% $^5\Delta_{u(1)}$, 13% $^5\Delta_{u(2)}$
	2_g	5904	85% $^5\Sigma_g^+$
	2_u	6265	21% $^5\Phi_{u(1)}$, 21% $^5\Phi_{u(2)}$, 24% $^5\Delta_{u(1)}$
	3_u	7195	38.85% $^5\Phi_{u(1)}$, 24.97% $^5\Phi_{u(2)}$

Finally, for the computed ionization energies for PuO_2 (IPs, see Table 4.14), our calculations could be grouped into three regions with respect to their energies: one below 8 eV, one between 8 and 10 eV and the last at energies higher than 10 eV. We see that, if one considers only the lowest EOM-IP-CCSD state ($\Omega = 3/2_u$), we observe a good agreement with the results of Rauh et al. [193] (and to a lesser extent, with the results of Capone et al. [194]) but poor agreement with a second measurement of Capone et al. [196] and of Santos et al. [195]. However, if we compare the first $\Omega = 1/2_u$ state to this second measurement of Capone, and the second $\Omega = 3/2_u$ state with that of Santos et al. [195], we see an overall good agreement between the calculated and experimental values. This leads us to suggest that experiments may have measured PuO_2^+ in different electronically excited states, something that would explain the rather different experimental values.

- Spin-free calculations

Beside calculations including spin-orbit coupling, it is informative to discuss the nature of PuO_2 ground-state at the scalar relativistic level (spin free). In our study, CASPT2 and UCCSD(T) calculations give the $^5\Sigma_g$ state ($(5f_\delta)^2(5f_\phi)^2$ occupations) lower in energy than the $^5\Phi_u$ state ($(5f_\delta)^2(5f_\phi)^1(7s)^1$) by 7994 cm^{-1} at the distance Pu-O of 1.804 Å, as found in the previous studies [174, 192]. With the ANO-RCC

AVTZ basis set, the equilibrium Pu−O distance is 1.818 Å and 1.808 Å at UCCSD(T) and CASPT2 levels, respectively, distances that are close to the fully-relativistic ones. These values are also in line with the SF-CASPT2 (CAS(12,14)) of La Macchia (d(Pu-O))= 1.792 Å), but significantly shorter by about 0.4/0.5 Å than the estimations Archibong and Ray [174]. These large discrepancies are probably related to the choice of a large-core RECP (78 electrons), which was proven to yield too long bond distances for actinide molecules [197], while the small-core ECP gives exactly the same distances that the all-electron Douglas-Kroll relativistic approach.

The ground state $^5\Sigma_g^+(1)$ is dominated up to 84% by the configuration that corresponds to the occupation of the two $5f_\delta$ and two $5f_{\Phi}$ orbitals carrying one electron each. It corresponds to the description of the ground state of Boguslawski *et al* [147]. and also to the $^5\Sigma_g^+(1)$ reported by La Macchia et al. [192]. The former study places the first excited state at 1800 cm^{-1} corresponding to $^5\Phi_u$ state, while in our SO-CASPT2 it appears at higher energy, of 5421 cm^{-1}. We note that in our SF-CASPT2 calculation, the spin-free spectrum is less dense than La Macchia's results [192]. Such differences can be explained by the choice of different active space, the fact that we computed a larger number of spin-free states, and most likely the change in the interatomic Pu−O distance. SO-coupling is not expected to change the energy of the $\Lambda = 0$ $^5\Sigma_g^+$ state, while it lifts the degeneracy of the $^5\Phi_u$ state. Given the small energy gap of 1800 cm^{-1} between the $^5\Sigma_g^+$ and $^5\Phi_u$ state, the 1_u state becomes the ground state in their study, while in our work, it remains a state of g symmetry.

TABLE 4.17: Standard enthalpies of formation $\Delta_f H^\circ$ of PuO_2, $PuO_2(OH)_2$, PuO_3 in kJ mol^{-1} in the gas phase calculated at various level of theory and extrapolated to the CBS-CE limit, and from the average of five reactions listed in Table 4.3, except for $^2DC^M$-CCSD(T). The standard deviations $\Delta\Delta_f H^\circ$ includes the uncertainty on the average value as well as the experimental error bars.

$\Delta_f H^\circ$	PuO_2	$PuO_2(OH)_2$	PuO_3
UCCSD + ΔE_{SO}	-348.4 $\pm$ 28.2		
UCCSD(T) + ΔE_{SO}	-404.3 $\pm$ 22.6	-518.8 $\pm$ 32.9	+599.1 $\pm$ 28.3
CASPT2 + ΔE_{SO}	-364.4 $\pm$17.8	-1008.7 $\pm$ 34.3	-539.8 $\pm$ 24.1
Reference	-410 $\pm$ 20 [198] ;	-1018.2 $\pm$3.3[199]	-562.8 $\pm$5[199] ;
	-412 $\pm$ 20 [139] ;		-567.6 $\pm$ 15 [141]
	-440$\pm$ 7 [138];		
	-428.7 $\pm$ 7[138];		
	-428.7 $\pm$ 20 [141];		

4.4.2 Thermodynamic properties

TABLE 4.16: Standard enthalpies of formation $\Delta_f H^\circ$ of PuO_2, $PuO_2(OH)_2$, PuO_3 in kJ mol^{-1} in the gas phase calculated at various level of theory and extrapolated to the CBS-TE limit, and from the average of five reactions listed in Table 4.3, except for $^2DC^M$-CCSD(T). The standard deviations $\Delta\Delta_f H^\circ$ includes the uncertainty on the average value as well as the experimental error bars.

$\Delta_f H^\circ$	PuO_2	$PuO_2(OH)_2$	PuO_3
ΔE_{SO} [1]	34.4	46.9	59.0
B3LYP + ΔE_{SO}	-304.1 $\pm$ 16.4	-787.0 $\pm$ 30.1	-397.3 $\pm$ 21.6
$^2DC^M$-CCSD(T)	-432		
UCCSD + ΔE_{SO}	-347.6$\pm$ 21.1		
UCCSD(T) + ΔE_{SO}	-406.6 $\pm$ 9.3	-260.9 $\pm$ 26.9	+438.0 $\pm$ 8.5
CASPT2 + ΔE_{SO}	-367.3$\pm$17.1	-1009.3 $\pm$ 44.5	-545.0 $\pm$ 23.3
Reference	-410 $\pm$ 20 [198] ;	-1018.2 $\pm$3.3[199]	-562.8 $\pm$5[199] ;
	-412 $\pm$ 20 [139] ;		-567.6 $\pm$ 15 [141]
	-440$\pm$ 7 [138];		
	-428.7 $\pm$ 7[138];		
	-428.7 $\pm$ 20 [141];		

[1] ΔE_{SO} is estimation of the SO contribution.

All the values of enthalpy of formation can be found in the Table 4.16. From our discussion of the electronic structures of the different Pu molecules detailed in section 4.4.1, one will not be surprised to see that the single-reference methods, here DFT and CCSD(T), fail at describing $PuO_2(OH)_2$ and PuO_3 thermodynamic properties,

while they should be in principle usable for PuO_2 molecule. Thus, for this methods, we will focus only on the PuO_2 molecule. One can observe that the enthalpy obtained with the B3LYP functional and the $+\Delta E_{SO}$ correction gives a value about 25% off the experimental one (100 kJ mol^{-1}). A change in the density functional will not ensure a better agreement with experience as observed previously for actinide systems [200] or for transition metal molecules [201]. The $\Delta_f H^{\ominus}$(298.15 K) computed with ^{2}DC^M approach (^{2}DC^M) is in almost perfect agreement with the available results [138, 141]. Note that the absence of error value is because the calculation was done only for the reaction R_4, as the other reactions involved species with a multideterminantal character. UCCSD+ΔE_{SO} result (-385.0$\pm$21.1kJ mol^{-1}) is lower than ^{2}DC^M-CCSD(T) one, while the UCCSD(T)+ΔE_{SO} agrees with the best theoretical estimations and the experimental data, thus highlighting the importance of the perturbative triple contributions. For the reaction 4, UCCSD(T) + ΔE_{SO} and CASPT2 + ΔE_{SO} give -416.22 kJ mol^{-1} and -387.7 kJ mol^{-1}, respectively. The SO-CASPT2 value deviates by about 40 kJ mol^{-1} from both ^{2}DC^M-CCSD(T) and experiments, probably because of the incompleteness of the active space. Nevertheless, the SO-CASPT2 results for $PuO_2(OH)_2$ and PuO_3 show great agreement with the experiment values by Krikorian et al. [199].

4.5 Conclusion and Perspectives

Concerning PuO_2, where the static correlation is not important and the wave function can be described by single-reference methods that include the dynamic correlation such as UCCSD(T) the $\Delta_f H^{\circ}$ could be reproduced. The distance Pu-O found for the linear PuO_2 is 1.808 Å and the ground state a 0_g mainly composed by the spin-free state ^5A_g.

About $PuO_2(OH)_2$, SO-CASPT2 method is enough to reproduce the only experimental data available but the enthalpy of formation given by this method for PuO_3 is smaller than expected. Since the detection of PuO_3 is complicated one could argue on the validity of the two measurements but we would rather point out the fact that our active space size might not be large enough and could lead to a mistreatment of the static correlation. In order to improve the description, larger active spaces can be handled with the DMRG method recently implemented in Molcas. Exploratory DMRG calculations will be performed in coming weeks.

Our thermodynamics data are about to be implemented by our IRSN colleagues (F. Virot) in the accident simulation code to quantify the amounts of each volatile Pu species released.

Chapter 5

How well are the f-elements described by a Double-Hybrid Functional ?

Contents

Our interest here is to see how double hybrids work for the geometries and thermochemistry of species containing actinides and lanthanides. This project was triggered by two reasons: the first is that we have seen that the B3LYP is not accurate to compute the thermochemistry of PuO_2, thus raising the question of whether other functionals and double hybrids in particular could be more accurate for such f-element complexes. The second, because we are involved in the implementation and benchmarking of double-hybrids four-component-based methods in Dirac in a collaboration with Benjamin Helmich-Paris (Mulheim) and Lucas Visscher (Amsterdam); therefore, we want to investigate if there are significant changes between spin-free (Molpro) and SOC (Dirac) calculations. This chapter presents the first step of the study. It consists in a systematic comparison of structural and thermodynamic properties computed at the spin-free level with the state of the art CCSD(T) method as reference. This is, to the best of our knowledge, the first application of double-hybrid B2-BLYP to actinide chemistry. However, we can refer to recent assessments of double hybrid, in particular B2-PLYP for transition metal thermochemistry [202, 203], leading to average uncertainties of up to 8 kcal.mol^{-1}, which is about 4 kcal.mol^{-1} better than B3LYP. After a brief description of the current development of double-hybrids and the B2-PLYP functional and a review of the available thermodynamic data, we will reach the aim of this chapter and present the first results regarding the f element properties.

5.1 Motivations for double-hybrid functionals

One of the biggest weakness of DFT is not accounting for the dispersion effects as we have seen in the Section 2.3.4. A widely used solution is the Grimme dispersion correction [49–51] which we have used in the Chapter 3. We have seen that even if it lead to good qualitative results, this correction could not be used as quantitative method for such a large system. When the system has a reasonable size, MP2 is a good but expensive solution to include dispersion effects.

The idea of double-hybrids (B2-PLYP) [204] is to add non-locality responsible for dispersive (van der Waals) interactions to hybrid functionals by considering virtuals orbitals and having a well-balanced performance for properties (energetics, etc). It relies on a combination of KS-DFT (Kohn Sham Density Functional Theory) and Perturbation Theory (PT) where the exchange-correlation energy is expressed as:

$$E_{xc} = (1 - a_x)E_x^{GGA} + a_x E_x^{HF} + bE_c^{GGA} + cE_c^{PT2} \tag{5.1}$$

where

$$E_c^{PT2} = \frac{1}{4}\sum_{ia}\sum_{jb}\frac{[(ia|jb) - (ib|ja)]^2}{\epsilon_i + \epsilon_j - \epsilon_a - \epsilon_b} \tag{5.2}$$

with ϵ_i being the KS eigenvalue of the orbital i, the bracket terms corresponding to the two electrons integrals over the KS orbitals. The parameters a_x, b and c were parametrised to reproduce thermodynamic properties of light elements namely the G2/97 set of heat of formation. During this parametrisation, the relation $b + c = 1$ was found and confirmed [205] and $c \leq a_x$, leading to only two parameters with a value of 0.53 and 0.27 for a_x and c, respectively. The GGA functional used is the BLYP one. Multiple rigorous analysis were done concerning the parametrisation [205–207] and showing that the value of a_x and c are very close to a theoretical optimum.

Even if it is not used in this thesis we can note that it is also possible to perform TDDFT with double hybrid [208, 209] or to add long-range dispersion [210].

During the past 10 years the development of many other double-hybrid functionals was done [207, 211–233] and listed and compared in a review of Grimme *et al* [234]. This work exposes the functional DSD-BLYP-D3 [221] and PWPB95-D3 [203] as the most accurate and robust ones though we have not evaluated them in this thesis.

Most specific performances are also tested such as: spin-state energetics [235], ionisation energies and aqueous redox potentials of organic molecules [236], non-linear optical properties [237] and thermochemistry of 3d transition metals [202]. This last study is particularly interesting since it states that the Mean Average Deviation (MAD) of B2-PLYP is 32.6 kJ.mol^{-1} for the determination of enthalpies of formation. Since the DIRAC implementation concerns only the B2-PLYP functional, it will be compared to HF, CCSD(T), B3LYP hybrid functional, PBE GGA functional and the limiting cases of B2-PLYP, MP2 and BLYP functional.

5.2 Literature review of the available enthalpies of formation $\Delta_r H^\ominus$.

The enthalpies of formation theoretical and experimental of the reactions listed in the Table 5.1 are only reported for reaction including UF_6. The enthalpies are extracted from the work of Peterson *et al.* and [184] Privalov *et al*. The former study includes four-component CCSD(T) calculations with a pseudopotential (PP) [179] or all electron basis sets [238]. The latter one includes SCF, MP2, B3LYP and CCSD(T) single point energy using geometries obtained at the HF level with a scalar relativistic pseudopotential or experimental data.

All the reactions were chosen for the fact that they involve close shell species and because the information about the structures are readily accessible.

TABLE 5.1: Reactions used to calculate $\Delta_r H^\ominus$ and their previously reported values.

Reactions	$\Delta_r H^\ominus$ in kJ.mol^{-1}
R_1: $H_2 + F_2 \longrightarrow 2\,HF$	
R_2: $La^{3+} + H_2O \longrightarrow LaH_2O^{3+}$	
R_3: $CeF_4 + CeO_2 \longrightarrow 2\,CeOF_2$	
R_4: $ThF_4 + ThO_2 \longrightarrow 2\,ThOF_2$	
R_5: $UO_2^{2+} + H_2O \longrightarrow UO_2(H_2O)^{2+}$	
R_6: $Ac^{3+} + H_2O \longrightarrow AcH_2O^{3+}$	
R_7: $UF_6 + SO_3 \longrightarrow UO_3 + SF_6$	4C-CCSD(T): 525.5 [1]; 527.2 [2][184] Exp: 528.9 [184]
R_8: $UF_6 + 3\,H_2O \longrightarrow UO_3 + 6\,HF$	4C-CCSD(T): 481.6 [1]; 479.9 [2][184] SCF: 539 ; MP2: 487, 534[*]; CCSD(T): 558, 464[*][239] B3LYP: 627, 500 [*]; Exp: 435 [239]
R_9: $UF_6 + H_2O \longrightarrow UOF_4 + {}_2HF$	
R_{10}: $UF_6 + 2\,H_2O \longrightarrow UO_2F_2 + {}_4HF$	4C-CCSD(T): 204.2[1], 202.1 [2][184] SCF: 170; MP2: 232, 263 [*]; CCSD(T): 232, 263 [*][239] B3LYP: 332, 246[*]; Exp: 187 [239]
R_{11}: $UO_2^{2+} + 4\,H_2O \longrightarrow UO_2(H_2O)_4^{2+}$	
R_{12}: $PaO_2^{+} + H_2O \longrightarrow PaO_2(H_2O)^{+}$	

[1] Values FC-CCSD(T)/CBS with pseudo potential.
[2] Values FC-CCSD(T)/CBS with the all electron basis sets.
[*] Corrected values

We aim to reproduce results as close as possible to the experimental ones or to the corresponding method in use.

Concerning the geometries of the molecules, when possible it will be compared to experimental data, otherwise the quantum chemical method used to determined them will be specified.

5.3 Computational details

As in the previous Chapters, the geometry of the molecules under interest is a key information for the description of thermodynamic properties. Therefore the different molecules were first optimised for each of the quantum chemistry methods at the spin-free level with the Molpro2015.1 package [156], followed by an harmonic frequency calculation. The reaction enthalpies are computed as in Chapter 4 in equation 4.3:

$$\Delta_r H^\ominus = \sum_i (E_i + ZPE_i + H_{corr,i}) \tag{5.3}$$

The light elements (first and second rows) are described with aug-cc-pVQZ basis sets [cite], for actinides the scalar relativistic effects were included with the relativistic pseudopotential with 60 e- in core, namely ECP60MDF [cite] with the corresponding quadruple-ζ quality basis sets[cite]. For lanthanides,the small-core relativistic pseudo potential with 28 e - in core, namely ECP28WB, [171, 240] and the corresponding quadruple-ζ basis sets were used. Peterson *et al.* [184] reportes that quadruple-ζ basis sets used are close enough from the CBS for us to overcome the need of CBS extrapolations. Since all the molecules involved in the reactions under study (see Table 5.1) are closed-shell, no spin state problem should appear and spin-orbit coupling is expected to be negligible [184].

In most of the reactions the bonding picture changes a lot from the reactants to the products resulting in large differences of dynamical correlation across the reactions making it then relevant for benchmarking correlation methods. A particular attention will be paid to the R_1 since its enthalpy of reaction is computationally challenging because as mentioned in the reference [239], Privalov *et al.* could not reproduce it.

5.4 Results and Discusions

The optimisations of $UO_2(H_2O)_4{}^{2+}$ are still in progress, thus, the results of the reaction R_{11} will not be reported. Table 5.2 presents the reported geometries of molecules with an f-element with the corresponding reference data.

5.4.1 Geometries and total energies

TABLE 5.2: Geometries of the various molecules under study, the distance are given in Å and angles in degree symmetry is given in parenthesis.

Molecule		CCSD(T)	MP2	B2PLYP	B3LYP	BLYP	PBE	HF	Literature
ThF_4 (Td)	r(Th-F)	2.112	2.113	2.116	2.117	2.132	2.113	2.116	Exp: 2.124 [241]
	angle(F-Th-F)	109.5	109.5	109.5	109.5	109.4	109.4	109.5	107.2
$ThOF_2$ (Cs)	r(Th-O)	1.890	1.896	1.895	1.888	1.906	1.890	1.870	Exp: 1.886 [242]
	r(Th-F)	2.138	2.136	2.139	2.141	2.152	2.130	2.154	Exp: 2.157
	angle(F-Th-F)	106.9	120.6	106.0	106.1	104.8	103.8	110.6	107
	angle(F-Th-O)	106.9	120.6	106.0	106.1	104.8	103.8	110.6	
ThO_2 (C_{2v})	r(Th-O)	1.907	1.912	1.913	1.905	1.923	1.906	1.891	CCSD(T): 1.905 [243]
	angle(O-Th-O)	117.0	114.4	117.8	119.9	119.0	119.2	120.4	117
UF_6 (O_h)	r(U-F)	2.000	1.999	2.016	2.014	2.041	2.022	1.984	Exp: 1.999 [244]
UO_3 (C_{2v})	r(U-O_{apical})	1.8	1.865 [1]	1.871[1]	1.81162	1.880	1.863	1.747	4C-CCSD(T): 1.801[184]
	r(U-O)	1.9	1.865[1]	1.871[1]	1.852977	1.854	1.829	1.828	1.852
	angle(O_{apical}-U-O)	99.4	119.9[1]	120[1]	101.4286	106.5	103.1	97.7	99.5
UO_2F_2 (C_{2v})	r(U-O)	1.769	1.788	1.798	1.788	1.816	1.816	1.713	4C-CCSD(T): 1.768 [184]
	r(U-F)	2.076	2.073	2.077	2.073	2.093	2.093	2.092	2.075
	angle(O-U-O)	169.1	169.5	166.4	169.5	163.9	163.9	170.2	169.2
	angle(F-U-F)	114.0	112.8	111.7	112.8	118.6	118.6	118.9	114.1
$UO_2H_2O^2+$ (Cs)	r(U-O)	1.713	1.732	1.734	1.716	1.748	1.733	1.660	CCSD(T): 1.789 [243]
	r(U-OH_2)	2.324	2.317	2.325	2.330	2.343	2.314	2.373	2.453
	angle(O-U-O)	89.8	88.8	89.5	90.1	90.1	89.4	90.7	90.0
LaF_3 (C_{3v})	r(La-F)	2.120	2.120	2.123	2.123	2.134	2.112	2.138	Exp: 2.12 [245]
	angle(F-La-F)	116.2	115.9	115.8	115.8	115.1	114.3	119.5	
CeO_2 (C_{2v})	r(Ce-O)	1.821	1.822	1.819	1.835	1.850	1.829	1.790	HF: 1.82 [246]
	angle(O-Ce-O)	121.8	115.4	128.4	139.1	132.6	132.9	116.6	132
CeF_4 (Td)	r(Ce-F)	2.028	2.026	2.036	2.042	2.070	2.049	2.031	CISD: 2.04 [247]
$CeOF_2$ (C_s)	r(Ce-O)	1.786	1.787	1.804	1.791	1.832	1.811	1.748	B3LYP: 1.794 [248]
	r(Ce-F)	2.082	2.078	2.087	2.090	2.109	2.086	2.098	2.091
	angle(F-Ce-F)	110.5	110.7	109.0	109.6	109.2	108.3	114.9	110.5
AcF_3 (C_{3v})	r(Ac-F)	2.195	2.195	2.197	2.197	2.209	2.186	2.210	MP2: 2.272 [249]
	angle(F-Ac-F)	113.4	113.3	113.0	112.7	111.6	110.9	116.7	
PaO_2^+ ($D_{\infty h}$)	r(Pa-O)	1.773	1.794	1.784	1.775	1.799	1.784	1.738	CCSD(T): 1.776 [243]
$PaO_2H_2O^+$ ($D_{\infty h}$)	r(Pa-O)	1.789	1.799	1.801	1.791	1.816	1.800	1.754	CCSD(T): 1.788 [243]
	r(Pa-OH_2)	2.449	2.441	2.455	2.465	2.475	2.442	2.511	2.447
	angle(O-Pa-OH_2)	88.7	88.7	89.1	89.6	88.5	88.8	90.6	98.5

[1] The symmetry is D_{3h}

Looking at Table 5.2 the B2-PLYP presents good performances at reproducing the literature data. This is highligted in Figures 5.1 and 5.2 presenting the bond length and angular deviation with respect to CCSD(T). Unfortunately, B2-PLYP and MP2 predict the wrong symmetry for UO_3 giving it as a D_{3h} symmetry for the molecule instead the expected C_{2v}.

Concerning the distances, it is the functional B3LYP that is the closest to CCSD(T) with a MAD of 0.006 Å followed by MP2 with 0.012 Å. B2-PLYP functional arrives third with an average error of 0.014 Å. However, while UO_3 is taken out of the set, the MAD of MP2 and B2-PLYP are reduced to 0.007 Å and 0.008 Å, respectively.

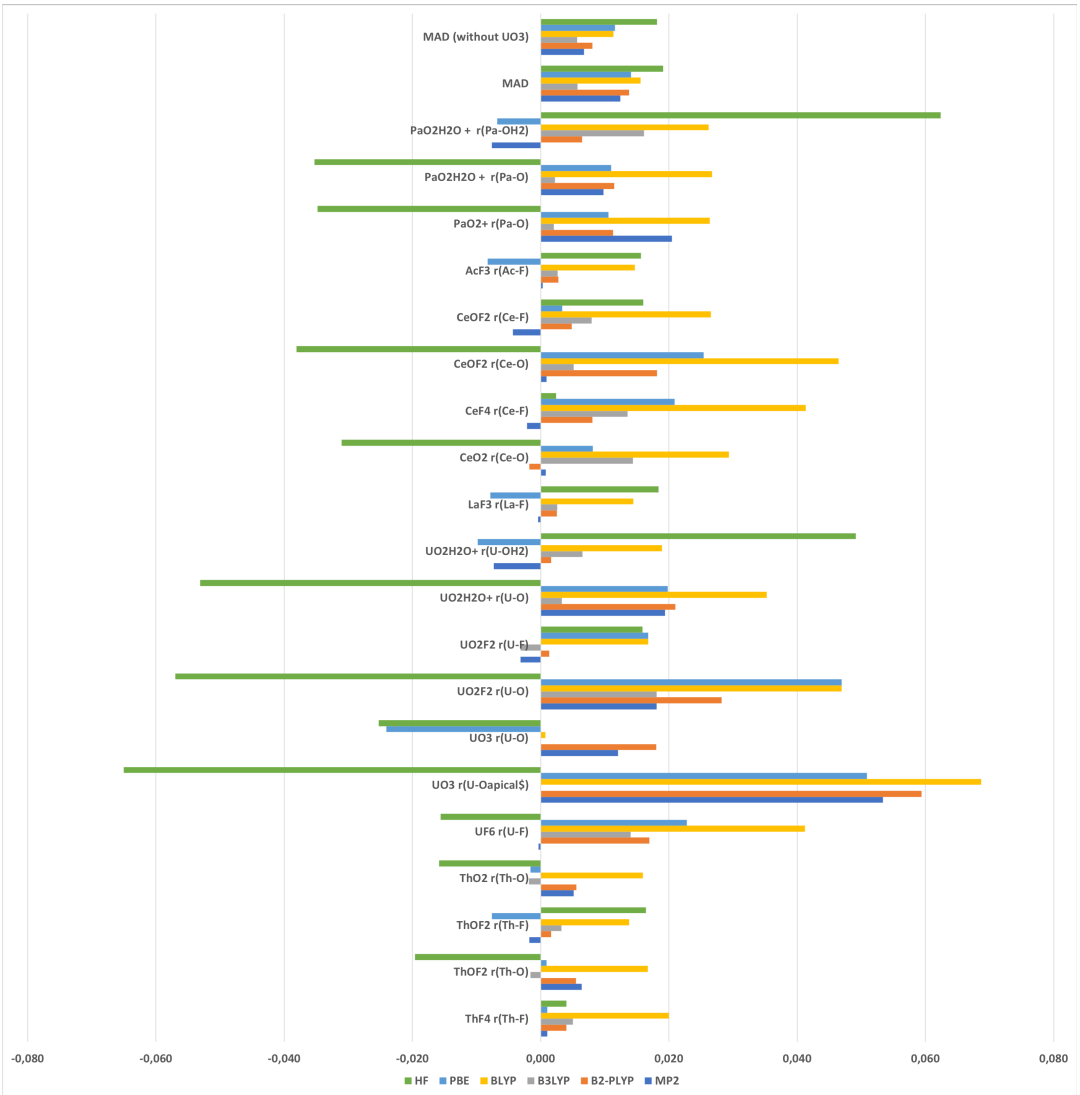

FIGURE 5.1: Error in the bond length in Å with respect to CCSD(T) values and MAD over all complexes

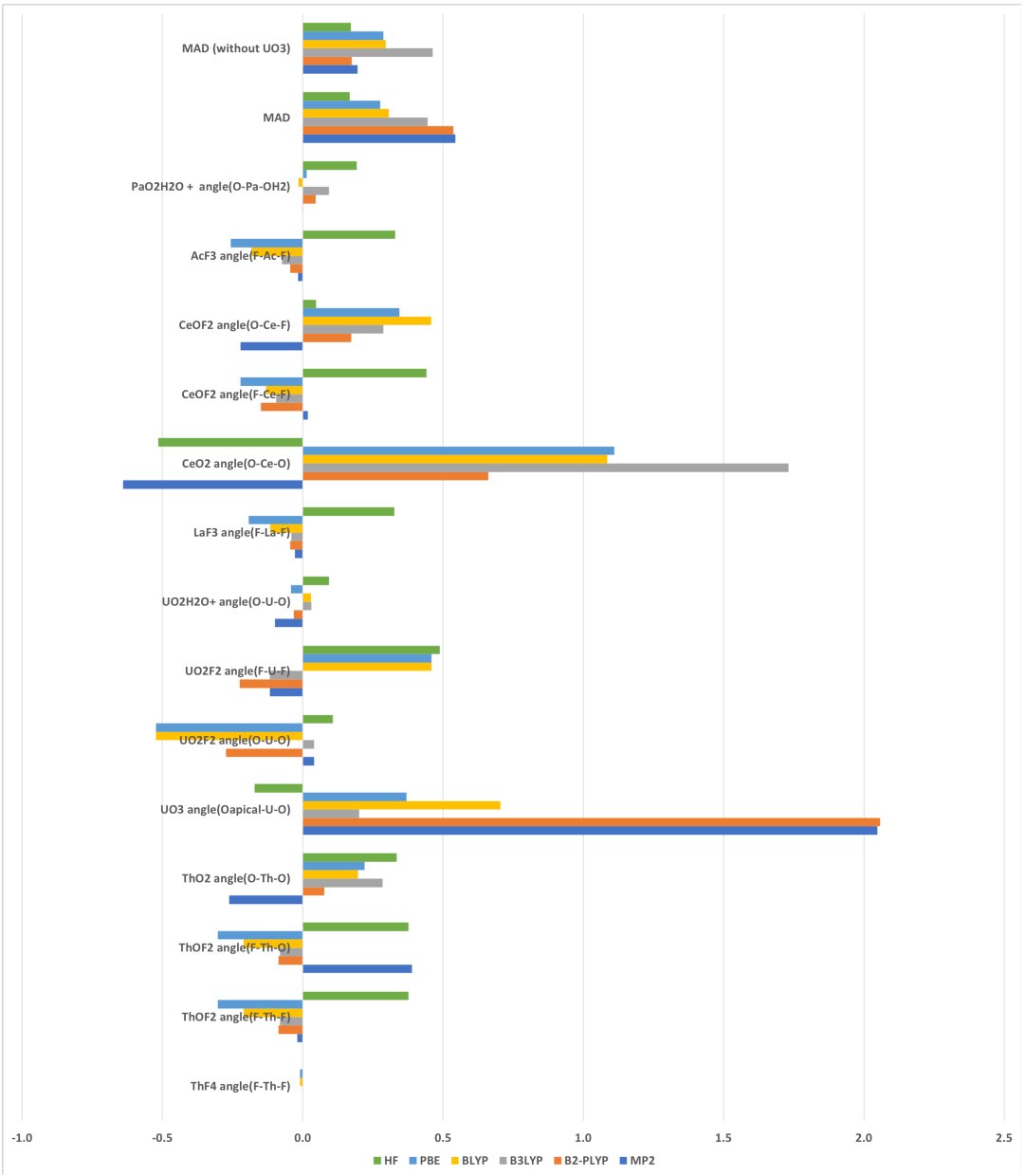

FIGURE 5.2: Differences in the angles (in degrees) with respect to CCSD(T) and the MAD over all complexes

For the intramolecular angles, MP2 and B2-PLYP perform the worst with a MAD of 5.4 due to the bad description of UO_3. While this molecule is taken off the set the MAD of B2-PLYP is the best with 1.7 degrees and MP2 the second best value with MADs of 2.0 degrees. Explanations about the failure of MP2 and B2-PLYP to describe UO_3 are still under investigation.

This small B2-PLYP MAD makes use confident about its capability in giving very accurate geometries while MP2 is performing well.

In Table 5.3, we reported the difference in total energies. One can note that the behaviour of each method/functional depends on the actinide/lanthanide present. Nonetheless, in every cases containing an heavy atom, the B2-PLYP is the closest to CCSD(T) after MP2. MP2 underestimates the total energies while all other methods overestimate it. So far, the smallest MAD is obtained with B2-PLYP attesting its good performance.

5.4.2 Enthalpies of Reactions

As mentioned previously, only scarce experimental values of reaction enthalpies are available for f elements. The only ones to benchmark with are those studying reactions R7, R8, R10 and R12. Thus, we will start the discussion by scrutinize the results obtained for these four reactions. For the reactions R_8 and R_{10} we could see that computed reaction enthalpies were far from the experimental values (see Table 5.3) . This was already noticed in [184] by Peterson *et al.*, thus we decided to correct the results in the same way they did. Peterson *et al.* attributed the error to the description of HF, and because of that they took the difference between the experimental value and theirs for reaction R_{10}. This difference was then divided by 4 (the number of HF molecules in reaction R_{10}) to obtain the correction factor for each HF molecule. This correction was then apply to each reaction involving HF.

Table 5.3 presents the enthalpies of reaction of the chosen reactions. The results obtained on reactions R_8 and R_{10} validate our correction since in reaction R_8 we are closer to the experimental enthalpy of reaction. Figure 5.3 exposes the differences in between the enthalpies of reactions with respect to CCSD(T) values. So far the smallest MAD is HF's with 27.8 kJ.mol^{-1}. The second lowest MAD is the one is given by the B2-PLYP functional (with 28.4 kJ.mol^{-1}). All the other MADs are above 35 kJ.mol^{-1}.

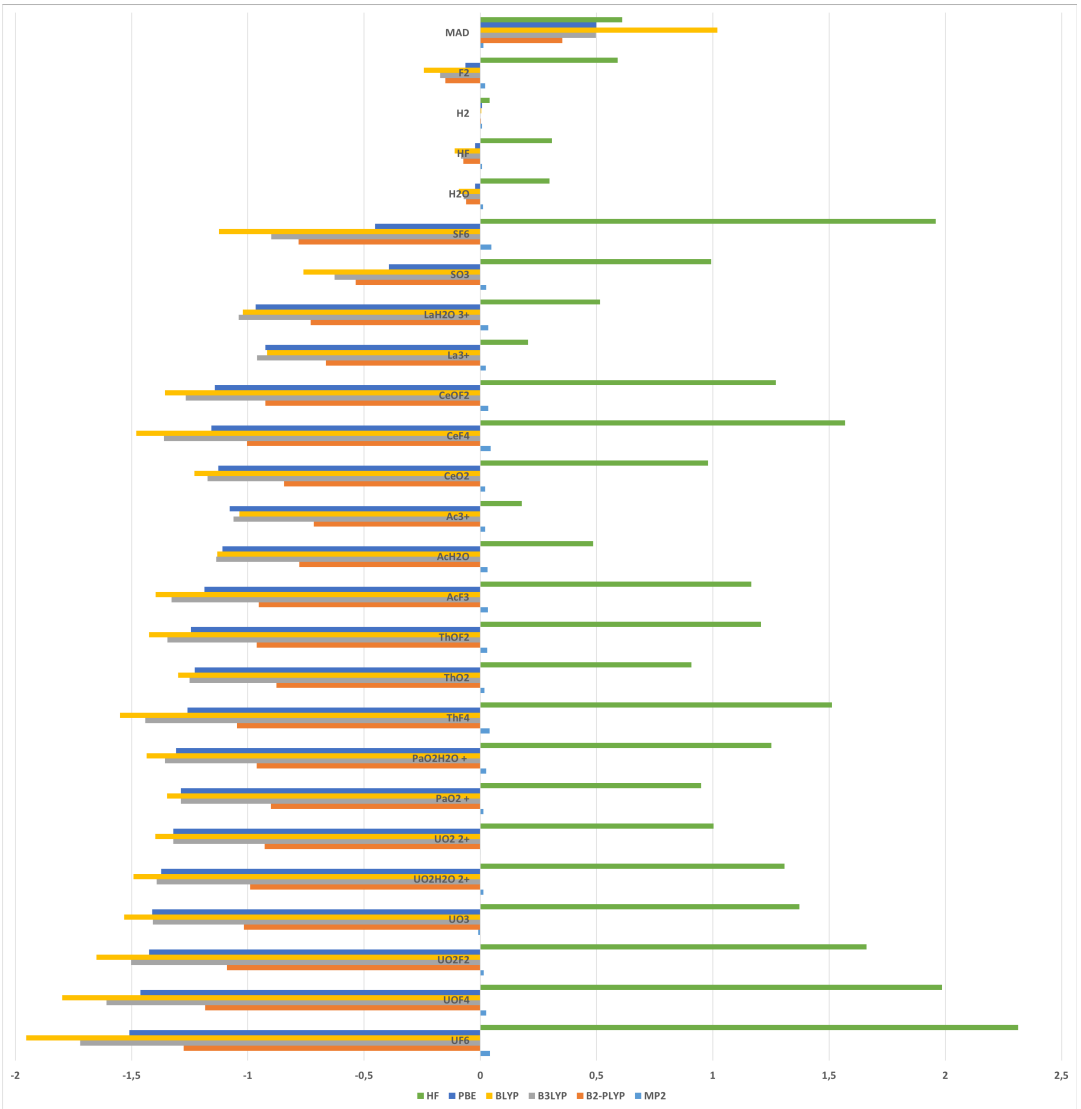

FIGURE 5.3: Difference in energy between the total energy given by the CCSD(T) and the considered method and functionals in a.u.

TABLE 5.3: $\Delta_r H^{\ominus}$ in kJ.mol^{-1} for the reaction under study.

	CCSD(T)	MP2	B2-PLYP	B3LYP	BLYP	PBE	HF	Exp
R_1	-547.3	-612.6	-578.1	-563.5	-533.0	-544.5	-617.7	
R_2	-381.0	-383.4	-391.7	-401.0	-413.7	-428.5	-345.8	
R_3	-146.0	-136.1	-147.6	-148.0	-162.2	-143.8	-164.5	
R_4	13.3	16.4	13.6	11.0	11.2	11.4	2.8	
R_5	-275.9	-276.8	-276.8	-278.3	-280.5	-356.1	-250.2	
R_6	-338.2	-340.4	-344.6	-347.1	-348.9	-360.9	-310.4	
R_7	539.2	457.1	570.2	643.6	686.7	635.2	604.6	539.3
R_8	468.7	356.0	472.2	545.0	553.2	553.2	527.9	
$R_{8,corrected}$	456.9	424.9	401.6	420.2	553.2	377.9	550.8	435
R_9	43.7	56.4	110.3	140.3	158.6	160.4	75.5	
$R_{9,corrected}$	39.8	79.4	86.8	98.7	99.1	102.0	83.2	
R_{10}	194.9	141.1	234.1	270.2	306.1	303.8	171.7	
$R_{10,corrected}$	187.0	187.0	187.0	187.0	187.0	187.0	187.0	187
R_{12}	-152.4	-155.6	-151.3	-146.8	-117.6	-149.7	-132.8	

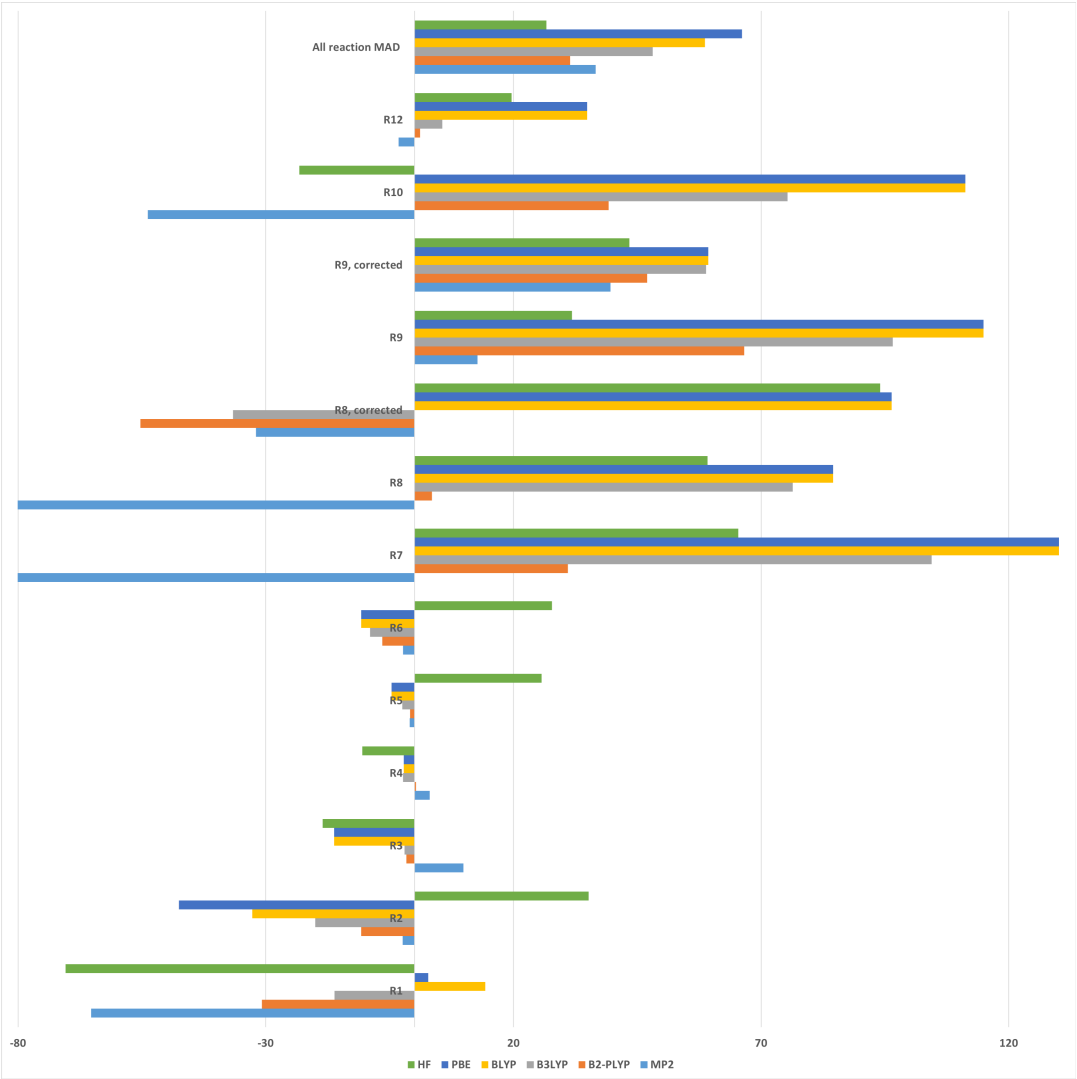

FIGURE 5.4: Differences in the enthalpies of reaction with respect to CCSD(T) values in kJ.mol^{-1}

5.5 Conclusion and Perspectives

Even if we can observe in B2-PLYP some imperfection of MP2, such as the inaccuracies in the description of the geometry of UO_3, it still yields to good results in the description of the geometry. The thermodynamic properties of f-element are even better describe with B2-PLYP than MP2, which is what was desired. The MAD reported for B2-PLYP (28.4 kJ.mol^{-1}) is smaller than the one found in the study of Wilson *et al.* on transition metals (32.6 kJ.mol^{-1}). All of this, demonstrate that this double hybrid is suitable to answer this kind of problems. The follow-up of the current work will be to use the double-hybrid implementation in DIRAC program to assess the importance of SOC to our results.

Chapter 6

Conclusions and perspectives

With respect to the quantum chemical methods used in this thesis to study actinides several conclusions need to be drawn. First, for closed-shell systems or for systems with a dominant single reference character, DFT with hybrid methods, such as semi-empirical dispersion corrections or double hybrid functional, performs well. For large systems it is cheap and efficient. With B2-PLYP, enough correlation can be included to describe properly closed-shell systems. Nonetheless, DFT is still failing for multireference systems. For this type of systems, we chose the CAS method. This method is neither black-box nor cheap. The choice of active space can be tedious and we have seen that in cases, where very accurate results are wanted, this method may fail because of the limited size of active space and probably a lack of accurate dynamic electron correlation treatment.

To the question raised in the introduction about the efficiency of the available tools to describe the structure, the bonding and the thermodynamics of actinide systems, we can not give a simple answer.

First, concerning the geometries, the three studies showed that the structures of actinides and f-elements systems can have their geometries reproduced or unravelled. We have seen that the X-ray structures were well reproduced for the catalysts in Chapter 3 as well as structural experimental values in Chapter 5 with the double-hybrid (B2-BLYP) functional, proving its capability, in most cases, at being as accurate as other quantum chemistry methods but also being predictive. It is worth noticing the failure of the DFT at converging to the expected triplet state for the uranium complexes in Chapter 3. In Chapter 5, only UO_3 structure turned out to be problematic both at MP2 and B2-PLYP levels; and the explanations of this failure are expected soon. Finally, for PuO_2, in Chapter 4 we reported a bond length and a ground state different from what was reported before at spin-orbit level [151].

Chapters 3 and 4 were focusing on the bonding. In the case of closed-shell systems, the exploration of the bonding via the determination of the electronic structure is

rather easy and the ETS-NOCV is a powerful tool to analyse and explore the metal arene chemical bonds and determine the main forces driving them. In particular we have seen that the zirconium-arene bond was mainly covalent while the thorium-arene one was mostly driven by electrostatic forces. In cases of open-shell systems, like in Chapter 4, the electronic wave functions are more difficult to describe. The CAS methods present the main disadvantages to include a limited number of orbitals in the active space thus requiring a thorough analysis of results. For example, in PuO_3, the full valence active space is (34; 26) but we could only compute a active space of (14,14) which might not be large enough.

The third properties we wanted to reproduce were thermodynamics. This part is particularly satisfactory in Chapter 5 where the double hybrid B2-PLYP already exhibits great performances at the spin-free level, compared to either experimental or state-of-the-art CCSD(T) data. In Chapter 4, multireference methods were needed to predict the enthalpies of formation of plutonium oxyhydroxide $PuO_2(OH)_2$ and trioxide PuO_3. The enthalpy of formation of $PuO_2(OH)_2$ was within very good agreement with experimental data but its uniqueness imposes to confirm this value with another method. For PuO_2, the single reference method UCCSD(T) perform very well. Regarding PuO_3 and PuO_2, the results with SO-CASPT2 method are good but not excellent, demonstrating the limit of actual relativistic multireference method accuracy.

As perspectives, the study of the alkyl cation catalysts calls for a further investigation of the possible transition states to have a better comprehension of the catalytic mechanism. Concerning the thermodynamic properties of plutonium oxides and oxyhydroxyde, in the next weeks, we will use the DMRG methods to be able to handle all valence orbitals in the active space to confirm our conclusions on PuO_3 and $PuO_2(OH)_2$. With DMRG we can expect to also be able to predict other thermodynamic values such as the one of uranyl complexes or RuO_2 (also important for nuclear safety) for which it is not easy to properly describe because of a ground and first excited states close to each other in energy [201].

To shed light on the possible formation of PuO_3 we wait for the results of IRSN on accident simulation. At the moment, the double hybrid B2-PLYP is tested on PuO_2 hoping to obtain results as good as the one computed with UCCSD(T) method. In addition we plan to benchmark the implementation of the double hybrid in the DIRAC package to have results in the fully relativistic context.

Finally, the broad range of uses and theoretical challenges to describe actinides makes them a wonderful subject for the development of both experimental and computational chemistry.

Appendix A

Geometries

Contents

A.1 Geometries from the Chapter Coordination of Alkyl cations $[(XA_2)X(CH_2Y)]$ (X = Th, U or Zr; Y = $SiMe_3$, H) with an arene for Ethylene polymerisation: Exploration of the bonding

A.1.1 X-Ray structures of Alkyl cations containing Thorium

X-Ray structure of η^6-2-Th

Th	13.572531	10.195293	14.464022	C	15.992251	5.394201	12.387399
Si	13.448412	7.436393	17.277993	H	16.053977	4.497544	12.079063
O	13.505595	7.925594	13.428804	C	13.429707	5.120134	12.400889
N	11.533051	9.429158	13.797651	C	12.203748	6.048476	12.562765
C	10.901366	5.592226	12.256356	C	12.283644	7.315836	13.063811
H	10.792612	4.709827	11.921041	C	14.695748	7.239794	13.098499
N	15.572197	9.327770	13.767395	C	14.706170	5.945503	12.620578
C	9.770801	6.390663	12.427868	C	13.455092	4.557743	10.957491
C	9.943419	7.681786	12.928914	H	14.231605	3.970005	10.849573
H	9.184008	8.241008	13.042613	H	13.515482	5.299149	10.319620
C	11.204383	8.166551	13.264229	H	12.633689	4.050799	10.791760
C	15.830055	8.022389	13.295063	C	13.364508	3.990600	13.406835
C	17.066703	7.444156	13.025269	H	14.146097	3.409198	13.296990
H	17.857644	7.959021	13.135114	H	12.548182	3.469398	13.260375
C	17.163700	6.111844	12.593599	H	13.357828	4.361303	14.314499

C	8.348976	5.918571	12.065573
C	7.779819	6.834239	10.992178
H	8.336952	6.780376	10.188578
H	7.767795	7.756243	11.323640
H	6.867297	6.553835	10.776343
C	7.451151	6.026297	13.322042
H	6.543973	5.726883	13.102353
H	7.423094	6.957806	13.624597
H	7.815893	5.462322	14.035069
C	8.306757	4.470612	11.572236
H	8.871372	4.380313	10.776343
H	7.383012	4.228230	11.348692
H	8.638899	3.874953	12.275627
C	18.537694	5.516184	12.265992
C	18.968436	6.042139	10.890042
H	19.001303	7.021174	10.909313
H	18.322590	5.749062	10.211703
H	19.856375	5.690446	10.668426
C	19.586226	5.912234	13.316261
H	19.631919	6.889686	13.381782
H	20.462942	5.562126	13.052248
H	19.332644	5.538363	14.185383
C	18.498147	3.962084	12.196616
H	17.836267	3.681681	11.531766
H	18.253115	3.600887	13.073446
H	19.380741	3.623065	11.938385
C	10.472762	10.428789	13.873193
C	10.172685	11.186036	12.726568
C	9.254284	12.234777	12.826778
H	9.026354	12.740136	12.055938
C	8.673102	12.538943	14.058195
H	8.101807	13.294606	14.133351
C	8.919737	11.759517	15.162423
H	8.481245	11.960710	15.981440
C	9.815959	10.660082	15.104610
C	10.781122	10.877117	11.366036
H	11.297639	10.024818	11.460464
C	9.726444	10.645824	10.302277
H	10.164668	10.450967	9.446644
H	9.173319	11.449013	10.211703
H	9.162631	9.886992	10.562435
C	11.757240	11.941700	10.901605
H	12.117974	11.696149	10.024774
H	12.492068	12.016157	11.547183
H	11.292295	12.803504	10.834156
C	9.943419	9.745998	16.303266
H	10.739170	9.161429	16.151025
C	8.720398	8.835083	16.416965
H	8.582785	8.366160	15.569041
H	7.928121	9.373711	16.627019
H	8.866028	8.179225	17.131919
C	10.164668	10.484236	17.638746
H	10.950266	11.065637	17.563589
H	10.311634	9.828377	18.353700
H	9.376399	11.024448	17.848800
C	16.641839	10.305221	13.803817
C	16.846522	11.122668	12.674537
C	17.778016	12.168240	12.782454
H	17.943151	12.724294	12.030885
C	18.463142	12.405870	13.969548
H	19.054745	13.147276	14.036996
C	18.287585	11.566244	15.052578
H	18.774175	11.726248	15.852325
C	17.389492	10.468394	14.985130
C	16.145630	10.888207	11.350619
H	15.295100	10.403441	11.558746
C	15.757374	12.150814	10.599050
H	15.225626	12.729047	11.184888
H	15.228298	11.910016	9.808939
H	16.567020	12.626074	10.317693
C	16.978523	9.955113	10.454518
H	17.216340	9.148755	10.955564
H	17.793514	10.417699	10.171234
H	16.452120	9.706393	9.666334
C	17.314406	9.490942	16.152952
H	16.553660	8.865183	15.975659
C	18.583654	8.652900	16.289776
H	18.771503	8.199819	15.441852
H	18.458867	7.984368	16.995095
H	19.335316	9.235886	16.522955
C	17.031965	10.205416	17.496141
H	16.991884	9.543221	18.216876
H	16.176893	10.679092	17.442182
H	17.748088	10.848602	17.681143
C	13.547547	9.235886	16.700249
H	14.365210	9.589163	17.131919
H	12.791343	9.684215	17.155044
C	14.955744	6.496804	16.715665
H	14.894285	5.568463	17.020147
H	15.760046	6.911865	17.095304
H	15.009186	6.518983	15.738626
C	11.928254	6.550667	16.636654
H	11.925582	5.627078	16.964261
H	11.938943	6.549083	15.655760
H	11.123952	7.011669	16.952699
C	13.372792	7.379204	19.153447
H	13.320419	6.446110	19.450220
H	12.580247	7.865553	19.463710
H	14.178163	7.795848	19.525377
C	14.776713	12.922319	15.844616
H	15.589031	12.871625	16.334100
C	14.819467	13.261338	14.414708
H	15.634457	13.438769	13.963767
C	13.654431	13.302527	13.796109
H	13.670464	13.348469	12.847976
C	12.434617	13.285101	14.391583
H	11.639668	13.468868	13.904027
C	12.398544	12.980935	15.784876
H	11.562177	12.987272	16.237745
C	13.560908	12.672016	16.503684
H	13.528842	12.315571	17.384369

A.1.2 X-Ray structures of Alkyl cations containing Uranium

X-Ray structure of η^6-2-U

U	26.777247	13.503446	-5.391782
C	25.497402	16.315921	-4.020626
C	27.893793	16.400190	-4.055059
C	25.430473	17.597350	-3.505585
C	26.632399	18.515068	-3.328096
C	27.914952	17.674466	-3.553844
O	26.717354	15.703364	-4.374315
Si	26.631072	16.262875	-8.133831
C	24.096018	18.044889	-3.237884
H	23.961710	18.921763	-2.897945
C	30.257583	16.196670	-4.027539
H	31.048407	15.690409	-4.171598
C	29.183435	18.242011	-3.352548
H	29.244576	19.142671	-3.056607
C	23.158568	15.962366	-3.969999
H	22.400133	15.407714	-4.110156
C	29.007950	15.612476	-4.269500
N	28.754519	14.348168	-4.765203
C	30.354856	17.521319	-3.574698
C	24.403820	15.486983	-4.276868

C	26.755000	14.493941	-7.517706
H	27.582991	14.155731	-7.942175
H	26.014113	14.031340	-7.983711
C	22.984861	17.224017	-3.464068
C	26.656266	19.034331	-1.896880
H	25.852805	19.570197	-1.730358
H	27.452665	19.589755	-1.764128
H	26.678646	18.277243	-1.275016
C	21.507655	19.145925	-2.621513
H	20.581249	19.405101	-2.434346
H	21.882572	19.742619	-3.302546
H	22.038066	19.213498	-1.800228
C	32.136413	17.576864	-1.871746
H	32.160015	16.597673	-1.903774
H	31.477376	17.866163	-1.206623
H	33.021484	17.917039	-1.624046
C	29.814411	13.343790	-4.831172
C	26.579170	19.651369	-4.322192
H	25.768992	20.181213	-4.169628
H	26.565710	19.288665	-5.232495
H	27.368347	20.221366	-4.209327
C	32.773442	17.694354	-4.294861
H	32.799566	16.715508	-4.334237
H	33.655035	18.034497	-4.035020
H	32.532489	18.050408	-5.175523
C	20.679690	17.628652	-4.399922
H	19.773461	17.946297	-4.204289
H	20.641089	16.697617	-4.703401
H	21.076323	18.185034	-5.102414
C	31.739727	18.132602	-3.271332
C	21.540230	17.718094	-3.127766
C	21.880182	11.161747	-5.093721
H	21.309073	10.407725	-5.181944
C	30.161611	13.499830	-8.495930
H	30.124018	14.174566	-9.205638
H	29.294009	13.049366	-8.427158
H	30.855745	12.841255	-8.707738
C	30.028630	12.532901	-3.691824
C	30.498085	14.192065	-7.136667
H	29.750695	14.825877	-6.937473
C	30.568704	13.211348	-5.982792
C	23.382822	12.479164	-3.740216
C	29.288062	12.758400	-2.363339
H	28.420965	13.210892	-2.571568
C	22.127932	11.928080	-6.176361
H	21.683459	11.738521	-6.994313
C	23.479803	13.182263	-8.621181
H	24.294972	12.647655	-8.520836
H	23.601289	13.830272	-9.346231
H	22.726360	12.592456	-8.833046
C	31.705241	19.675266	-3.193034
H	31.461049	20.041413	-4.068639
H	32.589621	20.009073	-2.934462
H	31.043203	19.953795	-2.526301
C	31.661489	11.272571	-4.984758
H	32.262332	10.539710	-5.051257
C	24.012019	12.762677	-2.362468
H	24.560907	13.592982	-2.458987
C	30.954213	11.502818	-3.788722
H	31.113026	10.944549	-3.036663
C	21.928421	14.794371	-7.448177
H	21.753414	15.271735	-6.610376
H	21.165420	14.217298	-7.660837
H	22.059889	15.442003	-8.171844
C	31.745780	15.016128	-7.290026
H	31.958778	15.448323	-6.436657
H	31.602658	15.700958	-7.976267
H	32.489374	14.436399	-7.557159
C	22.448796	11.451407	-3.829330
H	22.198153	10.955051	-3.059089
C	23.048285	13.020830	-6.113177
C	31.476420	12.117041	-6.057834
H	31.962150	11.966677	-6.860292
C	23.189072	13.937936	-7.294136
H	23.957727	14.552269	-7.115890
C	20.956590	16.798913	-2.077153
H	20.050732	17.095963	-1.850022
H	21.518646	16.821537	-1.274675
H	20.922369	15.883851	-2.426315
C	25.101379	17.176726	-7.485641
H	25.116140	17.184210	-6.505788
H	24.291945	16.720178	-7.796677
H	25.105468	18.098108	-7.819462
N	24.756569	14.219735	-4.803727
C	23.685898	13.247855	-4.894962
C	26.550285	16.284225	-9.996505
H	27.327675	15.813040	-10.362619
H	26.551612	17.211739	-10.312920
H	25.729063	15.839122	-10.292976
C	30.108673	13.705849	-1.494609
H	30.289149	14.530998	-1.991562
H	30.956523	13.277097	-1.254409
H	29.607625	13.918315	-0.679593
C	28.969588	11.466217	-1.616584
H	28.468832	10.863644	-2.205283
H	28.430628	11.671200	-0.824164
H	29.804747	11.033975	-1.340758
C	28.129862	17.204837	-7.576894
H	28.938128	16.746716	-7.888707
H	28.139472	17.254471	-6.598197
H	28.103473	18.110796	-7.949675
C	22.932561	13.064852	-1.345834
H	23.345893	13.263844	-0.479850
H	22.342390	12.287750	-1.255243
H	22.410354	13.838636	-1.644066
C	24.938240	11.680020	-1.885629
H	25.315200	11.931837	-1.016786
H	25.663250	11.561272	-2.534237
H	24.440404	10.840785	-1.794868
C	25.637524	10.440018	-5.444645
H	24.825993	10.249767	-4.988849
C	28.009889	10.501915	-5.432921
H	28.839978	10.383985	-4.986235
C	25.574737	10.778353	-6.701535
H	24.732888	10.854368	-7.135190
C	27.995367	10.828474	-6.763773
H	28.812288	10.915857	-7.240763
C	26.776345	11.033079	-7.419501
H	26.751681	11.334091	-8.320222
C	26.829335	10.342762	-4.735580
H	26.831194	10.172242	-3.801014

X-Ray structure of η^6-3-U-endo

U	26.475973	25.967895	3.207091
Si	26.597014	23.130531	0.474077
O	26.538359	23.792852	4.259045
N	24.504125	25.166614	3.840404
N	28.481946	25.255346	3.786880
C	24.048222	21.259237	5.310425
H	23.984236	20.362409	5.620104
C	22.872472	22.003952	5.071475
C	22.987114	23.307995	4.618426
H	22.200615	23.824542	4.480790
C	24.205522	23.867324	4.368006
C	28.855200	24.003590	4.354625
C	30.092271	23.499720	4.627984
H	30.857441	24.030527	4.436824
C	30.273566	22.232120	5.176613
C	29.135141	21.430363	5.409828

H	29.252449	20.549381	5.746270
C	26.607678	20.975611	5.337187
C	25.333282	21.839164	5.094414
C	25.338614	23.081412	4.593575
C	27.751435	23.102010	4.606956
C	27.802091	21.904128	5.149850
C	26.676997	19.864877	4.362271
H	25.906494	19.270689	4.488437
H	26.663666	20.227727	3.452350
H	27.506154	19.357837	4.499906
C	26.610344	20.497092	6.790003
H	26.565020	21.271913	7.388334
H	25.834509	19.918750	6.944843
H	27.434169	19.996390	6.969694
C	21.502097	21.374905	5.390712
C	21.038195	21.912050	6.730744
H	20.166380	21.523848	6.954401
H	21.688724	21.672791	7.422743
H	20.955546	22.888102	6.681042
C	20.462318	21.761523	4.278161
H	20.763587	21.414517	3.414118
H	19.587837	21.374905	4.499906
H	20.385001	22.737575	4.228459
C	21.563417	19.798328	5.425121
H	21.864686	19.465583	4.553431
H	22.189950	19.509949	6.120943
H	20.670273	19.441815	5.618192
C	31.689265	21.763108	5.572314
C	31.739921	20.352902	6.065507
H	31.364000	19.755546	5.384977
H	32.670389	20.100967	6.241374
H	31.217365	20.275262	6.891318
C	32.270474	22.716977	6.616048
H	32.227817	23.635987	6.277694
H	31.750585	22.650427	7.443770
H	33.203609	22.476133	6.793826
C	32.585074	21.896206	4.301100
H	32.555747	22.819969	3.976128
H	33.510211	21.660115	4.528580
H	32.254478	21.292511	3.603366
C	23.429687	26.152173	3.796438
C	23.240394	27.003049	4.897519
C	22.304593	28.069418	4.782823
H	22.149959	28.655683	5.513054
C	21.606074	28.245297	3.557488
H	21.006202	28.974167	3.452350
C	21.792701	27.378576	2.544340
H	21.296807	27.508505	1.745291
C	22.664516	26.313792	2.601688
C	22.768494	25.302881	1.470020
H	23.515002	24.669081	1.678385
C	21.440776	24.478941	1.317092
H	21.536756	23.837218	0.581126
H	21.256815	23.995668	2.148638
H	20.699600	25.087388	1.122109
C	23.080428	26.017490	0.086022
H	23.141748	25.344078	-0.623182
H	22.363247	26.649706	-0.124254
H	23.930914	26.500763	0.152928
C	23.901587	26.768543	6.237551
H	24.760071	26.293193	6.046391
C	23.056433	25.803583	7.147472
H	23.515002	25.675238	8.003869
H	22.171288	26.194954	7.306135
H	22.952455	24.936861	6.700158
C	24.280173	28.048819	7.028953
H	24.701417	27.795299	7.877704
H	24.909372	28.585965	6.501352
H	23.472344	28.573289	7.208644
C	29.564383	26.263088	3.689388
C	29.828327	27.045831	4.811497
C	30.777458	28.126459	4.668127
H	31.009409	28.684204	5.402182
C	31.366667	28.322938	3.337654
H	31.963873	29.047054	3.192372
C	31.070729	27.498998	2.324506
H	31.475977	27.663785	1.481490
C	30.220243	26.435798	2.429644
C	30.084272	25.456577	1.278860
H	29.313769	24.848129	1.468109
C	31.353336	24.612039	1.169899
H	31.265355	23.979823	0.426287
H	32.123839	25.198304	1.009325
H	31.489307	24.116090	2.003357
C	29.806998	26.201292	-0.032497
H	29.721683	25.553232	-0.764640
H	28.975175	26.711501	0.049702
H	30.548174	26.812909	-0.223657
C	29.191129	26.747944	6.164910
H	28.724561	25.863794	6.103739
C	30.278898	26.641783	7.264080
H	30.929426	25.954110	7.015572
H	30.734801	27.505336	7.355837
H	29.860320	26.402524	8.116654
C	28.156682	27.803221	6.505175
H	27.754101	27.598821	7.376864
H	28.585924	28.682619	6.541495
H	27.455498	27.807975	5.818910
C	26.517031	24.898833	1.110640
H	25.714535	25.260099	0.661414
H	27.284867	25.331402	0.655679
C	28.159348	22.157648	1.118286
H	28.156682	22.148141	2.098937
H	28.132687	21.237054	0.781844
H	28.972509	22.598139	0.797137
C	26.655668	23.116271	-1.372529
H	26.695659	22.189338	-1.691766
H	25.853172	23.548839	-1.729998
H	27.450166	23.601128	-1.678385
C	25.066672	22.141803	1.022706
H	25.013350	22.137050	1.999534
H	24.258844	22.558526	0.653767
H	25.135991	21.221208	0.693911
C	26.319739	28.335614	1.288418
H	26.314407	27.849172	0.472165
C	27.476827	28.606563	1.856164
H	28.284655	28.354628	1.422230
C	27.535481	29.267300	3.096792
H	28.367304	29.392475	3.542195
C	26.378393	29.722051	3.664537
C	25.167984	29.420996	3.052825
H	24.354824	29.685608	3.465731
C	25.133325	28.725400	1.825578
H	24.309500	28.538429	1.389733
C	26.429049	30.560252	4.859287
H	25.517243	30.796342	5.128823
H	26.866290	30.067472	5.585695
H	26.935608	31.376269	4.666216

X-Ray structure of η^6-5-U-endo

O	-0.156498	15.730261	3.745891
U	-0.224668	17.934927	4.767428
Si	-0.080636	15.164970	7.520860
N	-2.182485	17.109810	4.142043
N	1.792832	17.216825	4.188683
C	-2.629433	13.191173	2.747389
H	-2.694950	12.297283	2.430165
C	-3.796538	13.913524	2.975866
C	-3.704761	15.241769	3.425267
H	-4.496004	15.750090	3.561221

C	-2.457020	15.816188	3.670739
C	2.133414	15.964120	3.655633
C	3.403436	15.499864	3.338408
H	4.159136	16.060119	3.474362
C	3.574522	14.206241	2.819142
C	2.462856	13.408350	2.615212
H	2.586197	12.533345	2.265888
C	-0.069761	12.936225	2.720954
C	-1.349862	13.745133	2.973978
C	-1.328112	15.030886	3.440373
C	1.064718	15.108000	3.415826
C	1.153046	13.844279	2.907890
C	-0.003183	11.777945	3.716056
H	-0.029178	12.132039	4.629964
H	0.830236	11.279066	3.581991
H	-0.769228	11.181494	3.576327
C	-0.089655	12.396429	1.282115
H	-0.877981	11.829879	1.155603
H	0.721483	11.869223	1.119726
H	-0.122015	13.147108	0.651443
C	-5.172129	13.310778	2.654865
C	-6.205282	13.724674	3.716056
H	-5.920402	13.395760	4.595976
H	-7.076897	13.340679	3.489468
H	-6.275839	14.701973	3.740603
C	-5.615364	13.841131	1.280227
H	-5.625974	14.821578	1.295333
H	-6.514565	13.509070	1.076297
H	-4.989371	13.531103	0.592907
C	-5.141095	11.766929	2.598218
H	-4.554360	11.478933	1.867469
H	-6.047723	11.426999	2.441494
H	-4.801043	11.414409	3.446038
C	5.005021	13.753001	2.481147
C	5.575576	14.687809	1.425621
H	6.517217	14.464336	1.263233
H	5.509263	15.614748	1.739069
H	5.068947	14.588663	0.592907
C	5.888572	13.850574	3.736827
H	5.572924	13.213205	4.409040
H	5.838175	14.760201	4.099369
H	6.816951	13.644413	3.498909
C	5.056480	12.308299	1.954328
H	4.790433	11.691389	2.668083
H	5.968148	12.098990	1.665428
H	4.442954	12.213874	1.195256
C	-3.244550	18.098125	4.197558
C	-4.012452	18.241336	5.364490
C	-4.911388	19.330371	5.428690
H	-5.421730	19.470435	6.216086
C	-5.055684	20.186491	4.369387
H	-5.639236	20.932449	4.446805
C	-4.361257	19.983478	3.177908
H	-4.514572	20.554749	2.435830
C	-3.434470	18.930639	3.072166
C	-2.726250	18.678839	1.748510
H	-1.867367	18.205140	1.948664
C	-3.572931	17.753474	0.872367
H	-3.684336	16.889485	1.319880
H	-3.127309	17.619705	0.011329
H	-4.453564	18.159501	0.723196
C	-2.385402	19.952003	0.987550
H	-3.212190	20.381636	0.683543
H	-1.827579	19.728530	0.213371
H	-1.896545	20.564191	1.576680
C	-3.917227	17.260890	6.521981
H	-3.177707	16.618800	6.321828
C	-5.216161	16.453556	6.669264
H	-5.960190	17.064171	6.852423
H	-5.124649	15.819335	7.409454
H	-5.392553	15.964120	5.838438
C	-3.595212	17.951766	7.838084
H	-2.793093	18.502579	7.730455
H	-3.437653	17.278201	8.531068
H	-4.347464	18.521464	8.100550
C	2.832615	18.217730	4.301411
C	3.138450	18.984146	3.155249
C	4.053566	20.035411	3.302532
H	4.283804	20.567339	2.549124
C	4.630221	20.310817	4.539329
H	5.204225	21.061496	4.633741
C	4.379029	19.509779	5.621290
H	4.816958	19.689186	6.444563
C	3.484337	18.422318	5.538208
C	3.340571	17.484363	6.705140
H	2.567630	16.876895	6.518204
C	4.597861	16.615653	6.867529
H	4.747993	16.102610	6.046144
H	4.474784	16.000316	7.619048
H	5.371333	17.191645	7.039359
C	3.055692	18.224025	8.028796
H	3.822267	18.793723	8.255385
H	2.912456	17.569345	8.744439
H	2.254634	18.777985	7.926832
C	2.522272	18.696150	1.793828
H	2.116703	17.783375	1.833481
C	1.416440	19.670301	1.472827
H	0.681695	19.553844	2.111052
H	1.087529	19.505058	0.564584
H	1.758614	20.586224	1.535139
C	3.570278	18.680413	0.713755
H	3.867360	19.596335	0.532484
H	3.190970	18.290122	-0.101965
H	4.334201	18.140616	1.008320
C	-0.198142	16.931976	6.892076
H	0.546417	17.391511	7.356583
H	-1.023869	17.275054	7.320706
C	1.435008	14.266044	6.886411
H	1.432355	14.270765	5.906415
H	1.424398	13.339105	7.209300
H	2.241371	14.714563	7.213077
C	0.005040	15.189835	9.397770
H	0.769228	15.732779	9.682895
H	0.114058	14.273913	9.731989
H	-0.822278	15.573830	9.756536
C	-1.594159	14.203094	6.995929
H	-2.389912	14.602826	7.401901
H	-1.506626	13.273008	7.290495
H	-1.673734	14.231421	6.019709
C	-0.328911	20.403669	6.686258
H	-0.342174	20.025969	7.558625
C	-1.509278	20.693239	6.042368
H	-2.339514	20.527995	6.476663
C	-1.499199	21.225166	4.756477
H	-2.310336	21.404574	4.295746
C	-0.297081	21.483261	4.174899
C	0.901853	21.182675	4.771582
H	1.721479	21.325886	4.316517
C	0.885938	20.664911	6.055586
H	1.705564	20.487078	6.506875
F	-0.272413	22.093876	2.962649

A.1.3 X-Ray structures of Alkyl cations containing Zirconium

X-Ray structure of η^6-3'-Zr-exo

Zr	7.285954	8.774163	15.782526
O	8.282123	10.391022	14.632517
N	6.037782	10.513949	15.737937
N	8.621293	7.924604	14.345425
C	7.683726	13.944571	13.954353
H	8.083844	14.707173	13.554143
C	6.413363	14.079126	14.540962
C	5.844292	12.955691	15.147673
H	4.984944	13.030522	15.547883
C	6.501660	11.731730	15.178739
C	9.525022	8.743962	13.625413
C	10.531792	8.332530	12.766515
H	10.671907	7.404743	12.623974
C	11.343474	9.257527	12.106808
C	11.096220	10.627797	12.284070
H	11.640386	11.257814	11.827209
C	9.764440	12.571519	13.303783
C	8.378486	12.736923	13.939733
C	7.752986	11.682390	14.572028
C	9.358702	10.107644	13.766126
C	10.070439	11.091258	13.115556
C	9.834116	13.312058	11.969750
H	9.634537	14.260729	12.110463
H	10.734898	13.220060	11.591469
H	9.179132	12.929556	11.348419
C	10.797486	13.166765	14.268673
H	10.611125	14.119810	14.400249
H	10.744894	12.702701	15.131226
H	11.695268	13.057588	13.892220
C	12.440608	8.749381	11.182122
C	13.324447	7.701830	11.956958
H	13.740545	8.134607	12.731793
H	12.761565	6.958546	12.260313
H	14.023335	7.358586	11.361211
C	11.825687	8.061895	10.014386
H	11.207569	7.370662	10.330534
H	11.335317	8.715614	9.471636
H	12.529310	7.648445	9.471636
C	13.413114	9.838731	10.772775
H	13.789554	10.258385	11.575022
H	14.135691	9.446844	10.239162
H	12.943058	10.511657	10.240989
C	5.689633	15.432942	14.502585
C	6.524951	16.475573	15.222598
H	7.412773	16.524700	14.809596
H	6.085299	17.350191	15.154982
H	6.615473	16.228322	16.165558
C	4.317907	15.369288	15.149500
H	3.771037	14.697344	14.690812
H	4.413528	15.121533	16.094288
H	3.883354	16.243402	15.083712
C	5.517302	15.862992	13.031494
H	4.977773	15.196934	12.558186
H	5.065259	16.732238	12.996773
H	6.396836	15.935524	12.607527
C	4.635503	10.649064	16.114390
C	4.260817	10.961367	17.426494
C	2.913795	11.137363	17.715230
H	2.652761	11.333561	18.608849
C	1.934866	11.036785	16.730238
C	2.325160	10.725841	15.440063
H	1.660592	10.635369	14.767565
C	3.667875	10.537688	15.094677
C	4.020244	10.264885	13.632723
H	5.013773	10.190733	13.552315
C	3.534732	11.429597	12.735448
H	3.766245	11.240789	11.801625
H	2.561892	11.521268	12.819511
H	3.967172	12.261118	13.018702
C	3.391500	8.966358	13.128348
H	3.640094	8.826729	12.190870
H	3.716534	8.215453	13.667444
H	2.416275	9.025349	13.203274
C	5.298783	11.151457	18.550371
H	6.087771	10.578845	18.329250
C	5.793157	12.598983	18.628951
H	6.121621	12.880460	17.749951
H	5.053736	13.180551	18.904895
H	6.518045	12.660645	19.285003
C	4.786192	10.718832	19.930090
H	4.468725	9.792612	19.882577
H	5.512989	10.781503	20.582487
H	4.048384	11.303261	20.202379
C	0.476312	11.367248	17.050041
H	0.375806	11.343025	18.044169
C	0.167541	12.787874	16.595007
H	0.818146	13.405717	16.987907
H	0.220425	12.837202	15.617325
H	-0.735038	13.033770	16.885571
C	-0.505722	10.357198	16.467086
H	-0.273983	9.458964	16.781406
H	-1.414166	10.580861	16.757650
H	-0.458407	10.382440	15.489404
C	8.724414	6.550147	13.901357
C	7.912949	6.118556	12.826820
C	8.096091	4.819031	12.346203
H	7.544826	4.513116	11.635328
C	9.052372	3.957291	12.870679
C	9.808169	4.402191	13.950698
H	10.450845	3.813735	14.330806
C	9.663728	5.672445	14.497103
C	6.864113	7.023863	12.198180
H	6.530177	7.631103	12.918193
C	7.428729	7.903651	11.098060
H	6.714230	8.464996	10.728916
H	8.134606	8.476678	11.465376
H	7.801984	7.342060	10.387184
C	5.647374	6.247618	11.660912
H	5.283776	5.679046	12.371787
H	4.960606	6.881427	11.364866
H	5.924244	5.689371	10.904351
C	10.476433	6.072451	15.719662
H	9.989020	6.820522	16.171041
C	11.869091	6.582939	15.366966
H	12.345549	6.825247	16.187488
H	12.364905	5.883029	14.895486
H	11.790337	7.372226	14.789494
C	10.597018	4.916060	16.741203
H	11.127022	5.215100	17.510556
H	9.703872	4.651283	17.042731
H	11.038640	4.151161	16.317236
C	9.260431	2.545222	12.327929
H	10.246890	2.386918	12.364477
C	8.642170	1.500104	13.241650
H	8.911817	1.676107	14.168163
H	7.666109	1.541500	13.172207
H	8.951510	0.610315	12.974843
C	8.883953	2.312729	10.968311
H	9.290919	2.995402	10.394494
H	9.193640	1.425966	10.690540
H	7.908521	2.357655	10.886076
C	8.775268	9.430622	17.320502
H	8.307558	9.853784	18.069754
H	9.275254	8.652146	17.643959
H	9.398000	10.073301	16.918465
C	6.607178	7.309345	18.119095
C	7.250882	6.408794	17.260196
H	8.069384	6.017177	17.537968
C	6.744188	6.074138	16.035810
H	7.186440	5.422365	15.504024
C	5.590706	6.675344	15.562502
H	5.258827	6.458109	14.698122
C	4.931415	7.581915	16.339165
H	4.138094	7.994394	16.019363
C	5.427308	7.904468	17.607411
H	4.960818	8.539566	18.139196
C	7.083585	7.573345	19.498814
H	6.495514	8.231630	19.926435
H	7.071395	6.740065	20.014153
H	7.998037	7.924672	19.467747

A.1.4 Optimised geometries of Alkyl cations containing Thorium

Optimised geometry of η^6-2-Th and the name of the fragment f in the ETS-NOCV in which each atom belongs

Th	13.5411509	10.1377154	14.5509358 f=U	C	10.2305495	10.3306062	10.2068517 f=U
Si	13.4112173	7.5322504	17.4978204 f=U	H	10.8007652	10.0548590	9.3166019 f=U
O	13.4985180	7.8349960	13.6124273 f=U	H	9.5010599	11.0900207	9.9142923 f=U
N	11.5227749	9.3960006	13.7995967 f=U	H	9.6858193	9.4486246	10.5451961 f=U
C	10.9455192	5.5470351	12.3276461 f=U	C	11.9584772	12.0530811	10.7679995 f=U
H	10.8362841	4.5394039	11.9548734 f=U	H	12.5061723	11.7733943	9.8652660 f=U
N	15.5376637	9.3173458	13.8106982 f=U	H	12.6859752	12.4209590	11.4964693 f=U
C	9.8258568	6.3633255	12.4096511 f=U	H	11.3042754	12.8873466	10.5044660 f=U
C	9.9815248	7.6658022	12.8964944 f=U	C	9.6856998	9.7777687	16.0817399 f=U
H	9.1316192	8.3345344	12.9572021 f=U	H	10.5426491	9.1050062	16.0069246 f=U
C	11.2234660	8.1309948	13.3013923 f=U	C	8.4251433	8.9127275	16.1276204 f=U
C	15.7913673	8.0286696	13.3459828 f=U	H	8.3418233	8.2784856	15.2451328 f=U
C	17.0187729	7.5006963	12.9720467 f=U	H	7.5263993	9.5319572	16.1895833 f=U
H	17.8956188	8.1335073	13.0341862 f=U	H	8.4433803	8.2625803	17.0056007 f=U
C	17.1226427	6.1945221	12.4820930 f=U	C	9.8119876	10.5679219	17.3819215 f=U
C	15.9685601	5.4300640	12.3804617 f=U	H	10.7036482	11.1984294	17.3977057 f=U
H	16.0374282	4.4192964	12.0068144 f=U	H	9.8739262	9.8845784	18.2319737 f=U
C	13.4451964	5.0751477	12.6312720 f=U	H	8.9464597	11.2129345	17.5505540 f=U
C	12.2213251	5.9770285	12.7095653 f=U	C	16.6044161	10.2635307	13.8450668 f=U
C	12.3047788	7.2583693	13.1939544 f=U	C	16.7787840	11.1528864	12.7545679 f=U
C	14.6742893	7.2043935	13.2214293 f=U	C	17.7877195	12.1065971	12.8322780 f=U
C	14.7078764	5.9193695	12.7389865 f=U	H	17.9362931	12.7967494	12.0117006 f=U
C	13.4425255	4.2973168	11.3110614 f=U	C	18.6182955	12.1910936	13.9374748 f=U
H	14.3003684	3.6274961	11.2517737 f=U	H	19.4005878	12.9405693	13.9717481 f=U
H	13.4715311	4.9718018	10.4535549 f=U	C	18.4522472	11.3108758	14.9886070 f=U
H	12.5523668	3.6736791	11.2287250 f=U	H	19.1161199	11.3728628	15.8433492 f=U
C	13.4074615	4.0789474	13.8032364 f=U	C	17.4577070	10.3361746	14.9682044 f=U
H	14.2796188	3.4222287	13.7710610 f=U	C	15.9297148	11.0708127	11.4977558 f=U
H	12.5082246	3.4614699	13.7473022 f=U	H	14.9128837	10.7741860	11.7951912 f=U
H	13.4059143	4.5973764	14.7637199 f=U	C	15.8265003	12.3878320	10.7349313 f=U
C	8.4395024	5.8845547	11.9793421 f=U	H	15.5639355	13.2360915	11.3706355 f=U
C	7.9176908	6.7810542	10.8503947 f=U	H	15.0700117	12.3039652	9.9530766 f=U
H	8.5838292	6.7503773	9.9846807 f=U	H	16.7676868	12.6329311	10.2376493 f=U
H	7.8214859	7.8214193	11.1686322 f=U	C	16.4421692	9.9914081	10.5407292 f=U
H	6.9292862	6.4430363	10.5290679 f=U	H	16.4464425	9.0022685	10.9946364 f=U
C	7.4777847	5.9633618	13.1704677 f=U	H	17.4630052	10.2261678	10.2276067 f=U
H	6.4876781	5.6046543	12.8780991 f=U	H	15.8179199	9.9548450	9.6445553 f=U
H	7.3622998	6.9872296	13.5318342 f=U	C	17.3648884	9.3733850	16.1341247 f=U
H	7.8299581	5.3480955	14.0018572 f=U	H	16.4718301	8.7616463	15.9910548 f=U
C	8.4539888	4.4440075	11.4745932 f=U	C	18.5702046	8.4333869	16.1724097 f=U
H	9.0968831	4.3240268	10.5991082 f=U	H	18.6555576	7.8490821	15.2572107 f=U
H	7.4433857	4.1532997	11.1803993 f=U	H	18.4762324	7.7339345	17.0065442 f=U
H	8.7837445	3.7442284	12.2464610 f=U	H	19.4997500	8.9918326	16.3103739 f=U
C	18.4863186	5.6656603	12.0377325 f=U	C	17.2415441	10.0901175	17.4769903 f=U
C	18.9881421	6.5088337	10.8587986 f=U	H	17.1033516	9.3630039	18.2805042 f=U
H	19.0965641	7.5610272	11.1309185 f=U	H	16.3937546	10.7770891	17.5005999 f=U
H	18.2996336	6.4479457	10.0124772 f=U	H	18.1402206	10.6649430	17.7121421 f=U
H	19.9653575	6.1483343	10.5274803 f=U	C	13.4931435	9.2830186	16.8053328 f=U
C	19.4892647	5.7671788	13.1915918 f=U	H	14.3816515	9.7454179	17.2697837 f=U
H	19.6540149	6.8018053	13.4986825 f=U	H	12.6316977	9.8147787	17.2471611 f=U
H	20.4560660	5.3615223	12.8833908 f=U	C	14.9126528	6.5317840	16.9803795 f=U
H	19.1473189	5.2033597	14.0628291 f=U	H	14.8187365	5.5078077	17.3538912 f=U
C	18.4249925	4.2074922	11.5900877 f=U	H	15.8303965	6.9446519	17.4074739 f=U
H	17.7678338	4.0709094	10.7278683 f=U	H	15.0428410	6.4776692	15.8967079 f=U
H	18.0861434	3.5483540	12.3932988 f=U	C	11.8474905	6.6589310	16.9367496 f=U
H	19.4228595	3.8776437	11.2937161 f=U	H	11.8420964	5.6339427	17.3191504 f=U
C	10.5226752	10.4095246	13.7394240 f=U	H	11.7489874	6.6064370	15.8496706 f=U
C	10.3924842	11.1763814	12.5587559 f=U	H	10.9543500	7.1515076	17.3302000 f=U
C	9.4745988	12.2211291	12.5401612 f=U	C	13.3884479	7.6116642	19.3749136 f=U
H	9.3631736	12.8172040	11.6410803 f=U	H	13.3422745	6.6090710	19.8097699 f=U
C	8.6829065	12.5007577	13.6402780 f=U	H	12.5222756	8.1700561	19.7406040 f=U
H	7.9697568	13.3162732	13.6040570 f=U	H	14.2860040	8.0995391	19.7649674 f=U
C	8.7817089	11.7146781	14.7742515 f=U	C	14.9635327	13.0048072	15.1370528 f=B
H	8.1297067	11.9162214	15.6167982 f=U	H	16.0276938	13.0028906	14.9293386 f=B
C	9.6845539	10.6577207	14.8487296 f=U	C	14.0518998	13.2555576	14.1108529 f=B
C	11.1667063	10.8589817	11.2945455 f=U	H	14.4129924	13.4643714	13.1114026 f=B
H	11.8752658	10.0584404	11.5264475 f=U	C	12.6851956	13.2744506	14.3762951 f=B

```
H    11.9749179   13.4871561   13.5868063 f=B
C    12.2238385   13.0253003   15.6668106 f=B
H    11.1596929   13.0395968   15.8654698 f=B
C    13.1300729   12.7600194   16.6864401 f=B
H    12.7760406   12.5675868   17.6921270 f=B
C    14.4981855   12.7588473   16.4235351 f=B
H    15.2011788   12.5782390   17.2268758 f=B
```

Optimised geometry of η^6-2′-Th and the name of the fragment f in the ETS-NOCV in which each atom belongs

```
 C     6.448660     8.349540    15.663848 f=B
 C     7.300386     9.148847    14.911264 f=B
 C     6.925039    10.448375    14.570928 f=B
 C     5.699877    10.954523    14.987350 f=B
 C     4.845149    10.153568    15.744930 f=B
 C     5.217007     8.854583    16.079916 f=B
 H     8.256217     8.763558    14.578559 f=B
Th     7.164431    10.644975    17.851354 f=U
 C     9.379337    10.971753    16.902655 f=U
 O     8.269407    11.505852    19.921606 f=U
 C     8.688510    10.620761    20.908436 f=U
 C     9.324873    11.041861    22.054830 f=U
 C     9.682854    12.512835    22.223304 f=U
 C     8.678455    13.348153    21.439599 f=U
 C     8.078501    12.823486    20.321152 f=U
 C     8.365939     9.300966    20.626994 f=U
 C     8.713481     8.339491    21.572384 f=U
 C     9.353649     8.701681    22.755722 f=U
 C     9.650656    10.046886    22.973504 f=U
 C     8.355137    14.672802    21.748207 f=U
 C     7.480591    15.423653    20.971475 f=U
 C     6.917940    14.836237    19.833472 f=U
 C     7.203610    13.520925    19.493551 f=U
 C     9.736427     7.670919    23.817652 f=U
 C     9.081644     8.043433    25.153185 f=U
 N     7.699676     9.092247    19.423501 f=U
 C     7.296067     7.779314    19.050671 f=U
 C     8.212604     6.884735    18.461359 f=U
 C     7.754086     5.636466    18.050225 f=U
 C     6.433287     5.239485    18.194469 f=U
 C     5.549754     6.133385    18.792223 f=U
 C     5.948273     7.386616    19.238601 f=U
 N     6.689588    12.792345    18.424627 f=U
 C     5.804834    13.415369    17.499156 f=U
 C     4.411124    13.178389    17.596127 f=U
 C     3.571541    13.739065    16.642895 f=U
 C     4.046292    14.544896    15.611789 f=U
 C     5.411699    14.775050    15.549290 f=U
 C     6.308386    14.229095    16.463696 f=U
 C     7.088977    16.853075    21.347217 f=U
 C     7.854314    17.363808    22.565489 f=U
 C     9.714309    12.913093    23.695877 f=U
 C    11.079816    12.742952    21.614541 f=U
 C     9.681194     7.215740    18.284940 f=U
 C    10.126998     7.102465    16.828350 f=U
 C     5.978854     3.873659    17.737045 f=U
 C     4.915656     3.964707    16.644952 f=U
 C     4.961000     8.267096    19.984546 f=U
 C     3.505638     8.065806    19.579893 f=U
 C     3.819112    12.378437    18.744211 f=U
 C     2.457881    11.761962    18.444061 f=U
 C     3.108121    15.160683    14.601050 f=U
 C     2.122265    16.121320    15.262480 f=U
 C     7.782213    14.549984    16.314864 f=U
 C     8.319906    14.149930    14.942119 f=U
 C     7.371238    17.801557    20.177554 f=U
 C     5.590301    16.887479    21.672558 f=U
 C    11.260601     7.659871    23.985513 f=U
 C     9.285294     6.260050    23.448736 f=U
 C     5.098534     8.071927    21.496682 f=U
 C    10.562128     6.323028    19.159695 f=U
 C     5.488537     3.024870    18.908129 f=U
 C     3.715116    13.226717    20.013531 f=U
 C     8.059835    16.032898    16.559612 f=U
 C     2.373532    14.098188    13.786825 f=U
 H    10.152131    10.330023    23.888875 f=U
 H     8.450525     7.308436    21.378778 f=U
 H     6.221636    15.391464    19.216544 f=U
 H     8.801289    15.121396    22.622734 f=U
 H    10.459639    12.330648    24.238107 f=U
 H    10.002900    13.958665    23.806240 f=U
 H     8.744294    12.767600    24.174469 f=U
 H    11.824988    12.142624    22.141416 f=U
 H    11.103007    12.465198    20.558827 f=U
 H    11.358488    13.796020    21.696255 f=U
 H     8.428081    17.782964    19.900585 f=U
 H     6.782925    17.546487    19.293858 f=U
 H     7.112413    18.826152    20.456160 f=U
 H     4.984813    16.574685    20.818948 f=U
 H     5.357082    16.227597    22.511691 f=U
 H     5.286129    17.901841    21.943617 f=U
 H     8.933574    17.373606    22.393645 f=U
 H     7.546741    18.388853    22.782707 f=U
 H     7.650387    16.766923    23.457643 f=U
 H    11.640703     8.634550    24.297409 f=U
 H    11.550679     6.930088    24.745862 f=U
 H    11.756464     7.390254    23.049753 f=U
 H     8.200520     6.195917    23.330624 f=U
 H     9.755592     5.905573    22.528094 f=U
 H     9.569888     5.568591    24.244652 f=U
 H     7.992544     8.059968    25.064985 f=U
 H     9.348778     7.310570    25.918811 f=U
 H     9.404244     9.024079    25.507326 f=U
 H     8.457690     4.940785    17.603033 f=U
 H     4.518457     5.831085    18.931744 f=U
 H     5.219483     9.316942    19.783169 f=U
 H     4.397689     8.719048    22.029836 f=U
 H     4.869599     7.036302    21.762049 f=U
 H     6.105086     8.298043    21.846915 f=U
 H     2.880197     8.812384    20.072817 f=U
 H     3.345861     8.153629    18.502933 f=U
 H     3.132745     7.088407    19.893355 f=U
 H     9.832313     8.249140    18.605377 f=U
 H    10.302822     6.411946    20.214725 f=U
 H    10.466955     5.272560    18.873125 f=U
 H    11.611734     6.604369    19.047000 f=U
 H     9.526918     7.732119    16.168719 f=U
 H    11.169676     7.411654    16.726623 f=U
 H    10.053588     6.074735    16.464599 f=U
 H     6.854906     3.374881    17.308324 f=U
 H     6.253572     2.933285    19.681652 f=U
 H     4.597109     3.460537    19.367043 f=U
 H     5.227143     2.020410    18.567851 f=U
 H     5.272237     4.536188    15.784462 f=U
 H     4.641388     2.967195    16.294703 f=U
 H     4.005624     4.444141    17.016024 f=U
 H     2.505624    13.557923    16.711566 f=U
 H     5.794312    15.410401    14.756373 f=U
 H     4.509890    11.552785    18.975309 f=U
 H     3.298689    12.635573    20.832968 f=U
 H     4.681936    13.614883    20.330078 f=U
 H     3.048178    14.075460    19.840086 f=U
 H     2.443194    11.181806    17.518788 f=U
 H     2.166043    11.098397    19.259802 f=U
 H     1.681735    12.526691    18.367518 f=U
 H     8.328201    13.979937    17.070267 f=U
```

H	9.130050	16.234179	16.471880 f=U	H	1.498399	16.605965	14.508211 f=U
H	7.543497	16.656840	15.825489 f=U	H	1.457184	15.594541	15.951904 f=U
H	7.742040	16.343841	17.554241 f=U	H	9.871404	10.025805	16.646618 f=U
H	9.397846	14.319703	14.894657 f=U	H	9.413709	11.606802	16.011060 f=U
H	8.138224	13.095654	14.726289 f=U	H	10.003158	11.456396	17.663952 f=U
H	7.860456	14.737197	14.143512 f=U	H	7.590831	11.058690	13.973750 f=B
H	3.726010	15.742515	13.908517 f=U	H	5.407176	11.967868	14.736753 f=B
H	3.071820	13.431188	13.275369 f=U	H	3.884992	10.544719	16.056569 f=B
H	1.726274	13.487868	14.422540 f=U	H	4.550204	8.224420	16.654750 f=B
H	1.741605	14.566840	13.029173 f=U	H	6.736682	7.341461	15.938480 f=B
H	2.640904	16.899829	15.825484 f=U				

Optimised geometry of η^6-3-Th-endo and the name of the fragment f in the ETS-NOCV in which each atom belongs

Th	26.469113	25.919467	3.054570 f=Th	C	23.437643	26.045708	3.736822 f=Th
Si	26.498129	23.187135	0.209239 f=Th	C	23.193232	26.811633	4.899734 f=Th
O	26.545771	23.688876	4.136458 f=Th	C	22.251709	27.832567	4.840704 f=Th
N	24.479648	25.075114	3.757777 f=Th	H	22.052590	28.425707	5.726678 f=Th
N	28.517924	25.221841	3.760973 f=Th	C	21.550486	28.094794	3.676630 f=Th
C	24.105598	21.278497	5.415433 f=Th	H	20.820296	28.895638	3.649621 f=Th
H	24.052209	20.284913	5.836461 f=Th	C	21.758117	27.308521	2.557807 f=Th
C	22.935505	22.003301	5.237570 f=Th	H	21.170142	27.492155	1.666019 f=Th
C	23.021269	23.288249	4.689001 f=Th	C	22.679653	26.264577	2.564402 f=Th
H	22.129472	23.886926	4.549660 f=Th	C	22.752016	25.336264	1.369209 f=Th
C	24.244585	23.822236	4.316302 f=Th	H	23.644763	24.718343	1.483349 f=Th
C	28.834930	23.976126	4.298954 f=Th	C	21.543678	24.396568	1.366107 f=Th
C	30.095976	23.511931	4.639610 f=Th	H	21.603724	23.704147	0.522898 f=Th
H	30.946854	24.165120	4.489640 f=Th	H	21.492525	23.805016	2.280166 f=Th
C	30.271912	22.231574	5.176165 f=Th	H	20.611991	24.960193	1.271014 f=Th
C	29.152555	21.435039	5.371738 f=Th	C	22.833622	26.056432	0.026414 f=Th
H	29.274497	20.444078	5.784788 f=Th	H	22.931493	25.326972	-0.780787 f=Th
C	26.640519	20.976713	5.274151 f=Th	H	21.934328	26.641345	-0.179127 f=Th
C	25.365650	21.783038	5.072275 f=Th	H	23.689098	26.732023	-0.040362 f=Th
C	25.380943	23.041064	4.525425 f=Th	C	23.882047	26.522059	6.217689 f=Th
C	27.754998	23.120629	4.514888 f=Th	H	24.563594	25.682679	6.062735 f=Th
C	27.858350	21.862623	5.053187 f=Th	C	22.873655	26.093737	7.283140 f=Th
C	26.668153	19.821188	4.259757 f=Th	H	23.391056	25.834750	8.209990 f=Th
H	25.803826	19.169318	4.401271 f=Th	H	22.169142	26.897423	7.509556 f=Th
H	26.648363	20.196642	3.234743 f=Th	H	22.301963	25.222208	6.962220 f=Th
H	27.572801	19.223325	4.386791 f=Th	C	24.703823	27.707821	6.711773 f=Th
C	26.670432	20.405166	6.697648 f=Th	H	25.221499	27.453694	7.639612 f=Th
H	26.651614	21.203516	7.441974 f=Th	H	25.456603	28.016314	5.981290 f=Th
H	25.815150	19.752300	6.873370 f=Th	H	24.071507	28.575248	6.916668 f=Th
H	27.568157	19.807784	6.858219 f=Th	C	29.534589	26.220856	3.708390 f=Th
C	21.565837	21.440444	5.616069 f=Th	C	29.742928	27.052520	4.833574 f=Th
C	20.892009	22.367916	6.633781 f=Th	C	30.701983	28.055733	4.751219 f=Th
H	19.915904	21.967019	6.917791 f=Th	H	30.877429	28.696796	5.607479 f=Th
H	21.495885	22.461869	7.539534 f=Th	C	31.453602	28.241287	3.604421 f=Th
H	20.728952	23.368796	6.228016 f=Th	H	32.200623	29.025774	3.564420 f=Th
C	20.690088	21.347737	4.361113 f=Th	C	31.264721	27.406359	2.519459 f=Th
H	21.148432	20.701537	3.608780 f=Th	H	31.876719	27.539654	1.634518 f=Th
H	19.711579	20.932108	4.615291 f=Th	C	30.319452	26.384784	2.546155 f=Th
H	20.524517	22.327814	3.909266 f=Th	C	30.216109	25.460988	1.351702 f=Th
C	21.661712	20.047701	6.233881 f=Th	H	29.349086	24.815817	1.506254 f=Th
H	22.092698	19.321863	5.540052 f=Th	C	31.446241	24.558303	1.250698 f=Th
H	22.256036	20.047567	7.150917 f=Th	H	31.355726	23.889038	0.391749 f=Th
H	20.660483	19.696860	6.492125 f=Th	H	32.356540	25.148614	1.117881 f=Th
C	31.679939	21.758846	5.537326 f=Th	H	31.566469	23.942200	2.141915 f=Th
C	31.690734	20.333640	6.084065 f=Th	C	30.025468	26.218907	0.039455 f=Th
H	31.307353	19.614486	5.356066 f=Th	H	29.851268	25.518546	-0.780545 f=Th
H	32.716728	20.044169	6.320659 f=Th	H	29.177639	26.906995	0.078308 f=Th
H	31.106100	20.243909	7.002891 f=Th	H	30.910057	26.805036	-0.220261 f=Th
C	32.268408	22.686666	6.606896 f=Th	C	29.008315	26.849444	6.143433 f=Th
H	32.339373	23.718410	6.255516 f=Th	H	28.164802	26.176540	5.954794 f=Th
H	31.657825	22.678132	7.513038 f=Th	C	29.909590	26.164717	7.172527 f=Th
H	33.276153	22.359312	6.874867 f=Th	H	30.266565	25.198930	6.815215 f=Th
C	32.571260	21.798332	4.290836 f=Th	H	30.778685	26.788618	7.397685 f=Th
H	32.672828	22.810963	3.895951 f=Th	H	29.364612	26.001022	8.105411 f=Th
H	33.574293	21.439714	4.535737 f=Th	C	28.457855	28.149350	6.722713 f=Th
H	32.168149	21.163421	3.498296 f=Th	H	27.861080	27.941690	7.613142 f=Th

H	29.258894	28.827417	7.024926	f=Th
H	27.826359	28.679312	6.006731	f=Th
C	26.484300	24.957442	0.858341	f=Th
H	25.609820	25.448510	0.394133	f=Th
H	27.365781	25.442901	0.403947	f=Th
C	28.047737	22.290222	0.770925	f=Th
H	28.154622	22.260180	1.858087	f=Th
H	28.022145	21.257050	0.412318	f=Th
H	28.950212	22.749567	0.359284	f=Th
C	26.484766	23.216983	-1.668929	f=Th
H	26.497324	22.202336	-2.077350	f=Th
H	25.591738	23.716558	-2.054552	f=Th
H	27.356506	23.743600	-2.067007	f=Th
C	24.987683	22.236778	0.789041	f=Th
H	24.893503	22.203574	1.877209	f=Th
H	24.064604	22.661076	0.385989	f=Th
H	25.048904	21.204938	0.430768	f=Th
C	26.827615	28.441463	1.316750	f=A
H	27.085837	27.949098	0.386075	f=A
C	27.820063	28.983913	2.131822	f=A
H	28.865567	28.874316	1.869306	f=A
C	27.470234	29.689727	3.274113	f=A
H	28.253011	30.128912	3.882477	f=A
C	26.133457	29.867310	3.638993	f=A
C	25.150973	29.272326	2.846033	f=A
H	24.105505	29.373111	3.116053	f=A
C	25.490418	28.582979	1.686483	f=A
H	24.702520	28.189350	1.055050	f=A
C	25.764723	30.726492	4.805827	f=A
H	24.755135	30.515800	5.157193	f=A
H	26.459298	30.603577	5.638495	f=A
H	25.799387	31.780010	4.512007	f=A

Optimised geometry of η^6-4-Th-endo and the name of the fragment f in the ETS-NOCV in which each atom belongs

C	-0.405504	20.474935	6.472660	f=B
H	-0.451964	19.897584	7.391840	f=B
C	-1.580961	20.887258	5.843236	f=B
H	-2.548584	20.589392	6.230125	f=B
C	-1.525375	21.714859	4.730646	f=B
H	-2.437800	22.049040	4.254497	f=B
C	-0.289387	22.128361	4.248432	f=B
C	0.890761	21.705107	4.846807	f=B
H	1.848502	22.028407	4.460721	f=B
C	0.828943	20.882566	5.963866	f=B
H	1.751910	20.590332	6.451028	f=B
Br	-0.214734	23.294165	2.778681	f=B
O	-0.137029	15.618435	3.854669	f=Th
Th	-0.207254	17.846730	4.922957	f=Th
Si	-0.118522	15.157580	7.798293	f=Th
N	-2.193952	17.020068	4.221336	f=Th
N	1.830457	17.131702	4.248284	f=Th
C	-2.590922	13.195811	2.629948	f=Th
H	-2.649661	12.196827	2.222161	f=Th
C	-3.759238	13.920825	2.819720	f=Th
C	-3.667255	15.213281	3.349689	f=Th
H	-4.558044	15.812622	3.494180	f=Th
C	-2.438551	15.756988	3.687913	f=Th
C	2.153015	15.892179	3.702890	f=Th
C	3.412718	15.428971	3.359864	f=Th
H	4.264951	16.080615	3.510567	f=Th
C	3.584121	14.146308	2.825456	f=Th
C	2.462686	13.351421	2.632720	f=Th
H	2.583210	12.359043	2.222378	f=Th
C	-0.052978	12.900052	2.731413	f=Th
C	-1.326425	13.706023	2.946988	f=Th
C	-1.306004	14.970620	3.477839	f=Th
C	1.070082	15.041016	3.483720	f=Th
C	1.168536	13.781983	2.949052	f=Th
C	-0.017853	11.736482	3.735730	f=Th
H	-0.029700	12.103119	4.763913	f=Th
H	0.885644	11.139244	3.596541	f=Th
H	-0.882813	11.084915	3.595519	f=Th
C	-0.034995	12.340189	1.302920	f=Th
H	-0.892939	11.689904	1.129312	f=Th
H	0.861273	11.743464	1.130502	f=Th
H	-0.059071	13.144276	0.565289	f=Th
C	-5.133420	13.357466	2.459291	f=Th
C	-6.023893	13.339843	3.706953	f=Th
H	-5.581815	12.728508	4.497247	f=Th
H	-7.003768	12.922166	3.462486	f=Th
H	-6.185632	14.343492	4.105414	f=Th
C	-5.780717	14.244655	1.389207	f=Th
H	-5.918110	15.270121	1.739052	f=Th
H	-6.765218	13.852638	1.121674	f=Th
H	-5.170988	14.274494	0.482843	f=Th
C	-5.051963	11.934404	1.913275	f=Th
H	-4.461375	11.881833	0.995315	f=Th
H	-6.056915	11.579727	1.675306	f=Th
H	-4.624376	11.241402	2.642110	f=Th
C	4.991460	13.666076	2.472793	f=Th
C	5.605641	14.606920	1.429624	f=Th
H	6.611113	14.269476	1.165878	f=Th
H	5.689967	15.629811	1.802986	f=Th
H	5.005237	14.626711	0.516798	f=Th
C	5.863277	13.672319	3.733919	f=Th
H	5.445883	13.018721	4.503511	f=Th
H	5.958830	14.674531	4.156801	f=Th
H	6.869528	13.318038	3.496458	f=Th
C	4.995106	12.251723	1.898777	f=Th
H	4.601785	11.521239	2.610039	f=Th
H	6.020457	11.958932	1.663655	f=Th
H	4.415627	12.184283	0.974691	f=Th
C	-3.237475	17.989542	4.256989	f=Th
C	-4.030672	18.149565	5.415555	f=Th
C	-5.001467	19.147346	5.425738	f=Th
H	-5.621181	19.275276	6.305987	f=Th
C	-5.207280	19.962933	4.328997	f=Th
H	-5.976300	20.726544	4.355224	f=Th
C	-4.442450	19.787016	3.189331	f=Th
H	-4.626331	20.416672	2.326806	f=Th
C	-3.455403	18.810081	3.123461	f=Th
C	-2.699432	18.621235	1.823636	f=Th
H	-1.814047	18.009960	2.034213	f=Th
C	-3.546606	17.848541	0.810246	f=Th
H	-3.840670	16.870516	1.190998	f=Th
H	-2.986463	17.698609	-0.115853	f=Th
H	-4.453714	18.407897	0.566263	f=Th
C	-2.233279	19.937665	1.209300	f=Th
H	-3.075021	20.541094	0.863108	f=Th
H	-1.603845	19.742514	0.338989	f=Th
H	-1.658794	20.545727	1.911388	f=Th
C	-3.908763	17.243891	6.622137	f=Th
H	-3.024594	16.619234	6.479860	f=Th
C	-5.115906	16.310986	6.727828	f=Th
H	-6.041430	16.878823	6.853081	f=Th
H	-5.010901	15.650904	7.592229	f=Th
H	-5.217683	15.685165	5.840912	f=Th
C	-3.743717	18.023576	7.925264	f=Th
H	-2.909258	18.729106	7.886016	f=Th
H	-3.560794	17.337950	8.755902	f=Th
H	-4.642262	18.594119	8.171093	f=Th
C	2.801737	18.172617	4.277836	f=Th
C	2.987104	18.971199	3.124594	f=Th
C	3.880039	20.034852	3.186067	f=Th
H	4.035063	20.650536	2.307169	f=Th
C	4.586737	20.313735	4.342532	f=Th

H	5.281749	21.145330	4.368413 f=Th	C	3.290381	18.176866	0.766672 f=Th
C	4.424848	19.510406	5.456396 f=Th	H	4.036423	18.942970	0.540609 f=Th
H	5.008658	19.715130	6.346571 f=Th	H	2.773134	17.930509	-0.163594 f=Th
C	3.550639	18.426862	5.449285 f=Th	H	3.813374	17.283323	1.109274 f=Th
C	3.499367	17.521187	6.661331 f=Th	C	-0.186655	16.922252	7.134223 f=Th
H	2.662577	16.833095	6.525282 f=Th	H	0.666802	17.451565	7.594321 f=Th
C	4.772863	16.678442	6.753621 f=Th	H	-1.089616	17.373716	7.581814 f=Th
H	4.912909	16.065453	5.862802 f=Th	C	1.445115	14.287914	7.233342 f=Th
H	4.723898	16.009073	7.615874 f=Th	H	1.548189	14.256041	6.145824 f=Th
H	5.654796	17.312999	6.873193 f=Th	H	1.438215	13.255484	7.595246 f=Th
C	3.289628	18.282035	7.968393 f=Th	H	2.341017	14.763455	7.640635 f=Th
H	4.139740	18.926328	8.203837 f=Th	C	-0.122014	15.200019	9.675767 f=Th
H	3.179184	17.580687	8.798633 f=Th	H	0.740214	15.748334	10.065100 f=Th
H	2.396106	18.911775	7.947592 f=Th	H	-0.084483	14.188510	10.090308 f=Th
C	2.292167	18.676893	1.811438 f=Th	H	-1.023474	15.682360	10.063522 f=Th
H	1.574111	17.869313	1.983082 f=Th	C	-1.613888	14.177721	7.228798 f=Th
C	1.528826	19.884834	1.276874 f=Th	H	-2.542246	14.587068	7.635410 f=Th
H	0.798356	20.263812	1.996235 f=Th	H	-1.533799	13.147503	7.588106 f=Th
H	0.994162	19.621003	0.361992 f=Th	H	-1.712607	14.141432	6.140946 f=Th
H	2.200758	20.710783	1.033392 f=Th				

Optimised geometry of η^6-5-Th-endo and the name of the fragment f in the ETS-NOCV in which each atom belongs

O	-0.113290	15.647010	3.880077 f=Th	H	4.960728	14.632329	0.470099 f=Th
Th	-0.166280	17.900891	4.905746 f=Th	C	5.885668	13.677860	3.668690 f=Th
Si	-0.087969	15.235443	7.805776 f=Th	H	5.484188	13.024211	4.446653 f=Th
N	-2.165704	17.090403	4.182502 f=Th	H	5.989379	14.680056	4.089744 f=Th
N	1.866667	17.148530	4.243142 f=Th	H	6.886933	13.323698	3.410802 f=Th
C	-2.582531	13.236490	2.659033 f=Th	C	4.978106	12.256545	1.852919 f=Th
H	-2.647753	12.231946	2.266731 f=Th	H	4.600553	11.526823	2.573438 f=Th
C	-3.744286	13.977853	2.822147 f=Th	H	5.997753	11.962887	1.595146 f=Th
C	-3.642578	15.277400	3.331435 f=Th	H	4.377755	12.188769	0.942284 f=Th
H	-4.527883	15.890055	3.450659 f=Th	C	-3.232968	18.037255	4.205087 f=Th
C	-2.411730	15.815317	3.675216 f=Th	C	-4.047439	18.169601	5.351552 f=Th
C	2.177651	15.904927	3.703822 f=Th	C	-5.047945	19.137940	5.350668 f=Th
C	3.429527	15.439816	3.335895 f=Th	H	-5.683965	19.244069	6.222313 f=Th
H	4.284286	16.093500	3.460955 f=Th	C	-5.262442	19.950175	4.253546 f=Th
C	3.589099	14.153768	2.806751 f=Th	H	-6.053750	20.690938	4.270148 f=Th
C	2.463456	13.358168	2.644887 f=Th	C	-4.477767	19.797994	3.123648 f=Th
H	2.575219	12.362194	2.241297 f=Th	H	-4.670010	20.423302	2.259974 f=Th
C	-0.051179	12.912731	2.797166 f=Th	C	-3.461474	18.850414	3.068484 f=Th
C	-1.316937	13.737753	2.983853 f=Th	C	-2.686820	18.683362	1.775485 f=Th
C	-1.287019	15.010633	3.495873 f=Th	H	-1.760730	18.142998	2.005339 f=Th
C	1.087975	15.057754	3.505926 f=Th	C	-3.470813	17.825691	0.779073 f=Th
C	1.175797	13.793946	2.980461 f=Th	H	-3.694297	16.837867	1.180846 f=Th
C	-0.022519	11.789710	3.847225 f=Th	H	-2.897702	17.696742	-0.142317 f=Th
H	-0.029347	12.196750	4.860118 f=Th	H	-4.415323	18.311951	0.520501 f=Th
H	0.876608	11.181124	3.729836 f=Th	C	-2.312948	20.009436	1.119460 f=Th
H	-0.893001	11.140054	3.734421 f=Th	H	-3.194104	20.538000	0.749816 f=Th
C	-0.040024	12.295266	1.392980 f=Th	H	-1.669647	19.828636	0.256191 f=Th
H	-0.902325	11.644219	1.247149 f=Th	H	-1.782123	20.680727	1.796939 f=Th
H	0.850499	11.684131	1.243645 f=Th	C	-3.918135	17.263826	6.558240 f=Th
H	-0.059345	13.068393	0.622849 f=Th	H	-3.021209	16.656145	6.422648 f=Th
C	-5.119217	13.426088	2.446149 f=Th	C	-5.108788	16.309217	6.655917 f=Th
C	-6.039502	13.454456	3.671479 f=Th	H	-6.045253	16.859893	6.776672 f=Th
H	-5.623928	12.862134	4.490162 f=Th	H	-4.996685	15.650719	7.520671 f=Th
H	-7.017604	13.039826	3.415047 f=Th	H	-5.194104	15.681975	5.768721 f=Th
H	-6.200833	14.471030	4.035639 f=Th	C	-3.777868	18.042059	7.864942 f=Th
C	-5.727284	14.295041	1.338655 f=Th	H	-2.946677	18.750839	7.837847 f=Th
H	-5.854070	15.331563	1.658642 f=Th	H	-3.603172	17.355608	8.696696 f=Th
H	-6.712233	13.912474	1.059194 f=Th	H	-4.683927	18.606127	8.098320 f=Th
H	-5.097090	14.290747	0.445920 f=Th	C	2.840200	18.187015	4.265407 f=Th
C	-5.047940	11.988066	1.939097 f=Th	C	3.047763	18.953298	3.095430 f=Th
H	-4.440792	11.902783	1.034528 f=Th	C	3.896610	20.052422	3.158550 f=Th
H	-6.053188	11.641543	1.690572 f=Th	H	4.059220	20.652462	2.270186 f=Th
H	-4.644479	11.308689	2.694082 f=Th	C	4.546634	20.388381	4.333813 f=Th
C	4.988060	13.671321	2.425766 f=Th	H	5.202499	21.250933	4.365176 f=Th
C	5.581391	14.610664	1.369169 f=Th	C	4.386708	19.598153	5.458293 f=Th
H	6.580098	14.271050	1.083497 f=Th	H	4.940889	19.840506	6.357663 f=Th
H	5.675937	15.633130	1.741149 f=Th	C	3.556916	18.479574	5.448482 f=Th

```
C     3.541588    17.557385     6.650437 f=Th
H     2.690467    16.882410     6.539847 f=Th
C     4.807905    16.696664     6.659002 f=Th
H     4.896362    16.103399     5.748857 f=Th
H     4.792615    16.007682     7.506909 f=Th
H     5.701321    17.320076     6.749304 f=Th
C     3.412374    18.278769     7.988585 f=Th
H     4.275761    18.914900     8.195622 f=Th
H     3.352749    17.549112     8.799206 f=Th
H     2.518608    18.904182     8.048089 f=Th
C     2.400678    18.593323     1.773874 f=Th
H     1.888765    17.637203     1.900539 f=Th
C     1.363050    19.627863     1.350755 f=Th
H     0.560101    19.731821     2.088269 f=Th
H     0.901674    19.343836     0.402473 f=Th
H     1.808500    20.617403     1.223588 f=Th
C     3.442791    18.400287     0.673786 f=Th
H     3.967942    19.330621     0.445382 f=Th
H     2.959241    18.061882    -0.245333 f=Th
H     4.185743    17.653395     0.957927 f=Th
C    -0.160675    16.994646     7.128982 f=Th
H     0.680462    17.537292     7.596724 f=Th
H    -1.072379    17.438398     7.565636 f=Th
C     1.477541    14.358441     7.256920 f=Th
H     1.590072    14.320769     6.170590 f=Th
H     1.464248    13.327870     7.623986 f=Th
H     2.371390    14.832884     7.669985 f=Th
C    -0.097001    15.293656     9.683222 f=Th
H     0.763556    15.846266    10.070285 f=Th
H    -0.059517    14.285856    10.106740 f=Th
H    -1.000217    15.778226    10.064110 f=Th
C    -1.582102    14.249737     7.242728 f=Th
H    -2.510253    14.662636     7.646296 f=Th
H    -1.502411    13.222293     7.609940 f=Th
H    -1.681352    14.205223     6.155251 f=Th
C    -0.653737    20.458107     6.769763 f=F
H    -0.802646    20.044086     7.759425 f=F
C    -1.744219    20.879930     6.011475 f=F
H    -2.752289    20.766436     6.389852 f=F
C    -1.551659    21.460755     4.766006 f=F
H    -2.387660    21.804933     4.170855 f=F
C    -0.257589    21.607648     4.291723 f=F
C     0.846552    21.174993     5.010291 f=F
H     1.845147    21.305425     4.609919 f=F
C     0.637143    20.613982     6.267054 f=F
H     1.496325    20.321749     6.858551 f=F
F    -0.068418    22.190126     3.114084 f=F
```

Optimised geometry of η^1-5-Th-vertical and the name of the fragment f in the ETS-NOCV in which each atom belongs

```
F     3.119340    -0.636733     0.186344 f=F
C     2.014853    -0.687149     1.035935 f=F
C     1.700597     0.445550     1.745456 f=F
C     0.593352     0.379012     2.581655 f=F
C    -0.145619    -0.791110     2.675385 f=F
C     0.212898    -1.907548     1.933512 f=F
C     1.315831    -1.867080     1.090968 f=F
H    -1.008557    -0.832425     3.328262 f=F
H     0.310538     1.251594     3.157492 f=F
H     2.291261     1.348372     1.649296 f=F
H     1.616679    -2.720310     0.496932 f=F
H    -0.367118    -2.819419     2.004548 f=F
C     4.109276     1.348825    -3.220747 f=Th
C     5.101309     0.353378    -3.075817 f=Th
C     4.981896    -0.877438    -3.766851 f=Th
C     3.868138    -1.085298    -4.570686 f=Th
C     2.884339    -0.121193    -4.700504 f=Th
C     3.009147     1.080217    -4.030536 f=Th
N     6.200583     0.550602    -2.193367 f=Th
C     7.470551     0.855122    -2.671320 f=Th
C     8.509243     0.643006    -1.763948 f=Th
C     9.836814     0.844015    -2.042634 f=Th
C    10.123126     1.343938    -3.319057 f=Th
C     9.135744     1.602238    -4.260843 f=Th
C     7.802587     1.338081    -3.925835 f=Th
O     8.054338     0.176101    -0.536288 f=Th
C     8.991264    -0.369642     0.333479 f=Th
C    10.344190    -0.245064     0.146417 f=Th
C    10.923629     0.553459    -1.015309 f=Th
C    11.152432    -0.871807     1.102749 f=Th
C    10.628904    -1.591390     2.168493 f=Th
C     9.237881    -1.679481     2.302074 f=Th
C     8.397146    -1.065383     1.387935 f=Th
Th    5.638157    -0.067164    -0.105750 f=Th
N     7.006346    -1.067641     1.375915 f=Th
C     6.241745    -1.808171     2.321446 f=Th
C     5.901495    -1.245931     3.574189 f=Th
C     5.120501    -1.993551     4.449196 f=Th
C     4.665589    -3.253578     4.113293 f=Th
C     4.984336    -3.792908     2.881007 f=Th
C     5.771922    -3.098067     1.968828 f=Th
C    11.477026     1.884262    -0.478818 f=Th
C    12.059239    -0.237780    -1.675428 f=Th
C    11.521915    -2.305854     3.182466 f=Th
C    11.251282    -3.813960     3.113269 f=Th
C     9.457161     2.164247    -5.645014 f=Th
C     8.740421     3.508102    -5.823638 f=Th
C     6.373052     0.122556     4.013963 f=Th
C     7.475555     0.022295     5.068638 f=Th
C     6.161005    -3.775823     0.668605 f=Th
C     7.457071    -4.571961     0.836244 f=Th
C     6.039514    -1.958288    -3.692289 f=Th
C     5.447996    -3.309395    -3.300225 f=Th
C     4.234459     2.718295    -2.590626 f=Th
C     4.590786     3.765419    -3.646902 f=Th
C     5.380478     2.084610     0.936174 f=Th
Si    6.586760     3.519221     1.137846 f=Th
C     5.733265     4.944052     2.014684 f=Th
C     8.068775     2.997617     2.165803 f=Th
C     7.185553     4.128737    -0.532651 f=Th
C    13.006470    -2.074558     2.913146 f=Th
C    11.209640    -1.801578     4.595647 f=Th
C    10.952872     2.391555    -5.846906 f=Th
C     8.972531     1.185563    -6.721003 f=Th
C     5.227287     0.979348     4.552066 f=Th
C     5.067161    -4.677179     0.106418 f=Th
C     6.802168    -2.077842    -5.011726 f=Th
C     2.973444     3.136102    -1.837771 f=Th
H    12.224542    -0.790430     0.997994 f=Th
H     8.797646    -2.244560     3.114924 f=Th
H     7.009004     1.505719    -4.644286 f=Th
H    11.155768     1.536107    -3.572384 f=Th
H    10.691904     2.475491    -0.003748 f=Th
H    11.903692     2.474509    -1.292638 f=Th
H    12.260406     1.700796     0.259655 f=Th
H    12.861150    -0.435421    -0.963686 f=Th
H    12.497338     0.325262    -2.499861 f=Th
H    11.700636    -1.192661    -2.063707 f=Th
H    11.371860    -0.723895     4.674046 f=Th
H    11.859943    -2.295894     5.321670 f=Th
H    10.178051    -2.011493     4.885263 f=Th
H    10.210704    -4.050631     3.345842 f=Th
H    11.880578    -4.342493     3.833882 f=Th
H    11.473106    -4.206509     2.117891 f=Th
H    13.309291    -2.456498     1.935134 f=Th
H    13.597312    -2.600926     3.665640 f=Th
```

```
H    13.271260   -1.015787    2.970150 f=Th
H     9.199021    1.578924   -7.715184 f=Th
H     7.893633    1.023996   -6.669715 f=Th
H     9.466364    0.215883   -6.620761 f=Th
H     9.062271    4.227903   -5.067339 f=Th
H     7.655977    3.403263   -5.749219 f=Th
H     8.965376    3.925969   -6.808159 f=Th
H    11.356882    3.110821   -5.130232 f=Th
H    11.126408    2.794355   -6.846933 f=Th
H    11.522107    1.462210   -5.765337 f=Th
H     4.864216   -1.577139    5.416301 f=Th
H     4.059349   -3.818053    4.812273 f=Th
H     4.622356   -4.781875    2.630661 f=Th
H     6.371557   -2.996093   -0.078895 f=Th
H     8.282693   -3.938901    1.161342 f=Th
H     7.739590   -5.044894   -0.107411 f=Th
H     7.318435   -5.360952    1.580171 f=Th
H     4.910659   -5.557293    0.732995 f=Th
H     5.353072   -5.041284   -0.881110 f=Th
H     4.108492   -4.159270    0.015172 f=Th
H     6.796481    0.623345    3.140931 f=Th
H     7.115790   -0.498071    5.960250 f=Th
H     7.798398    1.020792    5.373451 f=Th
H     8.348981   -0.508823    4.691395 f=Th
H     4.368458    0.995917    3.876609 f=Th
H     5.564066    2.007833    4.701832 f=Th
H     4.873618    0.614392    5.519097 f=Th
H     3.769718   -2.019910   -5.111020 f=Th
H     2.023116   -0.304910   -5.332371 f=Th
H     2.243110    1.837275   -4.151726 f=Th
H     5.063609    2.682650   -1.880322 f=Th
H     5.530565    3.525093   -4.146533 f=Th
H     4.697625    4.751023   -3.187300 f=Th
H     3.809476    3.834332   -4.408152 f=Th
H     2.134978    3.306497   -2.516800 f=Th
H     3.146004    4.070953   -1.299125 f=Th
H     2.654951    2.379898   -1.114592 f=Th
H     6.764722   -1.670735   -2.924705 f=Th
H     4.858407   -3.246758   -2.382183 f=Th
H     6.244384   -4.041422   -3.146204 f=Th
H     4.792273   -3.702770   -4.080098 f=Th
H     6.129983   -2.365536   -5.824199 f=Th
H     7.578559   -2.842665   -4.933536 f=Th
H     7.280938   -1.136547   -5.283185 f=Th
H     4.495565    2.496989    0.419390 f=Th
H     5.041364    1.824459    1.953486 f=Th
H     7.682408    3.350048   -1.117148 f=Th
H     7.903993    4.941016   -0.388200 f=Th
H     6.366284    4.528934   -1.135367 f=Th
H     4.873490    5.305651    1.443879 f=Th
H     6.416696    5.787062    2.151182 f=Th
H     5.373528    4.646483    3.003464 f=Th
H     7.785475    2.771763    3.196918 f=Th
H     8.793504    3.816215    2.204449 f=Th
H     8.582200    2.121517    1.760960 f=Th
```

Optimised geometry of η^1-6-Th-vertical and the name of the fragment f in the ETS-NOCV in which each atom belongs

```
C     4.078764    1.565437   -3.050514 f=Th
C     5.030930    0.527165   -2.946449 f=Th
C     4.836050   -0.691409   -3.642015 f=Th
C     3.684864   -0.846600   -4.403004 f=Th
C     2.734396    0.156473   -4.485450 f=Th
C     2.934893    1.347033   -3.815138 f=Th
N     6.162369    0.670264   -2.095322 f=Th
C     7.430896    0.913081   -2.610829  f=Th
C     8.483694    0.653722   -1.732622 f=Th
C     9.810616    0.795029   -2.047467 f=Th
C    10.084329    1.280235   -3.332383 f=Th
C     9.084245    1.583530   -4.246690 f=Th
C     7.749982    1.380733   -3.874439 f=Th
O     8.040745    0.213266   -0.491716 f=Th
C     8.977886   -0.343145    0.370068 f=Th
C    10.329551   -0.273421    0.150201 f=Th
C    10.913483    0.456930   -1.052797 f=Th
C    11.136795   -0.894597    1.111143 f=Th
C    10.612384   -1.557060    2.212713 f=Th
C     9.222070   -1.594250    2.376417 f=Th
C     8.383198   -0.984963    1.457557 f=Th
Th    5.636555    0.132242    0.028979 f=Th
N     6.993453   -0.939845    1.471774 f=Th
C     6.220227   -1.657165    2.427791 f=Th
C     5.896511   -1.074947    3.675143 f=Th
C     5.097548   -1.794245    4.558420  f=Th
C     4.613341   -3.046480    4.235518 f=Th
C     4.921946   -3.608331    3.009891 f=Th
C     5.725620   -2.942906    2.090410 f=Th
C    11.577514    1.758740   -0.574766 f=Th
C    11.964343   -0.428668   -1.734546 f=Th
C    11.502358   -2.263437    3.234948 f=Th
C    11.185153   -3.763964    3.223550 f=Th
C     9.392734    2.134550   -5.638229 f=Th
C     8.743624    3.515727   -5.788870 f=Th
C     6.407116    0.283407    4.103825 f=Th
C     7.480844    0.158208    5.185059 f=Th
C     6.103149   -3.642394    0.798155 f=Th
C     7.408332   -4.425175    0.961629 f=Th
C     5.852038   -1.814352   -3.616612 f=Th
C     5.228428   -3.148810   -3.215350 f=Th
C     4.293886    2.930944   -2.434616 f=Th
C     4.639183    3.956515   -3.515604 f=Th
C     5.620042    2.325287    1.011215 f=Th
Si    6.938723    3.661012    1.147061 f=Th
C     6.222560    5.169963    2.007215 f=Th
C     8.392545    3.044094    2.163031 f=Th
C     7.541505    4.189147   -0.550068 f=Th
C    12.987905   -2.087212    2.931452 f=Th
C    11.232233   -1.700966    4.634799 f=Th
C    10.891620    2.283058   -5.885091 f=Th
C     8.824362    1.189687   -6.703267 f=Th
C     5.280708    1.189373    4.600252 f=Th
C     5.014271   -4.569271    0.268321 f=Th
C     6.557403   -1.948440   -4.966379 f=Th
C     3.093561    3.407109   -1.620197 f=Th
H    12.208586   -0.853680    0.980892 f=Th
H     8.780525   -2.116841    3.216411 f=Th
H     6.945245    1.587587   -4.569907 f=Th
H    11.117635    1.425217   -3.613421 f=Th
H    10.853809    2.414681   -0.087310 f=Th
H    12.011851    2.297453   -1.419600 f=Th
H    12.375117    1.540513    0.138528 f=Th
H    12.777492   -0.666422   -1.048109 f=Th
H    12.406044    0.081888   -2.590747 f=Th
H    11.523895   -1.364632   -2.082675 f=Th
H    11.427004   -0.626483    4.671786 f=Th
H    11.881587   -2.188819    5.366067 f=Th
H    10.200708   -1.869758    4.950247 f=Th
H    10.142049   -3.960210    3.481174 f=Th
H    11.810755   -4.286365    3.951852 f=Th
H    11.377434   -4.197386    2.239015 f=Th
H    13.261049   -2.512648    1.962659 f=Th
H    13.576756   -2.604336    3.691920 f=Th
H    13.284984   -1.035580    2.945536 f=Th
H     9.043208    1.575581   -7.702110 f=Th
H     7.740150    1.087110   -6.621436 f=Th
H     9.267039    0.193917   -6.621330 f=Th
```

```
 H     9.127029     4.212860    -5.040090 f=Th
 H     7.658080     3.468032    -5.680088 f=Th
 H     8.959433     3.926795    -6.778373 f=Th
 H    11.354732     2.977804    -5.180085 f=Th
 H    11.056027     2.679185    -6.889378 f=Th
 H    11.412924     1.324563    -5.821879 f=Th
 H     4.853451    -1.362474     5.522080 f=Th
 H     3.993886    -3.589217     4.940224 f=Th
 H     4.537993    -4.591784     2.770733 f=Th
 H     6.292596    -2.874550     0.033839 f=Th
 H     8.235989    -3.781799     1.258826 f=Th
 H     7.677063    -4.916187     0.023104 f=Th
 H     7.287128    -5.199781     1.723594 f=Th
 H     4.897848    -5.451873     0.900632 f=Th
 H     5.283562    -4.928152    -0.726187 f=Th
 H     4.042611    -4.074482     0.202487 f=Th
 H     6.869724     0.754782     3.234024 f=Th
 H     7.081457    -0.328732     6.078620 f=Th
 H     7.839505     1.148091     5.477433 f=Th
 H     8.338687    -0.417041     4.837217 f=Th
 H     4.450282     1.244452     3.892156 f=Th
 H     5.655793     2.202610     4.762568 f=Th
 H     4.876331     0.840262     5.553245 f=Th
 H     3.529299    -1.770865    -4.947950 f=Th
 H     1.842714     0.012878    -5.084808 f=Th
 H     2.198488     2.137326    -3.904363 f=Th
 H     5.157083     2.863906    -1.768336 f=Th
 H     5.536758     3.669606    -4.065705 f=Th
 H     4.818721     4.936989    -3.067869 f=Th
 H     3.820816     4.060831    -4.232634 f=Th
 H     2.222873     3.591417    -2.253632 f=Th
 H     3.327995     4.346190    -1.113450 f=Th
 H     2.794779     2.680269    -0.859331 f=Th
 H     6.615762    -1.562552    -2.874836 f=Th
 H     4.691691    -3.081667    -2.266555 f=Th
 H     6.004046    -3.911970    -3.115653 f=Th
 H     4.521149    -3.503737    -3.968456 f=Th
 H     5.844227    -2.205432    -5.753937 f=Th
 H     7.308716    -2.740665    -4.924660 f=Th
 H     7.058284    -1.022465    -5.249815 f=Th
 H     4.747326     2.800377     0.530224 f=Th
 H     5.297204     2.117033     2.045484 f=Th
 H     7.979068     3.367171    -1.122148 f=Th
 H     8.307811     4.962700    -0.444202 f=Th
 H     6.732680     4.618500    -1.147378 f=Th
 H     5.381798     5.586728     1.445801 f=Th
 H     6.974278     5.957904     2.109915 f=Th
 H     5.861564     4.923797     3.009556 f=Th
 H     8.099523     2.844076     3.197231 f=Th
 H     9.175338     3.807654     2.193349 f=Th
 H     8.837228     2.130146     1.760861 f=Th
 F     3.345025    -1.481475    -0.490926 f=F
 C     2.119049    -1.320570     0.075798 f=F
 C     1.980962    -0.294753     0.983390 f=F
 C     0.784881    -0.050183     1.611934 f=F
 C    -0.288853    -0.875503     1.301136 f=F
 C    -0.149713    -1.908246     0.384984 f=F
 C     1.067182    -2.143236    -0.243382 f=F
 H    -1.243297    -0.704784     1.782551 f=F
 H     0.701750     0.763088     2.321850 f=F
 F     3.078675     0.469421     1.224273 f=F
 H     1.200370    -2.939922    -0.964282 f=F
 H    -0.996023    -2.541678     0.151729 f=F
```

Optimised geometry of η^6-6-Th-exo and the name of the fragment f in the ETS-NOCV in which each atom belongs

```
Th    -0.281113    17.831764     4.911994     f=Th
C     -0.248155    16.989317     7.160963     f=Th
Si    -0.24196     15.23722      7.860108     f=Th
C     -1.754947    14.280659     7.296585     f=Th
O     -0.164173    15.574553     3.903963     f=Th
C     -1.318106    14.91378      3.501055     f=Th
C     -1.312083    13.649344     2.969776     f=Th
C     -0.022972    12.855171     2.808123     f=Th
C      1.179131    13.774005     2.984742     f=Th
C      1.054975    15.034538     3.512378     f=Th
C     -2.464197    15.689364     3.676764     f=Th
C     -3.676546    15.142323     3.290531     f=Th
C     -3.741652    13.848166     2.76099 f=Th
C     -2.562585    13.130362     2.612753     f=Th
C     2.47734 13.379133     2.641788     f=Th
C     3.57822 14.209343     2.802916     f=Th
C      3.380938    15.488882     3.334663     f=Th
C      2.115015    15.92237      3.69658 f=Th
C     -5.100945    13.269596     2.369893     f=Th
C     -4.988055    11.860749     1.793468     f=Th
N     -2.241223    16.948176     4.2235  f=Th
C     -3.245783    17.954284     4.205437     f=Th
C     -3.991708    18.246676     5.372253     f=Th
C     -4.865779    19.330257     5.345308     f=Th
C     -5.040672    20.088579     4.20115 f=Th
C     -4.347868    19.763923     3.048091     f=Th
C     -3.44775     18.704281     3.022264     f=Th
N     1.76643 17.166117     4.218433     f=Th
C      2.732905    18.210672     4.294504     f=Th
C      2.856484    19.118901     3.212685     f=Th
C      3.778295    20.154575     3.317757     f=Th
C      4.572619    20.301384     4.440955     f=Th
C      4.452285    19.408963     5.488504     f=Th
C      3.542185    18.356762     5.444033     f=Th
C      4.986747    13.778283     2.395037     f=Th
C     5.026606    12.343647     1.875173     f=Th
C     0.02478 11.756221     3.883116     f=Th
C     0.017556    12.207192     1.419024     f=Th
C     -3.951601    17.358069     6.598062     f=Th
C     -3.92761     18.122359     7.918485     f=Th
C     -2.748502    18.370494     1.721278     f=Th
C     -1.914368    19.539057     1.205064     f=Th
C     2.075338    18.957791     1.92197 f=Th
C     2.849176    18.099312     0.918023     f=Th
C     3.497213    17.389482     6.607388     f=Th
C     3.326807    18.101479     7.948185     f=Th
C     1.303546    14.318728     7.321671     f=Th
C     -0.260035    15.312201     9.736378     f=Th
C     -6.001784    13.209024     3.609237     f=Th
C     -5.75538     14.166961     1.313112     f=Th
C     5.493951    14.7054 1.283616     f=Th
C     5.927876    13.874592     3.600798     f=Th
C     -3.751143    17.921202     0.658789     f=Th
C     -5.146988    16.401185     6.586023     f=Th
C     4.750558    16.514524     6.649415     f=Th
C     1.699775    20.283493     1.26817 f=Th
H     -2.602629    12.130476     2.205642     f=Th
H     -4.575276    15.736566     3.404082     f=Th
H     4.215594    16.169515     3.451285     f=Th
H     2.619199    12.38852      2.234932     f=Th
H     -0.004211    12.18446      4.886884     f=Th
H     0.941742    11.170719     3.788102     f=Th
H     -0.826733    11.080924     3.775273     f=Th
H     -0.826217    11.530886     1.280256     f=Th
H     0.923554    11.614261     1.292158     f=Th
H     -0.012956    12.961481     0.630822     f=Th
H     -5.559367    12.580722     4.385874     f=Th
H     -6.975508    12.7884 3.345799     f=Th
H     -6.174942    14.199875     4.034494     f=Th
H     -5.927582    15.178463     1.687297     f=Th
```

```
H      -6.724998      13.756196      1.020849       f=Th
H      -5.133574      14.236883      0.41727 f=Th
H      -4.378992      11.838134      0.886366       f=Th
H      -5.982982      11.496944      1.52869 f=Th
H      -4.564572      11.157096      2.514345       f=Th
H      6.502625       14.412677      0.981197       f=Th
H      5.535299       15.746676      1.61056 f=Th
H      4.848104       14.652528      0.403747       f=Th
H      5.581759       13.242885      4.422376       f=Th
H      6.012054       14.898128      3.971398       f=Th
H      6.931326       13.545533      3.319558       f=Th
H      4.695699       11.626595      2.630632       f=Th
H      6.052482       12.084893      1.605048       f=Th
H      4.412005       12.215142      0.980827       f=Th
H      -5.44129       19.570313      6.231481       f=Th
H      -5.734165      20.921685      4.202689       f=Th
H      -4.512585      20.344411      2.147274       f=Th
H      -2.075264      17.529096      1.904839       f=Th
H      -4.329667      17.060317      0.996199       f=Th
H      -3.228245      17.638182      -0.257597      f=Th
H      -4.449483      18.723644      0.408664       f=Th
H      -2.535591      20.406589      0.971254       f=Th
H      -1.388597      19.255214      0.29084 f=Th
H      -1.166225      19.866104      1.933001       f=Th
H      -3.04863       16.747082      6.536484       f=Th
H      -6.088161      16.956609      6.613188       f=Th
H      -5.118174      15.746689      7.460443       f=Th
H      -5.147701      15.77017       5.697109       f=Th
H      -3.117166      18.853664      7.974199       f=Th
H      -3.797397      17.424474      8.748503       f=Th
H      -4.862626      18.657729      8.09746 f=Th
H      3.886251       20.857989      2.502037       f=Th
H      5.29168 21.110866      4.493911       f=Th
H      5.088496       19.52232       6.358975       f=Th
H      2.640493       16.729379      6.457757       f=Th
H      4.861795       15.92641       5.738864       f=Th
H      4.698659       15.819438      7.490939       f=Th
H      5.649484       17.123481      6.775975       f=Th
H      4.211344       18.687144      8.208871       f=Th
H      3.177128       17.372161      8.74767 f=Th
H      2.471649       18.781537      7.948544       f=Th
H      1.146756       18.416474      2.151127       f=Th
H      1.201931       20.969888      1.955569       f=Th
H      1.030363       20.104885      0.425196       f=Th
H      2.577412       20.795753      0.868861       f=Th
H      3.796011       18.582884      0.6631  f=Th
H      2.273597       17.98332       -0.003543      f=Th
H      3.068113       17.106852      1.310168       f=Th
H      0.643776       17.48359       7.584048       f=Th
H      -1.114091      17.499365      7.62023 f=Th
H      1.42187 14.278972      6.235756       f=Th
H      1.26273 13.288474      7.687351       f=Th
H      2.206297       14.771139      7.740047       f=Th
H      0.612141       15.845947      10.123696      f=Th
H      -0.251521      14.307574      10.168866      f=Th
H      -1.152619      15.823456      10.107362      f=Th
H      -2.677746      14.715474      7.688992       f=Th
H      -1.698561      13.255714      7.675054       f=Th
H      -1.84645       14.226011      6.208844       f=Th
H    0.595273    20.216477    7.644759 f=F
H   -1.724150    19.942888    6.795392 f=F
H   -2.381456    20.956813    4.618841 f=F
F    1.674463    22.764851    4.116384   f=F
H    2.239873    21.564320    6.332672   f=F
C    1.226557    21.414600    5.981901   f=F
C    0.310571    20.648822    6.693492   f=F
C   -0.983923    20.477976    6.209266   f=F
C   -1.370641    21.058694    4.999987   f=F
C   -0.455906    21.828848    4.306887   f=F
C    0.834873    22.010228    4.799450   f=F
F   -0.797031    22.418000    3.173317   f=F
```

Optimised geometry of η^6-6-Th-side and the name of the fragment f in the ETS-NOCV in which each atom belongs

```
 C     3.5195    18.3662     5.4188 f=Th
 C     2.7095    18.2118     4.2703 f=Th
 C     2.8311    19.1136     3.1830 f=Th
 C     3.7529    20.1500     3.2812 f=Th
 C     4.5473    20.3045     4.4031 f=Th
 C     4.4278    19.4196     5.4563 f=Th
 N     1.7483    17.1617     4.2002 f=Th
 C     2.1015    15.9165     3.6854 f=Th
 C     1.0439    15.0252     3.5055 f=Th
 C     1.1700    13.7640     2.9799 f=Th
 C     2.4691    13.3710     2.6379 f=Th
 C     3.5684    14.2038     2.7982 f=Th
 C     3.3687    15.4847     3.3259 f=Th
 O    -0.1754    15.5628     3.8986 f=Th
 C    -1.3279    14.9029     3.4919 f=Th
 C    -1.3210    13.6386     2.9604 f=Th
 C    -0.0314    12.8436     2.8055 f=Th
 C    -2.5709    13.1211     2.5989 f=Th
 C    -3.7499    13.8398     2.7440 f=Th
 C    -3.6857    15.1336     3.2747 f=Th
 C    -2.4739    15.6793     3.6644 f=Th
Th    -0.2921    17.8204     4.9105 f=Th
 N    -2.2490    16.9363     4.2129 f=Th
 C    -3.2448    17.9495     4.2049 f=Th
 C    -3.9851    18.2377     5.3762 f=Th
 C    -4.8335    19.3418     5.3692 f=Th
 C    -4.9881    20.1259     4.2400 f=Th
 C    -4.3056    19.8036     3.0799 f=Th
 C    -3.4329    18.7221     3.0337 f=Th
 C     0.0141    11.7507     3.8868 f=Th
 C     0.0124    12.1876     1.4204 f=Th
 C    -5.1084    13.2624     2.3482 f=Th
 C    -5.7586    14.1606     1.2894 f=Th
 C     4.9781    13.7740     2.3931 f=Th
 C     5.9169    13.8740     3.6005 f=Th
 C    -3.9619    17.3294     6.5874 f=Th
 C    -5.1780    16.3993     6.5659 f=Th
 C    -2.7521    18.3861     1.7234 f=Th
 C    -3.7733    17.9355     0.6788 f=Th
 C     2.0465    18.9466     1.8950 f=Th
 C     1.6891    20.2710     1.2282 f=Th
 C     3.4768    17.4061     6.5883 f=Th
 C     4.7386    16.5444     6.6435 f=Th
 C    -0.2605    16.9679     7.1552 f=Th
Si    -0.2301    15.2151     7.8508 f=Th
 C    -0.2439    15.2851     9.7273 f=Th
 C    -1.7380    14.2495     7.2880 f=Th
 C     1.3214    14.3103     7.3068 f=Th
 C    -4.9949    11.8536     1.7718 f=Th
 C    -6.0135    13.2023     3.5845 f=Th
 C     5.0210    12.3385     1.8760 f=Th
 C     5.4858    14.6999     1.2809 f=Th
 C    -3.9160    18.0764     7.9167 f=Th
 C    -1.9251    19.5511     1.1880 f=Th
 C     2.8050    18.0674     0.8976 f=Th
 C     3.2900    18.1265     7.9222 f=Th
 H    -2.6107    12.1214     2.1914 f=Th
 H    -4.5845    15.7280     3.3870 f=Th
 H     4.2016    16.1677     3.4402 f=Th
 H     2.6132    12.3799     2.2330 f=Th
 H    -0.0171    12.1846     4.8881 f=Th
 H     0.9315    11.1650     3.7971 f=Th
```

H	-0.8370	11.0745	3.7809	f=Th
H	-0.8307	11.5099	1.2838	f=Th
H	0.9189	11.5942	1.2991	f=Th
H	-0.0167	12.9370	0.6276	f=Th
H	-5.5740	12.5737	4.3626	f=Th
H	-6.9866	12.7823	3.3178	f=Th
H	-6.1875	14.1932	4.0093	f=Th
H	-5.9312	15.1721	1.6633	f=Th
H	-6.7276	13.7508	0.9939	f=Th
H	-5.1337	14.2303	0.3957	f=Th
H	-4.3829	11.8306	0.8667	f=Th
H	-5.9893	11.4907	1.5037	f=Th
H	-4.5744	11.1494	2.4939	f=Th
H	6.4953	14.4079	0.9806	f=Th
H	5.5253	15.7418	1.6060	f=Th
H	4.8413	14.6446	0.4001	f=Th
H	5.5705	13.2427	4.4223	f=Th
H	5.9981	14.8982	3.9699	f=Th
H	6.9216	13.5467	3.3216	f=Th
H	4.6902	11.6223	2.6323	f=Th
H	6.0478	12.0809	1.6080	f=Th
H	4.4080	12.2073	0.9810	f=Th
H	-5.4020	19.5802	6.2602	f=Th
H	-5.6589	20.9772	4.2577	f=Th
H	-4.4601	20.4018	2.1888	f=Th
H	-2.0765	17.5446	1.8987	f=Th
H	-4.3453	17.0747	1.0272	f=Th
H	-3.2672	17.6520	-0.2468	f=Th
H	-4.4764	18.7380	0.4422	f=Th
H	-2.5505	20.4168	0.9573	f=Th
H	-1.4146	19.2622	0.2668	f=Th
H	-1.1636	19.8763	1.9027	f=Th
H	-3.0725	16.7000	6.5137	f=Th
H	-6.1068	16.9744	6.6065	f=Th
H	-5.1589	15.7307	7.4298	f=Th
H	-5.1966	15.7825	5.6673	f=Th
H	-3.0985	18.7999	7.9661	f=Th
H	-3.7823	17.3685	8.7376	f=Th
H	-4.8436	18.6188	8.1124	f=Th
H	3.8599	20.8493	2.4619	f=Th
H	5.2607	21.1187	4.4541	f=Th
H	5.0586	19.5444	6.3287	f=Th
H	2.6277	16.7359	6.4386	f=Th
H	4.8622	15.9527	5.7367	f=Th
H	4.6885	15.8534	7.4885	f=Th
H	5.6304	17.1633	6.7727	f=Th
H	4.1622	18.7316	8.1793	f=Th
H	3.1508	17.4015	8.7276	f=Th
H	2.4232	18.7914	7.9122	f=Th
H	1.1103	18.4218	2.1321	f=Th
H	1.2185	20.9737	1.9187	f=Th
H	1.0044	20.0966	0.3965	f=Th
H	2.5718	20.7599	0.8112	f=Th
H	3.7592	18.5336	0.6379	f=Th
H	2.2269	17.9526	-0.0226	f=Th
H	3.0088	17.0751	1.2979	f=Th
H	0.6127	17.4848	7.5906	f=Th
H	-1.1450	17.4551	7.6034	f=Th
H	1.4371	14.2727	6.2205	f=Th
H	1.2899	13.2794	7.6716	f=Th
H	2.2214	14.7699	7.7231	f=Th
H	0.6247	15.8256	10.1133	f=Th
H	-0.2251	14.2796	10.1573	f=Th
H	-1.1399	15.7876	10.1021	f=Th
H	-2.6624	14.6777	7.6842	f=Th
H	-1.6749	13.2235	7.6626	f=Th
H	-1.8319	14.1982	6.2003	f=Th
H	0.7754	20.6094	7.8893	f=F
H	-1.4835	19.9474	7.0719	f=F
H	-2.2297	20.6287	4.7985	f=F
F	2.4289	22.0678	6.5455	f=F
F	1.6304	22.8049	4.0976	f=F
C	0.8392	22.0435	4.8297	f=F
C	1.2567	21.6582	6.1014	f=F
C	0.4416	20.8740	6.8934	f=F
C	-0.8098	20.4888	6.4165	f=F
C	-1.2303	20.8749	5.1448	f=F
C	-0.3931	21.6493	4.3456	f=F
H	-0.7026	21.9890	3.3647	f=F

Optimised geometry of η^6-6-Th-endo and the name of the fragment f in the ETS-NOCV in which each atom belongs

C	3.477468	20.142211	3.344767	f=Th
C	2.559315	19.088440	3.248252	f=Th
C	2.482665	18.150969	4.324976	f=Th
C	3.333864	18.289348	5.460652	f=Th
C	4.236242	19.361504	5.493746	f=Th
C	4.311560	20.280776	4.452927	f=Th
C	3.333017	17.302216	6.618655	f=Th
C	3.195237	17.995976	7.984193	f=Th
N	1.507918	17.101124	4.268571	f=Th
Th	-0.533459	17.819405	4.989196	f=Th
C	-0.494988	17.083987	7.276719	f=Th
Si	-0.482609	15.376207	8.107996	f=Th
C	1.053759	14.398616	7.607217	f=Th
C	1.723698	18.942337	1.979396	f=Th
C	2.406115	18.000503	0.967958	f=Th
C	1.839100	15.830115	3.779553	f=Th
C	0.764358	14.932286	3.667148	f=Th
C	0.862964	13.644140	3.174496	f=Th
C	2.153385	13.234344	2.784401	f=Th
C	3.270364	14.073159	2.868375	f=Th
C	3.097551	15.377150	3.372513	f=Th
C	-0.357375	12.718472	3.099807	f=Th
C	-1.643475	13.546403	3.203586	f=Th
C	-1.631659	14.839892	3.690900	f=Th
O	-0.453344	15.498655	4.083853	f=Th
C	-2.908630	13.037519	2.847794	f=Th
C	-4.084463	13.788390	2.958177	f=Th
C	-3.998495	15.106810	3.446703	f=Th
C	-2.768903	15.653939	3.822391	f=Th
C	4.665638	13.622946	2.401651	f=Th
C	5.123397	14.525285	1.234421	f=Th
C	-0.305112	11.726233	4.290288	f=Th
C	-0.342346	11.923108	1.778110	f=Th
C	-5.456847	13.221585	2.555470	f=Th
C	-6.400777	13.241116	3.777006	f=Th
N	-2.524870	16.943124	4.311358	f=Th
C	-3.538014	17.954380	4.283612	f=Th
C	-4.366001	18.182676	5.421733	f=Th
C	-5.277176	19.246833	5.381445	f=Th
C	-5.396175	20.061272	4.258568	f=Th
C	-4.606308	19.814617	3.137509	f=Th
C	-3.674510	18.768702	3.118195	f=Th
C	-4.347827	17.272961	6.641699	f=Th
C	-4.218406	18.042000	7.965791	f=Th
C	-2.895131	18.496221	1.837869	f=Th
C	-2.320864	19.768224	1.198120	f=Th
C	-6.060843	14.091922	1.431800	f=Th
C	-5.366143	11.775274	2.044181	f=Th
C	5.671972	13.748004	3.565123	f=Th
C	4.678044	12.165473	1.914569	f=Th
C	-5.608046	16.387822	6.677836	f=Th
C	-3.770275	17.744425	0.816452	f=Th
C	1.404077	20.277556	1.293683	f=Th
C	4.604262	16.433185	6.610385	f=Th

```
 C    -0.471427    15.585210     9.985197 f=Th
 C    -2.017073    14.385438     7.627230 f=Th
H    -2.965340    12.018332     2.472338 f=Th
 H    -4.892167    15.726996     3.527480 f=Th
 H     3.942490    16.064544     3.428851 f=Th
 H     2.277808    12.224434     2.400483 f=Th
 H    -0.316346    12.256778     5.252441 f=Th
 H     0.611233    11.120656     4.242804 f=Th
 H    -1.170897    11.049255     4.261408 f=Th
 H    -1.198757    11.239206     1.722583 f=Th
 H     0.560458    11.303783     1.703258 f=Th
 H    -0.376553    12.593115     0.908300 f=Th
 H    -5.993828    12.638059     4.601693 f=Th
 H    -7.382474    12.827017     3.503170 f=Th
 H    -6.565281    14.261486     4.151325 f=Th
 H    -6.206624    15.133379     1.752528 f=Th
 H    -7.043305    13.696531     1.133970 f=Th
 H    -5.412471    14.096060     0.543285 f=Th
 H    -4.733420    11.693771     1.148039 f=Th
 H    -6.370083    11.421296     1.770411 f=Th
 H    -4.974774    11.091044     2.811444 f=Th
 H     6.122432    14.220084     0.889252 f=Th
 H     5.182168    15.581774     1.532878 f=Th
 H     4.431354    14.450383     0.382782 f=Th
 H     5.364892    13.132712     4.423394 f=Th
 H     5.774933    14.786671     3.909533 f=Th
 H     6.667068    13.408945     3.241206 f=Th
 H     4.383026    11.463745     2.708743 f=Th
 H     5.695385    11.895208     1.598171 f=Th
 H     4.015051    12.013435     1.050113 f=Th
 H    -5.921687    19.429277     6.243422 f=Th
 H    -6.118018    20.879785     4.249134 f=Th
 H    -4.726458    20.442717     2.253369 f=Th
 H    -2.051979    17.829057     2.091184 f=Th
 H    -4.140740    16.794486     1.221944 f=Th
 H    -3.192679    17.525278    -0.093460 f=Th
 H    -4.637390    18.357142     0.527336 f=Th
 H    -3.113966    20.430876     0.823727 f=Th
 H    -1.691045    19.505138     0.336729 f=Th
 H    -1.708584    20.351708     1.901867 f=Th
 H    -3.478377    16.606637     6.545334 f=Th
 H    -6.517675    16.999610     6.772797 f=Th
 H    -5.569561    15.706669     7.540479 f=Th
 H    -5.700417    15.775681     5.771744 f=Th
 H    -3.333090    18.693837     7.984412 f=Th
 H    -4.131997    17.337331     8.805462 f=Th
 H    -5.100231    18.669656     8.161716 f=Th
 H     3.552629    20.866310     2.533384 f=Th
 H     5.023729    21.106360     4.500254 f=Th
 H     4.896917    19.474033     6.355028 f=Th
 H     2.471925    16.631763     6.484291 f=Th
 H     4.703074    15.863125     5.678533 f=Th
 H     4.576344    15.713996     7.442063 f=Th
 H     5.505725    17.052042     6.733456 f=Th
 H     4.085104    18.594790     8.226879 f=Th
 H     3.085498    17.244483     8.779482 f=Th
 H     2.327291    18.668415     8.030274 f=Th
 H     0.762601    18.463715     2.257426 f=Th
 H     0.978739    21.022373     1.982710 f=Th
 H     0.685747    20.118055     0.478692 f=Th
 H     2.301666    20.722697     0.841236 f=Th
 H     3.378129    18.416970     0.663404 f=Th
 H     1.786247    17.895722     0.065420 f=Th
 H     2.577976    17.000976     1.384641 f=Th
 H     0.392815    17.627078     7.669152 f=Th
 H    -1.378263    17.622782     7.686297 f=Th
 H     1.156048    14.285857     6.517678 f=Th
 H     1.002177    13.388115     8.041568 f=Th
 H     1.974959    14.864700     7.986421 f=Th
 H     0.415108    16.143120    10.322337 f=Th
 H    -0.461987    14.607667    10.491441 f=Th
 H    -1.360338    16.131884    10.334409 f=Th
 H    -2.938335    14.847574     8.011473 f=Th
 H    -1.954808    13.378425     8.068246 f=Th
 H    -2.127379    14.263890     6.539381 f=Th
 C    -0.440917    20.878248     4.959267 f=F
 C     0.686687    20.974758     5.795315 f=F
 C     0.499284    21.108800     7.167083 f=F
 C    -0.795351    21.136173     7.709972 f=F
 C    -1.910581    21.033135     6.885139 f=F
 C    -1.736120    20.905798     5.501965 f=F
 H     1.701367    20.979875     5.391659 f=F
 F     1.549265    21.222137     7.989030 f=F
 H    -0.298818    20.869337     3.875138 f=F
 F    -0.939957    21.259180     9.032545 f=F
 H    -2.904213    21.072415     7.331658 f=F
 H    -2.612225    20.862404     4.852201 f=F
```

Optimised geometry of η^2-E-Th and the name of the fragment f in the ETS-NOCV in which each atom belongs

```
 C    21.847110    13.218075     0.029437 f=Th
 C    22.243178    14.460897    -0.521528 f=Th
 C    22.901704    15.420206     0.287493 f=Th
 C    23.187838    15.096854     1.609350   f=Th
 C    22.835709    13.868886     2.140739   f=Th
 C    22.165940    12.947590     1.356963   f=Th
 N    22.070791    14.724384    -1.905604   f=Th
Th    23.908423    14.003799    -2.987916   f=Th
 C    23.084229    11.927646    -3.860379   f=Th
Si    21.697883    11.549284    -5.081391   f=Th
 C    20.052949    12.186872    -4.439322   f=Th
 C    23.247791    16.804657    -0.217781   f=Th
 C    24.701966    17.176531     0.052609   f=Th
 C    21.020343    12.216908    -0.746789   f=Th
 C    19.548569    12.316697    -0.339403   f=Th
 N    24.791161    14.944346    -4.836444   f=Th
 C    24.132397    15.719102    -5.786060   f=Th
 C    22.797790    16.006050    -5.492148   f=Th
 C    21.977409    16.778136    -6.274645   f=Th
 C    22.546441    17.274150    -7.453608   f=Th
 C    23.863218    17.019077    -7.812680   f=Th
 C    24.651912    16.234930    -6.962407   f=Th
 C    20.526660    17.045459    -5.891159   f=Th
 C    20.293051    16.664835    -4.434125   f=Th
 C    21.190648    15.893936    -3.741004   f=Th
 O    22.379862    15.435881    -4.295372   f=Th
 C    19.143598    17.044362    -3.730178   f=Th
 C    18.922276    16.683373    -2.407646   f=Th
 C    19.886205    15.908000    -1.752104   f=Th
 C    21.032539    15.497390    -2.411557   f=Th
 C    24.479529    17.580554    -9.093641   f=Th
 C    25.658547    18.491474    -8.730240   f=Th
 C    20.194110    18.526593    -6.103935   f=Th
 C    19.611404    16.186171    -6.780334   f=Th
 C    17.663067    17.102832    -1.650041   f=Th
 C    16.725998    17.950498    -2.506254   f=Th
 C    26.189652    14.692150    -4.883797   f=Th
 C    26.690753    13.547550    -5.549312   f=Th
 C    28.059350    13.297847    -5.510715   f=Th
 C    28.925987    14.138571    -4.840708   f=Th
 C    28.434409    15.256543    -4.190849   f=Th
 C    27.077603    15.560784    -4.195965   f=Th
 C    25.807251    12.610126    -6.342315   f=Th
 C    25.981023    12.834353    -7.845391   f=Th
 C    26.608574    16.837360    -3.524103   f=Th
 C    27.441588    17.220654    -2.305338   f=Th
```

```
 C    21.556337     9.693661    -5.327932   f=Th
 C    22.046343    12.342433    -6.747187   f=Th
 C    16.899678    15.851437    -1.200520   f=Th
 C    18.057876    17.924322    -0.417095   f=Th
 C    22.313323    17.851305     0.391058   f=Th
 C    21.505198    10.778902    -0.582707   f=Th
 C    24.982946    16.428185    -9.970074   f=Th
 C    23.480451    18.397508    -9.908823   f=Th
 C    26.593957    18.005753    -4.513307   f=Th
 C    26.067152    11.141571    -6.010772   f=Th
 H    18.403131    17.640124    -4.243753   f=Th
 H    25.689493    16.036231    -7.202942   f=Th
 H    21.930287    17.876857    -8.104671   f=Th
 H    19.750293    15.620154    -0.716474   f=Th
 H    23.993529    11.452306    -4.266859   f=Th
 H    22.845056    11.369858    -2.937494   f=Th
 H    19.153008    18.731197    -5.853497   f=Th
 H    20.329780    18.810298    -7.147745   f=Th
 H    20.828381    19.166539    -5.488042   f=Th
 H    15.846936    18.224247    -1.919149   f=Th
 H    16.374447    17.407263    -3.386815   f=Th
 H    17.201168    18.877693    -2.836083   f=Th
 H    26.437082    17.952507    -8.185970   f=Th
 H    25.330448    19.329205    -8.109954   f=Th
 H    26.111410    18.899364    -9.637442   f=Th
 H    18.563102    16.361530    -6.529147   f=Th
 H    19.820358    15.122552    -6.649563   f=Th
 H    19.759717    16.436451    -7.832991   f=Th
 H    25.760654    15.846775    -9.470707   f=Th
 H    25.410792    16.820870   -10.895857   f=Th
 H    24.168582    15.749217   -10.233900   f=Th
 H    15.991836    16.137915    -0.663641   f=Th
 H    17.496537    15.229778    -0.529840   f=Th
 H    16.608551    15.239948    -2.057803   f=Th
 H    23.068753    13.636711     3.173546   f=Th
 H    25.312561    10.509711    -6.484817   f=Th
 H    26.043652    10.945384    -4.935711   f=Th
 H    27.039597    10.810052    -6.381602   f=Th
 H    24.769399    12.841190    -6.093934   f=Th
 H    25.570389    16.689314    -3.194245   f=Th
 H    21.868676    12.000128     1.790645   f=Th
 H    22.572295    10.671456    -0.794024   f=Th
 H    20.961852    10.120369    -1.263992   f=Th
 H    21.331968    10.403863     0.428502   f=Th
 H    22.624717    17.796978   -10.227329   f=Th
 H    23.969559    18.773129   -10.809929   f=Th
 H    23.110702    19.262915    -9.353352   f=Th
 H    29.988937    13.926889    -4.827043   f=Th
 H    23.086883    16.821504    -1.300458   f=Th
 H    29.126347    15.909962    -3.675236   f=Th
 H    19.148036    13.314623    -0.520607  f=Th
 H    19.422387    12.085167     0.721474 f=Th
 H    18.947403    11.606121    -0.911614   f=Th
 H    25.724413    13.853382    -8.134541   f=Th
 H    25.334249    12.155574    -8.406482   f=Th
 H    27.012710    12.640642    -8.150600   f=Th
 H    23.686132    15.824214     2.239806   f=Th
 H    28.453622    12.429123    -6.024642   f=Th
 H    21.083964    12.484010    -1.803559   f=Th
 H    17.163515    18.234697     0.128871   f=Th
 H    18.608267    18.823708    -0.703960   f=Th
 H    18.680543    17.350762     0.272926   f=Th
 H    20.066910    13.256462    -4.213680   f=Th
 H    19.737427    11.657622    -3.536595   f=Th
 H    19.279202    12.019808    -5.194489   f=Th
 H    22.484145     9.270753    -5.722601   f=Th
 H    20.756016     9.451336    -6.033046   f=Th
 H    21.334188     9.182422    -4.387272   f=Th
 H    25.940680    17.813661    -5.363341   f=Th
 H    27.603240    18.189088    -4.891442   f=Th
 H    26.250345    18.917060    -4.017965   f=Th
 H    27.553807    16.398692    -1.593680   f=Th
 H    26.974557    18.057049    -1.783747   f=Th
 H    28.442603    17.549106    -2.592028   f=Th
 H    22.925911    11.905868    -7.227014   f=Th
 H    22.201166    13.422959    -6.683780   f=Th
 H    21.198410    12.170292    -7.416715   f=Th
 H    22.547077    18.843158    -0.002793   f=Th
 H    22.425484    17.886803     1.477719   f=Th
 H    21.269054    17.635469     0.163155   f=Th
 H    24.933030    18.145381    -0.394781   f=Th
 H    25.399094    16.440821    -0.357896   f=Th
 H    24.906711    17.257959     1.122191   f=Th
 C    26.471504    12.963033    -1.559296 f=F
 C    25.496519    12.651090    -0.702519 f=F
 H    25.203156    13.312913     0.108506 f=F
 H    24.991800    11.689823    -0.748135 f=F
 H    26.798991    12.274123    -2.333134 f=F
 H    27.024737    13.894649    -1.485349 f=F
```

A.1.5 Optimised geometries of Alkyl cations containing Uranium

Optimised geometry of η^6-2-U

```
U    26.800801    13.592814    -5.510886
  C    25.491564    16.354392    -4.125418
  C    27.859184    16.450443    -4.100940
  C    25.374046    17.619561    -3.607720
  C    26.584983    18.512217    -3.372946
  C    27.866905    17.717483    -3.576799
  O    26.704269    15.785651    -4.471938
 Si    26.748725    16.263684    -8.357543
  C    24.072324    18.040990    -3.315238
  H    23.936071    19.035812    -2.915692
  C    30.220188    16.219437    -3.954170
  H    31.115029    15.624078    -4.087968
  C    29.126541    18.236029    -3.254768
  H    29.177043    19.237272    -2.851155
  C    23.154197    15.944873    -4.031913
  H    22.310559    15.281382    -4.176239
  C    28.996215    15.672194    -4.305170
  N    28.755425    14.406473    -4.835895
  C    30.300529    17.515419    -3.430218
  C    24.425166    15.485274    -4.344659
  C    26.778469    14.516861    -7.642928
  H    27.657731    14.009038    -8.081075
  H    25.897664    14.000468    -8.066364
  C    22.962081    17.231350    -3.514712
  C    26.545780    19.064114    -1.941638
  H    25.642966    19.653100    -1.776663
  H    27.397400    19.719182    -1.754472
  H    26.566917    18.256036    -1.208279
  C    21.519420    19.128052    -2.641993
  H    20.489393    19.409663    -2.413867
  H    21.897596    19.839603    -3.380282
  H    22.099150    19.239753    -1.722441
  C    32.345398    17.198517    -2.025562
  H    32.506732    16.185276    -2.399907
  H    31.744232    17.133317    -1.115349
  H    33.322367    17.608172    -1.757125
  C    29.805556    13.442668    -4.839113
  C    26.552193    19.680812    -4.371123
  H    25.642392    20.270138    -4.239342
  H    26.579185    19.320344    -5.401177
  H    27.409759    20.339120    -4.217147
  C    32.544149    18.151328    -4.327783
```

H	32.714518	17.158779	-4.749780
H	33.520806	18.578219	-4.086297
H	32.083187	18.772426	-5.099434
C	20.657882	17.624523	-4.411195
H	19.651565	17.978086	-4.173094
H	20.564615	16.604010	-4.787757
H	21.055466	18.248659	-5.215074
C	31.669022	18.093653	-3.070331
C	21.547648	17.694299	-3.165275
C	21.808269	11.226944	-4.874431
H	21.050588	10.451720	-4.879614
C	30.412511	13.398266	-8.542697
H	30.335210	14.119434	-9.359476
H	29.540937	12.743199	-8.604023
H	31.297555	12.788620	-8.737350
C	30.049640	12.697456	-3.662349
C	30.510203	14.133732	-7.209000
H	29.627020	14.765887	-7.098002
C	30.576414	13.219479	-6.001855
C	23.567820	12.412978	-3.712184
C	29.348920	12.993585	-2.351449
H	28.623463	13.791967	-2.528938
C	21.980390	12.037195	-5.980298
H	21.345209	11.894524	-6.847401
C	23.250793	13.168848	-8.503801
H	24.144407	12.542989	-8.454812
H	23.369329	13.856229	-9.344718
H	22.404839	12.517532	-8.736037
C	31.569684	19.504055	-2.494917
H	31.131538	20.206564	-3.208142
H	32.570526	19.867326	-2.252717
H	30.980681	19.529486	-1.574720
C	31.712367	11.412966	-4.857821
H	32.446786	10.615850	-4.869923
C	24.350617	12.624722	-2.430434
H	25.254524	13.194362	-2.679122
C	31.003709	11.687375	-3.700574
H	31.202326	11.107937	-2.805781
C	21.762270	14.806669	-7.349048
H	21.603122	15.430853	-6.469947
H	20.874611	14.185137	-7.491402
H	21.846915	15.466632	-8.215871
C	31.732670	15.055063	-7.232214
H	31.802451	15.653685	-6.324210
H	31.674671	15.740739	-8.080969
H	32.654880	14.476800	-7.331643
C	22.592172	11.423751	-3.750368
H	22.432412	10.798651	-2.879927
C	22.937241	13.048575	-5.996127
C	31.505942	12.182604	-5.988417
H	32.100533	11.991274	-6.874219
C	23.020567	13.949256	-7.211135
H	23.864406	14.626238	-7.063852
C	20.969504	16.776983	-2.080826
H	19.956329	17.094454	-1.821588
H	21.577117	16.810911	-1.173131
H	20.915606	15.738034	-2.413315
C	25.184386	17.157574	-7.836846
H	25.071592	17.224607	-6.752064
H	24.291556	16.669657	-8.236224
H	25.197361	18.177318	-8.232864
N	24.768544	14.225881	-4.841291
C	23.752146	13.222525	-4.857619
C	26.772624	16.154835	-10.232090
H	27.672651	15.648994	-10.592301
H	26.752358	17.151948	-10.681267
H	25.907894	15.604016	-10.612132
C	30.341608	13.507969	-1.308866
H	30.864947	14.397379	-1.661677
H	31.088627	12.748095	-1.066251
H	29.819117	13.767429	-0.385121
C	28.592478	11.784703	-1.807714
H	27.835621	11.426989	-2.509936
H	28.086699	12.042829	-0.874627
H	29.266299	10.951369	-1.594781
C	28.248346	17.245122	-7.805123
H	29.176377	16.814151	-8.189238
H	28.336417	17.315384	-6.718361
H	28.180909	18.263558	-8.199184
C	23.549502	13.464920	-1.433089
H	24.129666	13.627673	-0.521457
H	22.627970	12.946131	-1.155389
H	23.281318	14.437698	-1.844433
C	24.782199	11.321412	-1.764336
H	25.438511	11.534204	-0.918324
H	25.317446	10.663177	-2.451053
H	23.927313	10.767982	-1.370276
C	25.594100	9.997042	-5.377091
H	24.761453	9.589362	-4.817891
C	27.942134	10.519101	-5.548983
H	28.943723	10.506546	-5.135160
C	25.379494	10.515147	-6.646812
H	24.382527	10.508200	-7.068628
C	27.728898	11.028977	-6.828773
H	28.572872	11.381829	-7.408480
C	26.446421	11.034485	-7.375398
H	26.290706	11.407912	-8.380757
C	26.871514	10.003360	-4.827268
H	27.039543	9.581841	-3.843284

A.1.6 Optimised geometries of Alkyl cations containing Zirconium

Optimised geometry of η^6-2′-Zr and the name of the fragment f in the ETS-NOCV in which each atom belongs

C	6.765617	8.543203	16.019925	f=B
C	7.594672	9.346129	15.246965	f=B
C	7.196142	10.639722	14.906181	f=B
C	5.972804	11.130791	15.343249	f=B
C	5.154178	10.338319	16.152808	f=B
C	5.548108	9.046473	16.486256	f=B
H	8.549431	8.971886	14.901321	f=B
Zr	7.388531	10.680855	17.780436	f=Z
C	9.476823	11.030952	17.040068	f=Z
O	8.269054	11.440735	19.704398	f=Z
C	8.628986	10.555301	20.706789	f=Z
C	9.220970	10.971548	21.878665	f=Z
C	9.596177	12.436971	22.049428	f=Z
C	8.610252	13.271948	21.243984	f=Z
C	8.051034	12.749072	20.103447	f=Z
C	8.280057	9.255044	20.402336	f=Z
C	8.560596	8.286726	21.368180	f=Z
C	9.155616	8.635298	22.577247	f=Z
C	9.478542	9.973302	22.811748	f=Z
C	8.253111	14.586079	21.549236	f=Z
C	7.383513	15.319339	20.747801	f=Z
C	6.858483	14.724108	19.597930	f=Z
C	7.181169	13.414049	19.256415	f=Z
C	9.461558	7.595019	23.654881	f=Z
C	8.743402	7.979213	24.954065	f=Z
N	7.666527	9.057113	19.160128	f=Z
C	7.320155	7.685229	18.917442	f=Z
C	8.292561	6.787389	18.441989	f=Z

C	7.924372	5.462894	18.219243	f=Z
C	6.643436	4.992255	18.459809	f=Z
C	5.709381	5.895833	18.955297	f=Z
C	6.015533	7.228151	19.204871	f=Z
N	6.709354	12.678854	18.161878	f=Z
C	5.793790	13.422420	17.343529	f=Z
C	4.404791	13.321505	17.575246	f=Z
C	3.544369	14.075971	16.786534	f=Z
C	3.998873	14.939301	15.795797	f=Z
C	5.368096	15.023748	15.598507	f=Z
C	6.282390	14.286679	16.346818	f=Z
C	6.966115	16.747203	21.102858	f=Z
C	7.652049	17.254159	22.368855	f=Z
C	9.607344	12.844484	23.519379	f=Z
C	11.005365	12.649569	21.462693	f=Z
C	9.729930	7.193328	18.175972	f=Z
C	10.162820	6.891034	16.741693	f=Z
C	6.285478	3.546344	18.210695	f=Z
C	5.181821	3.405791	17.165219	f=Z
C	4.956975	8.131120	19.814740	f=Z
C	3.531246	7.793075	19.385413	f=Z
C	3.825036	12.445980	18.672675	f=Z
C	2.467497	11.840098	18.322728	f=Z
C	3.041172	15.761244	14.966304	f=Z
C	2.250963	16.743154	15.828516	f=Z
C	7.760670	14.445703	16.047375	f=Z
C	8.070690	14.297339	14.557208	f=Z
C	7.326302	17.694915	19.953681	f=Z
C	5.450141	16.785160	21.331705	f=Z
C	10.974200	7.554671	23.903527	f=Z
C	9.003939	6.193832	23.258062	f=Z
H	8.284576	7.261235	21.171217	f=Z
H	6.168539	15.273180	18.970894	f=Z
H	8.665378	15.040704	22.437342	f=Z
H	10.337666	12.256421	24.076020	f=Z
H	9.905766	13.887622	23.627945	f=Z
H	8.628259	12.712520	23.983202	f=Z
H	11.735101	12.043939	22.004695	f=Z
H	11.044661	12.367011	20.408760	f=Z
H	11.293617	13.699933	21.544630	f=Z
H	8.401770	17.687980	19.759981	f=Z
H	6.813361	17.427730	19.027610	f=Z
H	7.035820	18.717484	20.207501	f=Z
H	4.897447	16.481220	20.440229	f=Z
H	5.160581	16.122475	22.150918	f=Z
H	5.134555	17.799495	21.588964	f=Z
H	8.739628	17.275510	22.263279	f=Z
H	7.323190	18.274893	22.574635	f=Z
H	7.399525	16.647924	23.242254	f=Z
H	11.356428	8.520654	24.239192	f=Z
H	11.208964	6.817641	24.675722	f=Z
H	11.514543	7.277311	22.995038	f=Z
H	7.925012	6.149437	23.088775	f=Z
H	9.510072	5.835066	22.358283	f=Z
H	9.238419	5.494863	24.063640	f=Z
H	7.661076	8.015551	24.807948	f=Z
H	8.955785	7.241210	25.731701	f=Z
H	9.064587	8.953571	25.326710	f=Z
H	8.671252	4.766910	17.849489	f=Z
H	4.706281	5.543943	19.166778	f=Z
H	5.172311	9.157319	19.494083	f=Z
H	4.263650	8.778327	21.763931	f=Z
H	4.844233	7.109950	21.721998	f=Z
H	5.999277	8.447249	21.711694	f=Z
H	2.848548	8.577403	19.718800	f=Z
H	3.416166	7.685328	18.303492	f=Z
H	3.185581	6.861806	19.839551	f=Z
H	9.805655	8.271329	18.334010	f=Z
H	10.463436	6.757366	20.182720	f=Z
H	10.664756	5.426295	19.035438	f=Z
H	11.720952	6.837195	18.946788	f=Z
H	9.493775	7.335754	16.002418	f=Z
H	11.168315	7.277577	16.559820	f=Z
H	10.188352	5.815982	16.549550	f=Z
H	7.184001	3.061091	17.813897	f=Z
H	6.703419	2.902632	20.248589	f=Z
H	5.000618	3.260531	19.943677	f=Z
H	5.711505	1.773855	19.315796	f=Z
H	5.459866	3.884216	16.223342	f=Z
H	4.980056	2.351711	16.961921	f=Z
H	4.248396	3.858345	17.510703	f=Z
H	2.477136	13.996342	16.958363	f=Z
H	5.739936	15.694090	14.829888	f=Z
H	4.528812	11.622897	18.844284	f=Z
H	3.282134	12.555753	20.767863	f=Z
H	4.659292	13.580684	20.346768	f=Z
H	3.025055	14.059450	19.876922	f=Z
H	2.442099	11.371183	17.335437	f=Z
H	2.196899	11.083883	19.062567	f=Z
H	1.676357	12.592999	18.339442	f=Z
H	8.292559	13.658651	16.586978	f=Z
H	9.365763	15.875988	16.298718	f=Z
H	7.783310	16.618070	16.050233	f=Z
H	8.190092	15.901656	17.615256	f=Z
H	9.150252	14.237740	14.400297	f=Z
H	7.611651	13.408930	14.117843	f=Z
H	7.711329	15.156260	13.986028	f=Z
H	3.648979	16.346516	14.267533	f=Z
H	2.662673	14.200154	13.495038	f=Z
H	1.457407	14.279404	14.785979	f=Z
H	1.460087	15.495549	13.509926	f=Z
H	2.914448	17.396077	16.399301	f=Z
H	1.611544	17.370887	15.203804	f=Z
H	1.605797	16.217401	16.537449	f=Z
H	9.985759	10.086449	16.820017	f=Z
H	9.526360	11.652714	16.141655	f=Z
H	10.043300	11.537249	17.825413	f=Z
C	5.027882	8.119345	21.344000	f=Z
C	10.696641	6.513226	19.146332	f=Z
C	5.906079	2.831771	19.505962	f=Z
C	3.698954	13.206581	19.994957	f=Z
C	8.302917	15.788679	16.537731	f=Z
C	2.104801	14.880875	14.142108	f=Z
H	9.943884	10.244620	23.749566	f=Z
H	7.845085	11.258052	14.300136	f=B
H	5.659133	12.132494	15.081835	f=B
H	4.209622	10.729768	16.504973	f=B
H	4.914149	8.421604	17.099425	f=B
H	7.065048	7.538292	16.286669	f=B

Optimised geometry of η^6-2-Zr and the name of the fragment f in the ETS-NOCV in which each atom belongs

;lkjhgfdsdrftghjklp;

Optimised geometry of η^6-3′-Zr-exo and the name of the fragment f in the ETS-NOCV in which each atom belongs

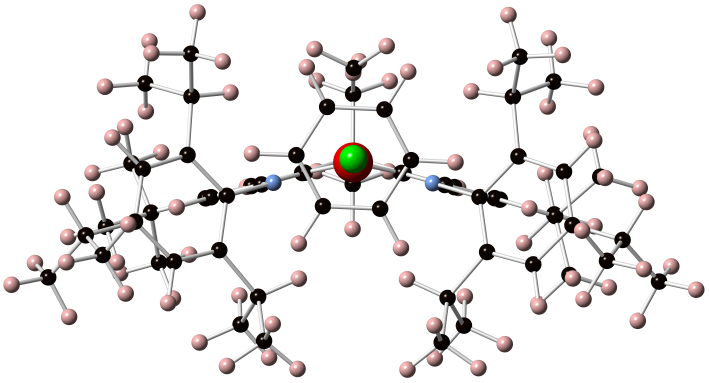

FIGURE A.1: **2'-Zr-a** molecule. Green: Pu; red: O; blue: N; black: C; pink: H

Zr	7.241484	8.778722	15.728818	f=Z
O	8.37604	10.43795	14.725539	f=Z
N	6.041734	10.575997	15.687056	f=Z
N	8.580454	7.966974	14.257685	f=Z
C	7.847188	13.982576	14.065712	f=Z
H	8.340867	14.845178	13.639288	f=Z
C	6.548546	14.119205	14.559059	f=Z
C	5.915737	13.007942	15.107004	f=Z
H	4.908206	13.088679	15.487045	f=Z
C	6.560912	11.770446	15.170919	f=Z
C	9.457686	8.790449	13.542351	f=Z
C	10.396445	8.399063	12.592137	f=Z
H	10.488642	7.34834	12.351078	f=Z
C	11.196338	9.338666	11.937741	f=Z
C	11.05044	10.685071	12.256195	f=Z
H	11.667627	11.41714	11.757684	f=Z
C	9.964387	12.575135	13.6375	f=Z
C	8.529419	12.771957	14.104719	f=Z
C	7.843191	11.714965	14.662143	f=Z
C	9.369295	10.147382	13.80374	f=Z
C	10.125937	11.125106	13.204583	f=Z
C	10.323614	13.539776	12.511312	f=Z
H	10.230982	14.57351	12.845571	f=Z
H	11.362163	13.407536	12.206714	f=Z
H	9.684256	13.397917	11.638253	f=Z
C	10.903549	12.832114	14.832205	f=Z
H	10.79525	13.860951	15.182735	f=Z
H	10.678964	12.163515	15.665722	f=Z
H	11.942768	12.671409	14.536719	f=Z
C	12.1962	8.858842	10.88479	f=Z
C	13.185709	7.877959	11.52368	f=Z
H	13.742256	8.35351	12.335036	f=Z
H	12.682995	6.997693	11.929344	f=Z
H	13.905614	7.533028	10.77715	f=Z
C	11.440193	8.149451	9.754941	f=Z
H	10.888694	7.279704	10.118005	f=Z
H	10.727811	8.825013	9.275063	f=Z
H	12.143268	7.802524	8.993403	f=Z
C	12.993337	10.009111	10.27525	f=Z
H	13.583338	10.540351	11.026303	f=Z
H	13.68955	9.613599	9.532765	f=Z
H	12.348039	10.729747	9.766824	f=Z
C	5.86003	15.481822	14.481236	f=Z
C	6.682208	16.512038	15.264871	f=Z
H	7.691833	16.618366	14.863564	f=Z
H	6.201045	17.49216	15.215714	f=Z
H	6.76683	16.228464	16.316794	f=Z
C	4.449933	15.454959	15.065231	f=Z
H	3.796974	14.761958	14.528403	f=Z
H	4.45103	15.179758	16.12301	f=Z
H	4.006296	16.449677	14.986067	f=Z
C	5.76314	15.919013	13.014691	f=Z
H	5.176693	15.205728	12.430227	f=Z
H	5.276267	16.895079	12.945114	f=Z
H	6.74679	16.005144	12.549168	f=Z
C	4.660025	10.709227	16.060997	f=Z
C	4.300172	11.057838	17.376605	f=Z
C	2.948951	11.216177	17.674901	f=Z
H	2.66217	11.480989	18.686918	f=Z
C	1.946728	11.061465	16.728534	f=Z
C	2.332178	10.732959	15.4356	f=Z
H	1.569189	10.618426	14.672579	f=Z
C	3.662998	10.560343	15.074594	f=Z
C	3.983874	10.251212	13.623686	f=Z
H	5.052405	10.026627	13.558602	f=Z
C	3.714556	11.460192	12.726124	f=Z
H	3.984213	11.233569	11.691628	f=Z
H	2.654716	11.7277	12.743193	f=Z
H	4.290299	12.330043	13.043208	f=Z
C	3.214969	9.042157	13.093204	f=Z
H	3.522626	8.822293	12.068282	f=Z
H	3.37927	8.142452	13.691201	f=Z
H	2.13874	9.22657	13.073153	f=Z
C	5.328534	11.294083	18.46876	f=Z
H	6.224168	10.726947	18.197704	f=Z
C	5.738926	12.766197	18.558806	f=Z
H	6.185356	13.124851	17.63257	f=Z
H	4.868977	13.389582	18.783206	f=Z
H	6.466102	12.906057	19.362746	f=Z
C	4.866663	10.833415	19.850879	f=Z
H	4.443631	9.825299	19.853821	f=Z
H	5.707009	10.851923	20.549002	f=Z
H	4.105157	11.499925	20.261716	f=Z
C	0.49476	11.25608	17.095625	f=Z
H	0.467841	11.506463	18.16191	f=Z
C	-0.127385	12.421453	16.329699	f=Z
H	0.430775	13.346411	16.488697	f=Z
H	-0.148137	12.222629	15.25485	f=Z
H	-1.15738	12.585655	16.654351	f=Z
C	-0.31574	9.977254	16.898486	f=Z
H	0.102675	9.146664	17.471432	f=Z
H	-1.348565	10.125093	17.221968	f=Z
H	-0.339518	9.682131	15.845967	f=Z
C	8.723797	6.578796	13.92012	f=Z

```
C    7.933199    6.024248    12.890256    f=Z
C    8.114705    4.686552    12.560278    f=Z
H    7.505573    4.258712    11.772254    f=Z
C    9.050226    3.878302    13.195526    f=Z
C    9.811753    4.450824    14.202076    f=Z
H    10.54556    3.832723    14.709134    f=Z
C    9.67749    5.783626    14.583113    f=Z
C    6.901207    6.83332    12.125691    f=Z
H    6.596811    7.667998    12.76726    f=Z
C    7.484733    7.440819    10.84804    f=Z
H    6.719476    8.012559    10.316729    f=Z
H    8.322596    8.105118    11.055649    f=Z
H    7.835466    6.650299    10.178958    f=Z
C    5.65189    6.030165    11.767412    f=Z
H    5.258706    5.453637    12.608836    f=Z
H    4.865322    6.699292    11.412636    f=Z
H    5.84912    5.321333    10.960095    f=Z
C    10.571936    6.31737    15.685831    f=Z
H    10.126239    7.246935    16.047122    f=Z
C    11.974768    6.651486    15.173733    f=Z
H    12.597962    7.01566    15.994496    f=Z
H    12.454898    5.759762    14.761196    f=Z
H    11.955385    7.417182    14.399607    f=Z
C    10.700352    5.354788    16.866994    f=Z
H    11.163343    5.863011    17.716054    f=Z
H    9.740565    4.947067    17.192041    f=Z
H    11.338864    4.502893    16.622291    f=Z
C    9.235178    2.430524    12.807497    f=Z
H    10.030744    2.030424    13.44568    f=Z
C    7.974383    1.609377    13.067519    f=Z
H    7.66456    1.673585    14.113085    f=Z
H    7.142472    1.954414    12.447563    f=Z
H    8.147306    0.557217    12.83032    f=Z
C    9.68957    2.29021    11.356487    f=Z
H    10.606795    2.852447    11.169614    f=Z
H    9.878672    1.241744    11.115352    f=Z
H    8.925386    2.65484    10.664915    f=Z
C    8.68459    9.195491    17.393953    f=Z
H    8.219318    9.763178    18.20611    f=Z
H    9.140681    8.301301    17.826483    f=Z
H    9.489988    9.810183    16.983148    f=Z
C    6.399183    7.241748    18.048942 f=t
C    7.042913    6.322772    17.208383  f=t
H    7.925389    5.808493    17.567453 f=t
C    6.563710    6.045666    15.934283 f=t
H    7.070384    5.316600    15.317068 f=t
C    5.443818    6.721495    15.442507 f=t
H    5.069741    6.508599    14.449781 f=t
C    4.796711    7.643354    16.260262 f=t
H    3.923633    8.176336    15.908099 f=t
C    5.277655    7.904809    17.543025 f=t
H    4.761421    8.632196    18.154469 f=t
C    6.846925    7.436240    19.457397 f=t
H    6.599208    8.430215    19.827540    f=t
H    6.335326    6.708595    20.095550    f=t
H    7.918576    7.273051    19.566346    f=t
```

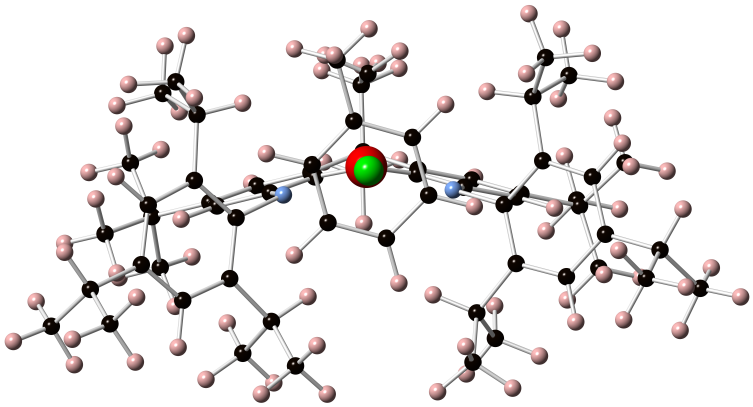

FIGURE A.2: **3'-Zr-a** molecule. Green: Pu; red: O; blue: N; black: C; pink: H

Optimised geometry of η^6-4′-Zr-exo and the name of the fragment f in the ETS-NOCV in which each atom belongs

Zr	7.199815	10.734381	18.139199	f=Z
C	9.010617	10.914767	16.901978	f=Z
N	6.732466	12.730258	18.505216	f=Z
C	7.237468	13.496107	19.551206	f=Z
C	8.127030	12.821728	20.372407	f=Z
C	8.721761	13.342691	21.493135	f=Z
C	8.396184	14.670369	21.785527	f=Z
C	7.524385	15.414368	20.995482	f=Z
C	6.946060	14.813874	19.871378	f=Z
C	9.704397	12.492366	22.289867	f=Z
C	9.311673	11.029192	22.120943	f=Z
C	8.686371	10.623636	20.964629	f=Z
O	8.317457	11.509919	19.963324	f=Z
C	9.579950	10.018531	23.040570	f=Z
C	9.237008	8.684177	22.809422	f=Z
C	8.598960	8.345833	21.617138	f=Z
C	8.306896	9.327319	20.674377	f=Z
C	7.167156	16.862897	21.330599	f=Z
C	7.546677	17.770764	20.155282	f=Z
C	9.727690	12.896902	23.760780	f=Z
C	11.111337	12.689274	21.693133	f=Z
C	9.566489	7.636205	23.872515	f=Z
C	11.085089	7.586506	24.080001	f=Z
N	7.644696	9.178804	19.459128	f=Z
C	7.301602	7.866091	19.023120	f=Z
C	8.278702	7.025886	18.452638	f=Z
C	7.894025	5.760398	18.020840	f=Z
C	6.592132	5.296211	18.127032	f=Z
C	5.647580	6.144083	18.697171	f=Z
C	5.968379	7.413734	19.158565	f=Z
C	9.729745	7.432499	18.297428	f=Z
C	10.204199	7.309467	16.849433	f=Z
C	6.219295	3.912676	17.651095	f=Z
C	5.172435	3.956146	16.540569	f=Z
C	4.900485	8.250931	19.839466	f=Z
C	3.486824	7.958775	19.349525	f=Z
C	5.818481	13.331859	17.592169	f=Z
C	6.296126	14.043585	16.472427	f=Z
C	5.368049	14.582774	15.588096	f=Z
C	3.997794	14.463192	15.772887	f=Z
C	3.554159	13.780257	16.900238	f=Z
C	4.428366	13.215366	17.819975	f=Z
C	7.770942	14.284981	16.222982	f=Z
C	8.199296	13.914005	14.804881	f=Z
C	3.860042	12.547012	19.056172	f=Z
C	2.702071	11.603131	18.746028	f=Z
C	3.026833	15.075727	14.791992	f=Z
C	2.190181	16.173872	15.445218	f=Z
C	9.091935	6.239915	23.478514	f=Z
C	8.885200	8.015287	25.192833	f=Z
C	5.658166	16.967870	21.582322	f=Z
C	7.893314	17.367613	22.574818	f=Z
C	10.641991	6.609766	19.208002	f=Z
C	5.753994	3.030976	18.808193	f=Z
C	4.963593	8.089279	21.359540	f=Z
C	3.419369	13.590835	20.084049	f=Z
C	2.133956	14.020750	14.143082	f=Z
C	8.140054	15.742239	16.505820	f=Z
H	10.071961	10.277875	23.968308	f=Z
H	8.301516	7.325759	21.416671	f=Z
H	6.249845	15.363208	19.249527	f=Z
H	8.838922	15.129311	22.656782	f=Z
H	10.454037	12.299617	24.312854	f=Z
H	10.037240	13.936769	23.869874	f=Z
H	8.749465	12.774499	24.228994	f=Z
H	11.837963	12.074331	22.228760	f=Z
H	11.138670	12.408082	20.638483	f=Z
H	11.412788	13.735928	21.774913	f=Z
H	8.616436	17.710773	19.940983	f=Z
H	7.003500	17.507786	19.245230	f=Z
H	7.306609	18.810306	20.392142	f=Z
H	5.078085	16.678940	20.703242	f=Z
H	5.353573	16.328814	22.414726	f=Z
H	5.389765	17.997863	21.830443	f=Z
H	8.978854	17.347302	22.450513	f=Z
H	7.605515	18.403378	22.766366	f=Z
H	7.634193	16.787180	23.463695	f=Z
H	11.481180	8.547794	24.412880	f=Z
H	11.336491	6.842235	24.839879	f=Z
H	11.599238	7.313721	23.155124	f=Z
H	8.008385	6.200588	23.340154	f=Z
H	9.571459	5.886366	22.562140	f=Z
H	9.346346	5.533664	24.271503	f=Z
H	7.799523	8.057223	25.076170	f=Z
H	9.115235	7.271574	25.959908	f=Z
H	9.220736	8.985946	25.562437	f=Z
H	8.642841	5.106947	17.584314	f=Z
H	4.626910	5.794792	18.793041	f=Z
H	5.112218	9.310802	19.632402	f=Z
H	4.198509	8.703377	21.840827	f=Z
H	4.778847	7.046900	21.632469	f=Z
H	5.934886	8.377892	21.760609	f=Z
H	2.790275	8.686098	19.768697	f=Z
H	3.400996	7.992781	18.260272	f=Z
H	3.146781	6.973663	19.676032	f=Z
H	9.817991	8.479446	18.595735	f=Z
H	10.369122	6.720232	20.257812	f=Z
H	10.596780	5.547755	18.953528	f=Z
H	11.678799	6.934698	19.093796	f=Z
H	9.557871	7.853322	16.157331	f=Z
H	11.216259	7.708092	16.749054	f=Z
H	10.232977	6.266238	16.526185	f=Z
H	7.128336	3.464428	17.235543	f=Z
H	6.509414	2.972740	19.594376	f=Z
H	4.833399	3.416440	19.254391	f=Z
H	5.550776	2.017132	18.456356	f=Z
H	5.511448	4.556798	15.693363	f=Z
H	4.961723	2.948284	16.176307	f=Z
H	4.230448	4.379850	16.898827	f=Z
H	2.487351	13.695155	17.075037	f=Z
H	5.727005	15.132477	14.723720	f=Z
H	4.661308	11.961003	19.520064	f=Z
H	3.029932	13.102346	20.980549	f=Z
H	4.246706	14.234883	20.382954	f=Z
H	2.626260	14.221795	19.674087	f=Z
H	2.962441	10.853683	17.994139	f=Z
H	2.393472	11.080161	19.653509	f=Z
H	1.827210	12.143424	18.378647	f=Z
H	8.332240	13.659450	16.919845	f=Z
H	9.208527	15.898556	16.339156	f=Z
H	7.596570	16.419022	15.841223	f=Z
H	7.916864	16.023364	17.535131	f=Z
H	9.283159	14.004305	14.706426	f=Z
H	7.923962	12.890358	14.544636	f=Z
H	7.751567	14.578374	14.061905	f=Z
H	3.625286	15.539494	14.000316	f=Z
H	2.723240	13.248947	13.642200	f=Z
H	1.496131	13.530410	14.883314	f=Z
H	1.480029	14.480297	13.398746	f=Z
H	2.821821	16.947082	15.887089	f=Z
H	1.540080	16.647416	14.706258	f=Z
H	1.552126	15.768846	16.235125	f=Z
H	9.538701	9.964884	16.794549	f=Z
H	8.710989	11.257021	15.903437	f=Z
H	9.711156	11.650599	17.307009	f=Z
C	5.335433	10.773110	15.476623	f=t
C	5.525781	9.667681	16.313699	f=t
C	6.337495	8.606945	15.891653	f=t
C	6.980050	8.669311	14.667198	f=t
C	6.796046	9.782767	13.856071	f=t
C	5.974804	10.831879	14.249578	f=t
Br	7.661406	9.865988	12.196192	f=t

```
 H     7.603622     7.850533    14.332358 f=t
 H     5.824671    11.681194    13.596222 f=t
 H     4.670173    11.577534    15.768395 f=t
 H     4.901991     9.545096    17.202458 f=t
 H     6.442404     7.722144    16.508373 f=t
```

Optimised geometry of η^6-4′-Zr-horizontal and the name of the fragment f in the ETS-NOCV in which each atom belongs

```
 C     1.148781     9.601211    14.619544 f=Z
 C     0.673990    10.683643    15.398187 f=Z
 C     0.555205    11.967135    14.828107 f=Z
 C     0.877636    12.126313    13.484817 f=Z
 C     1.327173    11.081041    12.694370 f=Z
 C     1.468641     9.831507    13.288947 f=Z
 N     0.323648    10.458942    16.760571 f=Z
 C    -1.008264    10.342883    17.141844 f=Z
 C    -1.188772    10.200101    18.510549 f=Z
 C    -2.393944    10.021929    19.139171 f=Z
 C    -3.509981     9.995356    18.296186 f=Z
 C    -3.405406    10.133943    16.915083 f=Z
 C    -2.140558    10.314812    16.342525 f=Z
 C    -2.457356     9.925330    20.660457 f=Z
 C    -1.117508     9.409622    21.175998 f=Z
 C     0.025033     9.602267    20.435973 f=Z
 O     0.018714    10.206175    19.189549 f=Z
 C     1.293988     9.186109    20.798453 f=Z
 C     1.438173     8.561830    22.032834 f=Z
 C     0.325322     8.354522    22.847404 f=Z
 C    -0.930438     8.773471    22.401611 f=Z
 C    -4.628998    10.060579    16.001102 f=Z
 C    -5.931041     9.908045    16.783116 f=Z
 C    -3.601916     9.017999    21.106840 f=Z
 C    -2.686008    11.339441    21.226728 f=Z
Zr     1.952082    10.409557    18.036020 f=Z
 C     0.441767     7.673773    24.211278 f=Z
 C    -0.421839     6.406751    24.224502 f=Z
 N     2.273716     9.444370    19.846307 f=Z
 C     3.601394     8.966923    20.053222 f=Z
 C     4.557828     9.769887    20.707707 f=Z
 C     5.842125     9.265130    20.878495 f=Z
 C     6.211278     7.996550    20.455108 f=Z
 C     5.244122     7.216088    19.832223 f=Z
 C     3.946550     7.664689    19.622511 f=Z
 C     4.223933    11.126257    21.290369 f=Z
 C     4.200484    11.071998    22.818928 f=Z
 C     7.607960     7.475617    20.699160 f=Z
 C     7.598198     6.285850    21.656917 f=Z
 C     2.934903     6.713715    19.015303 f=Z
 C     2.511977     5.648498    20.028610 f=Z
 C     0.088374    13.177657    15.608518 f=Z
 C    -1.290949    13.651900    15.151491 f=Z
 C     1.650904    11.297224    11.235080 f=Z
 C     3.129182    11.053835    10.939911 f=Z
 C     1.255845     8.195331    15.184761 f=Z
 C    -0.107129     7.502395    15.213686 f=Z
 C     2.117158    12.537237    18.628359 f=Z
 C    -4.726407    11.336766    15.158261 f=Z
 C    -4.484491     8.850128    15.070011 f=Z
 C    -0.048212     8.634482    25.301440 f=Z
 C     1.877829     7.273990    24.539736 f=Z
 C     5.187094    12.214211    20.819768 f=Z
 C     8.324365     7.122831    19.398196 f=Z
 C     3.442650     6.047997    17.740087 f=Z
 C     1.088070    14.330447    15.505460 f=Z
 C     2.262699     7.314899    14.455771 f=Z
 C     0.765447    10.444159    10.329609 f=Z
 H    -1.791650     8.600673    23.033093 f=Z
 H     2.421050     8.229484    22.337577 f=Z
 H    -2.027091    10.404964    15.269053 f=Z
 H    -4.485716     9.858622    18.738007 f=Z
 H    -3.658924     8.975175    22.194838 f=Z
 H    -4.560578     9.406600    20.762172 f=Z
 H    -3.481685     8.002451    20.725676 f=Z
 H    -2.721743    11.308468    22.317984 f=Z
 H    -1.884428    12.019301    20.931235 f=Z
 H    -3.630742    11.745886    20.858792 f=Z
 H    -4.814205    12.222189    15.792557 f=Z
 H    -3.856136    11.467314    14.511872 f=Z
 H    -5.608424    11.293276    14.514456 f=Z
 H    -3.591101     8.922962    14.445997 f=Z
 H    -4.421655     7.921366    15.642244 f=Z
 H    -5.349713     8.781375    14.405696 f=Z
 H    -6.104176    10.751811    17.455766 f=Z
 H    -6.769737     9.868012    16.084993 f=Z
 H    -5.951323     8.986084    17.369386 f=Z
 H    -1.091241     8.920483    25.153255 f=Z
 H     0.029522     8.159731    26.282824 f=Z
 H     0.551367     9.547839    25.317974 f=Z
 H     2.279856     6.559147    23.817026 f=Z
 H     2.544634     8.139139    24.579362 f=Z
 H     1.905476     6.795820    25.521025 f=Z
 H    -0.093701     5.700011    23.458299 f=Z
 H    -0.347239     5.912075    25.196225 f=Z
 H    -1.475559     6.629163    24.046163 f=Z
 H     6.581655     9.877803    21.384232 f=Z
 H     5.502852     6.211410    19.515345 f=Z
 H     2.039379     7.291088    18.762551 f=Z
 H     1.760770     4.985668    19.592276 f=Z
 H     3.368241     5.036358    20.324017 f=Z
 H     2.086880     6.095926    20.927566 f=Z
 H     2.647700     5.450121    17.288330 f=Z
 H     3.785214     6.776571    17.002139 f=Z
 H     4.274163     5.369710    17.944581 f=Z
 H     3.218604    11.391398    20.957663 f=Z
 H     3.475617    10.342469    23.183313 f=Z
 H     5.182185    10.804157    23.217997 f=Z
 H     3.929394    12.048709    23.226782 f=Z
 H     5.264702    12.251528    19.730738 f=Z
 H     4.852313    13.192887    21.171175 f=Z
 H     6.193719    12.056591    21.214065 f=Z
 H     8.169420     8.284706    21.178501 f=Z
 H     7.113650     6.539612    22.601786 f=Z
 H     7.065800     5.434335    21.224844 f=Z
 H     8.618643     5.962380    21.874307 f=Z
 H     8.377564     7.982089    18.725182 f=Z
 H     9.345603     6.793343    19.601906 f=Z
 H     7.815359     6.307713    18.875731 f=Z
 H     1.828258     9.006228    12.687072 f=Z
 H     0.773115    13.108742    13.035497 f=Z
 H     1.592295     8.269404    16.233328 f=Z
 H    -0.015899     6.498803    15.636409 f=Z
 H    -0.840265     8.054894    15.800117 f=Z
 H    -0.493622     7.403323    14.195809 f=Z
 H     3.245736     7.783301    14.375911 f=Z
 H     2.377135     6.368399    14.985307 f=Z
 H     1.919015     7.071413    13.447875 f=Z
 H     0.009751    12.888008    16.658622 f=Z
 H    -1.598901    14.525375    15.731253 f=Z
 H    -1.276771    13.941344    14.097500 f=Z
 H    -2.048440    12.879259    15.282607 f=Z
 H     0.811792    15.132069    16.194099 f=Z
 H     2.107569    14.015674    15.739302 f=Z
 H     1.101130    14.757085    14.499797 f=Z
 H     1.437713    12.348742    11.014946 f=Z
 H     3.767928    11.702558    11.544443 f=Z
 H     3.405091    10.014849    11.141816 f=Z
```

H	3.347912	11.254404	9.888684	f=Z
H	-0.293501	10.631874	10.517600	f=Z
H	0.968350	10.665448	9.279369	f=Z
H	0.949810	9.377701	10.484074	f=Z
H	3.036382	12.746366	19.183090	f=Z
H	2.073659	13.210702	17.768137	f=Z
H	1.275731	12.787666	19.283410	f=Z
Br	4.407454	11.206023	16.741043	f=t
C	5.293763	9.833134	15.735801	f=t
C	5.981724	8.848467	16.418211	f=t
C	6.668704	7.903664	15.667402	f=t
C	6.662601	7.965837	14.281666	f=t
C	5.963600	8.971677	13.630088	f=t
C	5.262890	9.923889	14.357237	f=t
H	5.960261	9.024021	12.547885	f=t
H	7.208921	7.228521	13.706043	f=t
H	4.709335	10.709690	13.860260	f=t
H	5.988764	8.812140	17.500800	f=t
H	7.217446	7.121333	16.177889	f=t

Optimised geometry of η^6-5′-Zr-exo and the name of the fragment f in the ETS-NOCV in which each atom belongs

C	5.537644	9.678384	16.311264	f=t
C	6.329164	8.599653	15.891837	f=t
C	6.959412	8.638335	14.661669	f=t
C	6.770844	9.748100	13.854006	f=t
C	5.973807	10.816795	14.229568	f=t
C	5.348104	10.777171	15.462709	f=t
H	7.571843	7.817650	14.310294	f=t
F	7.367646	9.784202	12.673467	f=t
H	5.839430	11.651137	13.553299	f=t
H	4.693620	11.589993	15.755161	f=t
H	4.912054	9.567614	17.200501	f=t
H	6.426936	7.721394	16.518662	f=t
C	6.301309	14.046565	16.468613	f=Z
C	5.823385	13.333500	17.587476	f=Z
C	4.432990	13.214396	17.813007	f=Z
C	3.559163	13.779248	16.892915	f=Z
C	4.003208	14.465242	15.767567	f=Z
C	5.373509	14.586207	15.584190	f=Z
N	6.736627	12.732991	18.501777	f=Z
C	7.240378	13.498687	19.548519	f=Z
C	8.127616	12.823494	20.371745	f=Z
C	8.719851	13.343995	21.494008	f=Z
C	8.394694	14.672015	21.785492	f=Z
C	7.525627	15.416832	20.993315	f=Z
C	6.949279	14.816662	19.867997	f=Z
O	8.318138	11.511676	19.962765	f=Z
C	8.686274	10.624969	20.963944	f=Z
C	9.308959	11.029850	22.121915	f=Z
C	9.699312	12.493265	22.294236	f=Z
C	9.577314	10.018302	23.040606	f=Z
C	9.236923	8.683736	22.807174	f=Z
C	8.601174	8.346100	21.613473	f=Z
C	8.309031	9.328402	20.671661	f=Z
Zr	7.200536	10.736097	18.137230	f=Z
N	7.648668	9.180079	19.455337	f=Z
C	7.305780	7.867236	19.019609	f=Z
C	8.282386	7.028363	18.446250	f=Z
C	7.898096	5.762522	18.015136	f=Z
C	6.597061	5.296615	18.124920	f=Z
C	5.653105	6.143085	18.698077	f=Z
C	5.973519	7.413241	19.158489	f=Z
C	9.714604	12.895924	23.765852	f=Z
C	11.109096	12.692277	21.705024	f=Z
C	9.566310	7.634770	23.869297	f=Z
C	9.095842	6.238076	23.471827	f=Z
C	7.169310	16.865846	21.327293	f=Z
C	5.659852	16.972833	21.575316	f=Z
C	9.732527	7.436883	18.287811	f=Z
C	10.647309	6.618527	19.199803	f=Z
C	6.224645	3.912821	17.649377	f=Z
C	5.766506	3.029187	18.807865	f=Z
C	4.905830	8.249180	19.841030	f=Z
C	4.964562	8.079041	21.360366	f=Z
C	3.864048	12.543749	19.047736	f=Z
C	3.430556	13.585624	20.080671	f=Z
C	3.032499	15.080256	14.787970	f=Z
C	2.136596	14.028098	14.138760	f=Z
C	7.776121	14.289557	16.220646	f=Z
C	8.144154	15.746347	16.507494	f=Z
C	9.006617	10.913195	16.891880	f=Z
C	8.880950	8.010272	25.188540	f=Z
C	11.084494	7.588027	24.080407	f=Z
C	7.893123	17.369939	22.573133	f=Z
C	7.552894	17.772942	20.152692	f=Z
C	10.205503	7.310334	16.839624	f=Z
C	5.172468	3.955187	16.543854	f=Z
C	3.492982	7.962947	19.345178	f=Z
C	2.701033	11.606301	18.737014	f=Z
C	2.198950	16.179353	15.443691	f=Z
C	8.205701	13.923379	14.801733	f=Z
H	10.067514	10.277122	23.969450	f=Z
H	8.305760	7.325812	21.411116	f=Z
H	6.254774	15.366510	19.244677	f=Z
H	8.835735	15.130606	22.657789	f=Z
H	10.438410	12.298455	24.321038	f=Z
H	10.022798	13.935857	23.878013	f=Z
H	8.733977	12.772169	24.228646	f=Z
H	11.833525	12.077313	22.243597	f=Z
H	11.142146	12.412485	20.650162	f=Z
H	11.409181	13.739091	21.789734	f=Z
H	8.622978	17.710981	19.940590	f=Z
H	7.011054	17.510916	19.241567	f=Z
H	7.314248	18.812943	20.388970	f=Z
H	5.081491	16.683658	20.695175	f=Z
H	5.352531	16.335012	22.407664	f=Z
H	5.392095	18.003396	21.821754	f=Z
H	8.978940	17.347873	22.451581	f=Z
H	7.606483	18.406241	22.763508	f=Z
H	7.630845	16.790308	23.461608	f=Z
H	11.477744	8.549562	24.415918	f=Z
H	11.335605	6.843003	24.839637	f=Z
H	11.601518	7.317890	23.156354	f=Z
H	8.012671	6.196405	23.331187	f=Z
H	9.578092	5.887344	22.555793	f=Z
H	9.350275	5.531005	24.264075	f=Z
H	7.795475	8.050015	25.069251	f=Z
H	9.110716	7.265899	25.955056	f=Z
H	9.213449	8.981120	25.560398	f=Z
H	8.646520	5.110020	17.576524	f=Z
H	4.633080	5.792613	18.796756	f=Z
H	5.120969	9.309471	19.640278	f=Z
H	4.199801	8.692424	21.843070	f=Z
H	4.776612	7.035665	21.627247	f=Z
H	5.935612	8.363186	21.765294	f=Z
H	2.796710	8.689492	19.766203	f=Z
H	3.410948	8.003339	18.255863	f=Z
H	3.149482	6.976848	19.664960	f=Z
H	9.819225	8.484878	18.582882	f=Z
H	10.376230	6.732724	20.249673	f=Z
H	10.602694	5.555521	18.949375	f=Z
H	11.683557	6.944138	19.082454	f=Z
H	9.555955	7.849040	16.146453	f=Z
H	11.215834	7.712571	16.736349	f=Z
H	10.238110	6.266049	16.520170	f=Z

H	7.132587	3.466715	17.229142 f=Z	H	9.212542	15.903925	16.341530 f=Z
H	6.525946	2.971328	19.590185 f=Z	H	7.600308	16.424500	15.844586 f=Z
H	4.847569	3.412804	19.259047 f=Z	H	7.920571	16.024505	17.537478 f=Z
H	5.563128	2.015392	18.455984 f=Z	H	9.289211	14.018285	14.703534 f=Z
H	5.506041	4.557714	15.695795 f=Z	H	7.934759	12.899217	14.538856 f=Z
H	4.962473	2.947307	16.179249 f=Z	H	7.755577	14.587825	14.060289 f=Z
H	4.231125	4.376134	16.906999 f=Z	H	3.631026	15.543844	13.996236 f=Z
H	2.492292	13.692200	17.066114 f=Z	H	2.723559	13.255896	13.635752 f=Z
H	5.732714	15.137895	14.721184 f=Z	H	1.498770	13.537821	14.879016 f=Z
H	4.663630	11.952345	19.507924 f=Z	H	1.482549	14.490207	13.396134 f=Z
H	3.040624	13.095507	20.976064 f=Z	H	2.832812	16.950538	15.885919 f=Z
H	4.261410	14.224740	20.380348 f=Z	H	1.548995	16.655395	14.706215 f=Z
H	2.639533	14.221750	19.674652 f=Z	H	1.561048	15.774498	16.233811 f=Z
H	2.955123	10.859998	17.979873 f=Z	H	9.529982	9.961519	16.777541 f=Z
H	2.394102	11.079667	19.642905 f=Z	H	8.702572	11.261323	15.896745 f=Z
H	1.826796	12.152215	18.376552 f=Z	H	9.712619	11.644496	17.295639 f=Z
H	8.337490	13.662454	16.916066 f=Z				

Optimised geometry of η^6-5′-Zr-horizontal and the name of the fragment f in the ETS-NOCV in which each atom belongs

C	4.956835	9.670408	15.943967 f=t	C	0.880813	11.904527	13.405515 f=Z
C	6.074845	9.090378	16.485056 f=t	C	1.247849	10.824287	12.618656 f=Z
C	7.174465	8.969835	15.644581 f=t	C	1.330568	9.576793	13.227951 f=Z
C	7.111237	9.424195	14.334801 f=t	C	1.033743	9.384055	14.570482 f=Z
C	5.948883	10.003554	13.846154 f=t	C	0.190685	13.027025	15.528276 f=Z
C	4.831654	10.137945	14.661571 f=t	C	1.189759	14.166133	15.321952 f=Z
H	5.901550	10.355603	12.822990 f=t	C	1.082086	7.981728	15.150044 f=Z
H	7.975236	9.326106	13.689307 f=t	C	2.095292	7.071836	14.465544 f=Z
H	3.905863	10.575787	14.308477 f=t	C	1.563285	11.007138	11.152977 f=Z
F	3.840492	9.798254	16.789883 f=t	C	0.697886	10.117671	10.264513 f=Z
H	6.086304	8.748216	17.513100 f=t	C	1.835201	7.353448	24.602246 f=Z
H	8.082719	8.517133	16.023156 f=t	C	-0.507519	6.590262	24.338905 f=Z
Zr	1.957971	10.200814	17.974402 f=Z	C	-4.579021	8.838280	15.177185 f=Z
C	2.450817	12.321618	18.285107 f=Z	C	-5.952936	10.016339	16.871308 f=Z
N	0.315954	10.318194	16.720485 f=Z	C	4.146719	11.063438	22.780140 f=Z
C	-1.011543	10.271017	17.131581 f=Z	C	7.604667	6.117442	21.585506 f=Z
C	-1.171727	10.201249	18.508356 f=Z	C	2.492683	5.577057	20.061481 f=Z
C	-2.372519	10.104767	19.162902 f=Z	C	-0.300668	7.328617	15.131634 f=Z
C	-3.503793	10.083021	18.340215 f=Z	C	3.048064	10.783840	10.871098 f=Z
C	-3.418946	10.150087	16.952844 f=Z	C	-1.210755	13.506898	15.148438 f=Z
C	-2.158107	10.250734	16.353050 f=Z	H	-1.784182	8.809318	23.093551 f=Z
C	-2.414460	10.086404	20.687169 f=Z	H	2.398468	8.220895	22.368177 f=Z
C	-1.094992	9.523728	21.203745 f=Z	H	-2.060312	10.288158	15.274929 f=Z
C	0.045315	9.636727	20.444364 f=Z	H	-4.475842	10.007903	18.804166 f=Z
O	0.049582	10.193124	19.171042 f=Z	H	-3.637572	9.284335	22.286909 f=Z
C	-0.923093	8.920918	22.448425 f=Z	H	-4.540647	9.693696	20.849303 f=Z
C	0.316192	8.456899	22.894700 f=Z	H	-3.543061	8.230137	20.867002 f=Z
C	1.428025	8.588118	22.063395 f=Z	H	-2.569304	11.561846	22.277407 f=Z
C	1.298852	9.180478	20.811920 f=Z	H	-1.721569	12.156096	20.843054 f=Z
C	-4.660352	10.088124	16.062613 f=Z	H	-3.481472	11.977436	20.813764 f=Z
C	-4.723246	11.334359	15.172732 f=Z	H	-4.771581	12.245514	15.773948 f=Z
C	-3.598816	9.268753	21.197396 f=Z	H	-3.856965	11.409659	14.512300 f=Z
C	-2.553448	11.537445	21.185548 f=Z	H	-5.614584	11.298342	14.541448 f=Z
C	0.416176	7.812628	24.277364 f=Z	H	-3.696604	8.853189	14.533858 f=Z
C	-0.013382	8.828766	25.342488 f=Z	H	-4.539262	7.930397	15.783949 f=Z
N	2.279183	9.365119	19.844578 f=Z	H	-5.459315	8.776705	14.532308 f=Z
C	3.602887	8.884245	20.073960 f=Z	H	-6.083436	10.892918	17.510817 f=Z
C	4.559056	9.695379	20.717595 f=Z	H	-6.804828	9.978996	16.189225 f=Z
C	5.838225	9.184165	20.910376 f=Z	H	-5.996068	9.120695	17.495837 f=Z
C	6.205662	7.909449	20.505403 f=Z	H	-1.043128	9.160480	25.196734 f=Z
C	5.241759	7.127195	19.879657 f=Z	H	0.053360	8.380801	26.337169 f=Z
C	3.947203	7.578453	19.657898 f=Z	H	0.629775	9.711947	25.324439 f=Z
C	4.236476	11.073988	21.253058 f=Z	H	2.193092	6.598726	23.897115 f=Z
C	5.250411	12.123041	20.799128 f=Z	H	2.543733	8.185712	24.608442 f=Z
C	7.604569	7.393801	20.748203 f=Z	H	1.851726	6.903954	25.597245 f=Z
C	8.361292	7.188359	19.437332 f=Z	H	-0.223123	5.845359	23.591642 f=Z
C	2.938576	6.628517	19.043934 f=Z	H	-0.445128	6.122409	25.324658 f=Z
C	3.457552	5.950739	17.779368 f=Z	H	-1.551308	6.858166	24.164962 f=Z
C	0.642687	10.501407	15.345133 f=Z	H	6.577157	9.800951	21.411715 f=Z
C	0.582503	11.782891	14.758700 f=Z	H	5.501027	6.120475	19.570066 f=Z

H	2.048391	7.208580	18.775639 f=Z	H	-0.255199	6.325269	15.562157 f=Z
H	1.741317	4.915783	19.623133 f=Z	H	-1.034834	7.907335	15.691802 f=Z
H	3.340064	4.961611	20.374783 f=Z	H	-0.655608	7.236020	14.101757 f=Z
H	2.060793	6.038582	20.950412 f=Z	H	3.087826	7.524191	14.405501 f=Z
H	2.667536	5.347381	17.326643 f=Z	H	2.181156	6.133199	15.014659 f=Z
H	3.804223	6.672452	17.035804 f=Z	H	1.780248	6.815210	13.451781 f=Z
H	4.288866	5.276447	17.995905 f=Z	H	0.180323	12.771817	16.590235 f=Z
H	3.254720	11.357955	20.868128 f=Z	H	-1.465301	14.406413	15.714133 f=Z
H	3.380245	10.372287	23.133446 f=Z	H	-1.261269	13.757330	14.085456 f=Z
H	5.100957	10.770871	23.225949 f=Z	H	-1.969342	12.753304	15.358050 f=Z
H	3.897163	12.060816	23.150004 f=Z	H	0.976357	14.981680	16.016172 f=Z
H	5.400559	12.111028	19.716994 f=Z	H	2.222481	13.848661	15.479827 f=Z
H	4.912857	13.121865	21.084551 f=Z	H	1.123783	14.577055	14.311841 f=Z
H	6.225484	11.966685	21.266337 f=Z	H	1.332488	12.049227	10.906964 f=Z
H	8.132546	8.165908	21.318123 f=Z	H	3.669203	11.463874	11.459654 f=Z
H	7.080004	6.262356	22.531896 f=Z	H	3.343392	9.757665	11.107987 f=Z
H	7.121261	5.292248	21.056099 f=Z	H	3.268400	10.956848	9.815282 f=Z
H	8.628428	5.809061	21.808642 f=Z	H	-0.365186	10.282906	10.450359 f=Z
H	8.421725	8.117606	18.865025 f=Z	H	0.894563	10.327083	9.210776 f=Z
H	9.380852	6.848170	19.632193 f=Z	H	0.908182	9.058313	10.433046 f=Z
H	7.873536	6.433073	18.814542 f=Z	H	3.378294	12.432557	18.853548 f=Z
H	1.627538	8.723499	12.630716 f=Z	H	2.581884	12.812227	17.314974 f=Z
H	0.821798	12.885097	12.944358 f=Z	H	1.660679	12.854688	18.822414 f=Z
H	1.376605	8.056921	16.208835 f=Z				

Optimised geometry of η^2-E′-Zr-horizontal and the name of the fragment f in the ETS-NOCV in which each atom belongs

C	7.558282	8.854639	16.089291 f=Z	C	14.890901	11.374616	16.931186 f=Z
C	8.153290	9.648401	15.078342 f=Z	C	12.093599	5.792469	16.850034 f=Z
C	7.667009	10.948369	14.824314 f=Z	C	11.071509	5.339423	17.887842 f=Z
C	6.595211	11.412500	15.579647 f=Z	C	15.049059	7.523058	20.529803 f=Z
C	5.996834	10.658307	16.576170 f=Z	C	15.873489	6.243283	20.655511 f=Z
C	6.502170	9.383756	16.816629 f=Z	C	5.490044	8.228339	10.911512 f=Z
N	9.263475	9.130158	14.357418 f=Z	C	6.642649	6.379226	9.734524 f=Z
Zr	11.046520	9.240895	15.415755 f=Z	C	16.115175	4.337158	13.529685 f=Z
C	11.761421	11.267041	14.913923 f=Z	C	16.371435	5.037955	11.167085 f=Z
C	8.251683	11.859960	13.765859 f=Z	C	7.297567	12.033327	12.582954 f=Z
C	8.608811	13.234999	14.332718 f=Z	C	3.568930	10.375914	17.146084 f=Z
C	4.833615	11.202755	17.369227 f=Z	C	7.469596	6.462294	15.319809 f=Z
C	5.162448	11.310860	18.856453 f=Z	C	12.891823	4.584485	16.354046 f=Z
C	8.021682	7.434911	16.362634 f=Z	C	13.963181	7.583101	21.601655 f=Z
C	7.684915	6.937324	17.762502 f=Z	C	16.315403	9.728787	15.700392 f=Z
N	12.807960	8.160428	15.283434 f=Z	H	9.300203	7.312590	9.451316 f=Z
C	13.331354	7.589170	14.131490 f=Z	H	7.014344	8.789188	12.761740 f=Z
C	12.535474	7.769066	13.008069 f=Z	H	15.143495	6.712897	14.837603 f=Z
C	12.792276	7.252753	11.764618 f=Z	H	14.241837	6.108341	10.691156 f=Z
C	13.984352	6.528825	11.651876 f=Z	H	11.121463	6.537547	8.811728 f=Z
C	14.845998	6.335662	12.727576 f=Z	H	12.767650	6.128993	9.230043 f=Z
C	14.505337	6.869671	13.976416 f=Z	H	11.431404	5.428841	10.157404 f=Z
C	11.836420	7.522869	10.606950 f=Z	H	11.664110	8.989793	9.010334 f=Z
C	10.453085	7.833021	11.170998 f=Z	H	12.387851	9.636361	10.489558 f=Z
C	10.322002	8.335418	12.444128 f=Z	H	13.335656	8.577165	9.436234 f=Z
O	11.397449	8.502465	13.300421 f=Z	H	17.378093	7.326077	12.316590 f=Z
C	9.261147	7.697449	10.461613 f=Z	H	17.267394	6.793030	13.998486 f=Z
C	8.019357	8.037219	11.003266 f=Z	H	18.269786	5.897727	12.858675 f=Z
C	7.961072	8.536759	12.304033 f=Z	H	16.019334	4.636078	14.575743 f=Z
C	9.127244	8.691326	13.045804 f=Z	H	15.280057	3.675013	13.288308 f=Z
C	16.148550	5.547313	12.588662 f=Z	H	17.040300	3.762981	13.435112 f=Z
C	17.331273	6.447567	12.964526 f=Z	H	16.438687	5.856158	10.445809 f=Z
C	11.783222	6.330474	9.653169 f=Z	H	17.312842	4.486385	11.123910 f=Z
C	12.337245	8.760653	9.839429 f=Z	H	15.578884	4.356799	10.847533 f=Z
C	6.760947	7.848753	10.155921 f=Z	H	7.723304	8.473041	8.292195 f=Z
C	6.857185	8.730396	8.904859 f=Z	H	5.964159	8.605085	8.287268 f=Z
C	13.411749	7.977729	16.555700 f=Z	H	6.937805	9.786527	9.173617 f=Z
C	14.365857	8.901124	17.037096 f=Z	H	5.348799	7.616794	11.806337 f=Z
C	14.863913	8.727117	18.323159 f=Z	H	5.485975	9.280829	11.206290 f=Z
C	14.475519	7.675444	19.141992 f=Z	H	4.623708	8.068808	10.266280 f=Z
C	13.560933	6.760006	18.632358 f=Z	H	6.570689	5.725488	10.607146 f=Z
C	13.022924	6.876392	17.358909 f=Z	H	5.745205	6.234887	9.127837 f=Z
C	14.899885	10.037793	16.191982 f=Z	H	7.498702	6.053457	9.140850 f=Z

```
H     6.211869    12.408856    15.384529 f=Z
H     6.045477     8.783068    17.593069 f=Z
H     9.120999     7.403883    16.264222 f=Z
H     7.825124     5.447897    15.516291 f=Z
H     6.377479     6.450296    15.365866 f=Z
H     7.762023     6.737305    14.306907 f=Z
H     8.152145     5.967058    17.934455 f=Z
H     8.020314     7.623258    18.544698 f=Z
H     6.609110     6.794469    17.885221 f=Z
H     9.167373    11.395839    13.392369 f=Z
H     7.071788    11.081971    12.101429 f=Z
H     6.356118    12.486056    12.904716 f=Z
H     7.744535    12.691525    11.834239 f=Z
H     9.210494    13.167229    15.241638 f=Z
H     9.172013    13.810845    13.595138 f=Z
H     7.713058    13.810680    14.576578 f=Z
H     4.640890    12.214298    16.995999 f=Z
H     3.311987    10.317290    16.086547 f=Z
H     3.691240     9.355654    17.519418 f=Z
H     2.724733    10.822073    17.676332 f=Z
H     6.046331    11.929730    19.026742 f=Z
H     4.327298    11.759011    19.399157 f=Z
H     5.348561    10.326569    19.294609 f=Z
H    13.264375     5.918623    19.248369 f=Z
H    15.595102     9.433720    18.701999 f=Z
H    11.548122     6.192245    15.987721 f=Z
H    12.216789     3.813811    15.974068 f=Z
H    13.579450     4.855213    15.553094 f=Z
H    13.472425     4.149515    17.171953 f=Z
H    10.526037     6.176114    18.329495 f=Z
H    10.345594     4.666380    17.426089 f=Z
H    11.541648     4.786226    18.703527 f=Z
H    14.258463    10.128337    15.313193 f=Z
H    16.686876    10.548867    15.081445 f=Z
H    17.002729     9.605699    16.541405 f=Z
H    16.344102     8.818135    15.101172 f=Z
H    15.145093    12.185008    16.244738 f=Z
H    13.916206    11.599404    17.371727 f=Z
H    15.626395    11.394079    17.738594 f=Z
H    15.723516     8.371150    20.690010 f=Z
H    13.390397     8.511226    21.539646 f=Z
H    13.264611     6.747531    21.506611 f=Z
H    14.408551     7.527417    22.597292 f=Z
H    16.669865     6.206345    19.909492 f=Z
H    16.331861     6.182525    21.644996 f=Z
H    15.249334     5.355276    20.525444 f=Z
H    10.939087    11.982021    14.833614 f=Z
H    12.458811    11.627763    15.678074 f=Z
H    12.296647    11.265589    13.958929 f=Z
C    10.924368     9.553377    18.192012 f=t
C    10.128037    10.543560    17.768890 f=t
H    10.525372    11.530788    17.554392 f=t
H     9.054213    10.413600    17.672924 f=t
H    10.518402     8.584812    18.471925 f=t
H    11.988135     9.695550    18.360094 f=t
```

A.2 Geometries from the Chapter Thermodynamic properties and electronic structures of Plutonium Oxides in Angstrom

A.2.1 Molecules containing Plutonium

$PuO_2(OH)_2$ coordinates in Å

Label	x	y	z
Pu	0.000000	0.967853	0.000000
O	-0.017474	0.880968	1.740764
O	0.017474	0.880968	-1.740764
O	1.676305	2.238293	0.001209
O	-1.676305	2.238293	-0.001209
H	2.063158	2.697914	0.750904
H	-2.063158	2.697914	-0.750904

PuO_3 coordinates in Å

Label	x	y	z
Pu	0.000000	0.000000	0.000000
O	1.934000	0.000000	0.000000

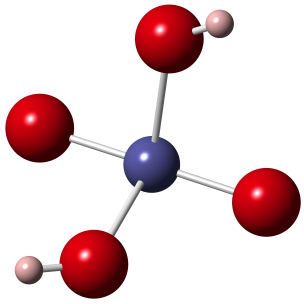

FIGURE A.3: $PuO_2(OH)_2$ molecule.Blue: Pu; red: O: pink; H.

O	-0.118952	0.000000	1.762992
O	-0.118952	0.000000	-1.762992

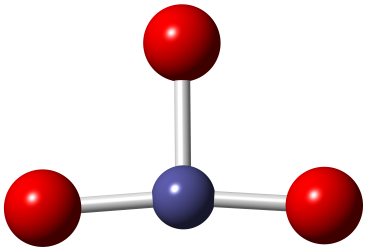

FIGURE A.4: PuO_3 molecule. Blue: Pu; red: O.

PuO_2 coordinates in Å

Label	x	y	z
Pu	0.000000	0.000000	0.000000
O	0.000000	0.000000	1.808000
O	0.000000	0.000000	-1.808000

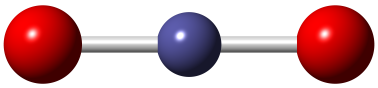

FIGURE A.5: PuO_2 molecule. Blue: Pu; red: O.

A.2.2 Organic Molecules

H_2O_2 coordinates in Å

Label	x	y	z
O	-0.275341	-0.185870	0.687291
O	-0.213172	0.301727	-0.678278
H	0.365257	0.397493	1.116183
H	0.173256	-0.463349	-1.125197

H_2O coordinates in Å

Label	x	y	z
O	0.000000	0.000000	0.000000
H	0.521742	0.000000	0.823124
H	0.521742	0.000000	-0.823124

O_2 coordinates in Å

Label	x	y	z
O	0.000000	0.000000	0.603760
O	0.000000	0.000000	-0.603760

OH coordinates in Å

Label	x	y	z
O	0.000000	0.000000	0.975370
H	0.000000	0.000000	0.000000

H_2 coordinates in Å

Label	x	y	z
H	0.000000	0.000000	0.372000
H	0.000000	0.000000	-0.372000

Appendix B

Electronic levels of Plutonium and Plutonium oxydes

TABLE B.1: Electronic levels (cm-1) of the plutonium atom and analysis of the various states obtained with the ano-cc-TZVP.

J-value	E (cm-1)	Character
0	0	54% ^7F , 38% ^5D , 7% ^3P
1	1806	64% ^7F , 32% ^5D
2	4208	82% ^7F , 17% ^5D
3	6353	88% ^7F , 10% ^5D
4	8091	93% ^7F
5	9552	90% ^7F
6	11010	85% ^7F , 10% ^5G
0	12499	44% ^7F , 21% ^5D , 8% ^3P
1	13612	66% ^9H , 9% ^7F , 7% ^7G
2	14399	82% ^9H , 14% ^7G
1	14845	38% ^5D, 20% ^7F , 9% ^9G
3	15551	89% ^9H , 8% ^7G
4	17026	86% ^9H , 6% ^7G
1	17032	66% ^9D , 29% ^7P

TABLE B.2: Energy electronic states (E < 16 000 cm^{-1}) of $PuO_2(OH)_2$ at SF-CASPT2 and SO-CASPT2 levels obtained with the ano-cc-TZVP.

	Term Symbol	Character : % [orbital(number of electron)]	E (cm^{-1})
SF	$^3B(1)$	49% 2a/Φ_u(1), 1b/δ_u(1)	0
		48% 1a/δ_u(1), 2b/Φ_u(1)	
	$^3A(1)$	41% 1a/δ_u(1) , 2a/Φ_u(1)	889
		59% 1b/δ_u(1) , 2b/Φ_u(1)	
	$^3B(2)$	75% 1a/δ_u(1), 1b/δ_u(1)	2136
		20% 2a/Φ_u(1), 2b/Φ_u(1)	
	$^3A(2)$	59% 1a/δ_u(1) , 2a/Φ_u(1)	4698
		41% 1b/δ_u(1) , 2b/Φ_u(1)	
	$^3B(3)$	52% 2a/Φ_u(1), 1b/δ_u(1)	5351
		46% 1a/δ_u(1), 2b/Φ_u(1)	
	$^1A(1)$	58% 1b/δ_u(1) , 2b/$\Phi_u(\bar{1})$	5764
		30% 1a/δ_u(1) , 2a/$\Phi_u(\bar{1})$	
		5% 2a/Φ_u(2)	
	$^1B(1)$	50% 1a/δ_u(1), 1b/$\delta_u(\bar{1})$	7444
		28% 2a/Φ_u(1), 2b/$\Phi_u(\bar{1})$	
		16% 1a/δ_u(1), 2b/$\Phi_u(\bar{1})$	
	$^1A(2)$	39% 1a/δ_u(1) , 2a/$\Phi_u(\bar{1})$	9626
		29 % 2a/Φ_u(2)	
		13% 1b/δ_u(1) , 2b/$\Phi_u(\bar{1})$	
		10% 1a/δ_u(2)	
		7 % 2a/Φ_u(2)	
	$^1A(3)$	44% 1b/δ_u(2)	10184
		33% 2a/Φ_u(2)	
		12% 2b/Φ_u(2)	
		9% 1a/δ_u(2)	
	$^1B(2)$	66% 2a/Φ_u(1), 2b/$\Phi_u(\bar{1})$	10287
		26% 1a/δ_u(1), 2b/$\Phi_u(\bar{1})$	
		8% 1a/δ_u(1), 1b/$\delta_u(\bar{1})$	
SO	X	46.1% $^3A(1)$, 41.4% $^3B(1)$, 6.4% $^3B(2)$	0
	a	45.3% $^3B(1)$, 44.8% $^3A(1)$, 6.3% $^3B(2)$	323
	b	34.9% $^3B(2)$, 24.7% $^3B(1)$, 14.4% $^1A(1)$, 12.5% $^3A(2)$, 10.1% $^3B(3)$	2222
	c	40.3% $^3A(2)$, 25.4% $^3B(2)$, 18.8% $^1B(1)$, 7.1% $^3B(1)$, 6.1% $^3A(1)$	3757
	d	35.5% $^3B(3)$, 34.3% $^3B(2)$, 14.3% $^1A(2)$, 11.1% $^3B(1)$,	4158
	e	63.5% $^3B(1)$, 30.1% $^3B(2)$	7268
	f	92.8% $^3A(1)$	7575
	g	32.4% $^1A(1)$, 28.1% $^3B(3)$, 27.8% $^3A(2)$, 6.3% $^3B(2)$,	10041
	h	41.1% $^3A(2)$, 24.1% $^3B(3)$, 15.3% $^3B(2)$, 10.5% $^3B(1)$, 6.1% $^1B(1)$	10142
	i	33.5% $^3A(2)$, 26.3% $^3B(2)$, 13.8% $^3B(3)$, 13.1% $^1B(1)$, 8.2% $^3B(1)$	10343
	j	29.3% $^3B(2)$, 25.6% $^3B(3)$, 22.0% $^3B(1)$, 16.6% $^1A(2)$	11089
	k	26.3% $^3B(3)$, 22.9% $^3A(1)$, 17.0% $^3B(1)$, 16.6% $^3A(2)$, 13.0% $^3B(2)$	12269
	l	26.1% $^3A(2)$, 23.6% $^3A(1)$, 21.3% $^3B(3)$, 15.4% $^3B(2)$, 9.6% $^3B(1)$	12311
	m	27.5% $^3B(3)$, 24.6% $^3A(2)$, 22.2% $^3A(1)$, 12.1% $^3B(1)$, 9.7% $^3B(2)$	13782
	n	34.8% $^3B(3)$, 21.8% $^3A(2)$, 17.7% $^3A(1)$, 13.0% $^3B(1)$, 8.5% $^3B(2)$	13783
	o	40.9% $^1A(1)$, 19.7% $^1A(3)$, 15.4% $^3B(2)$, 7.3% $^3B(4)$,	15696

TABLE B.3: Vertical transitions in cm^{-1} of the low-energy ($E < 16\,000\,cm^{-1}$) electronic states of PuO_3 at SF-CASPT2 and SO-CASPT2 levels obtained with the ANO-RCC-TZVP. Orbitals $1a_1$, $2a_1/\pi_u$, $3a_1$ always doubly occupied and do not appear in the following table.

	Term Symbol	Character : % [orbital(number of electron)]	E (cm^{-1})
SF	$^3B_2(1)$	36% [$4a_1/p^{(O)}(2)$, $1b_1/\Phi_u(1)$, $1b_2/p^{(O)}(\bar{1})$, $2b_2/\sigma_u(2)$, $3b_2/\delta_u(1)$, $1a_2/\delta_u(1)$]	0
		21% [$4a_1/p^{(O)}(2)$, $1b_1/\Phi_u(1)$, $1b_2/p^{(O)}(1)$, $2b_2/\sigma_u(2)$, $3b_2/\delta_u(\bar{1})$, $1a_2/\delta_u(1)$]	
		22% [$4a_1/p^{(O)}(2)$,$1b_1/\Phi_u(1)$,$1b_2/p^{(O)}(2)$,$2b_2/\sigma_u(2)$,$1a_2/\delta_u(1)$]	
	$^3A_2(1)$	43% [$4a_1/p^{(O)}(2)$, $5a_1/\Phi_u(1)$,$1b_2/p^{(O)}(\bar{1})$,$2b_2/\sigma_u(2)$,$3b_2/\delta_u(1)$,$1a_2/\delta_u(1)$]	3161
		23% [$4a_1/p^{(O)}(2)$, $5a_1/\Phi_u(1)$,$1b_2/p^{(O)}(1)$,$2b_2/\sigma_u(2)$,$3b_2/\delta_u(\bar{1})$,$1a_2/\delta_u(1)$]	
		17% [$4a_1/p^{(O)}(2)$, $5a_1/\Phi_u(1)$,$1b_2/p^{(O)}(2)$,$2b_2/\sigma_u(2)$,$1a_2/\delta_u(1)$]	
	$^3B_1(1)$	38% [$4a_1/p^{(O)}(2)$,$5a_1/\Phi_u(1)$,$1b_1/\Phi_u(1)$,$1b_2/p^{(O)}(\bar{1})$,$2b_2/\sigma_u(2)$,$3b_2/\delta_u(1)$]	4663
		12% [$4a_1/p^{(O)}(2)$, $5a_1/\Phi_u(1)$, $2b_1/\pi_u(1)$,$1b_2/p^{(O)}(\bar{1})$,$2b_2/\sigma_u(2)$,$3b_2/\delta_u(1)$]	
		12% [$4a_1/p^{(O)}(2)$, $5a_1/\Phi_u(1)$,$1b_1/\Phi_u(1)$,$2b_1/\pi_u(2)$,$1b_2/p^{(O)}(2)$]	
	$^1A_1(1)$	32% [$4a_1/p^{(O)}(2)$,$1b_2/p^{(O)}(1)$,$2b_2/\sigma_u(2)$,$3b_2/\delta_u(\bar{1})$,$1a_2/\delta_u(2)$]	7239
		28% [$4a_1/p^{(O)}(2)$,$1b_2/p^{(O)}(2)$,$2b_2/\sigma_u(2)$,$1a_2/\delta_u(2)$]	
		11% [$4a_1/p^{(O)}(1)$, $5a_1/\Phi_u(\bar{1})$,$1b_2/p^{(O)}(2)$,$2b_2/\sigma_u(2)$,$1a_2/\delta_u(2)$]	
	$^3A_2(2)$	20% [$4a_1/p^{(O)}(2)$,$1b_1/\Phi_u(1)$,$1b_2/p^{(O)}(1)$,$2b_2/\sigma_u(2)$,$3b_2/\delta_u(2)$]	7287
		18% [$4a_1/p^{(O)}(1)$,$5a_1/\Phi_u(\bar{1})$,$1b_1/\Phi_u(1)$,$1b_2/p^{(O)}(2)$,$2b_2/\sigma_u(2)$,$3b_2/\delta_u(1)$]	
		17% [$4a_1/p^{(O)}(2)$,$1b_1/\Phi_u(1)$,$1b_2/p^{(O)}(2)$,$2b_2/\sigma_u(2)$,$3b_2/\delta_u(1)$]	
	$^3B_1(2)$	31% [$4a_1/p^{(O)}(1)$,$5a_1/\Phi_u(\bar{1})$,$1b_2/p^{(O)}(2)$,$2b_2/\sigma_u(2)$,$3b_2/\delta_u(1)$,$1a_2/\delta_u(1)$]	8038
		11% [$4a_1/p^{(O)}(2)$,$5a_1/\Phi_u(1)$,$2b_1/\pi_u(1)$,$1b_2/p^{(O)}(\bar{1})$,$2b_2/\sigma_u(2)$,$3b_2/\delta_u(1)$]	
		10% [$4a_1/p^{(O)}(2)$,$1b_2/p^{(O)}(2)$,$2b_2/\sigma_u(2)$,$3b_2/\delta_u(1)$,$1a_2/\delta_u(1)$]	
		10% [$4a_1/p^{(O)}(2)$,$1b_1/\Phi_u(1)$,$2b_1/\pi_u(1)$,$1b_2/p^{(O)}(\bar{1})$,$2b_2/\sigma_u(2)$,$1a_2/\delta_u(1)$]	
	$^5B_2(1)$	47% [$4a_1/p^{(O)}(2)$, $1b_1/\Phi_u(\bar{1})(1)$, $1b_2/p^{(O)}(2)$, $2b_2/\sigma_u(1)$, $3b_2/\delta_u(1)$, $1a_2/\delta_u(1)$]	8962

Table B.3 – *Continued from previous page*

Term Symbol	Character : % [orbital(number of electron)]	E (cm^{-1})
	41% [$4a_1/p^{(O)}(2)$, $5a_1/\Phi_u(1)$, $1b_1/\Phi_u(\overline{1})(1)$, $1b_2/p^{(O)}(1)$, $2b_2/\sigma_u(2)$, $1a_2/\delta_u(1)$]	
$^3A_1(1)$	39% [$4a_1/p^{(O)}(2)$, $1b_1/\Phi_u(\overline{1})(1)$, $2b_1/\pi_u(1)$, $1b_2/p^{(O)}(\overline{1})$, $2b_2/\sigma_u(2)$, $3b_2/\delta_u(1)$]	9645
	11% [4(2), $1b_1/\Phi_u(\overline{1})(1)$, 8(1), $1b_2/p^{(O)}(\overline{1})$, $2b_2/\sigma_u(2)$, $3b_2/\delta_u(1)$]	
$^3B_2(2)$	15% [$4a_1/p^{(O)}(2)$, $2b_1/\pi_u(1)$, $1b_2/p^{(O)}(2)$, $2b_2/\sigma_u(2)$, $1a_2/\delta_u(1)$]]	9731
	15% [$4a_1/p^{(O)}(1)$, $5a_1/\Phi_u(\overline{1})$, $2b_1/\pi_u(1)$, $1b_2/p^{(O)}(2)$, $2b_2/\sigma_u(2)$, $1a_2/\delta_u(1)$]	
	12% [$4a_1/p^{(O)}(2)$, $2b_1/\pi_u(1)$, $1b_2/p^{(O)}(\overline{1})$, $2b_2/\sigma_u(2)$, $3b_2/\delta_u(1)$, $1a_2/\delta_u(1)$]	
$^1A_2(1)$	26% [$4a_1/p^{(O)}(2)$, $5a_1/\Phi_u(1)$, $1b_2/p^{(O)}(1)$, $2b_2/\sigma_u(2)$, $11(\overline{1})$, $1a_2/\delta_u(\overline{1})$]	10293
	24% [$4a_1/p^{(O)}(2)$, $5a_1/\Phi_u(1)$, $1b_2/p^{(O)}(\overline{1})$, $2b_2/\sigma_u(2)$, $3b_2/\delta_u(1)$, $1a_2/\delta_u(\overline{1})$]	
	18% [$4a_1/p^{(O)}(2)$, $1b_1/\Phi_u(1)$, $1b_2/p^{(O)}(\overline{1})$, $2b_2/\sigma_u(2)$, $1a_2/\delta_u(2)$]	
	16% [$4a_1/p^{(O)}(2)$, $5a_1/\Phi_u(1)$, $1b_2/p^{(O)}(2)$, $2b_2/\sigma_u(2)$, $1a_2/\delta_u(\overline{1})$]	
$^1B_2(1)$	30% [$4a_1/p^{(O)}(2)$, $1b_1/\Phi_u(1)$, $1b_2/p^{(O)}(\overline{1})$, $2b_2/\sigma_u(2)$, $3b_2/\delta_u(1)$, $1a_2/\delta_u(\overline{1})$]	10604
	22% [$4a_1/p^{(O)}(2)$, $1b_1/\Phi_u(1)$, $1b_2/p^{(O)}(1)$, $2b_2/\sigma_u(2)$, $3b_2/\delta_u(\overline{1})$, $1a_2/\delta_u(\overline{1})$]	
	16% [$4a_1/p^{(O)}(2)$, $1b_1/\Phi_u(1)$, $1b_2/p^{(O)}(2)$, $2b_2/\sigma_u(2)$, $1a_2/\delta_u(\overline{1})$]	
	15% [$4a_1/p^{(O)}(2)$, $5a_1/\Phi_u(1)$, $1b_2/p^{(O)}(\overline{1})$, $2b_2/\sigma_u(2)$, $1a_2/\delta_u(2)$]	
$^5A_1(1)$	27% [$4a_1/p^{(O)}(2)$, $5a_1/\Phi_u(1)$, $1b_1/\Phi_u(1)$, $1b_2/p^{(O)}(2)$, $2b_2/\sigma_u(1)$, $1a_2/\delta_u(1)$]	10662
	15% [$4a_1/p^{(O)}(2)$, $2b_1/\pi_u^*(1)$, $1b_1/\Phi_u(1)$, $1b_2/p^{(O)}(2)$, $2b_2/\sigma_u(1)$, $1a_2/\delta_u(1)$]	
	12% [$4a_1/p^{(O)}(2)$, $5a_1/\Phi_u(1)$, $1b_1/\Phi_u(1)$, $1b_2/p^{(O)}(1)$, $2b_2/\sigma_u(2)$, $1a_2/\delta_u(1)$]	
$^3B_1(3)$	26% [$4a_1/p^{(O)}(2)$, $1b_1/\Phi_u(1)$, $2b_1/\pi_u(1)$, $1b_2/p^{(O)}(\overline{1})$, $2b_2/\sigma_u(2)$, $1a_2/\delta_u(1)$]	11567
	17% [$4a_1/p^{(O)}(1)$, $5a_1/\Phi_u(\overline{1})$, $1b_2/p^{(O)}(2)$, $2b_2/\sigma_u(2)$, $3b_2/\delta_u(1)$, $1a_2/\delta_u(1)$]	
$^1B_1(1)$	34% [$4a_1/p^{(O)}(2)$, $1b_2/p^{(O)}(1)$, $2b_2/\sigma_u(2)$, $3b_2/\delta_u(2)$, $1a_2/\delta_u(\overline{1})$]	11632
	18% [$4a_1/p^{(O)}(1)$, $5a_1/\Phi_u(\overline{1})$, $1b_2/p^{(O)}(2)$, $2b_2/\sigma_u(2)$, $3b_2/\delta_u(1)$, $1a_2/\delta_u(\overline{1})$]	
	17% [$4a_1/p^{(O)}(2)$, $1b_2/p^{(O)}(2)$, $2b_2/\sigma_u(2)$, $3b_2/\delta_u(1)$, $1a_2/\delta_u(\overline{1})$]	
$^5B_1(1)$	36% [$4a_1/p^{(O)}(2)$, $1b_1/\Phi_u(1)$, $2b_1/\pi_u(1)$, $1b_2/p^{(O)}(2)$, $2b_2/\sigma_u(1)$, $1a_2/\delta_u(1)$]	12017

Table B.3 – *Continued from previous page*

Term Symbol	Character : % [orbital(number of electron)]	E (cm^{-1})
	15% [$4a_1/p^{(O)}(2)$, $1b_1/\Phi_u(1)$, $2b_1/\pi_u(1)$, $1b_2/p^{(O)}(1)$, $2b_2/\sigma_u(2)$, $1a_2/\delta_u(1)$]	
$^5A_2(1)$	36% [$4a_1/p^{(O)}(2)$, $1b_1/\Phi_u(1)$, $2b_1/\pi_u(1)$, $1b_2/p^{(O)}(2)$, $2b_2/\sigma_u(1)$, $1a_2/\delta_u(1)$]	12017
	15% [$4a_1/p^{(O)}(2)$, $1b_1/\Phi_u(1)$, $2b_1/\pi_u(1)$, $1b_2/p^{(O)}(1)$, $2b_2/\sigma_u(2)$, $1a_2/\delta_u(1)$]	
$^3B_2(3)$	24% [$4a_1/p^{(O)}(2)$, $1b_1/\Phi_u(1)$, $1b_2/p^{(O)}(1)$, $2b_2/\sigma_u(2)$, $3b_2/\delta_u(1)$, $1a_2/\delta_u(\overline{1})$]	12023
	11% [$4a_1/p^{(O)}(2)$, $5a_1/\Phi_u(1)$, $1b_2/p^{(O)}(1)$, $2b_2/\sigma_u(2)$, $3b_2/\delta_u(2)$]	
$^3A_2(3)$	17% [$4a_1/p^{(O)}(2)$, $1b_1/\Phi_u(1)$, $1b_2/p^{(O)}(1)$, $2b_2/\sigma_u(2)$, $1a_2/\delta_u(2)$]	12940
	15% [$4a_1/p^{(O)}(2)$, $5a_1/\Phi_u(1)$, $1b_2/p^{(O)}(1)$, $2b_2/\sigma_u(2)$, $3b_2/\delta_u(1)$, $1a_2/\delta_u(\overline{1})$]	
$^1A_1(2)$	21% [$4a_1/p^{(O)}(2)$, $5a_1/\Phi_u(2)$, $1b_2/p^{(O)}(1)$, $2b_2/\sigma_u(2)$, $3b_2/\delta_u(\overline{1})$]	13213
	10% [$4a_1/p^{(O)}(1)$, $5a_1/\Phi_u(\overline{1})$, $1b_2/p^{(O)}(2)$, $2b_2/\sigma_u(2)$, $3b_2/\delta_u(2)$]	
	10% [$4a_1/p^{(O)}(2)$, $5a_1/\Phi_u(2)$, $1b_2/p^{(O)}(2)$, $2b_2/\sigma_u(2)$]	
$^3A_1(2)$	44% [$4a_1/p^{(O)}(2)$, $5a_1/\Phi_u(1)$, $1b_1/\Phi_u(1)$, $1b_2/p^{(O)}(\overline{1})$, $2b_2/\sigma_u(2)$, $1a_2/\delta_u(1)$]	13421
	29% [$4a_1/p^{(O)}(2)$, $5a_1/\Phi_u(1)$, $2b_1/\pi_u(1)$, $1b_2/p^{(O)}(\overline{1})$, $2b_2/\sigma_u(2)$, $1a_2/\delta_u(1)$]	
$^3B_1(4)$	29% [$4a_1/p^{(O)}(2)$, $2b_1/\pi_u^*(1)$, $1b_1/\Phi_u(1)$, $1b_2/p^{(O)}(\overline{1})$, $2b_2/\sigma_u(2)$, $3b_2/\delta_u(1)$]	13518
	15% [$4a_1/p^{(O)}(2)$, $5a_1/\Phi_u(1)$, $2b_1/\pi_u(1)$, $1b_2/p^{(O)}(\overline{1})$, $2b_2/\sigma_u(2)$, $3b_2/\delta_u(1)$]	
	13% [$4a_1/p^{(O)}(2)$, $2b_1/\pi_u^*(1)$, $1b_1/\Phi_u(1)$, $1b_2/p^{(O)}(2)$, $2b_2/\sigma_u(2)$]	
	11% [$4a_1/p^{(O)}(2)$, $5a_1/\Phi_u(1)$, $2b_1/\pi_u^*(1)$, $1b_2/p^{(O)}(\overline{1})$, $2b_2/\sigma_u(2)$, $1a_2/\delta_u(1)$]	
$^5A_1(2)$	29% [$4a_1/p^{(O)}(2)$, $1b_1/\Phi_u(1)$, $2b_1/\pi_u(1)$, $1b_2/p^{(O)}(2)$, $2b_2/\sigma_u(1)$, $3b_2/\delta_u(1)$]	13575
	14% [$4a_1/p^{(O)}(2)$, $5a_1/\Phi_u(1)$, $1b_1/\Phi_u(1)$, $1b_2/p^{(O)}(2)$, $2b_2/\sigma_u(1)$, $1a_2/\delta_u(1)$]	
	13% [$4a_1/p^{(O)}(2)$, $1b_1/\Phi_u(1)$, $2b_1/\pi_u(1)$, $1b_2/p^{(O)}(1)$, $2b_2/\sigma_u(2)$, $3b_2/\delta_u(1)$]	
	12% [$4a_1/p^{(O)}(2)$, $5a_1/\Phi_u(1)$, $2b_1/\pi_u(1)$, $1b_2/p^{(O)}(2)$, $2b_2/\sigma_u(1)$, $1a_2/\delta_u(1)$]	
$^5B_1(2)$	30% [$4a_1/p^{(O)}(2)$, $5a_1/\Phi_u(1)$, $1b_1/\Phi_u(1)$, $1b_2/p^{(O)}(2)$, $2b_2/\sigma_u(1)$, $3b_2/\delta_u(1)$]	13970
	20% [$4a_1/p^{(O)}(2)$, $5a_1/\Phi_u(1)$, $1b_1/\Phi_u(1)$, $1b_2/p^{(O)}(1)$, $2b_2/\sigma_u(2)$, $3b_2/\delta_u(1)$]	
	16% [$4a_1/p^{(O)}(2)$, $5a_1/\Phi_u(1)$, $2b_1/\pi_u(1)$, $1b_2/p^{(O)}(2)$, $2b_2/\sigma_u(1)$, $3b_2/\delta_u(1)$]	

Table B.3 – *Continued from previous page*

Term Symbol	Character : % [orbital(number of electron)]	E (cm^{-1})
	10 % [$4a_1/p^{(O)}(2)$, $5a_1/\Phi_u(1)$, $2b_1/\pi_u(1)$, $1b_2/p^{(O)}(1)$, $2b_2/\sigma_u(2)$, $3b_2/\delta_u(1)$]	
$^5A_2(2)$	30% [$4a_1/p^{(O)}(2)$, $5a_1/\Phi_u(1)$, $1b_1/\Phi_u(1)$, $1b_2/p^{(O)}(2)$, $2b_2/\sigma_u(1)$, $3b_2/\delta_u(1)$]	13971
	20% [$4a_1/p^{(O)}(2)$, $5a_1/\Phi_u(1)$, $1b_1/\Phi_u(1)$, $1b_2/p^{(O)}(1)$, $2b_2/\sigma_u(2)$, $3b_2/\delta_u(1)$]	
	16% [$4a_1/p^{(O)}(2)$, $5a_1/\Phi_u(1)$, $2b_1/\pi_u(1)$, $1b_2/p^{(O)}(2)$, $2b_2/\sigma_u(1)$, $3b_2/\delta_u(1)$]	
	10% [$4a_1/p^{(O)}(2)$, $5a_1/\Phi_u(1)$, $2b_1/\pi_u(1)$, $1b_2/p^{(O)}(1)$, $2b_2/\sigma_u(2)$, $3b_2/\delta_u(1)$]	
$^5B_1(3)$	86% [$4a_1/p^{(O)}(1)$, $5a_1/\Phi_u(1)$, $1b_2/p^{(O)}(2)$, $2b_2/\sigma_u(2)$, $3b_2/\delta_u(1)$, $1a_2/\delta_u(1)$]	14055
$^5A_2(3)$	86% [$4a_1/p^{(O)}(1)$, $5a_1/\Phi_u(1)$, $1b_2/p^{(O)}(2)$, $2b_2/\sigma_u(2)$, $3b_2/\delta_u(1)$, $1a_2/\delta_u(1)$]	14056
$^5A_1(3)$	80% [$4a_1/p^{(O)}(1)$, $1b_1/\Phi_u(1)$, $1b_2/p^{(O)}(2)$, $2b_2/\sigma_u(2)$, $3b_2/\delta_u(1)$, $1a_2/\delta_u(1)$]	14139
$^3A_1(3)$	58% [$4a_1/p^{(O)}(1)$, $1b_1/\Phi_u(\bar{1})$, $1b_2/p^{(O)}(2)$, $2b_2/\sigma_u(2)$, $3b_2/\delta_u(1)$, $1a_2/\delta_u(1)$]	14236
	20% [$4a_1/p^{(O)}(1)$, $1b_1/\Phi_u(1)$, $1b_2/p^{(O)}(2)$, $2b_2/\sigma_u(2)$, $3b_2/\delta_u(\bar{1})$, $1a_2/\delta_u(1)$]	
	10% [$4a_1/p^{(O)}(1)$, $1b_1/\Phi_u(1)$, $1b_2/p^{(O)}(2)$, $2b_2/\sigma_u(2)$, $3b_2/\delta_u(1)$, $1a_2/\delta_u(\bar{1})$]	
$^3B_2(4)$	19% [$4a_1/p^{(O)}(1)$, $5a_1/\Phi_u(\bar{1})$, $1b_1/\Phi_u(1)$, $1b_2/p^{(O)}(2)$, $2b_2/\sigma_u(2)$, $1a_2/\delta_u(1)$]	14843
	18% [$4a_1/p^{(O)}(2)$, $5a_1/\Phi_u(1)$, $1b_2/p^{(O)}(1)$, $2b_2/\sigma_u(2)$, $3b_2/\delta_u(2)$]	
$^1A_1(3)$	27% [$4a_1/p^{(O)}(2)$, $1b_1/\Phi_u(2)$, $1b_2/p^{(O)}(1)$, $2b_2/\sigma_u(2)$, $3b_2/\delta_u(\bar{1})$]	14889
	13% [$4a_1/p^{(O)}(2)$, $1b_1/\Phi_u(2)$, $1b_2/p^{(O)}(2)$, $2b_2/\sigma_u(2)$]	
$^1A_2(2)$	47% [$4a_1/p^{(O)}(2)$, $1b_1/\Phi_u(1)$, $1b_2/p^{(O)}(\bar{1})$, $2b_2/\sigma_u(2)$, $3b_2/\delta_u(2)$]	14984
	10% [$4a_1/p^{(O)}(2)$, $5a_1/\Phi_u(1)$, $1b_2/p^{(O)}(\bar{1})$, $2b_2/\sigma_u(2)$, $3b_2/\delta_u(1)$, $1a_2/\delta_u(\bar{1})$]	
	9% [$4a_1/p^{(O)}(2)$, $5a_1/\Phi_u(1)$, $1b_2/p^{(O)}(1)$, $2b_2/\sigma_u(2)$, $3b_2/\delta_u(\bar{1})$, $1a_2/\delta_u(\bar{1})$]	
$^5B_2(2)$	64% [$4a_1/p^{(O)}(1)$, $5a_1/\Phi_u(1)$, $1b_1/\Phi_u(1)$, $1b_2/p^{(O)}(2)$, $2b_2/\sigma_u(2)$, $1a_2/\delta_u(1)$]	15035
	10% [$4a_1/p^{(O)}(1)$, 6(1), $1b_1/\Phi_u(1)$, $1b_2/p^{(O)}(2)$, $2b_2/\sigma_u(2)$, $1a_2/\delta_u(1)$]	
$^1B_1(2)$	33% [$4a_1/p^{(O)}(2)$, $5a_1/\Phi_u(1)$,$1b_1/\Phi_u(\bar{1})$, $1b_2/p^{(O)}(1)$, $2b_2/\sigma_u(2)$, $3b_2/\delta_u(\bar{1})$]	15593
	13% [$4a_1/p^{(O)}(2)$, $5a_1/\Phi_u(1)$,$1b_1/\Phi_u(\bar{1})$, $1b_2/p^{(O)}(2)$, $2b_2/\sigma_u(2)$,]	
	12% [$4a_1/p^{(O)}(2)$, $1b_2/p^{(O)}(1)$, $2b_2/\sigma_u(2)$, $3b_2/\delta_u(2)$, $1a_2/\delta_u(\bar{1})$]	

Table B.3 – *Continued from previous page*

	Term Symbol	Character : % [orbital(number of electron)]	E (cm^{-1})
		11% [$4a_1/p^{(O)}(2)$, $5a_1/\Phi_u(2)$, $1b_2/p^{(O)}(1)$, $2b_2/\sigma_u(2)$, $1a_2/\delta_u(\overline{1})$]	
SO	X	47.15% $^3B_2(1)$, 24.15% $^3A_2(1)$, 14.14% $^3B_1(1)$	0
	a	58.72% $^3B_2(1)$, 24.89% $^3A_2(1)$	1235
	b	73.37% $^3B_2(1)$	1783
	c	51.22% $^3A_2(1)$	3777
	d	23.54% $^3B_1(1)$, 18.35% $^1A_1(1)$, 16.73% $^3A_2(2)$, 10.23% $^3B_1(2)$	5660
	e	49.43% $^3B_1(1)$, 22.12% $^3A_1(1)$	6658
	f	43.87% $^3B_1(1)$, 19.21% $^3A_1(1)$, 11.3% $^3B_1(2)$	7062
	g	23.47% $^3B_2(1)$, 17.68% $^3A_2(1)$, 17.17% $^3B_1(2)$	7929
	h	26.14% $^3A_2(1)$, 21.08% $^5B_2(1)$, 18.73% $^3A_2(2)$	7973
	i	32.2% $^3A_2(2)$, 24.4% $^3A_2(1)$, 15% $^5B_2(1)$	8675
	j	28.2% $^3A_2(1)$, 22.38% $^3B_1(1)$, 11.46% $^5B_2(1)$	9096
	k	28.45% $^3A_2(1)$, 26.41% $^3B_2(1)$	9345
	l	30.77% $^3B_1(2)$, 19% $^3B_1(1)$	9399
	m	16.69% $^3B_2(1)$, 14.81% $^5B_2(1)$	9690
	n	28.51% $^3B_1(2)$, 11.78% $^3A_1(2)$, 10.3% $^3B_1(1)$	9879
	o	24.08% $^3A_2(2)$, 15.86% $^5B_1(1)$, 13.35% $^3B_2(2)$	10224
	p	25.31% $^3A_2(2)$, 14.83% $^3B_2(2)$, 9.57% $^5B_1(1)$	10235
	q	23.29% $^5B_2(1)$, 13.35% $^5B_1(3)$	10342
	r	29.37% $^5B_1(1)$, 24.74% $^5A_1(1)$, 10.19% $^5B_2(1)$, 10.05% $^5A_1(2)$	10686
	s	23.12% $^3B_2(2)$, 20.68% $^3B_1(3)$, 15.13% $^3B_1(2)$	10749

Table B.3 – *Continued from previous page*

Term Symbol	Character : % [orbital(number of electron)]	E (cm^{-1})
t	25.96% $^5B_1(1)$, 20.75% $^5A_1(1)$, 15.44% $^5B_2(1)$	10768
u	23.74% $^5B_2(1)$, 11.62% $^3B_1(3)$, 10.37% $^5A_1(1)$	11022
v	24.63% $^5B_2(1)$, 21.07% $^5A_1(1)$, 12.44% $^3B_1(1)$	11207
w	14.48% $^3A_1(1)$, 10.17% $^3A_1(2)$	11616
x	36.43% $^5A_1(1)$, 12.09% $^3B_1(2)$	12429
y	20.5% $^3A_2(2)$	12567
z	11.52% $^1A_1(1)$, 10.25% $^3B_1(3)$, 10.04% $^3B_2(3)$	12693
aa	14.11% $^1A_2(1)$	12794
ab	29.09% $^3B_2(2)$, 24.21% $^3A_2(3)$	12873
ac	16.43% $^3A_1(3)$, 15.09% $^5B_1(2)$, 14.7% $^3A_1(1)$, 10.89% $^5B_1(1)$	13058
ad	30.37% $^3A_2(3)$, 13.89% $^1A_1(1)$,	13309
ae	20.38% $^5B_1(2)$, 13.23% $^5A_1(3)$, 9.98% $^5B_2(2)$	13341
af	34.08% $^3B_2(3)$, 16.97% $^1A_2(1)$, 11.74% $^1A_2(2)$	13488
ag	24.73% $^3A_1(1)$, 12.48% $^5B_1(2)$, 11.36% $^5B_1(1)$	13582
ah	18.48% $^5B_1(2)$, 15.12% $^5A_1(3)$	13814
ai	27.31% $^5B_2(1)$, 14.88% $^1B_2(1)$, 12.3% $^3A_1(1)$	13936
aj	28.12% $^5B_2(1)$, 19.38% $^5A_1(1)$, 10% $^5B_1(2)$	13996
ak	17.59% $^5B_1(2)$, 14.15% $^5B_1(3)$, 11.94% $^5A_1(2)$, 11.41% $^5A_1(1)$	14024
al	53.19% $^1B_1(1)$, 12.49% $^3A_2(3)$	14216
am	22.79% $^5A_1(2)$, 12.86% $^5B_1(3)$, 10.57% $^3B_1(3)$	14257
an	31.62% $^5B_2(1)$, 10.41% $^3A_1(2)$	14680
ao	19.07% $^5B_1(1)$, 17.32% $^5B_1(2)$, 16.76% $^5A_1(3)$	14724
ap	21.09% $^5A_1(1)$, 10.26% $^5A_1(2)$, 10% $^5B_1(3)$	14750

Table B.3 – *Continued from previous page*

Term Symbol	Character : % [orbital(number of electron)]	E (cm^{-1})
aq	16.59% $^5B_1(3)$, 13.06% $^5B_1(2)$, 9.69% $^5A_1(2)$	14874
ar	16.33% $^5B_1(1)$	15129
as	20.39% $^5A_1(2)$, 20.07% $^5B_1(1)$, 12.66% $^5B_1(3)$, 10.85% $^3B_1(3)$, 9.82% $^5A_1(1)$	15141
at	28.7% $^3B_2(2)$, 12.63% $^5B_2(1)$	15375
au	15.53% $^3A_1(2)$, 12.26% $^5B_1(3)$, 10.67% $^5B_1(1)$, 9.55% $^3B_2(2)$	15439
av	25.7% $^3B_2(3)$, 10.77% $^3B_2(2)$, 10.04% $^5A_1(2)$	15494
aw	23.7% $^5B_1(3)$, 12.34% $^3A_1(2)$, 11.09% $^3B_1(3)$	15616
ay	12.56% $^5A_1(3)$, 11.67% $^3B_1(2)$, 10.58% $^3A_1(3)$, 10.25% $^3A_2(3)$	15708
az	15.14% $^5B_1(3)$, 10.79% $^3B_1(3)$	15906
ba	18.56% $^3B_2(3)$, 16.95% $^5B_1(3)$	15948

TABLE B.4: Vertical transitions in cm^{-1} of the low-energy ($E < 16\,000\,cm^{-1}$) electronic states of PuO_3 at SF-CASPT2 and SO-CASPT2 levels obtained with the ANO-RCC-TZVP. Orbitals $1a_1$, $2a_1/\pi_u$, $3a_1$ always doubly occupied and do not appear in the following table.

	Term Symbol	Character : % [orbital(number of electron)]	E (cm^{-1})
SF	$^5A_g(1)$	84% [$1a_u/\delta_u(1)$, $2b_{2u}/\Phi_u(1)$, $2b_{1u}/\delta_u(1)$, $2b_{3u}/\Phi_u(1)$]	0
	$^5A_g(2)$	45% [$1a_u/\delta_u(1)$, $3b_{2u}/\pi_u(1)$, $2b_{1u}/\delta_u(1)$, $2b_{3u}/\Phi_u(1)$]	4798
		45% [$1a_u/\delta_u(1)$, $2b_{2u}/\Phi_u(1)$, $2b_{1u}/\delta_u 3(1)$, $3b_{3u}/\pi_u(1)$]	
	$^5B_{3u}(1)$	85% [$3a_g(1)$, $1a_u/\delta_u(1)$, $2b_{1u}/\delta_u(1)$, $2b_{3u}/\Phi_u(1)$]	5421
	$^5B_{2u?}(1)$	85% [$3a_g(1)$, $1a_u/\delta_u(1)$, $2b_{1u}/\delta_u(1)$, $2b_{3u}/\Phi_u(1)$]	5421
	$^5B_{3g}(1)$	44% [$2b_{2u}/\Phi_u(1)$, $3b_{2u}/\pi_u 1(1)$, $2b_{1u}/\delta_u(1)$, $2b_{3u}/\Phi_u(1)$]	6019
		44% [$1a_u/\delta_u(1)$, $2b_{2u}/\Phi_u(1)$, $2b_{3u}/\Phi_u(1)$, $3b_{3u}/\pi_u(1)$]	
	$^5B_{2g}(1)$	44% [$2b_{2u}/\Phi_u(1)$, $3b_{2u}/\pi_u(1)$, $2b_{1u}/\delta_u(1)$, $2b_{3u}/\Phi_u(1)$]	6019
		44% [$1a_u/\delta_u(1)$, $2b_{2u}/\Phi_u(1)$, $2b_{3u}/\Phi_u(1)$, $3b_{3u}/\pi_u(1)$]	
	$^5A_g(3)$	45% [$1a_u/\delta_u(1)$, $3b_{2u}/\pi_u(1)$, $2b_{1u}/\delta_u(1)$, $2b_{3u}/\Phi_u(1)$]	6067
		45% [$1a_u/\delta_u(1)$, $2b_{2u}/\Phi_u(1)$, $2b_{1u}/\delta_u(1)$, $3b_{3u}/\pi_u(1)$]	
	$^5B_{1g}(1)$	44% [$1a_u/\delta_u(1)$, $2b_{2u}/\Phi_u(1)$, $3b_{2u}/\pi_u(1)$, $2b_{1u}/\delta_u(1)$]	6158
		44% [$1a_u/\delta_u(1)$, $2b_{1u}/\delta_u(1)$, $2b_{3u}/\Phi_u(1)$, $3b_{3u}/\pi_u(1)$]	
	$^3B_{3u}(1)$	59% [$3a_g(1)$,$1a_u/\delta_u(\bar{1})$, $2b_{2u}/\Phi_u(1)$, $2b_{1u}/\delta_u(1)$]	6855
		19% [$3a_g(1)$,$1a_u/\delta_u(1)$, $2b_{2u}/\Phi_u(\bar{1})$, $2b_{1u}/\delta_u(1)$]	
		10% [$3a_g(1)$,$1a_u/\delta_u(1)$, $2b_{2u}/\Phi_u(1)$, $2b_{1u}/\delta_u(\bar{1})$]	
	$^3B_{2u}(1)$	59% [$3a_g(1)$, $1a_u/\delta_u(\bar{1})$, $2b_{1u}/\delta_u(1)$, $2b_{3u}/\Phi_u(1)$]	6855
		20% [$3a_g(1)$, $1a_u/\delta_u(1)$, $2b_{1u}/\delta_u(\bar{1})$, $2b_{3u}/\Phi_u(1)$]	
	$^5B_{1g}(2)$	44% [$1a_u/\delta_u(1)$, $2b_{1u}/\delta_u(1)$, $2b_{3u}/\Phi_u(1)$, $3b_{3u}/\pi_u(1)$]	7293
		44% [$1a_u/\delta_u(1)$, $2b_{2u}/\Phi_u(1)$, $3b_{2u}/\pi_u(1)$, $2b_{1u}/\delta_u(1)$]	

Table B.4 – *Continued from previous page*

Term Symbol	Character : % [orbital(number of electron)]	E (cm^{-1})
$^5A_u(1)$	79% [$3a_g(1)$, $2b_{2u}/\Phi_u(1)$, $2b_{1u}/\delta_u(1)$, $2b_{3u}/\Phi_u(1)$]	7452
$^5B_{1u}(1)$	80% [$3a_g(1)$, $1a_u/\delta_u(1)$, $2b_{2u}/\Phi_u0(1)$, $2b_{3u}/\Phi_u(1)$]	7462
$^5B_{3g}(2)$	37% [$1a_u/\delta_u(1)$, $2b_{2u}/\Phi_u(1)$, $2b_{3u}/\Phi_u(1)$, $3b_{3u}/\pi_u(1)$]	7637
	33%[$2b_{2u}/\Phi_u(1)$, $3b_{2u}/\pi_u(1)$, $2b_{1u}/\delta_u3(1)$, $2b_{3u}/\Phi_u(1)$]	
	12% [$2b_{2u}/\Phi_u(1)$, $3b_{2u}/\pi_u(1)$, $2b_{1u}/\delta_u(1)$, $3b_{3u}/\pi_u(1)$]	
$^5B_{2g}(2)$	37% [$1a_u/\delta_u(1)$, $2b_{2u}/\Phi_u(1)$, $2b_{3u}/\Phi_u6(1)$, $3b_{3u}/\pi_u(1)$]	7637
	33%[$2b_{2u}/\Phi_u(1)$, $3b_{2u}/\pi_u(1)$, $2b_{1u}/\delta_u(1)$, $2b_{3u}/\Phi_u(1)$]	
	12% [$2b_{2u}/\Phi_u(1)$, $3b_{2u}/\pi_u(1)$, $2b_{1u}/\delta_u(1)$, $3b_{3u}/\pi_u(1)$]	
$^3B_{1u}(1)$	51%[$3a_g(1)$, $1a_u/\delta_u(1)$, $2b_{2u}/\Phi_u(\overline{1})$, $2b_{3u}/\Phi_u(1)$]	9586
	68%[$3a_g(1)$, $1a_u/\delta_u(1)$, $2b_{2u}/\Phi_u(\overline{1})$, $2b_{3u}/\Phi_u(1)$]	
$^3A_u(1)$	51% [$3a_g(1)$, $2b_{2u}/\Phi_u(\overline{1})$, $2b_{1u}/\delta_u(1)$, $2b_{3u}/\Phi_u(1)$]	9614
	17% [$3a_g(1)$, $2b_{2u}/\Phi_u(1)$, $2b_{1u}/\delta_u(\overline{1})$, $2b_{3u}/\Phi_u(1)$]	
$^3B_{3g}(1)$	38% [$1a_u/\delta_u(1)$, $2b_{2u}/\Phi_u(1)$, $2b_{1u}/\delta_u(2)$]	10101
	36% [$1a_u/\delta_u(2)$, $2b_{1u}/\delta_u(1)$, $2b_{3u}/\Phi_u(1)$]	
$^3B_{2g}(1)$	38% [$1a_u/\delta_u(1)$, $2b_{2u}/\Phi_u(1)$, $2b_{1u}/\delta_u(2)$]	10101
	36% [$1a_u/\delta_u(2)$, $2b_{1u}/\delta_u(1)$, $2b_{3u}/\Phi_u(1)$]	
$^3B_{1g}(1)$	24% [$1a_u/\delta_u(1)$, $2b_{2u}/\Phi_u(2)$, $2b_{1u}/\delta_u(1)$]	10308
	24% [$1a_u/\delta_u(1)$, $2b_{1u}/\delta_u(1)$, $2b_{3u}/\Phi_u(2)$]	
	19% [$2b_{2u}/\Phi_u(1)$, $2b_{1u}/\delta_u(2)$, $2b_{3u}/\Phi_u(1)$]	
	16% [$1a_u/\delta_u(1)$, $2b_{2u}/\Phi_u(1)$, $2b_{3u}/\Phi_u(1)$]	
$^5A_u(2)$	23% [$3a_g(1)$, $1a_u/\delta_u(1)$, $2b_{2u}/\Phi_u(1)$, $3b_{2u}/\pi_u(1)$]	11344
	23% [$3a_g(1)$, $1a_u/\delta_u(1)$, $2b_{3u}/\Phi_u(1)$, $3b_{3u}/\pi_u(1)$]	
	20% [$3a_g(1)$, $3b_{2u}/\pi_u(1)$, $2b_{1u}/\delta_u(1)$, $2b_{3u}/\Phi_u(1)$]	

Table B.4 – *Continued from previous page*

Term Symbol	Character : % [orbital(number of electron)]	E (cm^{-1})
	20% [$3a_g(1)$, $2b_{2u}/\Phi_u(1)$, $2b_{1u}/\delta_u(1)$, $3b_{3u}/\pi_u(1)$]	
$^5B_{1u}(2)$	23% [$3a_g(1)$, $2b_{1u}/\delta_u(1)$, $2b_{3u}/\Phi_u(1)$, $3b_{3u}/\pi_u(1)$]	11347
	23% [$3a_g(1)$, $2b_{2u}/\Phi_u(1)$, $3b_{2u}/\pi_u(1)$, $2b_{1u}/\delta_u(1)$]	
	19% [$3a_g(1)$, $1a_u/\delta_u(1)$, $2b_{2u}/\Phi_u(1)$, $3b_{3u}/\pi_u(1)$]	
	19% [$3a_g(1)$, $1a_u/\delta_u(1)$, 11(1), $2b_{3u}/\Phi_u(1)$]	
$^3B_{3g}(2)$	35%[$1a_u/\delta_u(2)$, $2b_{1u}/\delta_u(1)$, $2b_{3u}/\Phi_u(1)$]	11467
	33% [$1a_u/\delta_u(1)$, $3b_{2u}/\pi_u(1)$, $2b_{1u}/\delta_u(2)$]	
$^3B_{2g}(2)$	35%[$1a_u/\delta_u(2)$, $2b_{1u}/\delta_u(1)$, $2b_{3u}/\Phi_u(1)$]	11467
	33% [$1a_u/\delta_u(1)$, $3b_{2u}/\pi_u(1)$, $2b_{1u}/\delta_u(2)$]	
$^3B_{1g}(2)$	34% [$1a_u/\delta_u(2)$, $3b_{2u}/\pi_u(1)$, $2b_{3u}/\Phi_u(1)$]	12812
	33% [$3b_{2u}/\pi_u(1)$, $2b_{1u}/\delta_u(2)$, $2b_{3u}/\Phi_u(1)$]	
$^3A_g(1)$	51% [$1a_u/\delta_u(1)$, $2b_{2u}/\Phi_u(1)$, $2b_{1u}/\delta_u(\bar{1})$, $2b_{3u}/\Phi_u(1)$]	12815
	17% [$1a_u/\delta_u(1)$, $2b_{2u}/\Phi_u(\bar{1})$, $2b_{1u}/\delta_u(1)$, $2b_{3u}/\Phi_u(1)$]	
$^3B_{1u}(2)$	20%[$3a_g(1)$, $2b_{2u}/\Phi_u(\bar{1})$, $3b_{2u}/\pi_u(1)$, $2b_{1u}/\delta_u(1)$]	13398
	20%[$3a_g(1)$, $2b_{1u}/\delta_u(\bar{1})$, $2b_{3u}/\Phi_u(1)$, $3b_{3u}/\pi_u(1)$]	
	15%[$3a_g(1)$, $1a_u/\delta_u(\bar{1})$, $3b_{2u}/\pi_u(1)$, $2b_{3u}/\Phi_u(1)$]	
	15%[$3a_g(1)$, $1a_u/\delta_u(\bar{1})$, $2b_{2u}/\Phi_u(1)$, $3b_{3u}/\pi_u(1)$]	
$^3A_u(2)$	15% [$3a_g(1)$, $1a_u/\delta_u(\bar{1})$, $2b_{2u}/\Phi_u(1)$, $3b_{2u}/\pi_u(1)$]	13402
	15% [$3a_g(1)$, $1a_u/\delta_u(\bar{1})$, $2b_{3u}/\Phi_u(1)$, $3b_{3u}/\pi_u(1)$]	
	14% [$3a_g(1)$, $3b_{2u}/\pi_u(\bar{1})$, $2b_{1u}/\delta_u(1)$, $2b_{3u}/\Phi_u(1)$]	
	14% [$3a_g(1)$, $2b_{2u}/\pi_u(\bar{1})$, $2b_{1u}/\delta_u(1)$, $3b_{3u}/\pi_u(1)$]	
$^5B_{3g}(3)$	46% [$2b_{2u}/\Phi_u(1)$, $3b_{2u}/\pi_u(1)$, $2b_{1u}/\delta_u(1)$, $3b_{3u}/\pi_u(1)$]	13460
	45% [$1a_u/\delta_u(1)$, $3b_{2u}/\pi_u(1)$, $2b_{3u}/\Phi_u(1)$, $3b_{3u}/\pi_u(1)$]	

Table B.4 – *Continued from previous page*

Term Symbol	Character : % [orbital(number of electron)]	E (cm^{-1})
$^5B_{2g}(3)$	46% [$2b_{2u}/\Phi_u(1)$, $3b_{2u}/\pi_u(1)$, $2b_{1u}/\delta_u(1)$, $3b_{3u}/\pi_u(1)$]	13460
	45% [$1a_u/\delta_u(1)$, $3b_{2u}/\pi_u(1)$, $2b_{3u}/\Phi_u(1)$, $3b_{3u}/\pi_u(1)$]	
$^3B_{1g}(3)$	34% [$1a_u/\delta_u(1)$, $2b_{1u}/\delta_u(1)$, $2b_{3u}/\Phi_u(2)$]	13638
	34% [$1a_u/\delta_u(1)$, $3b_{2u}/\pi_u(2)$, $2b_{1u}/\delta_u(1)$]	
$^3A_g(2)$	47% [$1a_u/\delta_u(1)$, $2b_{2u}/\Phi_u(1)$, $2b_{1u}/\delta_u(1)$, $2b_{3u}/\Phi_u(\bar{1})$]	13659
	17% [$1a_u/\delta_u(1)$, $2b_{2u}/\Phi_u(\bar{1})$, $2b_{1u}/\delta_u(1)$, $2b_{3u}/\Phi_u(1)$]	
$^5B_{3u}(2)$	45% [$2a_g/\delta_u(1)$, $1a_u/\delta_u(1)$, $2b_{1u}/\delta_u(1)$, $2b_{3u}/\Phi_u6(1)$]	14688
	42% [$1b_{1g}/\delta_u(1)$, $1a_u/\delta_u(1)$, $2b_{2u}/\Phi_u0(1)$, $2b_{1u}/\delta_u(1)$]	
$^5B_{2u}(2)$	45% [$2a_g/\delta_u(1)$, $1a_u/\delta_u(1)$, $2b_{1u}/\delta_u(1)$, $2b_{3u}/\Phi_u(1)$]	14688
	42% [$1b_{1g}/\delta_u(1)$, $1a_u/\delta_u(1)$, $2b_{2u}/\Phi_u(1)$, $2b_{1u}/\delta_u(1)$]	
$^3B_{3u}(2)$	30% [$3a_g(1)$, $1a_u/\delta_u(1)$, $2b_{2u}/\Phi_u(1)$, $2b_{1u}/\delta_u(\bar{1})$]	15060
	22% [$3a_g(1)$, $1a_u/\delta_u(2)$, $2b_{3u}/\Phi_u(1)$]	
	22% [$3a_g(1)$, $2b_{1u}/\delta_u(2)$, $2b_{3u}/\Phi_u(1)$]	
	11% [$3a_g(1)$, $1a_u/\delta_u(\bar{1})$, $2b_{2u}/\Phi_u(1)$, $2b_{1u}/\delta_u(1)$]	
$^3B_{2u}(2)$	34% [$3a_g(1)$, $1a_u/\delta_u(1)$, $2b_{1u}/\delta_u(\bar{1})$, $2b_{3u}/\Phi_u(1)$]	15062
	22% [$3a_g(1)$, $1a_u/\delta_u(2)$, $2b_{2u}/\Phi_u(1)$]	
	22% [$3a_g(1)$, $2b_{2u}/\Phi_u(1)$, $2b_{1u}/\delta_u(3)$]	
	11% [$3a_g(1)$, $1a_u/\delta_u(\bar{1})$, $2b_{1u}/\delta_u(1)$, $2b_{3u}/\Phi_u(1)$]	
$^1B_{3u}(1)$	32% [$3a_g(1)$, $1a_u/\delta_u(1)$, $2b_{1u}/\delta_u(1)$, $2b_{3u}/\Phi_u(1)$]	15336
	21% [$3a_g(1)$, $3b_{2u}/\pi_u(1)$, $2b_{1u}/\delta_u(2)$]	
	21% [$3a_g(1)$, $1a_u/\delta_u(2)$, $3b_{2u}/\pi_u(1)$]	
$^1B_{2u}(1)$	32% [$3a_g(1)$, $1a_u/\delta_u(1)$, $2b_{1u}/\delta_u(1)$, $2b_{3u}/\Phi_u(1)$]	15336
	21% [$3a_g(1)$, $3b_{2u}/\pi_u(1)$, $2b_{1u}/\delta_u(2)$]	

Table B.4 – *Continued from previous page*

	Term Symbol	Character : % [orbital(number of electron)]	E (cm^{-1})
		21% [$3a_g(1)$, $1a_u/\delta_u(2)$, $3b_{2u}/\pi_u(1)$]	
	$^3B_{3u}(3)$	29% [$3a_g(1)$, $1a_u/\delta_u(1)$, $2b_{2u}/\Phi_u(\bar{1})$, $2b_{1u}/\delta_u(1)$]	15370
		24% [$3a_g(1)$, $2b_{1u}/\delta_u(2)$, $2b_{3u}/\Phi_u(1)$]	
		23% [$3a_g(1)$, $1a_u/\delta_u(2)$, $2b_{3u}/\Phi_u(1)$]	
	$^3B_{2u}(3)$	37% [$3a_g(1)$, $1a_u/\delta_u(1)$, $2b_{1u}/\delta_u(1)$, $2b_{3u}/\Phi_u(\bar{1})$]	15382
		24% [$3a_g(1)$, $2b_{2u}/\Phi_u(1)$, $2b_{1u}/\delta_u(3)$]	
		23% [$3a_g(1)$, $1a_u/\delta_u(2)$, $2b_{2u}/\Phi_u(1)$]	
	$^5A_g(4)$	64% [$2b_{2u}/\Phi_u(1)$, $3b_{2u}/\pi_u(1)$, $2b_{3u}/\Phi_u(1)$, $3b_{3u}/\pi_u(1)$]	15800
		20% [$2b_{2u}/\Phi_u(1)$, $3b_{2u}/\pi_u(1)$, $2b_{1u}/\delta_u(1)$, $2b_{3u}/\Phi_u(1)$]	
		23% [$1a_u/\delta_u(1)$, $3b_{2u}/\pi_u(1)$, $2b_{1u}/\delta_u(1)$, $3b_{3u}/\pi_u(1)$]	
		14% [$2b_{2u}/\Phi_u(2)$, $2b_{1u}/\delta_u(1)$, $3b_{3u}/\pi_u(1)$]	
		10% [$2b_{1u}/\delta_u(1)$, $2b_{3u}/\Phi_u(2)$, $3b_{3u}/\pi_u(1)$]	
	$^1B_{3u}(2)$	41% [$3a_g(1)$, $1a_u/\delta_u(1)$, 13(1), $2b_{3u}/\Phi_u(1)$]	15850
		23% [$3a_g(1)$, $2b_{2u}/\Phi_u(1)$, $2b_{1u}/\delta_u(2)$]	
		23% [$3a_g(1)$, $1a_u/\delta_u(2)$, $2b_{2u}/\Phi_u(1)$]	
	$^1B_{2u}(2)$	41% [$3a_g(1)$, $1a_u/\delta_u(1)$, $2b_{1u}/\delta_u(1)$, $2b_{3u}/\Phi_u(1)$]	15850
		23% [$3a_g(1)$, $2b_{2u}/\Phi_u(1)$, $2b_{1u}/\delta_u(2)$]	
		23% [$3a_g(1)$, $1a_u/\delta_u(2)$, $2b_{2u}/\Phi_u(1)$]	
SO	0_g^-	48% $^5A_g(1)$, 22.45% $^3B_{1g}(1)$	0
	1_g	67% $^5A_g(1)$, 14.59% $^3B_{1g}(1)$	2462
	1_u	27% $^5B_{2u}(1)$, 26.81% $^5B_{3u}(1)$, 13.24% $^5A_u(1)$, 12.77% $^5B_{1u}(1)$	5851
	2_g	85.58% $^5A_g(1)$	5904

Table B.4 – *Continued from previous page*

Term Symbol	Character : % [orbital(number of electron)]	E (cm^{-1})
2_u	24.14% $^5A_u(1)$, 21.34% $^5B_{2u}(1)$, 21.31% $^5B_{3u}(1)$	6266
3_u	38.85% $^5B_{3u}(1)$, 24.97% $^3B_{2u}(1)$	7197
a_g	49.54% $^5A_g(2)$, 36.86% $^5B_{1g}(1)$	7240
b_g	31.53% $^5A_g(3)$, 23.96% $^5B_{1g}(2)$, 18.11% $^3B_{3g}(2)$, 18.11% $^3B_{2g}(2)$	7595
c_u	22.24% $^3B_{2u}(1)$, 21.61% $^3B_{3u}(1)$, 12.23% $^3A_u(1)$, 10.77% $^5B_{2u}(1)$, 10.68% $^5B_{3u}(1)$	7911
d_g	47.71% $^5A_g(2)$, 28.33% $^5B_{1g}(1)$, 15.29% $^5B_{2g}(1)$	8738
e_g	32.7% $^5A_g(3)$, 23.46% $^5B_{1g}(2)$, 18.02% $^5A_g(1)$, 12.56% $^3B_{2g}(2)$, 12.56% $^3B_{3g}(2)$	8971
f_g	49.36% $^5B_{2g}(1)$, 49.3% $^5B_{3g}(1)$	9610
g_g	72.76% $^5A_g(2)$	10193
h_g	44.58% $^5A_g(3)$, 22.96% $^5B_{1g}(2)$, 17.34% $^5B_{3g}(2)$	10763
i_g	63.19% $^5B_{1g}(1)$, 10.62% $^5B_{2g}(1)$, 10.62% $^5B_{3g}(1)$	11038
j_u	44.22% $^5A_u(2)$, 43.57% $^5B_{1u}(2)$	11105
k_u	48.86% $^5A_u(1)$, 43.03% $^5B_{1u}(1)$	11239
l_u	29.76% $^5B_{3u}(1)$, 29.64% $^5B_{2u}(1)$	11362
m_u	21.94% $^5A_u(1)$, 21.78% $^5B_{1u}(1)$, 18.43% $^5B_{3u}(1)$, 18.4% $^5B_{2u}(1)$	11700
n_g	19.12% $^5B_{2g}(2)$, 19.07% $^5B_{3g}(2)$, 17.44% $^3B_{1g}(1)$, 14.82% $^1A_g(1)$	11817
o_u	42.88% $^3B_{2u}(1)$, 31.88% $^5B_{3u}(1)$	11850
p_g	36.81% $^5B_{2g}(1)$, 36.81% $^5B_{3g}(1)$, 9.67% $^5A_g(3)$	12253
q_g	30.81% $^5B_{1g}(1)$, 23.75% $^5A_g(2)$, 17.24% $^3B_{2g}(1)$, 10.5% $^5B_{3g}(1)$	12345
r_u	36.84% $^5B_{1u}(1)$, 14.5% $^3B_{3u}(1)$, 14.32% $^3B_{2u}(1)$, 9.93% $^3A_u(3)$	12539
s_u	26.69% $^3A_u(2)$, 26.67% $^3B_{1u}(2)$, 21.97% $^5A_u(2)$, 21.84% $^5B_{1u}(2)$	12545
t_g	53.19% $^5B_{1g}(2)$, 14.79% $^5B_{2g}(2)$, 14.79% $^5B_{3g}(2)$	12687
u_u	25.54% $^5A_u(1)$, 19.8% $^3B_{1u}(1)$, 19.02% $^5B_{1u}(1)$	13216

Table B.4 – *Continued from previous page*

Term Symbol	Character : % [orbital(number of electron)]	E (cm^{-1})
v_u	43.47% $^3A_u(1)$, 24.48% $^3B_{1u}(1)$	13241
w_g	28.83% $^5B_{1g}(2)$, 20.15% $^5B_{2g}(2)$, 19.79% $^5A_g(3)$, 12.91% $^5B_{3g}(2)$, 12.71% $^5B_{2g}(1)$	13394
x_g	58.26% $^5B_{2g}(1)$	13728
y_g	34.24% $^5B_{1g}(1)$, 21.57% $^3B_{3g}(1)$, 21.56% $^3B_{2g}(1)$, 20.21% $^5A_g(2)$	14074
z_g	45.19% $^5B_{3g}(2)$, 38.99% $^5B_{2g}(2)$	14162
aa_u	47.44% $^3B_{1u}(1)$, 14.08% $^1A_u(1)$, 12.08% $^5A_u(1)$	14253
ab_g	32.6% $^5B_{3g}(1)$, 32.6% $^5B_{2g}(1)$, 17.93% $^3B_{1g}(2)$, 10.46% $^5A_g(2)$	14698
ac_g	35.2% $^5B_{3g}(2)$, 35.19% $^5B_{2g}(2)$, 11.61% $^3B_{3g}(2)$, 11.61% $^3B_{2g}(2)$	14747
ad_g	27.69% $^5B_{3g}(1)$, 27.69% $^5B_{2g}(1)$, 16.03% $^3A_g(1)$, 13.05% $^5B_{1g}(1)$	14862
ae_u	48.62% $^5A_u(3)$, 48.07% $^5B_{1u}(3)$	14968
af_g	24.6% $^5B_{2g}(1)$, 24.55% $^5B_{3g}(1)$, 14.87% $^3B_{1g}(2)$, 12.76% $^3A_g(1)$	15217
ag_g	57.87% $^5B_{3g}(2)$, 12.24% $^3B_{2g}(2)$	15786
ah_u	32.7% $^5B_{3u}(2)$, 32.65% $^5B_{2u}(2)$, 15.35% $^5B_{3u}(1)$, 14.96% $^5B_{2u}(1)$	15843
ai_g	35.75% $^5B_{2g}(3)$, 35.52% $^5B_{3g}(3)$, 12.29% $^5B_{1g}(1)$	15851

Appendix C

Additional ETS-NOCV Results

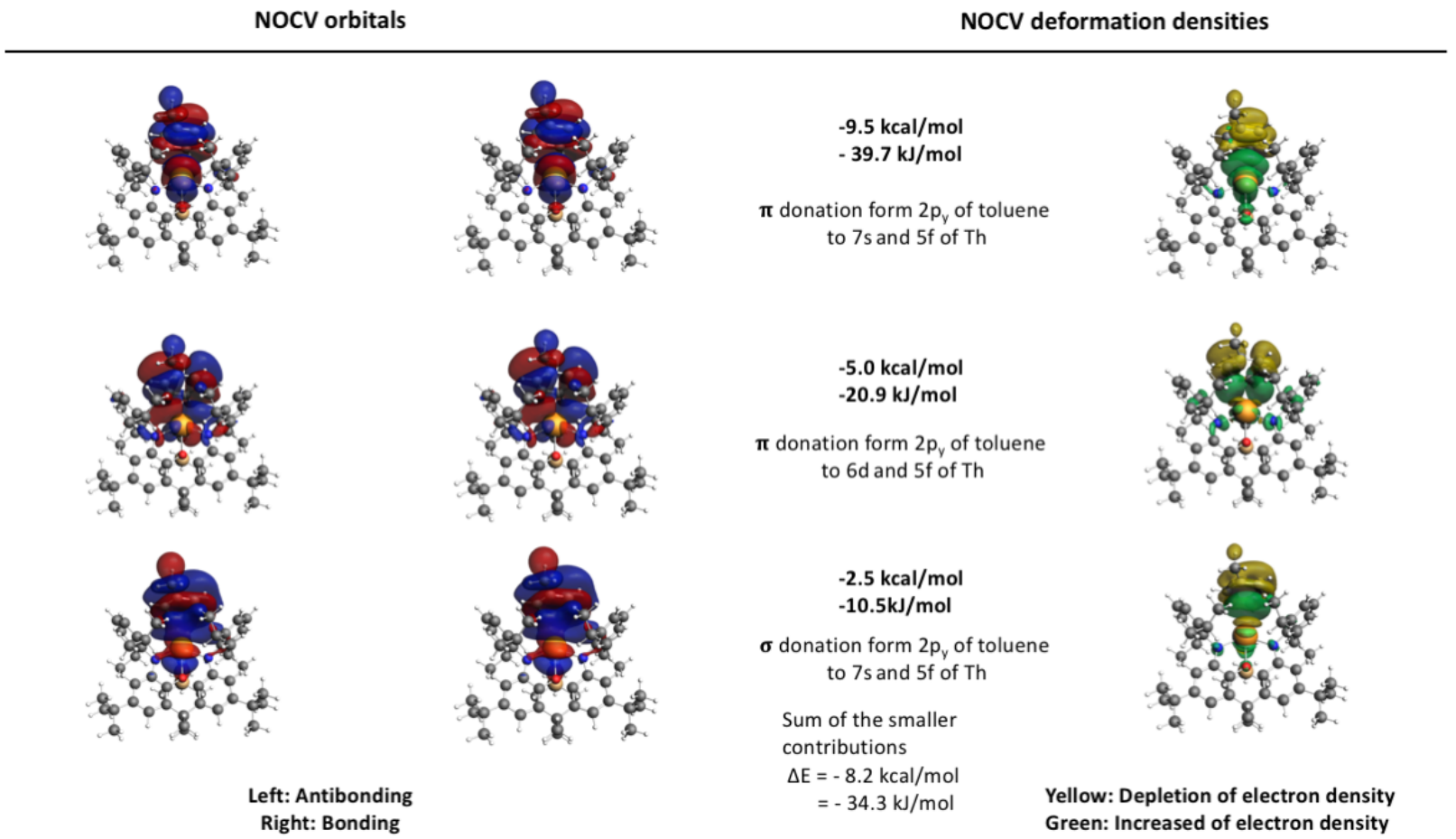

FIGURE C.1: On the left hand side: the NOCV Orbitals (with isosurfaces set to 0.01) and on the right hand side ETS-NOCV deformation density contributions, Increased (green) and decreased (yellow) electron density is presented relative to that in the isolated fragments (isosurfaces are set to 0.0001) for the molecule η^6**-3-Th-down**.

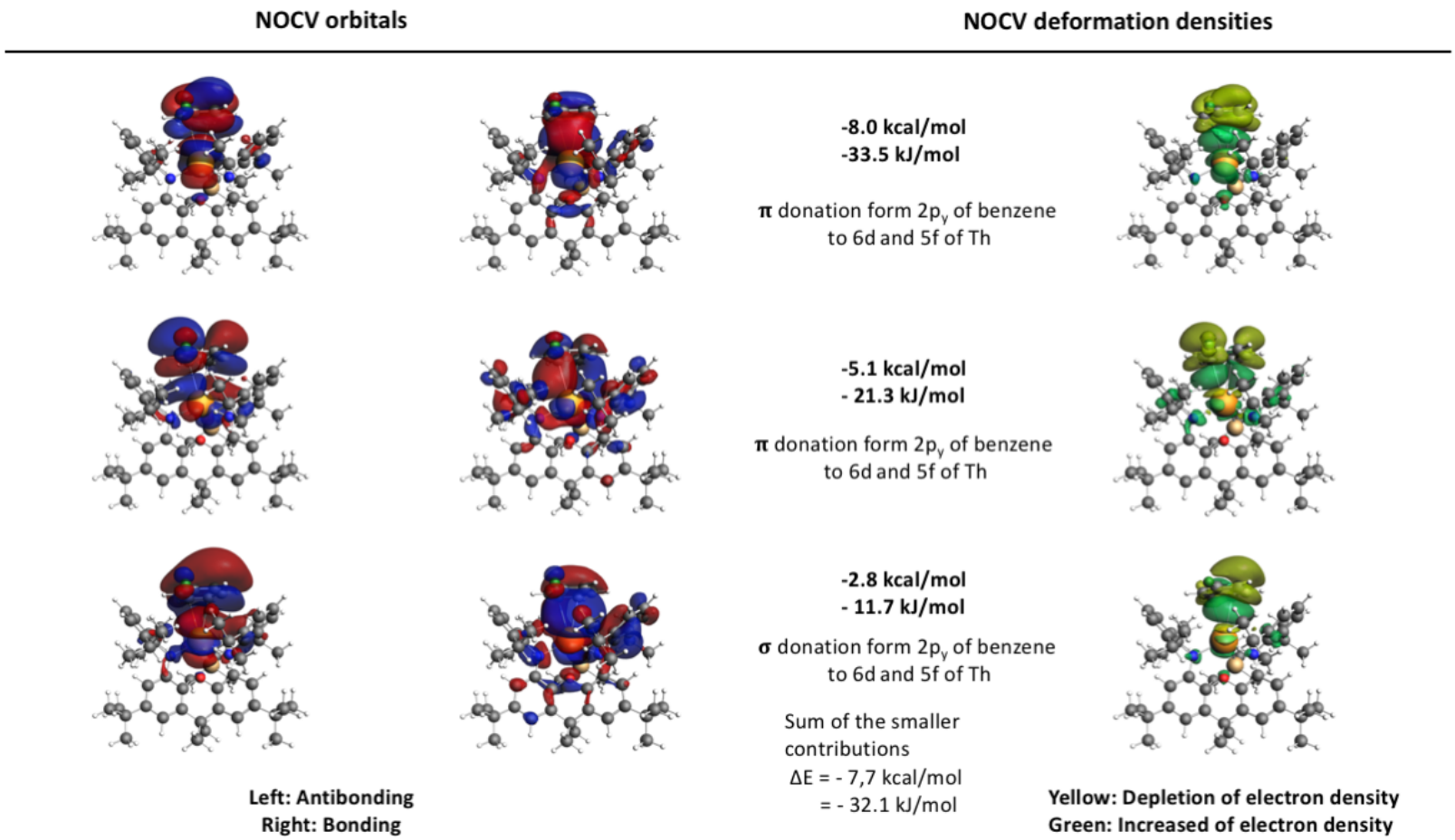

FIGURE C.2: On the left hand side: the NOCV Orbitals (with isosurfaces set to 0.01) and on the right hand side ETS-NOCV deformation density contributions, Increased (green) and decreased (yellow) electron density is presented relative to that in the isolated fragments (isosurfaces are set to 0.0001) for the molecule η^6**-5-Th-endo**.

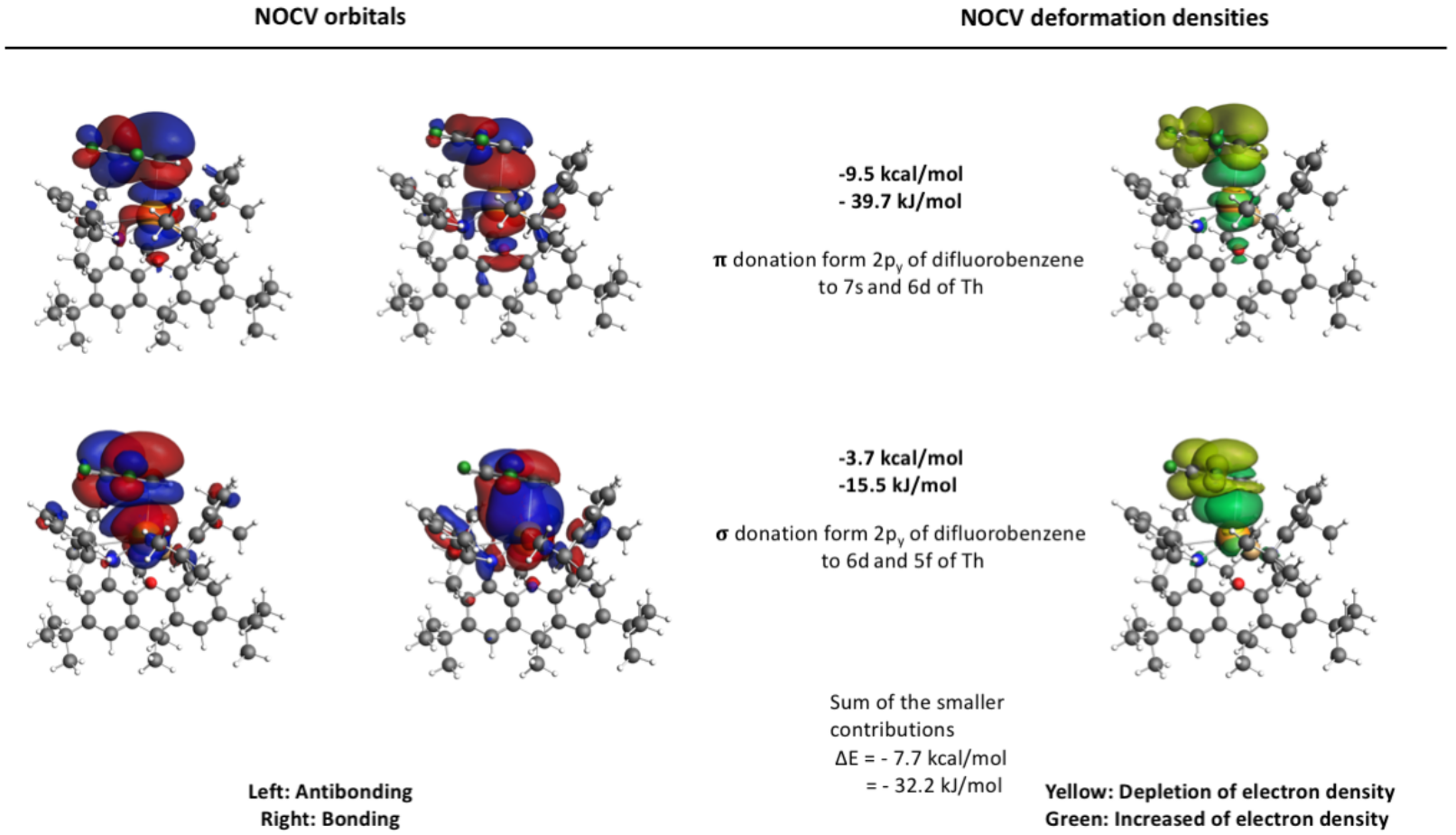

FIGURE C.3: On the left hand side: the NOCV Orbitals (with isosurfaces set to 0.01) and on the right hand side ETS-NOCV deformation density contributions, Increased (green) and decreased (yellow) electron density is presented relative to that in the isolated fragments (isosurfaces are set to 0.0001) for the molecule η^6**-6-Th-exo** .

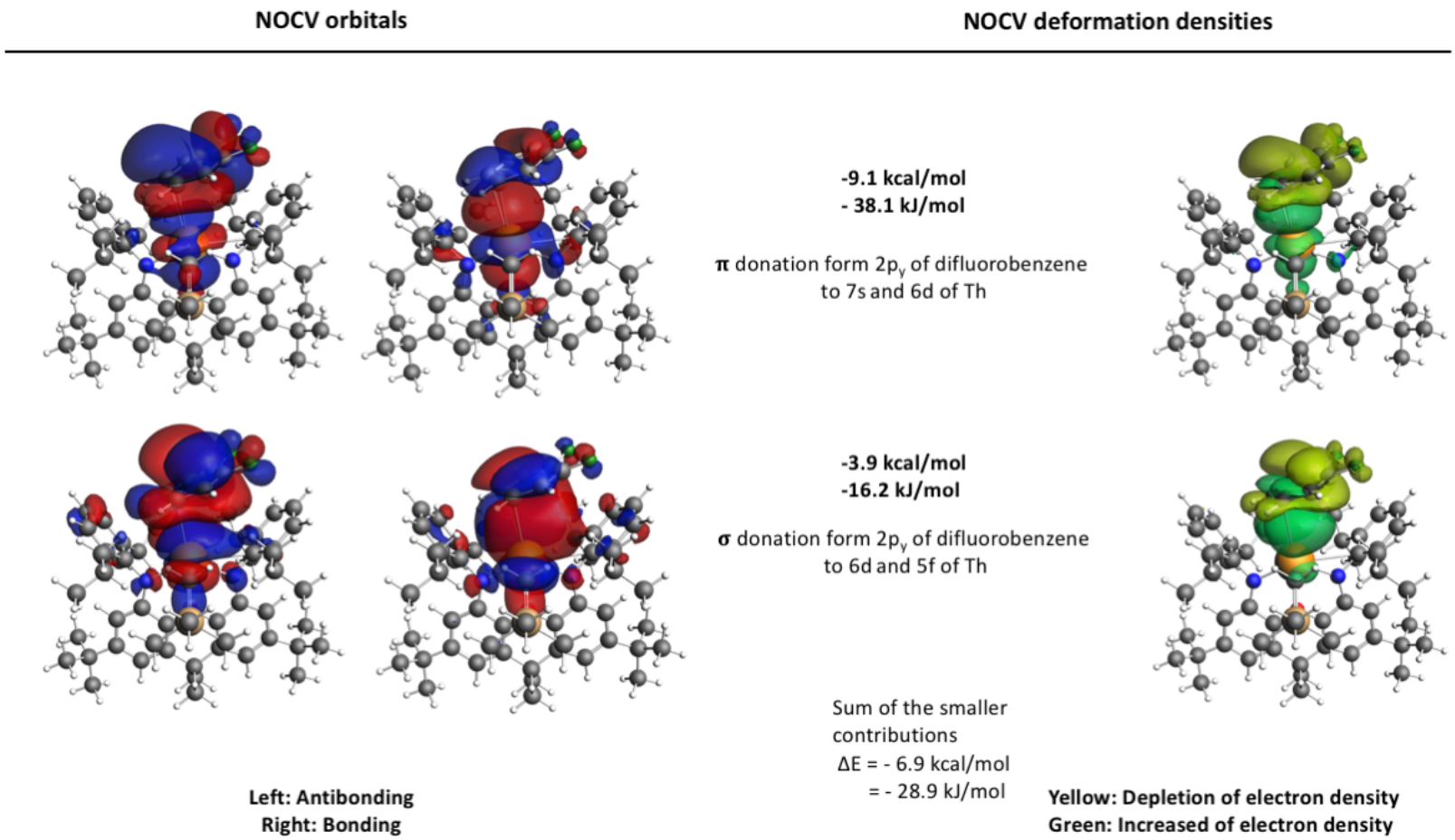

FIGURE C.4: On the left hand side: the NOCV Orbitals (with isosurfaces set to 0.01) and on the right hand side ETS-NOCV deformation density contributions, Increased (green) and decreased (yellow) electron density is presented relative to that in the isolated fragments (isosurfaces are set to 0.0001) for the molecule η^6**-6-Th-side**.

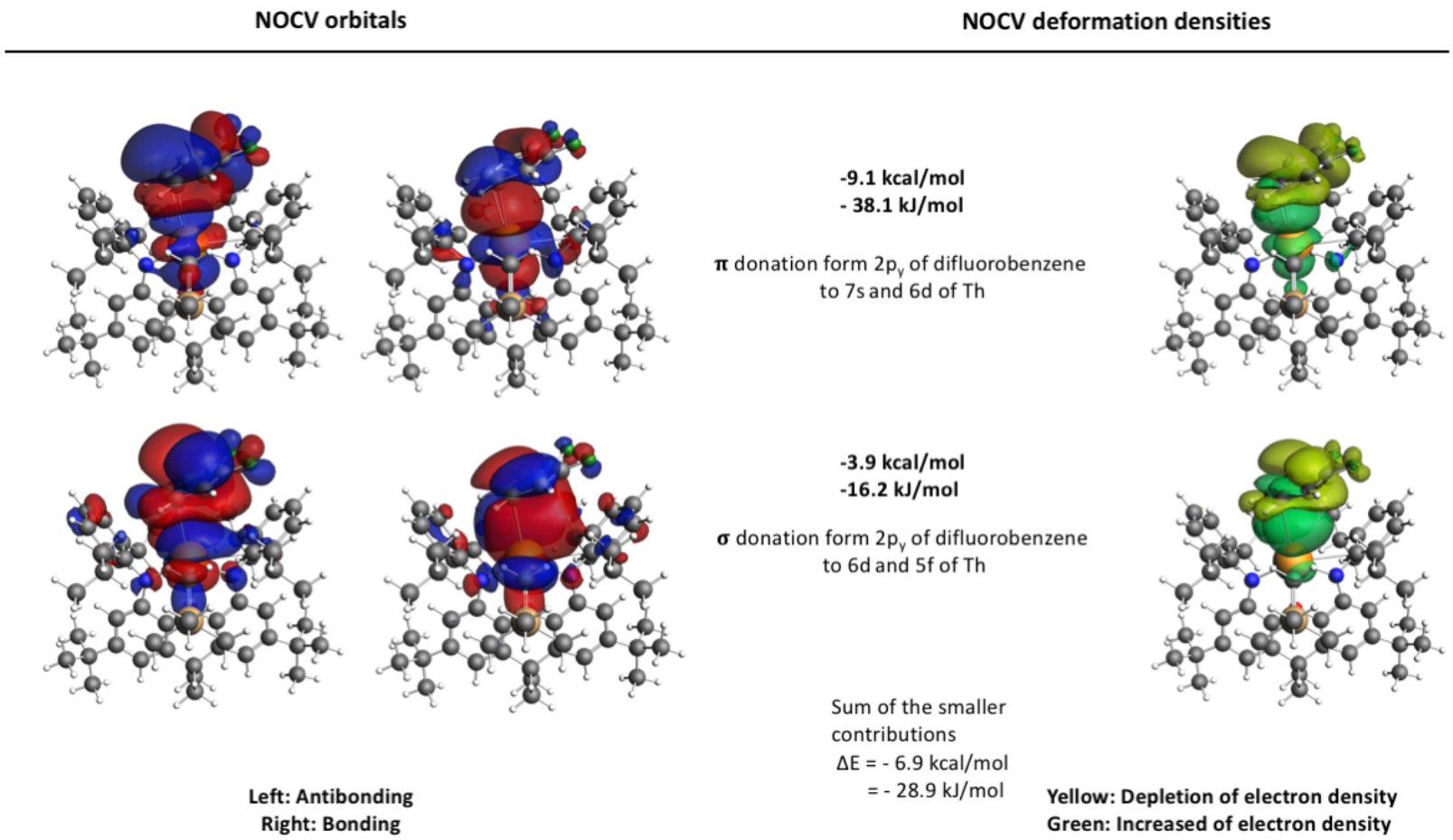

FIGURE C.5: On the left hand side: the NOCV Orbitals (with isosurfaces set to 0.01) and on the right hand side ETS-NOCV deformation density contributions, Increased (green) and decreased (yellow) electron density is presented relative to that in the isolated fragments (isosurfaces are set to 0.0001) for the molecule η^6**-6-Th-endo**.

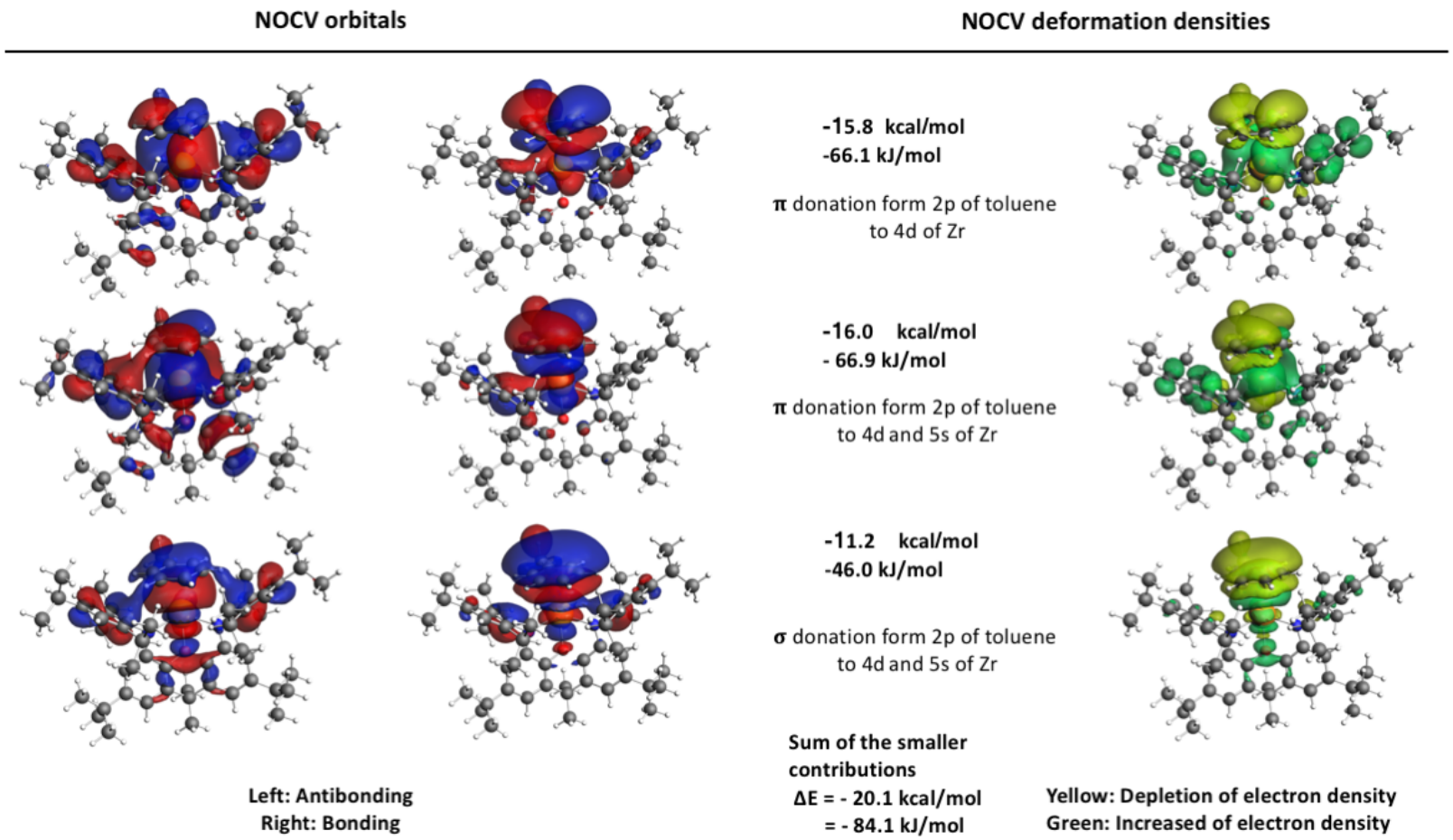

FIGURE C.6: On the left hand side: the NOCV Orbitals (with isosurfaces set to 0.01) and on the right hand side ETS-NOCV deformation density contributions, Increased (green) and decreased (yellow) electron density is presented relative to that in the isolated fragments (isosurfaces are set to 0.0001) for the molecule η^2-**E′-Zr**.

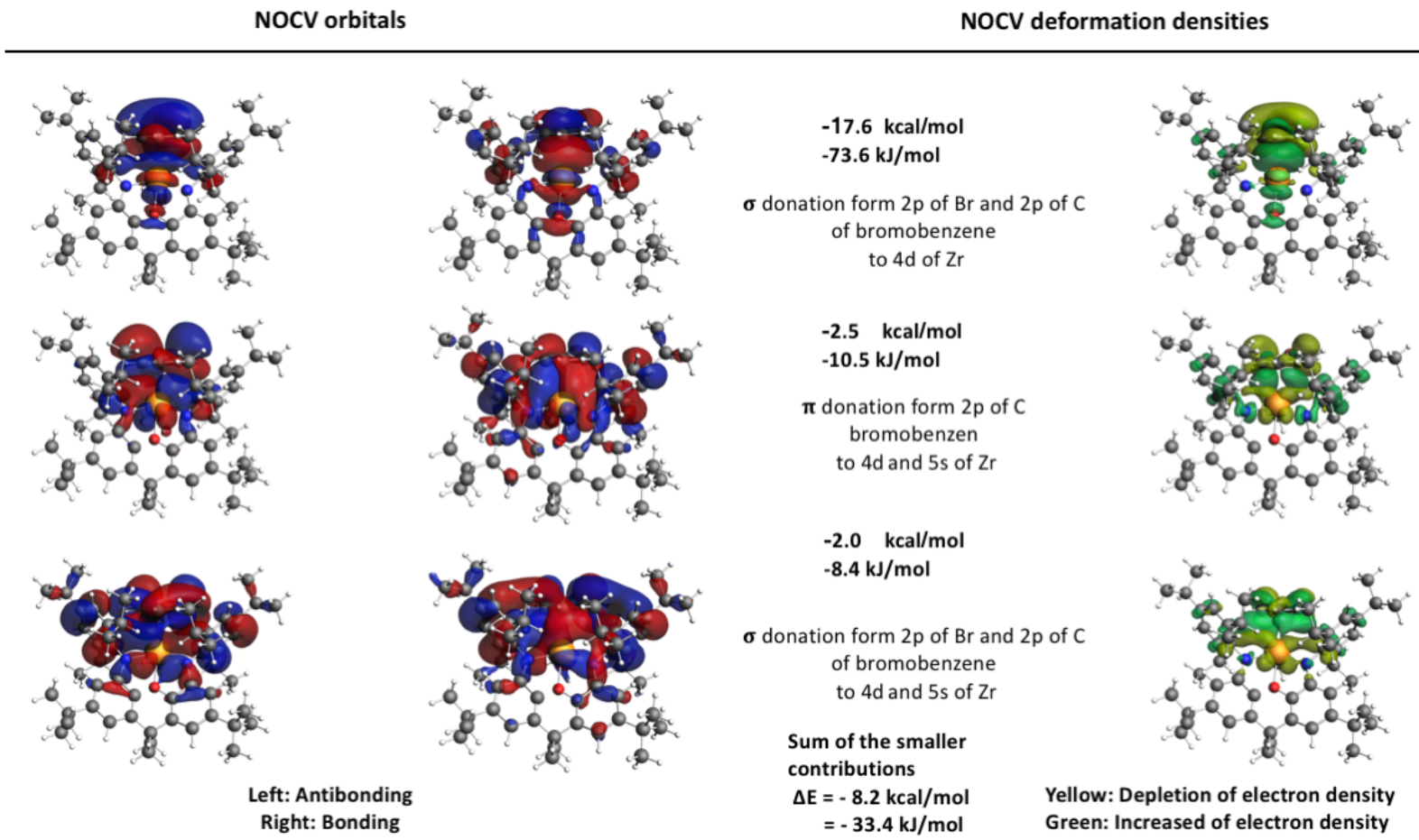

FIGURE C.7: On the left hand side: the NOCV Orbitals (with isosurfaces set to 0.01) and on the right hand side ETS-NOCV deformation density contributions, Increased (green) and decreased (yellow) electron density is presented relative to that in the isolated fragments (isosurfaces are set to 0.0001) for the molecule η^6**-4′-Zr-exo**.

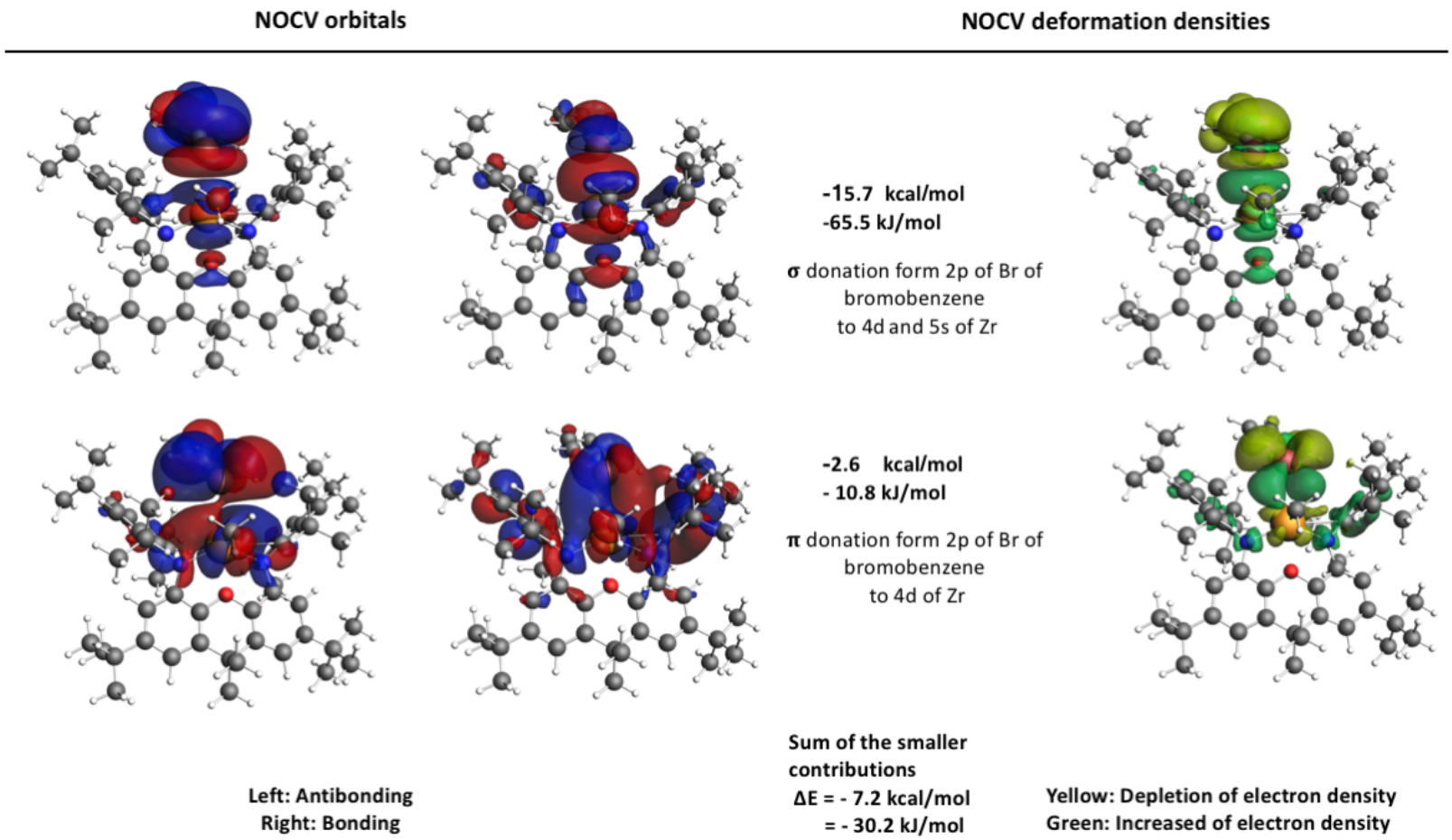

FIGURE C.8: On the left hand side: the NOCV Orbitals (with isosurfaces set to 0.01) and on the right hand side ETS-NOCV deformation density contributions, Increased (green) and decreased (yellow) electron density is presented relative to that in the isolated fragments (isosurfaces are set to 0.0001) for the molecule η^6**-4′-Zr-exo**.

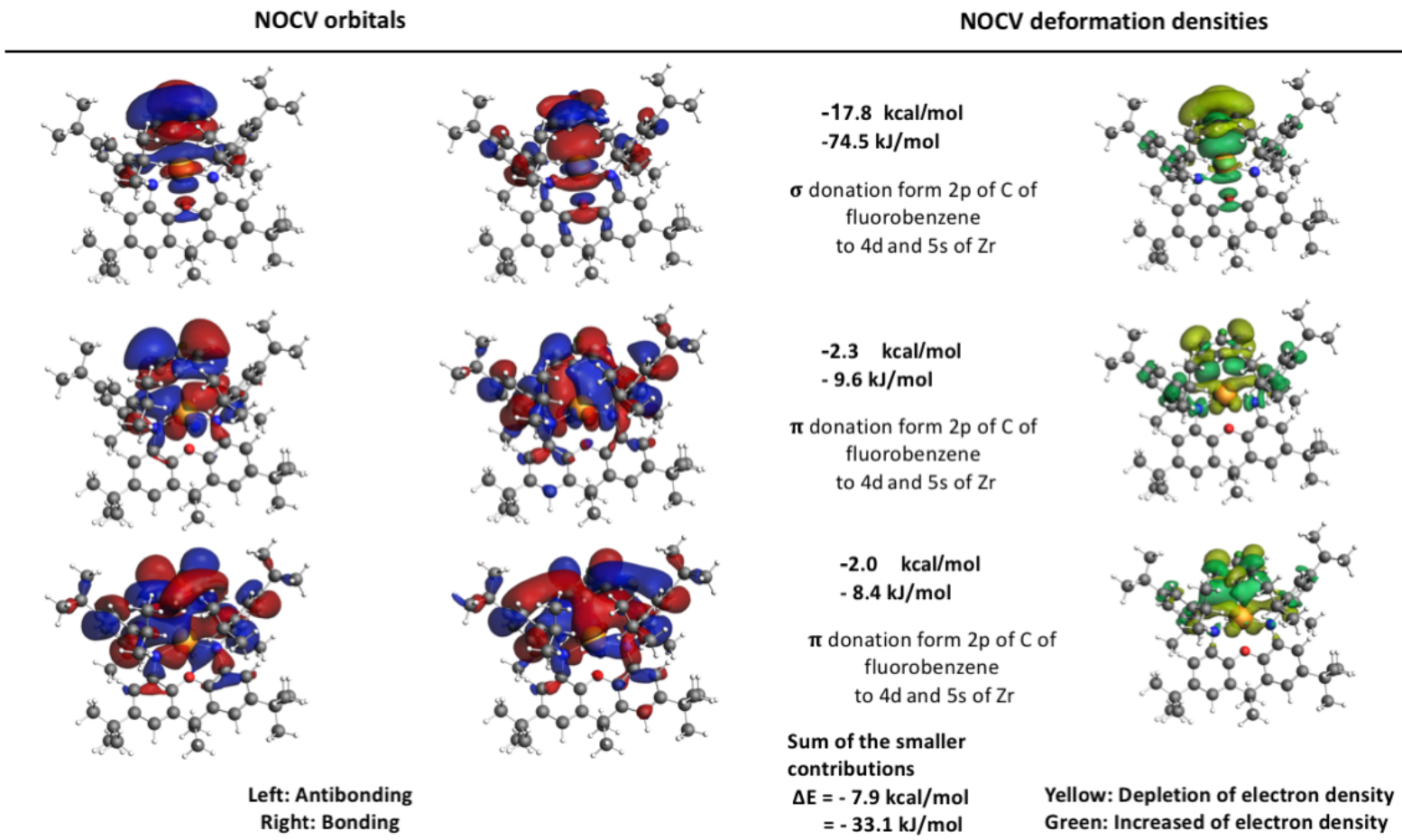

FIGURE C.9: On the left hand side: the NOCV Orbitals (with isosurfaces set to 0.01) and on the right hand side ETS-NOCV deformation density contributions, Increased (green) and decreased (yellow) electron density is presented relative to that in the isolated fragments (isosurfaces are set to 0.0001) for the molecule η^6**-5′-Zr-exo**.

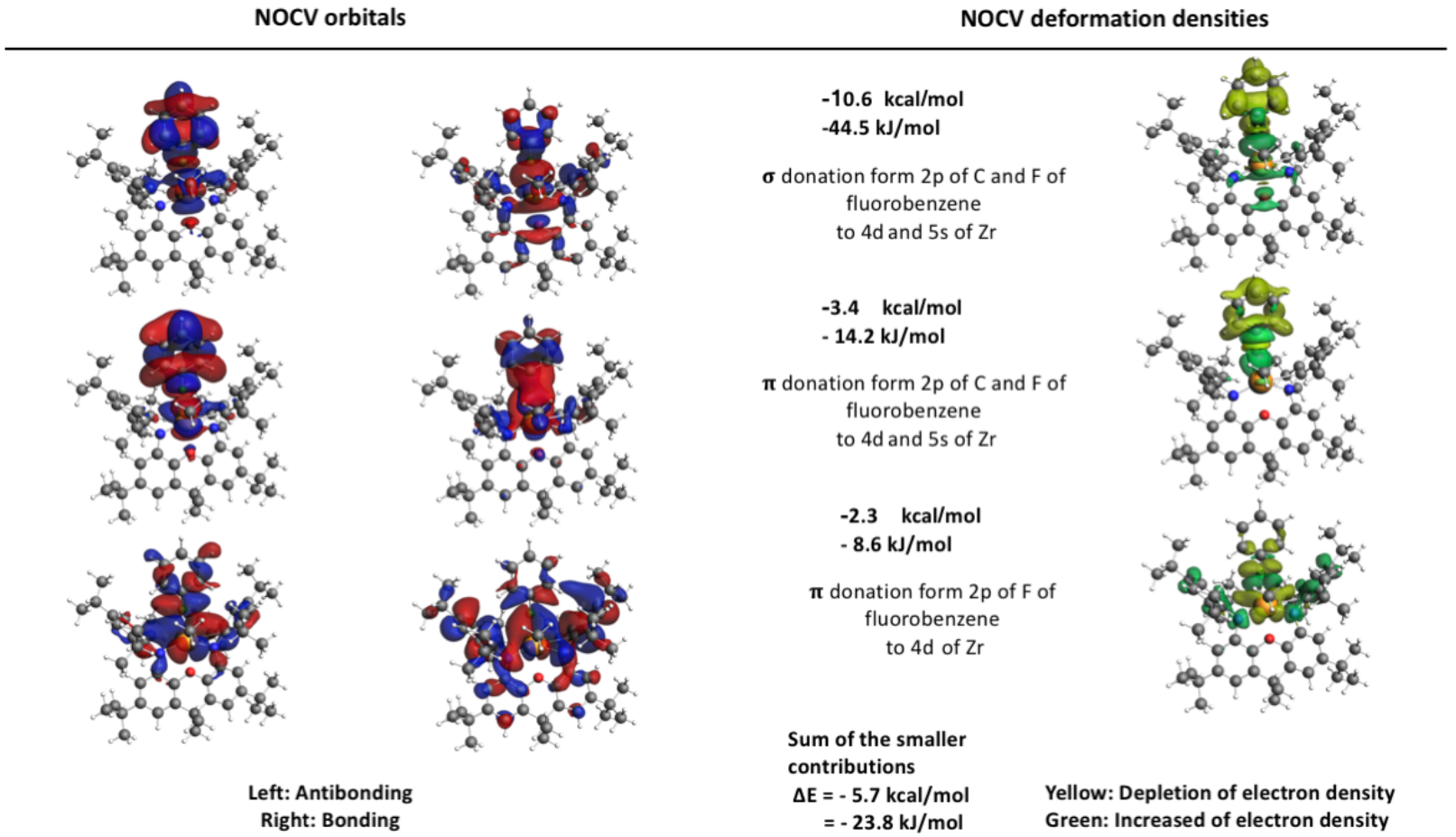

FIGURE C.10: On the left hand side: the NOCV Orbitals (with isosurfaces set to 0.01) and on the right hand side ETS-NOCV deformation density contributions, Increased (green) and decreased (yellow) electron density is presented relative to that in the isolated fragments (isosurfaces are set to 0.0001) for the molecule η^1**-5′-Zr-horizontal**.

Bibliography

[1] Bernd F. Straub. Organotransition Metal Chemistry. From Bonding to Catalysis. Edited by John?F. H Vol. 49. 42. WILEY-VCH Verlag, 2010, pp. 7622–7622. DOI: 10.1002/anie.201004890.

[2] Ataf Ali Altaf et al. "Zirconium complexes in homogeneous ethylene polymerization". In: Journal of Coordination Chemistry 64.10 (2011), pp. 1815–1836. DOI: 10.1080/00958972.2011.568616.

[3] Andrew J. Peacock and Allison Calhoun. "Polymer Chemistry". In: Polymer Chemistry. Carl Hanser Verlag GmbH & Co. KG, 2006, pp. I–XIX. ISBN: 978-3-446-22283-0. DOI: doi:10.3139/9783446433434.fm.

[4] M Salvatores. "Physics and Safety of transmutation Systems". In: NEA Nuclear Science Report 6090 (2006).

[5] R. P. Feynman. Quantum Electrodynamics. New York: WA. Benjamin, 1961.

[6] Attila Szabo and Neil S. Ostlund. Modern Quantum Chemistry: Introduction to Advanced Electroni First. Mineola: Dover Publications, Inc., 1996.

[7] Lev Davidovich Landau and Evgenii Mikhailovich Lifshitz. Quantum Mechanics: Non-Relativistic T Vol. 3. Elsevier, 2013.

[8] W. Pauli. "Uber den Zusammenhang des Abschlusses der Elektronengruppen im Atom mit der Komplexstruktur der Spektren". In: Zeitschrift fur Physik 31.1 (1925), pp. 765–783. DOI: 10.1007/BF02980631.

[9] J. C. Slater. "A Simplification of the Hartree-Fock Method". In: Phys. Rev. 81 (3 1951), pp. 385–390. DOI: 10.1103/PhysRev.81.385.

[10] Frank Jensen. Introduction to Computational Chemistry. John Wiley & Sons, 2006. ISBN: 0470011874.

[11] Per-Olov L
owdin. "Quantum Theory of Many-Particle Systems. III. Extension of the Hartree-Fock Scheme to Include Degenerate Systems and Correlation Effects". In: Phys. Rev. 97 (6 1955), pp. 1509–1520. DOI: 10.1103/PhysRev.97.1509.

[12] L. González, D. Escudero, and L. Serrano-Andrés. "Progress and Challenges in the Calculation of Electronic Excited States". In: ChemPhysChem 13 (2012), pp. 28–51. ISSN: 1439-7641. DOI: 10.1002/cphc.201100200.

[13] Chr. Møller and M. S. Plesset. "Note on an Approximation Treatment for Many-Electron Systems". In: Phys. Rev. 46 (7 1934), pp. 618–622. DOI: 10.1103/PhysRev.46.618.

[14] Bernard Levy and Gaston Berthier. "Generalized brillouin theorem for multiconfigurational SCF theories". In: International Journal of Quantum Chemistry 2.2 (), pp. 307–319. DOI: 10.1002/qua.560020210.

[15] T Koopmans. "Über die Zuordnung von Wellenfunktionen und Eigenwerten zu den Einzelnen Elektronen Eines Atoms". In: Physica 1.1 (1934), pp. 104 –113. DOI: https://doi.org/10.1016/S0031-8914(34)90011-2.

[16] R J Bartlett. "Many-Body Perturbation Theory and Coupled Cluster Theory for Electron Correlation in Molecules". In: Annual Review of Physical Chemistry 32.1 (1981), pp. 359–401. DOI: 10.1146/annurev.pc.32.100181.002043.

[17] A. Szabo and N. S. Ostlund. Modern Quantum Chemistry: Introduction to Advanced Electroni New York: McGraw-Hill, 1989.

[18] Jiří Čížek. In: The Journal of Chemical Physics 45.11 (1966), pp. 4256–4266. DOI: 10.1063/1.1727484.

[19] Čižek J. and Paldus J. In: International Journal of Quantum Chemistry 5.4 (), pp. 359–379. DOI: 10.1002/qua.560050402.

[20] "Coupled cluster theory for high spin, open shell reference wave functions". In: The Journal of Chemical Physics 99.7 (1993), pp. 5219–5227. DOI: 10.1063/1.465990.

[21] Peter J. Knowles, Claudia Hampel, and Hans-Joachim Werner. "Erratum: "Coupled cluster theory for high spin, open shell reference wave functions" [J. Chem. Phys. 99, 5219 (1993)]". In: The Journal of Chemical Physics 112.6 (2000), pp. 3106–3107. DOI: 10.1063/1.480886.

[22] R. J. Bartlett and M. Musiał. "Coupled-Cluster Theory In Quantum Chemistry". In: Reviews of Modern Physics 79 (2007), pp. 291–350.

[23] George D. Purvis and Rodney J. Bartlett. In: The Journal of Chemical Physics 76.4 (1982), pp. 1910–1918. DOI: 10.1063/1.443164.

[24] Watts John D. and Bartlett Rodney J. In: International Journal of Quantum Chemistry 48.27 (), pp. 51–66. DOI: 10.1002/qua.560480809.

[25] Krishnan Raghavachari et al. "A fifth-order perturbation comparison of electron correlation theories". In: Chemical Physics Letters 157.6 (1989), pp. 479 –483. ISSN: 0009-2614. DOI: https://doi.org/10.1016/S0009-2614(89)87395-6.

[26] Miles J.O. Deegan and Peter J. Knowles. "Perturbative corrections to account for triple excitations in closed and open shell coupled cluster theories". In: Chemical Physics Letters 227.3 (1994), pp. 321 –326. ISSN: 0009-2614. DOI: https://doi.org/10.1016/0009-2614(94)00815-9.

[27] Rodney J. Bartlett. "Coupled-cluster approach to molecular structure and spectra: a step toward predictive quantum chemistry". In: The Journal of Physical Chemistry 93.5 (1989), pp. 1697–1708. DOI: 10.1021/j100342a008.

[28] Peter M. W. Gill et al. In: The Journal of Chemical Physics 89.12 (1988), pp. 7307–7314. DOI: 10.1063/1.455312.

[29] Martin Rosenberg et al. "Excited State Aromaticity and Antiaromaticity: Opportunities for Photophysical and Photochemical Rationalizations". In: Chemical Reviews 114.10 (2014), pp. 5379–5425. DOI: 10.1021/cr300471v.

[30] Gustavo E. Scuseria. "The open-shell restricted Hartree—Fock singles and doubles coupled-cluster method including triple excitations CCSD (T): application to C+3". In: Chemical Physics Letters 176.1 (1991), pp. 27 –35. ISSN: 0009-2614. DOI: https://doi.org/10.1016/0009-2614(91)90005-T.

[31] Lee Timothy J. and Taylor Peter R. In: International Journal of Quantum Chemistry 36.S23 (), pp. 199–207. DOI: 10.1002/qua.560360824.

[32] Timothy J. Lee. "Comparison of the T1 and D1 diagnostics for electronic structure theory: a new definition for the open-shell D1 diagnostic". In: Chemical Physics Letters 372 (2003), pp. 362–367.

[33] Curtis L Janssen and Ida M B Nielsen. "New diagnostics for coupled-cluster and Møller-Plesset perturbation theory". In: Chem. Phys. Lett. 290 (1998), pp. 423–430.

[34] Timothy J Lee. "Comparison of the T1 and D1 diagnostics for electronic structure theory: a new definition for the open-shell D1 diagnostic". In: Chemical Physics Letters 372.3 (2003), pp. 362 –367. ISSN: 0009-2614. DOI: https://doi.org/10.1016/S0009-2614(03)00435-4.

[35] Matthew L. Leininger et al. "A new diagnostic for open-shell coupled-cluster theory". In: Chemical Physics Letters 328.4 (2000), pp. 431 –436. ISSN: 0009-2614. DOI: https://doi.org/10.1016/S0009-2614(00)00966-0.

[36] Wanyi Jiang, Nathan J. DeYonker, and Angela K. Wilson. "Multireference Character for 3d Transition-Metal-Containing Molecules". In: J. Chem. Theory Comput. 8 (2012), pp. 460–468.

[37] P. Tecmer et al. "Electronic spectroscopy of UO_2^{2+}, NUO^+ and NUN: An Evaluation of Time-Dependent Density Functional Theory for Actinides". In: Phys. Chem. Chem. Phys. 13 (2011), pp. 6249–6259.

[38] P. Hohenberg and W. Kohn. "Inhomogeneous Electron Gas". In: Phys. Rev. 136 (1964), B864–B871. DOI: 10.1103/PhysRev.136.B864.

[39] W. Kohn and L. J. Sham. In: Phys. Rev. 140 (1965), A1133–A1138.

[40] J. P. Perdew and Y. Wang. "Accurate and simple analytic representation of the electron-gas correlation energy". In: Phys. Rev. B 45 (1992), pp. 13244–13249. DOI: 10.1103/PhysRevB.45.13244.

[41] S. H. Vosko, L. Wilk, and M. Nusair. "Accurate spin-dependent electron liquid correlation energies for local spin-density calculations - A critical analysis". In: Can. J. Phys. 58 (1980), pp. 1200–1211. DOI: 10.1139/p80-159.

[42] J. P. Perdew et al. "Atoms, molecules, solids, and surfaces: Applications of the generalized gradient approximation for exchange and correlation". In: Phys. Rev. B 46 (1992), pp. 6671–6687. DOI: 10.1103/PhysRevB.46.6671.

[43] J. P. Perdew, K. Burke, and M. Ernzerhof. "Generalized gradient approximation made simple". In: Phys. Rev. Lett. 77 (1996), pp. 3865–3868.

[44] P. J. Stephens et al. "Ab Initio Calculation of Vibrational Absorption and Circular Dichroism Spectra Using Density Functional Force Fields". In: The Journal of Physical Che 98.45 (1994), pp. 11623–11627. DOI: 10.1021/j100096a001.

[45] Carlo Adamo and Vincenzo Barone. "Toward reliable density functional methods without adjustable parameters: The PBE0 model". In: The Journal of Chemical Physics 110.13 (1999), pp. 6158–6170. DOI: 10.1063/1.478522.

[46] John P. Perdew, Matthias Ernzerhof, and Kieron Burke. "Rationale for mixing exact exchange with density functional approximations". In: The Journal of Chemical Physics 105.22 (1996), pp. 9982–9985. DOI: 10.1063/1.472933.

[47] Christos P. Constantinides, Panayiotis A. Koutentis, and Jürgen Schatz. "A DFT Study of the Ground State Multiplicities of Linear vs Angular Polyheteroacenes". In: Journal of the American Chemical Society 126.49 (2004), pp. 16232–16241. DOI: 10.1021/ja045006t.

[48] Marcel Swart et al. "Validation of Exchange-Correlation Functionals for Spin States of Iron Complexes". In: The Journal of Physical Chemistry A 108.25 (2004), pp. 5479–5483. DOI: 10.1021/jp049043i.

[49] Stefan Grimme. "Semiempirical GGA-type density functional constructed with a long-range dispersion correction". In: Journal of Computational Chemistry 27.15 (), pp. 1787–1799. DOI: 10.1002/jcc.20495.

[50] Stefan Grimme et al. "A consistent and accurate ab initio parametrization of density functional dispersion correction (DFT-D) for the 94 elements H-Pu". In: The Journal of Chemical Physics 132.15 (2010), p. 154104. DOI: 10.1063/1.3382344.

[51] Stefan Grimme. "Accurate description of van der Waals complexes by density functional theory including empirical corrections". In: Journal of Computational Chemistry 25.12 (), pp. 1463–1473. DOI: 10.1002/jcc.20078.

[52] Pekka Pyykkö. "Relativistic effects in structural chemistry". EN. In: Chem. Rev. 88.3 (1988), pp. 563–594. ISSN: 0009-2665. DOI: 10.1021/cr00085a006.

[53] Albert A Michelson and Edward W Morley. In: Am. J. Sci. 134 (1887), p. 33.

[54] P. A. M. Dirac. "The quantum theory of the electron". In: Proc. R. Soc. London 117 (1928), p. 610.

[55] "A theory of electrons and protons". In: Proceedings of the Royal Society of London A: Mathematica 126.801 (1930), pp. 360–365. ISSN: 0950-1207. DOI: 10.1098/rspa.1930.0013. eprint: http://rspa.royalsocietypublishing.org/content/126/801/360.full.pdf.

[56] "IV. The triplets of helium". In: Philosophical Transactions of the Royal Society of London A: Mathe 228.659-669 (1929), pp. 151–196. ISSN: 0264-3952. DOI: 10.1098/rsta.1929.0004. eprint: http://rsta.royalsocietypublishing.org/content/228/659-669/151.full.pdf.

[57] G. Breit. "The Effect of Retardation on the Interaction of Two Electrons". In: Phys. Rev. 34 (4 1929), pp. 553–573. DOI: 10.1103/PhysRev.34.553.

[58] H. B. G. Casimir and D. Polder. "The Influence of Retardation on the London-van der Waals Forces". In: Phys. Rev. 73 (4 1948), pp. 360–372. DOI: 10.1103/PhysRev.73.360.

[59] Kenneth G Dyall and Knut Faegri Jr. Introduction to relativistic quantum chemistry. Oxford University Press, 2007.

[60] Markus Reiher and Alexander Wolf. Relativistic quantum chemistry: the fundamental theory of mo John Wiley Sons, 2014.

[61] Christoph van Wüllen. "Molecular density functional calculations in the regular relativistic approximation: Method, application to coinage metal diatomics, hydrides, fluorides and chlorides, and comparison with first-order relativistic calculations". In: The Journal of Chemical Physics 109.2 (1998), pp. 392–399. DOI: 10.1063/1.476576.

[62] Alexander Wolf, Markus Reiher, and Bernd Artur Hess. "The generalized Douglas–Kroll transformation". In: The Journal of Chemical Physics 117.20 (2002), pp. 9215–9226. DOI: 10.1063/1.1515314.

[63] Markus Reiher and Alexander Wolf. "Exact decoupling of the Dirac Hamiltonian. II. The generalized Douglas–Kroll–Hess transformation up to arbitrary order". In: The Journal of Chemical Physics 121.22 (2004), pp. 10945–10956. DOI: 10.1063/1.1818681.

[64] L. L. Foldy and S. A. Wouthuysen. "On the Dirac Theory of Spin 1/2 Particles and Its Non-Relativistic Limit". In: Physical Review 78 (1950), p. 29.

[65] Bernd Artur Hess et al. "A mean-field spin-orbit method applicable to correlated wavefunctions". In: Chem. Phys. Lett. 251 (1996), pp. 365–371.

[66] M Krauss and W J Stevens. "Effective potentials in molecular quantum chemistry". In: Annual Review of Physical Chemistry 35.1 (1984), pp. 357–385.

[67] M. Dolg and X. Cao. "Relativistic Pseudopotentials: Their Development And Scope Of Applications". In: Chem. Rev. 112 (2012), pp. 403–480.

[68] Helmut Eschrig. Optimized LCAO Method and Electronic Structure of Extended Systems, Berlin. Jan. 1989.

[69] J. C. Slater. "Atomic Shielding Constants". In: Phys. Rev. 36 (1 1930), pp. 57–64. DOI: 10.1103/PhysRev.36.57.

[70] "Electronic wave functions - I. A general method of calculation for the stationary states of any molecular system". In: Proceedings of the Royal Society of London A: Mat 200.1063 (1950), pp. 542–554. DOI: 10.1098/rspa.1950.0036.

[71] T. H. Dunning Jr. "Gaussian basis sets for use in correlated molecular calculations. I. The atoms boron through neon and hydrogen". In: J. Chem. Phys. 90 (1989), pp. 1007–1023. DOI: 10.1063/1.456153.

[72] J. M. L. Martin and A. Sundermann. "Correlation consistent valence basis sets for use with the Stuttgart-Dresden-Bonn relativistic effective core potentials: The atoms Ga-Kr and In-Xe". In: J. Chem. Phys. 114 (2001), pp. 3408–3420. DOI: 10.1063/1.1337864.

[73] Florian Weigend and Reinhart Ahlrichs. "Balanced basis sets of split valence, triple zeta valence and quadruple zeta valence quality for H to Rn: Design and assessment of accuracy". In: Phys. Chem. Chem. Phys. 7 (18 2005), pp. 3297–3305. DOI: 10.1039/B508541A.

[74] Florian Weigend. "Accurate Coulomb-fitting basis sets for H to Rn". In: Phys. Chem. Chem. Phy 8 (9 2006), pp. 1057–1065. DOI: 10.1039/B515623H.

[75] Per-Olof Widmark, B. Joakim Persson, and Björn O. Roos. "Density matrix averaged atomic natural orbital (ANO) basis sets for correlated molecular wave functions". In: Theoretica chimica acta 79.6 (1991), pp. 419–432. ISSN: 1432-2234. DOI: 10.1007/BF01112569.

[76] Jan Almlöf and Peter R Taylor. "Atomic natural orbital (ANO) basis sets for quantum chemical calculations". In: Advances in Quantum Chemistry 22 (1991), pp. 301–373. DOI: 10.1016/S0065-3276(08)60366-4.

[77] B. O. Roos et al. "Main group atoms and dimers studied with a new relativistic ANO basis set". In: J. Phys. Chem. A 108 (2004), pp. 2851–2858. DOI: 10.1021/jp031064+.

[78] B. O. Roos et al. "New relativistic ANO basis sets for actinide atoms". In: Chem. Phys. Lett. 409 (2005), pp. 295–299. DOI: 10.1016/j.cplett.2005.05.011.

[79] M. Gutowski et al. "The basis set superposition error in correlated electronic structure calculations". In: Chemical Physics Letters 124.4 (1986), pp. 370 – 375. ISSN: 0009-2614. DOI: https://doi.org/10.1016/0009-2614(86)85036-9.

[80] T. Helgaker, P. Jørgensen, and J. Olsen. Molecular Electronic-Structure Theory. New York: Wiley, 2000.

[81] David H. Bross and Kirk A. Peterson. "Theoretical spectroscopy study of the low-lying electronic states of UX and UX+, X = F and Cl". In: The Journal of Chemical Physics 143.18 (2015), p. 184313. DOI: 10.1063/1.4935492.

[82] Hans H. Brintzinger et al. "Stereospecific Olefin Polymerization with Chiral Metallocene Catalysts". In: Angewandte Chemie International Edition in English 34.11 (), pp. 1143–1170. DOI: 10.1002/anie.199511431.

[83] Raymond J. Butcher et al. In: Organometallics 15.5 (1996), pp. 1488–1496. DOI: 10.1021/om9508694.

[84] Li Jia et al. "Cationic d0/f0 metallocene catalysts. properties of binuclear organoborane Lewis acid cocatalysts and weakly coordinating counteranions derived therefrom". In: Organometallics 13.10 (1994), pp. 3755–3757. DOI: 10.1021/om00022a003.

[85] Xinmin. Yang, Charlotte. Stern, and Tobin J. Marks. "Models for organometallic molecule-support complexes. Very large counterion modulation of cationic actinide alkyl reactivity". In: Organometallics 10.4 (1991), pp. 840–842. DOI: 10.1021/om00050a008.

[86] Zerong Lin et al. "Models for organometallic molecule-support complexes. Synthesis and properties of cationic organoactinides". In: Journal of the American Chemical Society 109.13 (1987), pp. 4127–4129. DOI: 10.1021/ja00247a056.

[87] Ming Yuan He et al. "Supported organoactinides. Surface chemistry and catalytic properties of alumina-bound cyclopentadienyl and pentamethylcyclopentadienyl thorium and uranium hydrocarbyls and hydrides". In: Journal of the American Chemical S 107.3 (1985), pp. 641–652. DOI: 10.1021/ja00289a016.

[88] Paul J. Toscano and Tobin J. Marks. "Supported organoactinides. High-resolution solid-state carbon-13 NMR studies of catalytically active, alumina-bound pentamethylcyclopentadienyl)thorium methyl and hydride complexes". In: Journal of the American Ch 107.3 (1985), pp. 653–659. DOI: 10.1021/ja00289a017.

[89] William C. Finch et al. "Organometallic molecule-inorganic surface coordination and catalytic chemistry. In situ CPMAS NMR delineation of organoactinide adsorbate structure, dynamics, and reactivity". In: Journal of the American Chemical Society 112.17 (1990), pp. 6221–6232. DOI: 10.1021/ja00173a009.

[90] David. Hedden and Tobin J. Marks. "[(CH3)5C5]2Th(CH3)2 surface chemistry and catalysis. Direct NMR spectroscopic observation of surface alkylation and ethylene insertion/polymerization on MgCl2". In: Journal of the American Chemical Societ 110.5 (1988), pp. 1647–1649. DOI: 10.1021/ja00213a061.

[91] Tobin J. Marks. "Surface-bound metal hydrocarbyls. Organometallic connections between heterogeneous and homogeneous catalysis". In: Accounts of Chemical Research 25.2 (1992), pp. 57–65. DOI: 10.1021/ar00014a001.

[92] Li Jia et al. "Cationic Metallocene Polymerization Catalysts Based on Tetrakis(pentafluorophenyl and Its Derivatives. Probing the Limits of Anion "Noncoordination" via a Synthetic, Solution Dynamic, Structural, and Catalytic Olefin Polymerization Study". In: Organometallics 16.5 (1997), pp. 842–857. DOI: 10.1021/om960880j.

[93] Jayachandran Jayakumar et al. "One-Pot Synthesis of Highly Substituted Polyheteroaromatic Compounds by Rhodium(III)-Catalyzed Multiple C-H Activation and Annulation". In: Angewandte Chemie International Edition 53.37 (), pp. 9889–9892. DOI: 10.1002/anie.201405183.

[94] Dennis B Malpass. Introduction to industrial polyethylene: properties, catalysts, and processes Vol. 45. John Wiley & Sons, 2010.

[95] Paul G. Hayes, Warren E. Piers, and Masood Parvez. In: Journal of the American Chemical Soci 125.19 (2003). PMID: 12733887, pp. 5622–5623. DOI: 10.1021/ja034680s.

[96] Paul G. Hayes, Warren E. Piers, and Masood Parvez. "Arene Complexes of Diketiminato Supported Organoscandium Cations: Mechanism of Arene Exchange and Alkyne Insertion in Solvent Separated Ion Pairs". In: Chemistry – A European Journ 13.9 (2007), pp. 2632–2640. DOI: 10.1002/chem.200601087.

[97] Renato P. Orenha et al. "Nature of the Ru-àíNO Coordination Bond: Kohn–Sham Molecular Orbital and Energy Decomposition Analysis". In: ChemistryOpen 6.3 (), pp. 410–416. DOI: 10.1002/open.201700028.

[98] R. D. Shannon. "Revised effective ionic radii and systematic studies of interatomic distances in halides and chalcogenides". In: Acta Crystallographica Section A 32.5 (1976), pp. 751–767. DOI: 10.1107/S0567739476001551.

[99] Carlos A. Cruz et al. "Extremely Stable Thorium(IV) Dialkyl Complexes Supported by Rigid Tridentate 4,5-Bis(anilido)xanthene and 2,6-Bis(anilidomethyl)pyridine Ligands". In: Organometallics 26.3 (2007), pp. 692–701. DOI: 10.1021/om060914f.

[100] Carlos A. Cruz et al. In: Organometallics 28.6 (2009), pp. 1891–1899. DOI: 10.1021/om800624t.

[101] Carlos A. Cruz et al. "Single and Double Alkyl Abstraction from a Bis(anilido)xanthene Thorium(IV) Dibenzyl Complex: Isolation of an Organothorium Cation and a Thorium Dication". In: Organometallics 27.1 (2008), pp. 15–17. DOI: 10.1021/om7011503.

[102] Cassandra E. Hayes and Daniel B. Leznoff. "Diamido-Ether Uranium(IV) Alkyl Complexes as Single-Component Ethylene Polymerization Catalysts". In: Organometallics 29.4 (2010), pp. 767–774. DOI: 10.1021/om900546p.

[103] Paul J. Fagan et al. "Synthesis and properties of bis(pentamethylcyclopentadienyl) actinide hydrocarbyls and hydrides. A new class of highly reactive f-element organometallic compounds". In: Journal of the American Chemical Society 103.22 (1981), pp. 6650–6667. DOI: 10.1021/ja00412a021.

[104] Tobin J. Marks and William A. Wachter. "Tris(.eta.5-cyclopentadienyl)alkyl and -alkenyl compounds of thorium(IV)". In: Journal of the American Chemical Society 98.3 (1976), pp. 703–710. DOI: 10.1021/ja00419a011.

[105] Andrew Streitwieser and Norio Yoshida. "Di-.pi.-cyclooctatetraenethorium". In: Journal of the American Chemical Society 91.26 (1969), pp. 7528–7528. DOI: 10.1021/ja01054a061.

[106] Andrew Streitwieser and Ulrich Mueller-Westerhoff. "Bis(cyclooctatetraenyl)uranium (uranocene). A new class of sandwich complexes that utilize atomic f orbitals". In: Journal of the American Chemical Society 90.26 (1968), pp. 7364–7364. DOI: 10.1021/ja01028a044.

[107] F.T. Edelmann and W.A. Herrmann. Synthetic Methods of Organometallic and Inorganic Chemistry, Thieme, 2014. ISBN: 9783131792211.

[108] Nicholas R. Andreychuk. "NON-DONOR LIGANDS IN ORGANOACTINIDE CHEMISTRY". PhD thesis. McMaster Univerity, 2017.

[109] Kelly S. A. Motolko et al. "Zirconium Complexes of a Rigid, Dianionic Pincer Ligand: Alkyl Cations, Arene Coordination, and Ethylene Polymerization". In: Organometallics 36.16 (2017), pp. 3084–3093. DOI: 10.1021/acs.organomet.7b00424.

[110] Benedict M. Gardner et al. "The role of 5f-orbital participation in unexpected inversion of the [sigma]-bond metathesis reactivity trend of triamidoamine thorium(iv) and uranium(iv) alkyls". In: Chem. Sci. 5 (6 2014), pp. 2489–2497. DOI: 10.1039/C4SC00182F.

[111] Elena Domeshek et al. "Organoactinides in the polymerization of ethylene: is TIBA a better cocatalyst than MAO?" In: Dalton Trans. 42 (25 2013), pp. 9069–9078. DOI: 10.1039/C3DT00032J. URL: http://dx.doi.org/10.1039/C3DT00032J.

[112] Tobin J. Marks and Victor W. Day. "Actinide Hydrocarbyl and Hydride Chemistry". In: Fundamental and Technological Aspects of Organo-f-Element Chemistry. Ed. by Tobin J. Marks and Ignazio L. Fragalà. Dordrecht: Springer Netherlands, 1985, pp. 115–157. ISBN: 978-94-009-5406-9. DOI: 10.1007/978-94-009-5406-9_4.

[113] Axel D. Becke. In: The Journal of Chemical Physics 98.7 (1993), pp. 5648–5652. DOI: 10.1063/1.464913.

[114] John P. Perdew, Kieron Burke, and Matthias Ernzerhof. "Generalized Gradient Approximation Made Simple". In: Phys. Rev. Lett. 77 (18 1996), pp. 3865–3868. DOI: 10.1103/PhysRevLett.77.3865.

[115] Xiaoyan Cao, Michael Dolg, and Hermann Stoll. "Valence basis sets for relativistic energy-consistent small-core actinide pseudopotentials". In: The Journal of Chemical Physics 118.2 (2003), pp. 487–496. DOI: 10.1063/1.1521431.

[116] Xiaoyan Cao and Michael Dolg. "Segmented contraction scheme for small-core actinide pseudopotential basis sets". In: Journal of Molecular Structure: THEOCHEM 673.1 (2004), pp. 203 –209. ISSN: 0166-1280. DOI: https://doi.org/10.1016/j.theochem.2003.12.015.

[117] Paula L. Diaconescu et al. In: Journal of the American Chemical Society 122.25 (2000), pp. 6108–6109. DOI: 10.1021/ja994484e.

[118] "Applications of the ETS-NOCV method in descriptions of chemical reactions". In: Journal of Molecular Modeling 17.9 (2011), p. 2337. ISSN: 0948-5023. DOI: 10.1007/s00894-011-1023-6.

[119] Mariusz P. Mitoraj, Artur Michalak, and Tom Ziegler. "On the Nature of the Agostic Bond between Metal Centers and Hydrogen Atoms in Alkyl Complexes. An Analysis Based on the Extended Transition State Method and the Natural Orbitals for Chemical Valence Scheme (ETS-NOCV)". In: Organometallics 28.13 (2009), pp. 3727–3733. DOI: 10.1021/om900203m.

[120] Sung-Kwan Kim et al. In: Journal of the American Chemical Society 132.29 (2010). PMID: 20597488, pp. 9954–9955. DOI: 10.1021/ja101685u.

[121] E. Broclawik et al. "Formaldehyde activation by Cu(I) and Ag(I) sites in ZSM-5: ETS-NOCV analysis of charge transfer processes". In: Catalysis Today 169.1 (2011), pp. 45 –51. ISSN: 0920-5861. DOI: https://doi.org/10.1016/j.cattod.2010.08.020.

[122] Sylvester Ndambuki and Tom Ziegler. In: Inorganic Chemistry 51.14 (2012). PMID: 22731692, pp. 7794–7800. DOI: 10.1021/ic300824u.

[123] Mariusz P. Mitoraj and Artur Michalak. "On the asymmetry in molybdenum–oxygen bonding in the MoO3 structure: ETS–NOCV analysis". In: Structural Chemistry 23.5 (2012), pp. 1369–1375. ISSN: 1572-9001. DOI: 10.1007/s11224-012-0056-5.

[124] Holger Braunschweig et al. "Bond-strengthening backdonation in a transition-metal diborene complex". In: Nature Chemistry 5 (Dec. 2012), 115 EP –.

[125] Paul G. Hayes et al. "The Osmium–Silicon Triple Bond: Synthesis, Characterization, and Reactivity of an Osmium Silylyne Complex". In: Journal of the American Chemical 135.32 (2013), pp. 11780–11783. DOI: 10.1021/ja406799y.

[126] Ignacy Cukrowski, Jurgens H. de Lange, and Mariusz Mitoraj. In: The Journal of Physical Chem 118.3 (2014), pp. 623–637. DOI: 10.1021/jp410744x.

[127] Estefania Fernandez Villanueva, Otilia Mo, and Manuel Yanez. "On the existence and characteristics of [small pi]-beryllium bonds". In: Phys. Chem. Chem. Phys. 16 (33 2014), pp. 17531–17536. DOI: 10.1039/C4CP01992J.

[128] Wan-Lu Li et al. "Electronic Structure and Bonding Situation in M2O2 (M = Be, Mg, Ca) Rhombic Clusters". In: The Journal of Physical Chemistry A 122.10 (2018), pp. 2816–2822. DOI: 10.1021/acs.jpca.8b01335.

[129] Ndambuki Sylvester and Ziegler Tom. "An analysis of unsupported triple and quadruple metal–metal bonds between two homonuclear group 6 transition elements based on the combined natural orbitals for chemical valence and extended transition state method". In: International Journal of Quantum Chemistry 113.6 (), pp. 753–761. DOI: 10.1002/qua.24068.

[130] TURBOMOLE V5.10 2008, a development of University of Karlsruhe and Forschungszentrum Karls

[131] K. Eichkorn et al. "Auxiliary basis sets for main row atoms and transition metals and their use to approximate Coulomb potentials". In: Theoretical Chemistry Accounts 97 (1997), p. 119.

[132] Martin ulka, L. Cantrel, and V. Vallet. "Theoretical Study of Plutonium(IV) Complexes Formed within the PUREX Process: A Proposal of a Plutonium Surrogate in Fire Conditions". In: J. Phys. Chem. A 118 (2014), pp. 10073–10080.

[133] Tom Ziegler and Arvi Rauk. "On the calculation of bonding energies by the Hartree Fock Slater method". In: Theoretica chimica acta 46.1 (1977), pp. 1–10. DOI: 10.1007/BF02401406.

[134] RF Nalewajski, AM Köster, and K Jug. "Chemical valence from the two-particle density matrix". In: Theoretica chimica acta 85.6 (1993), pp. 463–484.

[135] Roman F. Nalewajski and Janusz Mrozek. "Modified valence indices from the two-particle density matrix". In: International Journal of Quantum Chemistry 51.4 (1994), pp. 187–200. DOI: 10.1002/qua.560510403.

[136] Slawomir M. Cybulski and Marion L. Lytle. "The origin of deficiency of the supermolecule second-order Møller-Plesset approach for evaluating interaction energies". In: The Journal of Chemical Physics 127.14 (2007), p. 141102. DOI: 10.1063/1.2795693.

[137] C. David Sherrill, Tait Takatani, and Edward G. Hohenstein. "An Assessment of Theoretical Methods for Nonbonded Interactions: Comparison to Complete Basis Set Limit Coupled-Cluster Potential Energy Curves for the Benzene Dimer, the Methane Dimer, Benzene-àíMethane, and Benzene-àíH2S". In: The Journal of Physical Chemistry A 113.38 (2009), pp. 10146–10159. DOI: 10.1021/jp9034375.

[138] P. Gotcu-Freis et al. "Mass spectrometric studies of the vapour phase in the (Pu+O) system". In: The Journal of Chemical Thermodynamics 43.8 (2011), pp. 1164 –1173. ISSN: 0021-9614. DOI: https://doi.org/10.1016/j.jct.2011.02.024.

[139] V.P. Glushko et al. Thermodynamic Properties of Individual Substances. Ed. by V.P. Glushko (Ed.) Vol. 1-4. Nauka, Moscow, 1978-1982.

[140] E. H. P. Cordfunke and R. J. M. Konings. "Thermochemical data for reactor materials and fission products: The ECN database". In: Journal of Phase Equilibria 14.4 (1993), pp. 457–464. ISSN: 1054-9714. DOI: 10.1007/BF02671964.

[141] Rudy J. M. Konings et al. "The Thermodynamic Properties of the f-Elements and their Compounds. Part 2. The Lanthanide and Actinide Oxides". In: Journal of Physical and Chemical Reference Data 43.1 (2014), p. 013101. DOI: 10.1063/1.4825256.

[142] R. J. Ackermann, R. L. Faircloth, and M. H. Rand. "A Thermodynamic Study of the Vaporization Behavior of the Substoichiometric Plutonium Dioxide Phase1". In: The Journal of Physical Chemistry 70.11 (1966), pp. 3698–3706. DOI: 10.1021/j100883a055.

[143] PARDUE WILLIAM M. and KELLER DONALD L. "Volatility of PuO2 in Nonreducing Atmospheres". In: Journal of the American Ceramic Society 47.12 (), pp. 610–614. DOI: 10.1111/j.1151-2916.1964.tb13116.x.

[144] D. R. Messier. "Evaporation of Hypostoichiometric Plutonium Dioxide from 2070 ° to 2380 °K". In: Journal of the American Ceramic Society 51.12 (), pp. 710–713. DOI: 10.1111/j.1151-2916.1968.tb15933.x.

[145] C Ronchi et al. "Volatile molecule PuO3 observed from subliming plutonium dioxide". In: J. Nucl. Mat. 280.1 (2000), pp. 111–115. ISSN: 0022-3115. DOI: 10.1016/S0022-3115(00)00058-1.

[146] Oscar H. Krikorian et al. "Transpiration studies on the volatilities of PuO3(g) and PuO2(OH)2(g) from PuO2(s) in the presence of steam and oxygen and application to plutonium volatility in mixed-waste thermal oxidation processors". In: Journal of Nuclear Materials 247 (1997). Thermodynamics of Nuclear Materials, pp. 161 –171. ISSN: 0022-3115. DOI: https://doi.org/10.1016/S0022-3115(97)00043-3.

[147] Katharina Boguslawski et al. "On the multi-reference nature of plutonium oxides: PuO22+, PuO2, PuO3 and PuO2(OH)2". In: Phys. Chem. Chem. Phys. 19 (6 2017), pp. 4317–4329. DOI: 10.1039/C6CP05429C.

[148] Attila Kovács. "Relativistic Multireference Quantum Chemical Study of the Electronic Structure of Actinide Trioxide Molecules". In: J. Phys. Chem. A, 121.12 (2017), pp. 2523–2530. DOI: 10.1021/acs.jpca.7b01344.

[149] Meng Sheng Liao, Tapas Kar, and Steve Scheiner. In: The Journal of Physical Chemistry A 108.15 (2004), pp. 3056–3063. DOI: 10.1021/jp036927d.

[150] E. F. Archibong and A. K. Ray. "An ab initio study of PuO_2 and of PuN_2". In: J. Mol. Struct. (THEOCHEM) 530 (2000), pp. 165–170. DOI: 10.1016/S0166-1280(00)00332-8.

[151] G. La Macchia et al. "A theoretical study of the ground state and lowest excited states of $PuO^{0/+/+2}$ and $PuO_2^{0/+/+2}$". In: Phys. Chem. Chem. Phys. 48 (2008), pp. 7278–7283.

[152] Lyudmila V. Moskaleva et al. "The heat of formation of gaseous PuO22+ from relativistic density functional calculations". In: Phys. Chem. Chem. Phys. 8 (32 2006), pp. 3767–3773. DOI: 10.1039/B607292E.

[153] Arie Landau et al. "Intermediate Hamiltonian Fock-space coupled-cluster method: Excitation energies of barium and radium". In: The Journal of Chemical Physics 113.22 (2000), pp. 9905–9910. DOI: 10.1063/1.1323258.

[154] Lucas Visscher, Ephraim Eliav, and Uzi Kaldor. "Formulation and implementation of the relativistic Fock-space coupled cluster method for molecules". In: The Journal of Chemical Physics 115.21 (2001), pp. 9720–9726. DOI: 10.1063/1.1415746.

[155] Arie Landau et al. "Intermediate Hamiltonian Fock-space coupled cluster method in the one-hole one-particle sector: Excitation energies of xenon and radon". In: The Journal of Chemical Physics 115.15 (2001), pp. 6862–6865. DOI: 10.1063/1.1405005.

[156] H.-J. Werner et al. MOLPRO, Version 2015.1, A Package Of Ab Initio Programs. 2015.

[157] Veryazov Valera, Malmqvist Per Åke, and Roos Björn O. "How to select active space for multiconfigurational quantum chemistry?" In: International Journal of Quantum Chemistr 111.13 (), pp. 3329–3338. DOI: 10.1002/qua.23068.

[158] Kerstin. Andersson et al. "Second-order perturbation theory with a CASSCF reference function". In: The Journal of Physical Chemistry 94.14 (1990), pp. 5483–5488. DOI: 10.1021/j100377a012.

[159] N. Forsberg and P.-Å. Malmqvist. "Multiconfiguration perturbation theory with imaginary level shift". In: Chem. Phys. Lett. 274 (1997), p. 196.

[160] J. Patrick Zobel, Juan J. Nogueira, and Leticia González. "The IPEA dilemma in CASPT2". In: Chem. Sci. 8 (2 2017), pp. 1482–1499. DOI: 10.1039/C6SC03759C.

[161] C. Angeli et al. "Introduction Of N-Electron Valence States For Multireference Perturbation Theory". In: J. Chem. Phys. 114 (2001), pp. 10252–10264.

[162] Kenneth G. Dyall. In: The Journal of Chemical Physics 102.12 (1995), pp. 4909–4918. DOI: 10.1063/1.469539.

[163] Per Åke Malmqvist, Björn O. Roos, and Bernd Schimmelpfennig. "The restricted active space (RAS) state interaction approach with spin–orbit coupling". In: Chemical Physics Letters 357.3 (2002), pp. 230 –240. ISSN: 0009-2614. DOI: https://doi.org/10.1016/S0009-2614(02)00498-0.

[164] Branko Ruscic et al. In: The Journal of Physical Chemistry A 110.21 (2006), pp. 6592–6601. DOI: 10.1021/jp056311j.

[165] J D Cox, Donald D Wagman, and V A Medvedev. CODATA key values for thermodynamics. New York: Hemisphere Pub. Corp., 1989.

[166] R.J. Lemire, NEA Data Bank, and OECD Nuclear Energy Agency. Chemical Thermodynamics o Chemical thermodynamics. Elsevier, 2001. ISBN: 9780444503794.

[167] National Institute of Standards and Technology data base, http://www.nist.gov/chemistry (accessed on March 13, 2014).

[168] A. D. Becke. "Density-functional thermochemistry. III. The role of exact exchange". In: J. Chem. Phys. 98 (1993), pp. 5648–5653.

[169] P. J. Stephens et al. "Ab Initio Calculation of Vibrational Absorption and Circular Dichroism Spectra Using Density Functional Force Fields". In: J. Chem. Phys. 98 (1994), pp. 11623–11627.

[170] M. J. Frisch et al. Gaussian 09, Revision C.02. Gaussian, Inc., Wallingford, CT, 2004.

[171] Xiaoyan Cao, Michael Dolg, and Hermann Stoll. "Valence basis sets for relativistic energy-consistent small-core actinide pseudopotentials". In: J. Chem. Phys. 118.2 (2003), pp. 487–496.

[172] B. O. Roos et al. "Main group atoms and dimers studied with a new relativistic ANO basis set". In: J. Phys. Chem. A 108 (2004), pp. 2851–2858. DOI: 10.1021/jp031064+.

[173] Björn O. Roos et al. "New Relativistic ANO Basis Sets for Actinide Atoms". In: Chem. Phys. Lett. 409 (2005), pp. 295–299.

[174] E. F. Archibong and A. K. Ray. "An ab initio study of PuO_2 and of PuN_2". In: J. Mol. Struct. (THEOCHEM) 530 (2000), pp. 165–170. DOI: 10.1016/S0166-1280(00)00332-8.

[175] "The molecular mean-field approach for correlated relativistic calculations." In: J. Chem. Phys. 131.12 (Sept. 2009), p. 124116. ISSN: 1089-7690. DOI: 10.1063/1.3239505.

[176] L. Visscher, T. J. Lee, and K. G. Dyall. "Formulation and implementation of a relativistic unrestricted coupled-cluster method including noniterative connected triples". In: J. Chem. Phys. 105.19 (1996), pp. 8769–8776. DOI: 10.1063/1.472655.

[177] L. Visscher, E. Eliav, and U. Kaldor. "Formulation and implementation of the relativistic Fock-space coupled cluster method for molecules". In: J. Chem. Phys. 115 (2001), pp. 9720–9726. DOI: 10.1063/1.1415746.

[178] DIRAC, a relativistic ab initio electronic structure program, Release DIRAC16 (2016), written by H. J. Aa. Jensen, R. Bast, T. Saue, and L. Visscher, with contributions from V. Bakken, K. G. Dyall, S. Dubillard, U. Ekström, E. Eliav,

T. Enevoldsen, E. Faßhauer, T. Fleig, O. Fossgaard, A. S. P. Gomes, T. Helgaker, J. Henriksson, M. Iliaš, Ch. R. Jacob, S. Knecht, S. Komorovský, O. Kullie, J. K. Lærdahl, C. V. Larsen, Y. S. Lee, H. S. Nataraj, M. K. Nayak, P. Norman, G. Olejniczak, J. Olsen, Y. C. Park, J. K. Pedersen, M. Pernpointner, R. di Remigio, K. Ruud, P. Sałek, B. Schimmelpfennig, J. Sikkema, A. J. Thorvaldsen, J. Thyssen, J. van Stralen, S. Villaume, O. Visser, T. Winther, and S. Yamamoto (see http://www.diracprogram.org).

[179] K. G. Dyall. "Relativistic double-zeta, triple-zeta, and quadruple-zeta basis sets for the 7*p* elements, with atomic and molecular applications". In: Theor. Chem. Acc. 131 (2012), pp. 1172–4. DOI: 10.1007/s00214-012-1172-4.

[180] K. G. Dyall. "Relativistic double-zeta, triple-zeta, and quadruple-zeta basis sets for the actinides Ac Lr". In: Theor. Chem. Acc. 117 (2007), pp. 491–500. DOI: 10.1007/s00214-006-0175-4.

[181] R. A. Kendall, T. H. Dunning Jr., and R. J. Harrison. "Electron affinities of the first-row atoms revisited. Systematic basis sets and wave functions". In: J. Chem. Phys. 96 (1992), pp. 6796–6806. DOI: 10.1063/1.462569.

[182] L. Visscher. "Approximate molecular relativistic Dirac-Coulomb calculations using a simple Coulombic correction". In: Theor. Chem. Acc. 98 (1997), pp. 68–70. DOI: 10.1007/s002140050280.

[183] J. D. Watts, J. Gauss, and R. J. Bartlett. "Coupled-cluster methods with noniterative triple excitations for restricted open-shell Hartree-Fock and other general single determinant reference functions. Energies and analytical gradients". In: J. Chem. Phys. 98 (1993), pp. 8718–8733.

[184] David H. Bross and Kirk A. Peterson. "Composite thermochemistry of gas phase U(VI)-containing molecules". In: J. Chem. Phys. 141.24 (2014), p. 244308. DOI: http://dx.doi.org/10.1063/1.4904721.

[185] A Shee et al. "Equation-of-Motion Coupled -Cluster Theory based on the 4-component Dirac–Coulomb(–Gaunt) Hamiltonian. Energies for single electron detachment, attachment and electronically excited states". In: The Journal of Chemical Physics (2018).

[186] Aquilante Francesco et al. "Molcas 8: New capabilities for multiconfigurational quantum chemical calculations across the periodic table". In: J. Comput. Chem. 37.5 (), pp. 506–541. DOI: 10.1002/jcc.24221.

[187] R. G. Denning and I. D. Morrison. "The electronic structure of actinyl ions: the excited-state absorption spectrum of $Cs_2UO_2Cl_4$". In: Chem. Phys. Lett. 180 (1991), p. 101.

[188] L. Bovey and S. Gerstenkorn. "Ground State of the First Spectrum of Plutonium (Pu i), from an Analysis of Its Atomic Spectrum". In: J. Opt. Soc. Am. 51.5 (1961), pp. 522–525. DOI: 10.1364/JOSA.51.000522.

[189] J. Blaise et al. In: C.R. Acad. Sci., Fr. 255 (1962), pp. 2403–2405.

[190] J. Blaise et al. In: Physica Scripta 22 (1980), pp. 224–230.

[191] Attila Kovács. "Relativistic Multireference Quantum Chemical Study of the Electronic Structure of Actinide Trioxide Molecules". In: J. Phys. Chem. A 121 (2017), pp. 2523–2530. ISSN: 1520-5215. DOI: 10.1021/acs.jpca.7b01344.

[192] G. La Macchia et al. "A theoretical study of the ground state and lowest excited states of $PuO^{0/+/+2}$ and $PuO_2^{0/+/+2}$". In: Phys. Chem. Chem. Phys. 48 (2008), pp. 7278–7283.

[193] E. G. Rauh and R. J. Ackermann. "First ionization potentials of some refractory oxide vapors". In: The Journal of Chemical Physics 60.4 (1974), pp. 1396–1400. DOI: 10.1063/1.1681210.

[194] F. Capone et al. "Mass Spectrometric Measurement Of the Ionization Energies and Cross Sections Of Uranium and Plutonium Oxide Vapors". In: The Journal of Physical Chemistry A 103.50 (1999), pp. 10899–10906. DOI: 10.1021/jp992405f.

[195] Marta Santos et al. "Gas-Phase Oxidation Reactions of Neptunium and Plutonium Ions Investigated via Fourier Transform Ion Cyclotron Resonance Mass Spectrometry". In: The Journal of Physical Chemistry A 106.31 (2002), pp. 7190–7194. DOI: 10.1021/jp025733f.

[196] F. Capone et al. "Controversy on the First Ionization Potential of PuO2 (Nearly) Settled by New Experimental Evidence". In: The Journal of Physical Chemistry A 109.51 (2005), pp. 12054–12058. DOI: 10.1021/jp055452i.

[197] E. R. Batista et al. "Density functional investigations of the properties and thermochemistry of UF_6 and UF_5 using valence-electron and all-electron approaches". In: J. Chem. Phys. 121 (2004), pp. 2144–2150. DOI: 10.1063/1.1768518.

[198] E. H. P. Cordfunke and R. J. M. Konings. "Thermochemical data for reactor materials and fission products: The ECN database". In: Journal of Phase Equilibria 14.4 (1993), pp. 457–464. ISSN: 1054-9714. DOI: 10.1007/BF02671964.

[199] Oscar H. Krikorian et al. "Transpiration studies on the volatilities of PuO3(g) and PuO2(OH)2(g) from PuO2(s) in the presence of steam and oxygen and application to plutonium volatility in mixed-waste thermal oxidation processors". In: Journal of Nuclear Materials 247 (1997). Thermodynamics of Nuclear Materials, pp. 161 –171. ISSN: 0022-3115. DOI: https://doi.org/10.1016/S0022-3115(97)00043-3.

[200] Attila Kovács et al. "Quantum Chemical Calculations and Experimental Investigations of Molecular Actinide Oxides". In: Chem. Rev. 115.4 (2015), pp. 1725–1759. DOI: 10.1021/cr500426s.

[201] Faoulat Miradji et al. "Thermodynamic Properties of Gaseous Ruthenium Species". In: J. Phys. Chem. A 119.20 (2015), pp. 4961–4971. DOI: 10.1021/acs.jpca.5b01645.

[202] Wanyi Jiang et al. "Comparative Study of Single and Double Hybrid Density Functionals for the Prediction of 3d Transition Metal Thermochemistry". In: Journal of Chemical Theory and Computation 8.11 (2012), pp. 4102–4111. DOI: 10.1021/ct300455e.

[203] Lars Goerigk and Stefan Grimme. "Efficient and Accurate Double-Hybrid-Meta-GGA Density Functionals—Evaluation with the Extended GMTKN30 Database for General Main Group Thermochemistry, Kinetics, and Noncovalent Interactions". In: Journal of Chemical Theory and Computation 7.2 (2011), pp. 291–309. DOI: 10.1021/ct100466k.

[204] Stefan Grimme. "Semiempirical hybrid density functional with perturbative second-order correlation". In: The Journal of Chemical Physics 124.3 (2006), p. 034108. DOI: 10.1063/1.2148954.

[205] Emmanuel Fromager. "Rigorous formulation of two-parameter double-hybrid density-functionals". In: The Journal of Chemical Physics 135.24 (2011), p. 244106. DOI: 10.1063/1.3671384.

[206] Julien Toulouse et al. "Communication: Rationale for a new class of double-hybrid approximations in density-functional theory". In: The Journal of Chemical Physics 135.10 (2011), p. 101102. DOI: 10.1063/1.3640019.

[207] Kamal Sharkas, Julien Toulouse, and Andreas Savin. "Double-hybrid density-functional theory made rigorous". In: The Journal of Chemical Physics 134.6 (2011), p. 064113. DOI: 10.1063/1.3544215.

[208] Tobias Schwabe and Lars Goerigk. "Time-Dependent Double-Hybrid Density Functionals with Spin-Component and Spin-Opposite Scaling". In: Journal of Chemical Theory 13.9 (2017), pp. 4307–4323. DOI: 10.1021/acs.jctc.7b00386.

[209] Stefan Grimme and Frank Neese. "Double-hybrid density functional theory for excited electronic states of molecules". In: The Journal of Chemical Physics 127.15 (2007), p. 154116. DOI: 10.1063/1.2772854.

[210] Tobias Schwabe and Stefan Grimme. "Double-hybrid density functionals with long-range dispersion corrections: higher accuracy and extended applicability". In: Phys. Chem. Chem. Phys. 9 (26 2007), pp. 3397–3406. DOI: 10.1039/B704725H.

[211] Juan Aragó, Enrique Ortí, and Juan C. Sancho-García. "Nonlocal van der Waals Approach Merged with Double-Hybrid Density Functionals: Toward the Accurate Treatment of Noncovalent Interactions". In: Journal of Chemical Theory and Computat 9.8 (2013), pp. 3437–3443. DOI: 10.1021/ct4003527.

[212] Tobias Benighaus et al. "Semiempirical Double-Hybrid Density Functional with Improved Description of Long-Range Correlation". In: The Journal of Physical Chemistry 112.12 (2008), pp. 2702–2712. DOI: 10.1021/jp710439w.

[213] Eric Brémond and Carlo Adamo. "Seeking for parameter-free double-hybrid functionals: The PBE0-DH model". In: The Journal of Chemical Physics 135.2 (2011), p. 024106. DOI: 10.1063/1.3604569.

[214] Jeng-Da Chai and Shan-Ping Mao. "Seeking for reliable double-hybrid density functionals without fitting parameters: The PBE0-2 functional". In: Chemical Physics Letter 538 (2012), pp. 121 –125. ISSN: 0009-2614. DOI: https://doi.org/10.1016/j.cplett.2012.04.045.

[215] Jeng-Da Chai and Martin Head-Gordon. "Long-range corrected hybrid density functionals with damped atom–atom dispersion corrections". In: Phys. Chem. Chem. Phys. 10 (44 2008), pp. 6615–6620. DOI: 10.1039/B810189B.

[216] Bun Chan and Leo Radom. "Obtaining Good Performance With Triple-Type Basis Sets in Double-Hybrid Density Functional Theory Procedures". In: Journal of Chemical Th 7.9 (2011), pp. 2852–2863. DOI: 10.1021/ct200396x.

[217] Lars Goerigk and Stefan Grimme. "A thorough benchmark of density functional methods for general main group thermochemistry, kinetics, and noncovalent interactions". In: Phys. Chem. Chem. Phys. 13 (14 2011), pp. 6670–6688. DOI: 10.1039/C0CP02984J.

[218] David C. Graham et al. "Optimization and Basis-Set Dependence of a Restricted-Open-Shell Form of B2-PLYP Double-Hybrid Density Functional Theory". In: The Journal of Physical Chemistry A 113.36 (2009). PMID: 19645437, pp. 9861–9873. DOI: 10.1021/jp9042864.

[219] Amir Karton et al. "Highly Accurate First-Principles Benchmark Data Sets for the Parametrization and Validation of Density Functional and Other Approximate Methods. Derivation of a Robust, Generally Applicable, Double-Hybrid Functional for Thermochemistry and Thermochemical Kinetics". In: The Journal of Physical Chemistry A 112.50 (2008), pp. 12868–12886. DOI: 10.1021/jp801805p.

[220] Sebastian Kozuch and Jan M. L. Martin. "Spin-component-scaled double hybrids: An extensive search for the best fifth-rung functionals blending DFT and perturbation theory". In: Journal of Computational Chemistry 34.27 (), pp. 2327–2344. DOI: 10.1002/jcc.23391.

[221] Sebastian Kozuch, David Gruzman, and Jan M. L. Martin. "DSD-BLYP: A General Purpose Double Hybrid Density Functional Including Spin Component Scaling and Dispersion Correction". In: The Journal of Physical Chemistry C 114.48 (2010), pp. 20801–20808. DOI: 10.1021/jp1070852.

[222] Sebastian Kozuch and Jan M. L. Martin. "DSD-PBEP86: in search of the best double-hybrid DFT with spin-component scaled MP2 and dispersion corrections". In: Phys. Chem. Chem. Phys. 13 (45 2011), pp. 20104–20107. DOI: 10.1039/C1CP22592H.

[223] Afshan Mohajeri and Mojtaba Alipour. "B2-PPW91: A promising double-hybrid density functional for the electric response properties". In: The Journal of Chemical Physics 136.12 (2012), p. 124111. DOI: 10.1063/1.3698284.

[224] Roberto Peverati and Martin Head-Gordon. "Orbital optimized double-hybrid density functionals". In: The Journal of Chemical Physics 139.2 (2013), p. 024110. DOI: 10.1063/1.4812689.

[225] J. C. Sancho-García and A. J. Pérez-Jiménez. "Assessment of double-hybrid energy functionals for conjugated systems". In: The Journal of Chemical Physics 131.8 (2009), p. 084108. DOI: 10.1063/1.3212881.

[226] Tobias Schwabe and Stefan Grimme. "Towards chemical accuracy for the thermodynamics of large molecules: new hybrid density functionals including non-local correlation effects". In: Phys. Chem. Chem. Phys. 8 (38 2006), pp. 4398–4401. DOI: 10.1039/B608478H.

[227] Sidi M. O. Souvi, Kamal Sharkas, and Julien Toulouse. "Double-hybrid density-functional theory with meta-generalized-gradient approximations". In: The Journal of Chemical Phy 140.8 (2014), p. 084107. DOI: 10.1063/1.4865963.

[228] Alex Tarnopolsky et al. "Double-Hybrid Functionals for Thermochemical Kinetics". In: The Journal of Physical Chemistry A 112.1 (2008), pp. 3–8. DOI: 10.1021/jp710179r.

[229] Julien Toulouse et al. "Communication: Rationale for a new class of double-hybrid approximations in density-functional theory". In: The Journal of Chemical Physics 135.10 (2011), p. 101102. DOI: 10.1063/1.3640019.

[230] Igor Ying Zhang et al. "Doubly hybrid density functional xDH-PBE0 from a parameter-free global hybrid model PBE0". In: The Journal of Chemical Physics 136.17 (2012), p. 174103. DOI: 10.1063/1.3703893.

[231] Igor Ying Zhang and Xin Xu. "Reaching a Uniform Accuracy for Complex Molecular Systems: Long-Range-Corrected XYG3 Doubly Hybrid Density Functional". In: The Journal of Physical Chemistry Letters 4.10 (2013), pp. 1669–1675. DOI: 10.1021/jz400695u.

[232] Ying Zhang, Xin Xu, and William A. Goddard. "Doubly hybrid density functional for accurate descriptions of nonbond interactions, thermochemistry, and thermochemical kinetics". In: Proceedings of the National Academy of Sciences (2009). ISSN: 0027-8424. DOI: 10.1073/pnas.0901093106.

[233] Igor Ying Zhang et al. "A fast doubly hybrid density functional method close to chemical accuracy using a local opposite spin ansatz". In: Proceedings of the National Acade 108.50 (2011), pp. 19896–19900. DOI: 10.1073/pnas.1115123108.

[234] Lars Goerigk and Stefan Grimme. "Double-hybrid density functionals". In: Wiley Interdisciplinary Reviews: Computational Molecular Science 4.6 (), pp. 576–600. DOI: 10.1002/wcms.1193.

[235] Liam Wilbraham, Carlo Adamo, and Ilaria Ciofini. "Communication: Evaluating non-empirical double hybrid functionals for spin-state energetics in transition-metal complexes". In: The Journal of Chemical Physics 148.4 (2018), p. 041103. DOI: 10.1063/1.5019641.

[236] Miho Isegawa, Frank Neese, and Dimitrios A. Pantazis. "Ionization Energies and Aqueous Redox Potentials of Organic Molecules: Comparison of DFT, Correlated ab Initio Theory and Pair Natural Orbital Approaches". In: Journal of Chemical Theory and Computation 12.5 (2016), pp. 2272–2284. DOI: 10.1021/acs.jctc.6b00252.

[237] Tomasz Seidler, Katarzyna Stadnicka, and Benoît Champagne. "Evaluation of the Linear and Second-Order NLO Properties of Molecular Crystals within the Local Field Theory: Electron Correlation Effects, Choice of XC Functional, ZPVA Contributions, and Impact of the Geometry in the Case of 2-Methyl-4-nitroaniline". In: Journal of Chemical Theory and Computation 10.5 (2014), pp. 2114–2124. DOI: 10.1021/ct5001654.

[238] Kirk A. Peterson. "Correlation consistent basis sets for actinides. I. The Th and U atoms". In: The Journal of Chemical Physics 142.7 (2015), p. 074105. DOI: 10.1063/1.4907596.

[239] Timofei Privalov et al. "Structure and Thermodynamics of Uranium(VI) Complexes in the Gas Phase: A Comparison of Experimental and ab Initio Data". In: The Journal of Physical Chemistry A 106.46 (2002), pp. 11277–11282. DOI: 10.1021/jp0260402.

[240] M. Dolg, H. Stoll, and H. Preuss. "Energy Aadjusted ab initio pseudopotentials for the rare earth elements". In: The Journal of Chemical Physics 90.3 (1989), pp. 1730–1734. DOI: 10.1063/1.456066.

[241] G. V. Girichev et al. "Molecular structure and vibrational characteristics of thorium tetrafluoride". In: Journal of Structural Chemistry 40.2 (1999), p. 207.

[242] Yu Gong et al. "Infrared Spectroscopic and Theoretical Investigations of the OUF2 and OThF2 Molecules with Triple Oxo Bond Character". In: Inorganic Chemistry 51.12 (2012), pp. 6983–6991. DOI: 10.1021/ic3009128.

[243] Monica Vasiliu et al. "Reliable Potential Energy Surfaces for the Reactions of H2O with ThO2, PaO2(+), UO2(2+), and UO2(.)" In: J. Phys. Chem. A 119.46 (2015), pp. 11422–11431. DOI: 10.1021/acs.jpca.5b08618.

[244] Georg Schreckenbach, P. Jeffrey Hay, and Richard L. Martin. "Density functional calculations on actinide compounds: Survey of recent progress and application to [UO2X4]2-(X=F, Cl, OH) and AnF6 (An=U, Np, Pu)". In: Journal of Computational Chem 20.1 (), pp. 70–90. DOI: 10.1002/(SICI)1096-987X(19990115)20:1<70::AID-JCC9>3.0.CO;2-F.

[245] R. D. Wesley and C. W. DeKock. "Geometry and Infrared Spectra of Matrix-Isolated Rare-Earth Halides. I. LaF3, CeF3, PrF3, NdF3, SmF3, and EuF3". In: The Journal of Chemical Physics 55.8 (1971), pp. 3866–3877. DOI: 10.1063/1.1676673.

[246] Roger L. De Kock et al. "A theoretical study of the linear versus bent geometry for several MX2 molecules: MgF2, CaH2, CaF2, CeO2 and YbCl2". In: Polyhedron 9.15 (1990), pp. 1919 –1934. DOI: https://doi.org/10.1016/S0277-5387(00)84004-8.

[247] V. G. Solomonik, A. Yu. Yachmenev, and A. N. Smirnov. "Structure, force fields, and vibrational spectra of cerium tetrahalides". In: Journal of Structural Chemistry 49.4 (2008), pp. 613–620. DOI: 10.1007/s10947-008-0085-5.

[248] Tanya Mikulas et al. "Reactions of Lanthanide Atoms with Oxygen Difluoride and the Role of the Ln Oxidation State". In: Inorganic Chemistry 53.1 (2014), pp. 446–456. DOI: 10.1021/ic402422h.

[249] V. Yu. Buz'ko, G. Yu. Chuiko, and Kh. B. Kushkhov. "Ab initio study of the structure and stability of AcF n (3 -àí n)+ of complexes (n = 1-àí7)". In: Russian Journal of Inorganic Chemistry 57.6 (2012), pp. 838–842.